Investigating the Role of Exercise-Induced Circulating Extracellular Vesicles in Adult Myogenesis and Neurogenesis

Bianca Paris

Thesis is submitted in partial fulfillment of the requirements of the award of Doctor of Philosophy at

Oxford Brookes University

Department of Biological and Medical Sciences

January 2019

Acknowledgements

I would like to thank Oxford Brookes University and Professor Nigel Groome for providing such generous funding for my research. I also owe a huge thank you to my supervisors Dr Ryan Pink and Professor Dave Carter for their invaluable guidance and encouragement, and to past and present members of the lab for all of the technical (and emotional) support which enabled me to complete this work. I would also like to thank all of the collaborators mentioned within this thesis for sharing their expertise, resources, and facilities.

Thank you to Fiona Revell and Gerard Ducker for instilling their enthusiasm for science, and for seeing a scientist in me even when I didn't; triple award and A-level chemistry came in handy in the end!

Finally, thank you to all of my wonderful family and friends - epecially my amazing mum and incredibly supportive boyfriend - for their love, patience, and kindness throughout my completion of this project. And a special thank you to Lia, for sharing this PhD journey with me from day one.

Author's Declaration

I, Bianca Paris, declare that this thesis titled 'Investigating the Role of Exercise-Induced Circulating Extracellular Vesicles in Adult Myogenesis and Neurogenesis' and submitted for assessment is an original work of my own. Any works of other authors used within this thesis or the work presented in it are properly acknowledged. A list of the references employed is included.

Abstract

Physical activity brings about a widespread physiological response and elicits the beneficial adaptation of several tissues and organs. Furthermore, regular participation in physical activity reduces the risk of developing major non-communicable diseases such as cardiovascular disease, diabetes, cancer, osteoporosis, and dementia. Two important processes known to occur following physical activity are adult myogenesis and adult neurogenesis; both of which involve the activation and proliferation of specialised tissue-resident stem cells, which subsequently integrate into the existing tissue by differentiating into mature functional cells. The molecular mechanisms regulating these processes following exercise are poorly understood to date. A possible contributing mechanism is the release of extracellular vesicles into the circulation during exercise: in many physiological and pathological conditions these vesicles carry functional cargo molecules which are protected from degradation in the circulating milieu by a robust lipid bilayer, enabling them to transfer signals over long distances and generate phenotypic changes in recipient cells. The origin and functional significance of circulating extracellular vesicles remain virtually unexplored in the context of physical activity and adult myogenesis or neurogenesis. This project therefore aimed to enrich and count small circulating extracellular vesicles from healthy rested and exercised volunteers, and to assess their effects on recipient muscle and neural stem cell proliferation and differentiation. Potential mechanistic actions were also explored by proteomic analyses.

The number of circulating extracellular vesicles did not increase following moderate intensity cycling exercise, but the proliferation of myoblasts treated with these vesicles did. Moreover, proteomic analysis of myoblasts treated with post-exercise vesicles revealed an increase in several post-translational modifications indicative of ERK1/2 and Akt pathway activation. Proliferating neural stem cells treated with plasma vesicles adhered to the culture surface in chain formations: potentially a sign of stem cell migration and the onset of differentiation. Differentiating neural stem cells treated with post-exercise plasma vesicles exhibited increased commitment to a neuronal fate over other (glial) neural cell types. Mass spectral analysis of the circulating extracellular vesicles confirmed enrichment of vesicle-associated proteins, but

also hinted at contamination with other blood components such as lipoproteins and plasma proteins which impeded identification of any vesicle cargo increased by exercise. Methods used to enrich small extracellular vesicles from human plasma were consequently evaluated for their ability to separate these vesicles from other plasma components, to help shed light on which molecules might mediate changes in stem cell behaviour following physical activity.

The work presented in this thesis suggests that exercise-induced circulating extracellular vesicles could play a role in mediating myoblast proliferation and neural stem cell migration processes, plus encourage commitment of neural stem cells to a neuronal fate. In the case of myoblasts, extracellular vesicles appear to be acting via ERK1/2 and Akt pathways to promote cell proliferation following exercise. Future technological advancements in separating plasma EVs from other blood components such as lipoproteins may allow subsequent work to further tease apart their origin and mechanistic action.

Contents

1 Introduction **1**

1.1 Physical Activity . . . 1

1.1.1 Physiological Benefits and Health Outcomes . . . 1

1.1.2 Recommending and Prescribing Exercise . . . 1

1.1.3 Physical Activity, Skeletal Muscle, and the Brain . . . 2

1.2 Extracellular Vesicles . . . 3

1.2.1 A Brief History . . . 3

1.2.2 Nomenclature . . . 4

1.2.3 Cargo . . . 6

1.2.4 Plasma EVs . . . 10

1.2.5 Extracting EVs from Plasma . . . 11

1.3 Skeletal Muscle . . . 14

1.3.1 Architecture and contraction . . . 14

1.3.2 Adult Myogenesis . . . 15

1.4 Brain . . . 18

1.4.1 Architecture . . . 18

1.4.2 Adult Neurogenesis . . . 18

1.4.3 Exercise training and brain function . . . 21

1.4.4 Exercise training and adult neurogenesis . . . 21

1.5 Secreted Factors . . . 22

1.5.1 Secreted Factors and Adult Myogenesis . . . 22

1.5.2 Secreted Factors and Adult Neurogenesis . . . 23

1.5.3 Exercise Factors . . . 23

1.5.4 Extracellular Vesicles as Novel Exercise Factors . . . 24

1.6 Project Aims . . . 25

2 Materials and Methods **29**

2.1 Introduction . . . 29
2.2 Chemicals and Reagents . . . 29
2.3 Cell Culture . . . 31
2.3.1 Description of Cell Lines and Primary Cells . . . 31
2.3.2 Maintenance and Subculturing . . . 31
2.3.3 Resazurin Cell Viability Assay . . . 34
2.3.4 BrdU Incorporation Assay . . . 34
2.3.5 Coating of Culture Surfaces . . . 35
2.4 Immunocytochemistry . . . 35
2.4.1 BrdU . . . 35
2.4.2 Myosin Heavy Chain . . . 36
2.4.3 GFAP, MAP2 and Tuj1 . . . 36
2.5 Microscopy . . . 37
2.5.1 Fluorescent Microscopy . . . 37
2.5.2 Transmission Electron Microscopy . . . 37
2.6 Image Analysis . . . 37
2.6.1 Automated Nuclei Counts . . . 38
2.6.2 Manual Cell Counts . . . 38
2.7 Fractionation of Whole blood and Platelet Depletion of Plasma . . . 38
2.8 Enriching EVs from Human Plasma . . . 39
2.8.1 Differential Centrifugation . . . 39
2.8.2 Size Exclusion Chromatography . . . 39
2.8.3 Polymer Precipitation . . . 40
2.9 Nanoparticle Tracking Analysis . . . 40
2.10 EV Fluorescent Labelling . . . 40
2.11 Protein Extraction and Quantification . . . 41
2.11.1 Protein Extraction . . . 41
2.11.2 Protein Quantification . . . 41
2.12 Western Blotting . . . 42

2.13 Dot blot Assays . . . 42

3 Circulating Vesicles and Adult Myogenesis 47

3.1 Introduction . . . 47

3.1.1 Background . . . 47

3.1.2 Aims and Objectives . . . 47

3.2 Establishing In vitro Models of Myoblast Proliferation and Differentiation . . . 48

3.2.1 Experiment Rationale . . . 48

3.2.2 Methods . . . 49

3.2.3 Results . . . 52

3.3 Enriching and Counting EVs from Pre- and Post-Exercise Plasma . . . 55

3.3.1 Experiment Rationale . . . 55

3.3.2 Methods . . . 55

3.3.3 Results . . . 57

3.4 Treating Myoblast Proliferation and Differentiation Models with Plasma EVs . 61

3.4.1 Experiment Rationale . . . 61

3.4.2 Methods . . . 61

3.4.3 Results . . . 62

3.5 Visualising C2C12 Uptake of plasma EVs . . . 65

3.5.1 Experiment Rationale . . . 65

3.5.2 Methods . . . 65

3.5.3 Results . . . 66

3.6 Treating Myoblast Proliferation Model with Other Plasma Components . . . 66

3.6.1 Experiment Rationale . . . 66

3.6.2 Methods . . . 67

3.6.3 Results . . . 67

3.7 Treating Primary Human Myoblasts with Plasma EVs . . . 69

3.7.1 Experiment Rationale . . . 69

3.7.2 Methods . . . 69

3.7.3 Results . . . 69

3.8 Discussion . . . 70
3.8.1 Discussion of Results . . . 70
3.8.2 Experimental Limitations . . . 72

4 Circulating Vesicles and Adult Neurogenesis 79
4.1 Introduction . . . 79
4.1.1 Background . . . 79
4.1.2 Aims and Objectives . . . 79
4.2 Treating Neural Stem Cell Proliferation and Differentiation models with Plasma EVs . . . 80
4.2.1 Experiment Rationale . . . 80
4.2.2 Methods . . . 81
4.2.3 Results . . . 83
4.3 Discussion . . . 87
4.3.1 Discussion of Results . . . 87
4.3.2 Experimental limitations . . . 90

5 Investigating Mechanisms of Action 95
5.1 Introduction . . . 95
5.1.1 Background . . . 95
5.1.2 Aims and Objectives . . . 95
5.2 Proteomic Profiling of Plasma EVs . . . 95
5.2.1 Rationale . . . 95
5.2.2 Methods . . . 96
5.2.3 Results . . . 97
5.3 Proteomic Analysis of Myoblasts Treated with Plasma EVs . . . 104
5.3.1 Rationale . . . 104
5.3.2 Methods . . . 105
5.3.3 Results . . . 105
5.4 Discussion . . . 106

5.4.1 Discussion of Results . . . 106
5.4.2 Experimental Strengths and Limitations . . . 112

6 Evaluating Methods of Circulating Vesicle Enrichment 117

6.1 Introduction . . . 117
6.1.1 Background . . . 117
6.1.2 Aims and Objectives . . . 117
6.2 Platelet Depletion of Plasma . . . 118
6.2.1 Experiment Rationale . . . 118
6.2.2 Methods . . . 118
6.2.3 Results . . . 119
6.3 EV Retention and Plasma Protein/Lipoprotein Contamination . . . 121
6.3.1 Experiment Rationale . . . 121
6.3.2 Methods . . . 121
6.3.3 Results . . . 122
6.4 Treating C2C12 Proliferation Model with SEC Plasma EVs . . . 127
6.4.1 Experiment Rationale . . . 127
6.4.2 Methods . . . 127
6.4.3 Results . . . 127
6.5 Discussion . . . 128
6.5.1 Discussion of Results . . . 128

7 Discussion & Future Directions 135

7.1 Summary of Key Findings . . . 135
7.2 Discussion and Future Work . . . 138
7.2.1 Sample Size and Exercise Interventions . . . 138
7.2.2 Blood Collection and Processing . . . 140
7.2.3 Enrichment and Characterisation of Plasma EVs . . . 141
7.2.4 *In vitro* Models of Myogenesis and Neurogenesis . . . 143
7.2.5 Supporting Literature . . . 146

7.2.6 Results in Context 146

Appendices **194**

A Participant Demographics **195**

A.1 Participant Demographics 196

B Mycoplasma Testing **197**

B.1 Mycoplasma Testing 197

C Power Estimation **198**

C.1 Power Estimation 198

D Proteomic Data **199**

D.1 Spectral analysis of pre- and post-exercise plasma EVs 200

D.2 Pathways analysis of proteins increased in post-exercise EVs 206

D.3 Enrichment of Cellular Components in All Plasma EVs 208

D.4 Enrichment of Biological Processes in post-exercise EVs 210

D.5 Protein Modifications in Mouse Myoblasts Treated with Pre- and Post-Exercise EVs 214

List of Figures

1.1 Subpopulations of extracellular vesicles 6
1.2 Architecture of human skeletal muscle 15
1.3 Schematic representation of adult myogenesis 17
1.4 Schematic representation of adult neurogenesis 20

3.1 Schematic representation of myoblast proliferation model 50
3.2 Schematic representation of myoblast differentiation model 51
3.3 Myoblast proliferation model: Total cell number, BrdU incorporation, and resazurin reduction of C2C12 cells 53
3.4 Myoblast differentiation model: Myoblast fusion index of C2C12 cells at days 0-7 of differentiation 54
3.5 Detection of protein markers in EV samples 58
3.6 Electron microscopy of plasma EVs 58
3.7 Number of EVs enriched from plasma of rested and exercised individuals 59
3.8 Size distribution of EVs enriched from plasma of rested and exercised individuals 60
3.9 Effect of pre- and post-exercise EVs on myoblast proliferation 63
3.10 Effect of pre- and post-exercise EVs on myoblast differentiation 64
3.11 Effect of pre- and post-exercise EVs on myoblast differentiation - normalised EV number 65
3.12 Plasma EV uptake by C2C12 cells 66
3.13 Effect of EV-depleted plasma on myoblast proliferation 68
3.14 Effect of pre- and post-exercise EVs on primary human myoblast proliferation . 70

4.1 Neural stem cell proliferation and differentiation models 80
4.2 SVZ and DG neurospheres cultured with plasma EVs 83
4.3 SVZ and DG neurospheres cultured with plasma EVs 84
4.4 Example images of EV-treated neural stem cell staining and morphology 85

4.5 Effect of pre- and post-exercise EVs on neural stem cell Fate Commitment . . 86

5.1 Volcano plot of significance vs protein fold change between pre- and post-exercise EVs 100
5.2 GO-terms analysis of all proteins detected in plasma EVs. 101
5.3 Genome-wide overview of pathway analysis results 103
5.4 HPA tissue enrichment of proteins increased in post-exercise EVs 104
5.5 Phosphorylation of proliferation-associated proteins in myoblasts incubated with plasma EVs 106
5.6 Schematic representation of cellular proliferation pathways assessed by PathScan assay 110

6.1 Platelet markers in platelet rich vs platelet depleted plasma 120
6.2 Optimisation of SEC to enrich EVs from human plasma 123
6.3 Particle retention and protein contamination of plasma EVs enriched by different methods 124
6.4 Lipoprotein contamination of plasma EVs enriched by different methods 125
6.5 Transmission electron microscopy of particles enriched by different methods . . 126
6.6 Proliferation of C2C12s treated with SEC-enriched plasma EVs and plasma proteins 128

7.1 Schematic representation of exercise-mediated tissue crosstalk 149

B.1 Mycoplasma testing of C2C12 cells 197

C.1 Power estimation for experimental biological replicates 198

List of Tables

2.1 General Chemicals and Reagents - Sources and Abbreviations Used 29
2.2 Cell Culture Solutions and Media 30
2.3 Primary Antibodies, Techniques & Dilutions 43
2.4 Secondary Antibodies, Techniques & Dilutions 43

5.1 Plasma EV proteins increased by exercise (fold change >2), sorted by p-value . 99
5.2 Pathways associated with ApoA-4, GSN, F5 and Serpina4, detected using Reactome (v67) software, and sorted by p-value. 102

A.1 Participant Demographics 196

D.1 Plasma EV proteins increased or decreased with exercise 200
D.2 Pathways enrichment in proteins significantly increased in post-exercise EVs . . 206
D.3 Cellular component GO terms enrichment in plasma EV proteins 208
D.4 Biological process GO terms enrichment of proteins increased in post-exercise EVs. 210
D.5 Protein modifications antibody array - raw data 214

Nomenclature

AHN Adult hippocampal neurogenesis, page 21

Akt Protein kinase B, page 110

Alix ALG-2 interacting protein X, page 5

AMPKα AMP-activated protein kinase, page 111

ApoA-4 Apolipoprotein A4, page 98

ASCM American College of Sports Medicine, page 1

BBB Blood brain barrier, page 90

BDNF Brain-derived neurotrophic factor, page 22

BrdU Bromodeoxyuridine, page 21

BSA Bovine serum albumin, page 30

CSF Cerebrospinal fluid, page 23

DC Differential centrifugation, page 12

DCX Neuronal migration protein doublecortin, page 19

DG Dentate gyrus, page 18

DMEM Dulbecco's modified eagle medium, page 30

DNA Deoxyribonucleic acid, page 8

DPBS Dulbecco's Phosphate buffered saline, page 30

DSHB Developmental Studies Hybridoma Bank, page 43

DTT Dithiothreitol, page 30

ERK Extracellular-signal-regulated kinase, page 111

ESCRT Endosomal sorting complexes required for transport, page 4

EV Extracellular vesicle, page 3

F5 Coagulation factor 5, page 98

GFP Green fluorescent protein, page 7

GO Gene ontology, page 97

GSN Gelsolin, page 98

HBSS Hanks' balanced salt solution, page 32

HCl Hydrochloric acid, page 30

HDL High density lipoprotein, page 121

HGF Hepatocyte growth factor, page 22

HPA Human Protein Atlas, page 97

HRP Horseradish peroxidase, page 30

HSC70 Heat shock cognate 71 kDa protein, page 112

HSkMC human skeletal muscle cell, page 31

HSP70 Heat shock protein 70, page 8

IGF-1 Insulin-like growth factor 1, page 23

LDL Low density lipoprotein, page 121

LFQ label-free quantitation, page 96

LIF Leukemia inhibitory factor, page 22

MFI Myoblast fusion index, page 51

MHC Myosin heavy chain, page 17

miRNA Micro-RNA, page 7

MRF Myogenic regulatory factor, page 16

MRF4 Myogenic regulatory factor 4, page 16

mRNA Messenger RNA, page 7

mTOR Mammalian target of rapamycin, page 110

mTORC1 mTOR complex 1, page 110

MVB Multivesicular body, page 4

Myf5 Myogenic factor 5, page 16

MyoD Myogenic differentiation protein, page 16

MyoG Myogenin, page 16

NeuN Neuronal nuclei antigen, page 19

NSC Neural stem cell, page 18

OB Olfactory bulb, page 88

Pax7 Paired box 7, page 16

PBS Phosphate buffered saline, page 30

PDGF Platelet derived growth factor, page 23

PDP Platelet-depleted plasma, page 39

PEG Polyethylene glycol, page 11

PFA Paraformaldehyde, page 30

PP Polymer precipitation, page 117

PRAS40 Proline-rich AKT1 substrate 1, page 110

RIPA Radioimmunoprecipitation assay, page 30

RNA Ribonucleic acid, page 7

RNase Ribonuclease, page 7

S6K Ribosomal S6 kinase, page 111

SDS Sodium dodecyl sulfate, page 30

SEC Size exclusion chromatography, page 12

SERPINA4 Serpin family A member 4, page 98

SVZ Subventricular zone, page 18

TBS Tris buffered saline, page 30

TGF-β Transforming growth factor-β, page 22

TGS Tris-glycine-sodium dodecyl sulfate, page 30

TNF-α Tumour necrosis factor-α , page 23

TSG101 tumour susceptibility gene 101, page 5

TuJ1 β-III-Tubulin, page 19

UA Uranyl acetate, page 30

VEGF Vascular endothelial growth factor, page 23

VLDL Very low density lipoprotein, page 13

Chapter 1

Introduction

1.1 Physical Activity

1.1.1 Physiological Benefits and Health Outcomes

Physical activity, defined as "any bodily movement produced by skeletal muscles that requires energy expenditure" (Caspersen et al., 1985), is an integral aspect of human life that positively influences overall health (reviewed by Bamman et al., 2014). An extensive and continually growing body of research describes that physical activity leads to a striking array of physiological benefits in men and women: when performed on a regular basis, physical activity leads to beneficial changes in bone and skeletal muscle mass (Dalsky et al., 1988), blood pressure (Duncan et al., 1985), blood lipid profiles (Haskell, 1986), immune function (Matthews et al., 2002), and insulin sensitivity (Koivisto et al., 1986; Poehlman et al., 2000). Moreover, a physically active lifestyle enhances feelings of well-being and quality of life (Pasco et al., 2011) and improves cognitive function (Sibley and Etnier, 2003; Colcombe and Kramer, 2003). Physical activity can delay all-cause mortality, and is a powerful preventative measure for over 25 chronic non-communicable medical conditions including cardiovascular disease, diabetes, cancer, obesity, osteoporosis, depression and anxiety (Greist et al., 1979; Broocks et al., 1998; Warburton et al., 2006, 2010; Warburton and Bredin, 2017). In accordance with this knowledge, a lack of regular physical activity has been identified by the World Health Organisation (WHO) as the fourth leading risk factor for global mortality (WHO, 2009), and increases the risk of developing type 2 diabetes (Tuomilehto et al., 2001), cardiovascular disease (Nocon et al., 2008), colon and breast cancer (Monninkhof et al., 2007; Wolin et al., 2009), dementia (Rovio et al., 2005) and depression (Paffenbarger Jr et al., 1994).

1.1.2 Recommending and Prescribing Exercise

In 2012, the American College of Sports Medicine (ACSM) announced that "Exercise is Medicine" (ACSM, 2012), and launched a global campaign urging physicians to assess and prescribe exercise: the planned, repetitive performance of structured physical activity sessions, which aim to improve or maintain physical fitness (Caspersen et al., 1985). This initiative has

however been difficult to implement; though the many health benefits of physical activity are irrefutable, the exact mechanisms by which exercise causes them are quite poorly understood, and questions regarding the type, amount, and intensity of physical activity that should be performed for optimal health remain unanswered. Determining an appropriate 'dose' of exercise is particularly challenging in the context of disease, as patients who may benefit from participating in regular physical activity often present with specific needs or limitations which require consideration (ASCM, 2013). International recommendations for regular physical activity have therefore varied greatly over the years (Powell et al., 2011), and will likely continue to do so as our understanding of exercise physiology evolves. Several large cohort and epidemiologic studies of healthy populations have determined a minimal threshold of energy expenditure (1000 kilocalories/week) that should be met to achieve beneficial health outcomes (reviewed by Oguma et al., 2002), and accordingly current international guidelines advise a minimum of 150 minutes of moderate-to-vigorous intensity physical activity per week for healthy adult populations (WHO, 2018) and some clinical populations (Colberg et al., 2016). At present it is estimated that globally 1 in 4 adults are not meeting these targets (WHO, 2018); improving current understanding of how physical activity mediates physiological adaptation at the molecular level could allow for a much more targeted approach to promoting and prescribing exercise.

1.1.3 Physical Activity, Skeletal Muscle, and the Brain

The effects of physical activity on skeletal muscle and the brain are of particular interest in today's climate, as functional independence of our aging population is most negatively impacted by decreased muscle mass and impaired cognitive performance (van Dam et al., 2018). Regular participation in physical activity preserves bone and skeletal muscle mass (Kortebein et al., 2008) and reduces the risk of falling (Montero-Fernandez and Serra-Rexach, 2013) in older adults. According to a comprehensive study of over 8000 participants, older adults classified as having poor skeletal muscle strength were 50% more likely to die of all-cause mortality than those with higher skeletal muscle strength (Ruiz et al., 2008). Physical activity is also associated with a lower risk of cognitive decline in older adults: a national prospective cohort

study performed in Canada from 1991-1997 associated regular physical activity with lower risk of cognitive impairment, Alzheimers disease, and dementia of any type (Laurin et al., 2001). Some mechanisms by which physical activity affects skeletal muscle and brain tissue have been elucidated (later discussed in sections 1.3 and 1.4), however several key pieces of this complex puzzle are missing. Revealing the complete picture could significantly contribute to the treatment of musculoskeletal and mental disorders, and to improving quality of life for older adults.

1.2 Extracellular Vesicles

Extracellular vesicles (EVs) are a heterogenous group of small membrane-enclosed particles that are released by cells into their surrounding environment. Collectively they range from 30nm to 5μm in diameter, and are released by a wide variety of cell types. Though once considered solely a means of cellular waste disposal, EVs are now known to embody a novel mechanism of long distance intercellular communication, and carry functional molecules between cells.

1.2.1 A Brief History

Cell-derived vesicles were first discovered in the 1940s by Chargaff and West, in a study which demonstrated that plasma contains subcellular factors with pro-coagulative effects on blood (Chargaff and West, 1946). Over 20 years later cell-free plasma was characterised by electron microscopy, and was seen to contain small platelet-derived vesicles which were at the time termed 'platelet dust' (Wolf, 1967). Numerous small vesicles of endosomal origin were also identified in commercially obtained foetal calf serum, and described as having an electron density distinct from virus particles of a similar size (Dalton, 1975). Within a separate line of research, vesicles also of endosomal origin were isolated from the conditioned culture medium of sheep reticulocytes, and were noted to carry transferrin receptor usually found on the plasma membrane of reticulocytes (Johnstone et al., 1987). This research led to the belief that EVs may aid cellular waste disposal by providing a mechanism of transmembrane protein removal,

however in the late 1990s it was discovered that EVs carry surface molecules capable of inducing signalling in target immune cells, thus demonstrating that they not only function as cellular 'trash cans', but also as potent intercellular communication devices (Raposo et al., 1996). Decades on, scientific interest in EVs has heightened, and as a result our understanding of these entities has significantly improved. A myriad of studies have shown that diverse cell types produce EVs: in fact most, if not all, cell types secrete and incorporate them (reviewed by Raposo and Stoorvogel, 2013). We also now know that these EVs contain several different functional molecules which can be incorporated and used by recipient cells (see section 1.2.3).

1.2.2 Nomenclature

EVs can be classified into several subpopulations, each with different means of biogenesis. These are termed exosomes, microvesicles, and apoptotic bodies (Akers et al., 2013). Overlap in the size, density and surface markers of the EV subpopulations means that these characteristics alone do not clearly differentiate them (see below). Such an overlap also makes obtaining one homogenous population of EVs extremely challenging. As a result, there is current consensus in the field that the umbrella term 'extracellular vesicles' be used for any population of EVs, unless the exact mechanism of EV biogenesis can be experimentally determined for that population (Gould and Raposo, 2013).

Exosomes arise from the endocytic pathway, which dynamically facilitates the internalisation of extracellular ligands or cellular components, their recycling to the plasma membrane, and/or their cellular degradation (Gould and Lippincott-Schwartz, 2009; Klumperman and Raposo, 2014). Endosomes form within a cell via invagination of the plasma membrane, and as they mature they accumulate vesicles in their lumen: at this stage they are therefore generally termed multivesicular bodies (MVBs) (Stoorvogel et al., 1991). In most cell types the predominant fate of MVBs is to fuse with lysosomes, where they are degraded by lysosomal hydrolases. They can however also fuse with the plasma membrane, thus releasing their intraluminal vesicles into the extracellular milieu (Jaiswal et al., 2002; Ostrowski et al., 2010). Endosomal sorting complexes required for transport (ESCRT) play a functional role in exosome biogenesis. These

proteins assemble to form a multisubunit machinery that mediates scission events to form intraluminal vesicles within endosomes/MVBs. This was first inferred by the presence of two ESCRT-associated proteins, tumour susceptibility gene 101 (TSG101) and ALG-2 interacting protein X (Alix) in exosomes from several different cell types (Théry et al., 2001). Exosomes have been reported to range from 30 to ∼100 nm in diameter and bear several surface markers (see figure 1.1) such as tetraspanins (CD9 antigen, CD81 antigen, CD63 antigen), Alix, and TSG101 (Raposo and Stoorvogel, 2013).

Microvesicles are not formed by the endosomal pathway, and are instead generated by outward budding of a cell's plasma membrane into the extracellular space. It has been demonstrated that in T lymphocytes this process occurs as a result of cell surface receptor oligomerisation (Fang et al., 2007). Interestingly, EVs budding from the plasma membrane require components of the ESCRT machinery to do so, which has historically led to their misidentification as exosomes (Booth et al., 2006). Microvesicles carry cytoplasmic contents and also bear tetraspanin surface markers, donated by the cell of origin's plasma membrane (see figure 1.1), and are generally larger than exosomes, ranging from 100 to 1000 nm in diameter (Muralidharan-Chari et al., 2009).

Apoptotic bodies are produced by dying cells when increased contractility of their actin cytoskeleton causes the plasma membrane to 'bleb' or bulge outwards (Charras et al., 2005). These bulges can dissociate entirely from the cell of origin, taking a portion of cytoplasm and organelles with them. Apoptotic bodies therefore also have cytoplasmic contents and bear tetraspanin surface markers (see figure 1.1). They are very diverse in diameter, ranging from 50 to 5000 nm (Hristov et al., 2004; Simpson et al., 2012).

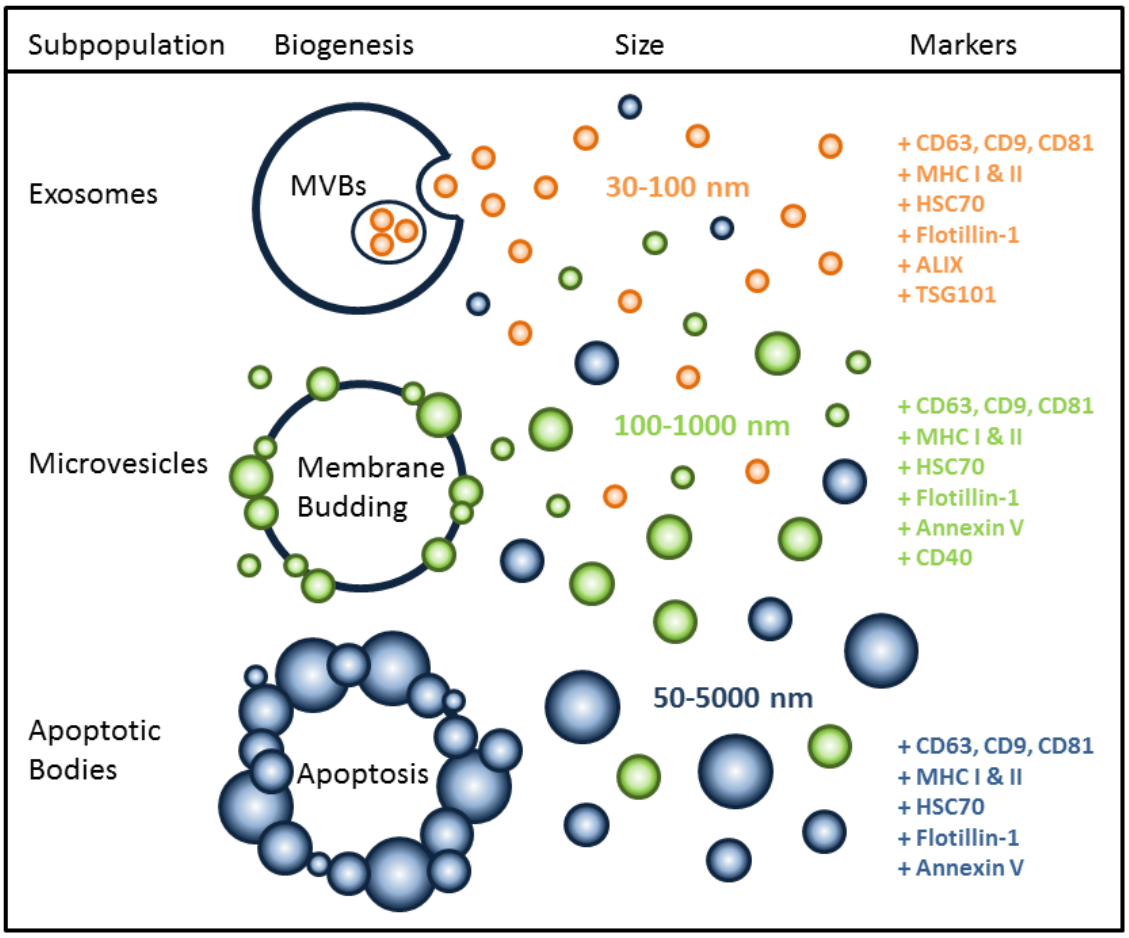

Figure 1.1: overview of the subpopulations of extracellular vesicles: biogenesis, size, and markers. Despite having different means of biogenesis, exosomes, microvesicles, and apoptotic bodies all have overlapping sizes and characteristic markers. This makes separating individual subpopulations of extracellular vesicles challenging.
ALIX, ALG-2-interacting protein X; CD, cluster of differentiation; HSC, heat shock cognate, MHC, major histocompatibility complex; MVB, multivesicular body; TSG, tumour susceptibility gene.

1.2.3 Cargo

EVs serve as mediators of intercellular communication by shuttling functional proteins, nucleic acids, and bioactive lipids from donor cells to recipient cells. Research to date suggests that EV cargo can exert biological effects on recipient cells via two main mechanisms:

a) Proteins and bioactive lipids on the EV surface directly activate recipient cell surface receptors

b) Cargo contained inside EVs are released into recipient cells via merging of the EV and recipient cell plasma membranes, or via endocytosis of the EV by the recipient cell.

EV cargo is effectively a small sampling of the donor cell's interior, with observed enrichment of certain proteins and RNAs: this suggests that cargo is at least in part actively sorted and packaged into EVs, though exactly how this sorting and packaging occurs is yet to be elucidated.

Nucleic Acids

EVs carry a multitude of RNAs and RNA fragments, predominantly less than 700 nucleotides long (Batagov and Kurochkin, 2013). The RNA species most extensively studied in EVs are messenger RNAs (mRNAs) and micro-RNAs (miRNAs) (Baj-Krzyworzeka et al., 2006; Mittelbrunn et al., 2011), however EVs also contain long non-coding RNA, piwi-interacting RNA, ribosomal RNA, and fragments of transfer RNA, vault RNA and Y RNA (Huang et al., 2013; Bellingham et al., 2012). There is currently great variability in the reported proportions of different RNA species present within EVs, likely caused by differences in EV source and the methodology used to obtain data (Mateescu et al., 2017).

Transfer of RNA-containing EVs from one cell to another can result in changes in recipient cell RNA and protein expression. Early experimental evidence that EVs transfer intact functional mRNA to recipient cells was performed by Ratajczak et al. (2006), who treated murine bone marrow mononuclear cells with EVs derived from embryonic stem cells enriched in *Oct4* mRNA, and demonstrated an increase of Oct4 protein expression in the bone marrow cells. Treating the EVs with ribonuclease (RNase) before adding to recipient cells abolished this effect. Similar findings in other cell types soon followed, one particularly elegant example arising from the work of Deregibus et al. (2007). They generated green fluorescent protein (*GFP*) mRNA expressing cells that produced EVs with no detectable levels of the protein, and demonstrated that recipient endothelial cells started to express GFP protein after incubation with these EVs. Moreover, the act of selectively disposing of specific RNA molecules inside EVs could also serve as a rapid means of regulating gene expression during cellular processes such as immune cell activation (Ostenfeld et al., 2014). At present it is difficult to determine the extent to which

individual EV mRNAs contribute to the effects observed in recipient cells, or to distinguish between effects generated by mRNAs and by non-coding RNAs that are also abundant in EVs. It is also unclear what proportion of EV RNA consists of intact mRNA which can be translated into functional protein, versus mRNA fragments that may instead play regulatory roles (Huang et al., 2013).

The presence of DNA in EVs has been comparatively less explored to date, but studies thus far show that small EVs contain single-stranded DNA, double-stranded DNA, and mitochondrial DNA (Guescini et al., 2010; Thakur et al., 2014; Waldenström et al., 2012). Small EVs stained for DNA have been observed in the cytosol and nuclei of recipient fibroblasts (Waldenström et al., 2012). Furthermore, tumour cell-derived EVs carry DNA that reflects the genetic status of the parental cells, for example an amplification of the *c-myc* mutation (Balaj et al., 2011). The physiological significance of DNA cargo in EVs is currently unexplored and whether the amounts of DNA found in EVs are sufficient to induce any meaningful physiological effects in *vivo* remains debated.

Proteins

EVs are most abundant in cytoskeletal, cytosolic, heat shock, and plasma membrane proteins. As previously discussed in section 1.2.2, proteins enriched in EVs that specifically reflect vesicle localisation, cellular origin and biogenesis/secretion are often used as characterisation markers (Gonzales et al., 2009), though they are not necessarily specific to EVs or to different EV subpopulations. These marker proteins include tetraspanins (CD9, CD63, and CD81), major histocompatibility complex molecules, and cytosolic proteins such as heat shock protein 70 (HSP70), Tsg101, and Alix (Witwer et al., 2013). It is assumed that some EV-shuttled proteins are embedded in or attached to the EV membrane whereas others are contained within their cytosolic interior; however, accurate identification of interior vs exterior EV proteins remains a work in progress in the field. In terms of EV function, protein ligands found on the EV surface have been proposed to bind the surface receptors of recipient cells and therefore initiate signalling cascades traditionally associated with direct cell-cell communication, thus allowing such communication to occur over long distances (reviewed by Simons and Raposo,

2009). Alternatively EVs may also deliver receptor proteins themselves, allowing recipient cells to receive new stimulatory or inhibitory signals (Harrison et al., 2014). EVs can shuttle transcription factors and therefore alter the rate of recipient cell gene transcription to modify fundamental cellular processes such as growth, division, migration, organization, and cell death (Ung et al., 2014). Incorporation of EV-associated growth factors and chemokines can also direct these processes via stimulation of major signalling cascades in recipient cells (Fitzgerald et al., 2018).

Lipids

EVs are enriched in several lipids which play a role in their biogenesis and function (Record et al., 2014). Enrichment of lipids such as cholesterol and sphingolipids provides EV membranes with a structural rigidity that may contribute to the resilience they exhibit in different extracellular environments. EVs also contain bioactive lipids which can be transferred between cells or activate recipient cell surface receptors such as growth factor receptors (Coskun et al., 2011). Like other cargo molecules, lipids are thought to be specifically sorted into EVs (reviewed by Simons and Sampaio, 2011).

Carbohydrates

Comparative to protein, nucleic acid and lipid EV cargo, investigation into EV-associated carbohydrates is scarce. Carbohydrate structures are found conjugated to EV lipids and proteins as glycans or as repeating glycosaminoglycan chains. Glycans are important structural components which play roles in cellular recognition, and are also involved in energy storage, protein trafficking and folding, and molecular recognition events (Varki and Lowe, 2009). Aberrant glycosylation can disrupt these essential functions and can therefore aid the progression of diseases such as cancer (Dube and Bertozzi, 2005). Microarray studies have shown that EVs bear highly glycosylated epitopes distinguishable from their parental cells (Batista et al., 2011). Moreover, different types of EVs carry distinct glycosylation patterns that might influence their uptake by target cells (Escrevente et al., 2011).

Metabolites

A selection of small cytosolic metabolites is enriched in EVs. Analysis of these metabolites could reveal dynamic changes in metabolism that occur downstream of genetic and proteomic regulation (Wei et al., 2014). Puhka et al. (2017) profiled over one hundred polar metabolites in urinary EVs and platelet EVs, along with the original source urine and platelet concentrates. They were able to divide the commonly detected metabolites into five classes: organic acids and their derivatives, nucleotides and sugars (and their derivatives), carnitines, vitamin B/related metabolites, and amines. Though overlap was observed within the metabolite profiles of urine, platelets, and their EVs, each group also contained unique metabolites. EVs from both sources were rich in metabolites involved in nucleic acid metabolism and the urea cycle.

1.2.4 Plasma EVs

Just as EVs are produced by many cell types, they are found in many biofluids including blood, urine, saliva, amniotic fluid, and even tears (reviewed by Jin et al., 2016). Biofluid EVs originate from a mixture of sources, including cells found in the fluid itself and/or cells from tissues the biofluid comes into regular contact with. EV lipid membranes encapsulate and protect their contents from degradation by enzymes also present in biofluids, allowing their cargo to travel unharmed (Skog et al., 2008; Ridder et al., 2014).

Blood EVs modulate many important physiological processes such as immune surveillance, tissue repair, stem cell maintenance, and blood coagulation (reviewed by Andaloussi et al., 2013). During pregnancy the number and origin of circulating EVs is altered (Sarker et al., 2014), and an increase in circulating EV number has also been reported in several pathologies such as obeisity, diabetes, cardiovascular disease, traumatic injury, and cancer (Diamant et al., 2002; Ueba et al., 2010; Gercel-Taylor et al., 2012; Stepanian et al., 2013; Hazelton et al., 2018). Blood EVs are therefore likely to play a role in the maintenance of healthy physiology, and indeed in the pathology of several diseases. As a result there is currently intense investigation into the use of EVs as disease biomarkers and prognostic indicators. The protein and RNA content of plasma-derived EVs have been noted to change in different pathophysiological states (Sato et al., 2016; Li, Li, Zhou, Liu, Liu, Li and Chen, 2017; Sun

et al., 2017): many studies have therefore proposed the clinical application of nucleic acid and protein profiles from blood EVs in diagnosis; however this research is still very much in its infancy. It has been proposed that studies of blood EVs should focus on those extracted from plasma rather than serum, since blood clotting could cause EV release in serum after a blood sample has been collected (Wolf, 1967; Ayers et al., 2011; Lacroix et al., 2012). A large proportion ($\sim$25%) of plasma EVs are reported to be positive for platelet-specific markers (Vagida et al., 2016). All other plasma EVs are thought to derive from a wide variety of cell types exposed to the blood as it circulates: larger EVs found in the peripheral blood may also originate from erythrocytes and white blood cells (Nieuwland et al., 2000), however the cellular origin of small EVs found in the peripheral blood is still unclear.

1.2.5 Extracting EVs from Plasma

As discussed in section 1.2.2, obtaining a homogeneous subpopulation of EVs is challenging due to overlap in EV size and markers, and this is further complicated by the presence of non EV-associated proteins and lipoproteins in human plasma (Karimi et al., 2018). Currently, there are no standardised protocols for isolation of EVs from plasma. Commonly used EV enrichment methods and their suitability for plasma EVs are discussed below.

Polymer Precipitation

Polyethylene glycol (PEG) is a polymer that has been used for over fifty years to concentrate and purify viruses which have similar biophysical properties to small extracellular vesicles (Albertsson and Frick, 1960). Methods using PEG to precipitate EVs simply involve mixing a concentrated stock solution of PEG into the EV-containing solution, incubating at 4 °C, and centrifuging at low speed (3000 *xg*) for 10-30 minutes. EVs can therefore be enriched very quickly and cost-effectively by PEG precipitation. PEG-enriched EV preparations contain a huge number of particles compared to other methods (Taylor et al., 2011), but when enriching EVs from blood a large proportion of these are likely to be contaminants, as PEG cannot distinguish between EVs and other particles present in solution such as plasma proteins and lipoproteins. There is also concern as to whether PEG that stays bound to the enriched EVs might interfere

with downstream analysis and applications (Mentkowski et al., 2018).

Differential Centrifugation

In the majority of EV studies, vesicles are isolated by differential centrifugation (DC) steps designed to enrich different types of EVs from solution based on their size. DC involves sequential centrifugations of increasing centrifugal force. With every step the pellet and supernatant are split, allowing the separation of smaller components each time. In general, cells and cellular debris are pelleted with centrifugal forces of 500-1000 *xg*, larger vesicles with a size of 100-800 nm are pelleted with centrifugal forces of 10,000-20,000 *xg*, and smaller vesicles with a diameter of less than 100 nm are pelleted with centrifugal forces of 100,000-200,000 *xg* (Konoshenko et al., 2018).

DC has several disadvantages. A multitude of factors can affect the efficiency of vesicle isolation including solution viscosity, temperature, centrifugation time and the type of rotor used for each centrifugation step. The greatest disadvantage when working with plasma is that plasma proteins and lipoproteins often co-sediment with EVs when using this approach (Konoshenko et al., 2018). Several additional steps have been introduced to DC protocols in an attempt to reduce contamination: one step known as "double pelleting" repeats the final centrifugation step to wash the EV pellet and therefore reduce aggregation between EVs and contaminants. However this often results in a significant loss of EVs, and it is debated whether impurities are in fact reduced by this additional wash step (Webber and Clayton, 2013). DC can be combined with density gradient centrifugation, which as the name suggests can separate particles based on their density in addition to size. This combination is the currently proposed "gold standard" for EV enrichment, but the process is time consuming, costly, and poorly reproducible in terms of EV yield. Moreover, many research groups do not have capacity to incorporate density gradient centrifugation into their protocols due to the associated costs and timings.

Size Exclusion Chromatography

Size exclusion chromatography (SEC) columns contain beads with a known pore size which trap and slow down small particles as they travel through. Particles of different sizes therefore

elute in different fractions collected from the column, with smaller particles eluting later than larger ones. SEC has been shown to perform well in separating EVs from contaminant plasma proteins and high density lipoproteins (HDLs) (Böing et al., 2014), however SEC-enriched EV fractions can still contain other lipoproteins such as chylomicrons and very low density lipoproteins (VLDLs) , which are similar in size to EVs (Karimi et al., 2018). Although the sample processing time is much shorter than differential ultracentrifugation, SEC still requires a manual aspect which may introduce user variability and impact the purity of resulting EV fractions.

Other Methods

Other less commonly used approaches for enriching biofluid EVs include ultrafiltration, immunoisolation, and microfluidic devices.

Ultrafiltration can be used to separate EVs from proteins and other macromolecules based on their size. It is relatively quick to perform, and can be employed independently or in conjunction with other techniques such as DC. Ultrafiltration may however result in non-specific binding of EVs to the filter membranes (Merchant et al., 2010), thus reducing EV yield. Although the pore size of commercially available filters is often well defined, increasing forces must be applied with decreasing pore size, which can result in the introduction of artefacts to an EV sample (Lawrie et al., 2009).

Immunoisolation uses antibody-coated magnetic or latex beads to enrich EVs by targeting marker proteins such as CD9, CD63 and CD81 (He et al., 2014). Immunoisolation has also been combined with microfluidics (discussed below), by modifying microchannel surfaces with antibodies or magnetic beads (Reátegui et al., 2018). Though immunoisolation could enable the specific enrichment of EVs with a marker of interest, there is still a poor understanding of which markers are present or absent in different EV subpopulations. The use of immunoisolation techniques to enrich EVs from complex mixtures may therefore lead to the loss of some less characterised EV populations (perhaps negative for the chosen EV marker, for example).

Further investigation is therefore required to realise the full potential of this method to selectively isolate pure or homogenous populations of EVs.

Microfluidic devices exploit the physical and chemical characteristics of liquids and gases at the microscale. They contain chambers and tunnels in which biofluid components such as EVs can become trapped as small volumes of fluids flow through (Manz et al., 1992). Portable microfluidic systems have attracted a lot of attention as they require very small sample volumes and would be particularly useful in a diagnostic setting (Gomez, 2013). Several groups have explored the possibility of using such systems to directly enrich and evaluate EVs from biofluids. Davies et al., for example, developed a microfluidic device which enriched small EVs from whole blood more efficiently than DC (81% EV retention compared with 23% for DC), and proposed that this device reduced co-purification of larger vesicles and protein aggregates (Davies et al., 2012). This technology is relatively new, but as it grows and improves, other EV features such as electric properties, shape, size and density could also be exploited in the development of customised chips.

1.3 Skeletal Muscle

1.3.1 Architecture and contraction

Skeletal muscle is the most abundant tissue of the human body, accounting for 35-45% of total body mass (Janssen et al., 2000). In addition to facilitating locomotion, skeletal muscle generates heat, stores protein reserves, and provides postural support whilst protecting internal tissues and organs. Adult skeletal muscle is made up of bundles of long multinucleated muscle cells (myofibers), each surrounded by layers of extracellular matrix (basement membrane) and connective tissue. Every myofiber has a plasma membrane (sarcolemma) which is positioned close to the basement membrane, forming a physical barrier which mediates signals between the muscle exterior, basement membrane and inner muscle cell (Gillies and Lieber, 2011). Individual myofibers are filled with a series of actin and myosin containing units known as sarcomeres,

which are surrounded by sarcoplasmic reticulum. Nerve impulses cause a wave of depolarisation across the sarcolemma which induces the sarcoplasmic reticulum to release stored calcium ions into the cytosol. This surge in cytosolic calcium exposes actin-myosin binding sites and drives the movement of actin and myosin filaments relative to one another, causing shortening of the sarcomere structure and therefore muscle contraction. Repeated binding and release of actin and myosin to generate muscle contraction is known as the cross-bridge cycle (Geeves, 1991).

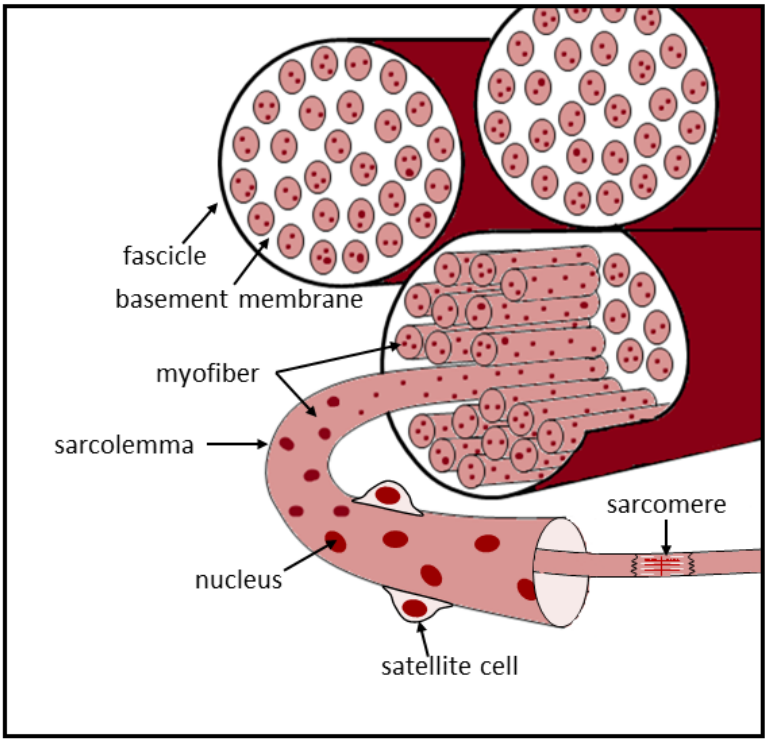

Figure 1.2: Architecture of human skeletal muscle

1.3.2 Adult Myogenesis

Physical activity requires the sustained and repeated contraction of skeletal muscle, which results in microscopic damage to myofibers (Faulkner et al., 1993). A prominent feature of skeletal muscle is its robust capacity to regenerate when such damage occurs, via a process known as adult myogenesis. This process is so efficient *in vivo* that skeletal muscle structure and function can be completely restored only a few weeks after a major injury (Studitsky,

1964). Skeletal myofibers are post-mitotic, so a local population of progenitor cells is required to create or repair myofibers. These are termed satellite cells, and are located in a niche on the surface of mature myofibers between the sarcolemma and the surrounding basal lamina (Mauro, 1961). Satellite cells are characterised by a common expression of the transcription factor paired box (Pax) 7 (Seale et al., 2000; Kassar-Duchossoy et al., 2005), and they are mitotically quiescent (G0 phase) with a low rate of metabolism and low RNA content in adult muscle (Cheung and Rando, 2013). Notch signalling maintains this quiescent state (Bjornson et al., 2012), but physical trauma and/or growth signals can quickly activate satellite cells to enter cell cycle, giving rise to progeny which proliferate as they migrate to the site of injury, differentiate, and then fuse to form new or repair existing myofibers (reviewed by Kuang et al., 2008).

Adult myogenesis is tightly associated with the serial activation of a family of muscle-specific transcription factors, known as myogenic regulatory factors (MRFs). The MRF family includes myogenic factor 5 (Myf5), myogenic differentiation protein-D (MyoD), myogenin (MyoG) and myogenic regulatory factor 4 (Mrf4), all of which are key players in orchestrating myogenic proliferation and differentiation (reviewed by Hernández-Hernández et al., 2017; Zammit, 2017). The MRF proteins contain a basic domain and a Helix–Loop–Helix motif, which together activate the transcription of many E-box-containing muscle specific genes (Weintraub et al., 1991).

Quiescent satellite cells generally express Pax7 and Myf5 proteins (Beauchamp et al., 2000; Kassar-Duchossoy et al., 2005). Approximately 3 hours following acute myoinjury, satellite cell levels of Myf5 are increased, activating them to enter cell cycle (Cooper et al., 1999). Activated satellite cells may undergo symmetric or asymmetric division, depending on the orientation of their mitotic spindle in relation to the host myofiber. Divisions parallel to the host myofiber result in the symmetric expansion of satellite cells, producing two MyoD positive 'myoblast' progeny which are committed to a myogenic lineage and destined for differentiation (Kitzmann et al., 1998). Conversely, divisions perpendicular to the myofiber give rise to two distinct cell types: one daughter cell is a myoblast ($MyoD^{+}$), whilst the other daughter cell maintains a stem cell ($MyoD^{-}$) identity and replenishes the satellite cell population (reviewed

by Kuang et al., 2008). Following several rounds of proliferation, myoblasts exit cell cycle and differentiate into mature myocytes. Levels of Pax7 in these differentiating cells begin to decline as MyoG protein is expressed, which in concert with MyoD activates transcription of several muscle specific genes (Füchtbauer and Westphal, 1992). Finally, myocytes fuse to one another to form new myofibers, expressing Mrf4 in the process (Pavlath et al., 2003). As newly formed myofibers develop, their levels of Mrf4 accumulate, as do levels of myosin heavy chain (MHC) protein which gives these cells their contractile capabilities (Kuang et al., 2008). According to the human Protein Atlas (Uhlén et al., 2015), MyoD, Myf5, Myogenin, and Mrf4 proteins and their corresponding genes are exclusively expressed by muscle cells. A series of experiments have shown that expression of these MRFs in non-muscle cells can induce muscle-specific traits such as myotube formation *in vitro* (Davis et al., 1987; Braun et al., 1989; Rhodes and Konieczny, 1989; Miner and Wold, 1990).

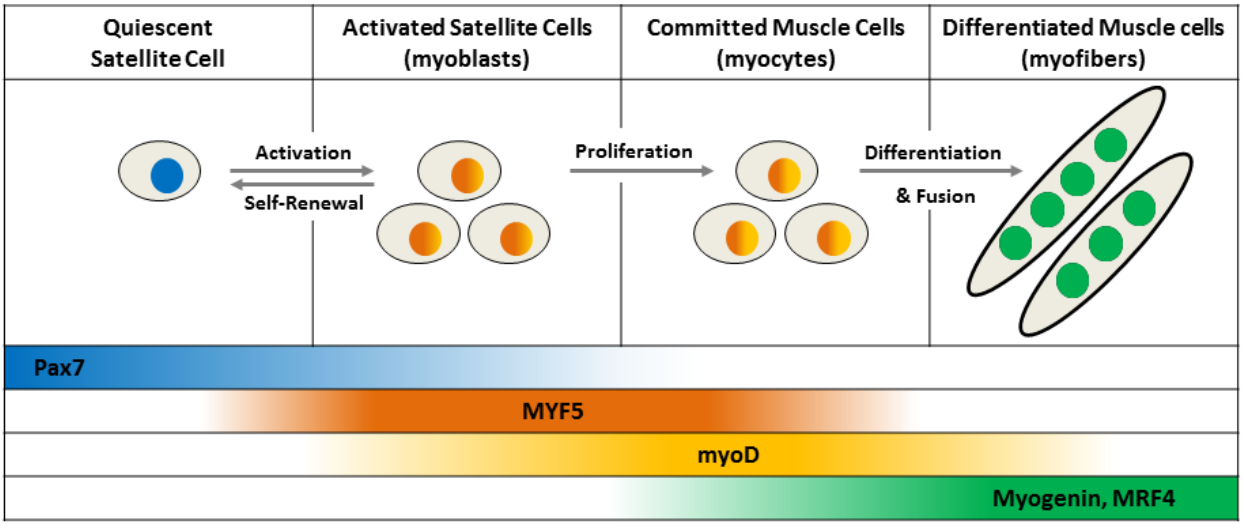

Figure 1.3: Schematic representation of adult myogenesis - stages and associated myogenic regulatory factors.
MRF4, myogenic regulatory factor 4; MYF5, myogenic factor 5; myoD, myoblast determination protein; Pax7, paired box protein 7.

1.4 Brain

1.4.1 Architecture

The brain controls all functions of the body, interprets information from the outside world, and governs intelligence, creativity, emotion, and memory. Protected within the skull, the brain is composed of the cerebral cortex, cerebellum, and brainstem (Snell, 2010). The cerebral cortex is the largest part of the brain, and is divided by a longitudinal fissure into right and left hemispheres, each of which are further divided into four lobes: frontal, temporal, parietal, and occipital. Each lobe can then be subdivided into individual structures that serve very specific functions (Snell, 2010). The brain is composed of two broad groups of cells: neurons, which are the primary signalling cells, and glial cells, which support and protect neurons, and include astrocytes and oligodendrocytes. Though glial cells outnumber neurons in some structures of the brain, neurons are considered the key players in mediating brain function (Hilgetag and Barbas, 2009).

1.4.2 Adult Neurogenesis

Neurogenesis describes the generation and development of new functional neurons. This occurs during early development to form the brain and peripheral nervous system, and to a lesser degree in the postnatal (adult) brain to maintain plasticity. Adult neurogenesis is largely restricted to two specific regions: the subventricular zone (SVZ) adjacent to each lateral ventricle (Altman, 1969), and the dentate gyrus (DG) of the hippocampus (Altman and Das, 1965). In these areas, referred to as neurogenic niches, neural stem cells (NSCs) proliferate and differentiate into new functional neurons throughout life.

Neurogenesis in the DG begins with the activation of NSCs (type-1 cells) in the subgranular zone of the dentate gyrus. These activated stem cells can divide symmetrically or asymmetrically to renew the stem cell population or to give rise to neural progenitor cells (NPCs) with a higher proliferative capacity. NPCs then differentiate through 3 stages (type-2a, 2b and type-3 cells) in which their proliferative capacity gradually decreases whilst their morphology and

protein expression become increasingly neuron specific (Filippov et al., 2003; Fukuda et al., 2003). Type-3 cells are considered to be the most differentiated of the progenitors and are also referred to as committed neuroblasts. They are characterised by expression of Neuronal migration protein doublecortin (DCX), which allows them to migrate short distances through the white matter before exiting cell cycle to mature into granule neurons (Brown et al., 2003). Maturing neuroblasts begin to extend long processes (neurites) which increase in length and complexity as the cells mature, to allow the formation of synaptic connections within the existing circuitry of the hippocampus. As this happens, neuroblast levels of DCX decrease, while levels of β-III-Tubulin (TuJ1), Microtubule-associated protein II (MAP2) and Neuronal nuclei antigen (NeuN) protein accumulate (figure 1.4 A) (Spalding et al., 2013).

Neurogenesis in the SVZ follows a similar process, whereby quiescent NSCs (type B cells) become activated to divide symetrically or asymmetrically and give rise to more NSCs or to transit-amplifying (type C) progenitor cells (Alvarez-Buylla and Garcıa-Verdugo, 2002). The type C cells in turn divide to give rise to DCX-positive neuroblasts (type A cells), which form long chains that migrate to the olfactory bulb guided by a channel of astrocytes (the rostal migratory stream). Within the olfactory bulb, these neuroblasts differentiate into NeuN-expressing granular neurons and periglomerular neurons, which integrate into the existing circuitry of the olfactory bulb (Merkle and Alvarez-Buylla, 2006; Curtis et al., 2007).

Hippocampal (DG) neurogenesis is currently of great interest due to its important role in emotions, learning, and memory, plus the striking clinical consequences of its deterioration (reviewed by Anand and Dhikav, 2012). For example, the hippocampus is the earliest and most severely affected brain structure in neuropsychiatric disorders such as dementia and epilepsy (Frisoni et al., 2010), and extensive bilateral damage to the hippocampus can result in complete inability to form and retain new memories (Clark et al., 2002). Olfactory bulb (SVZ) neurogenesis is well characterised in rodents, but its extent and functional relevance in humans remains unclear to date (reviewed by Braun and Jessberger, 2014).

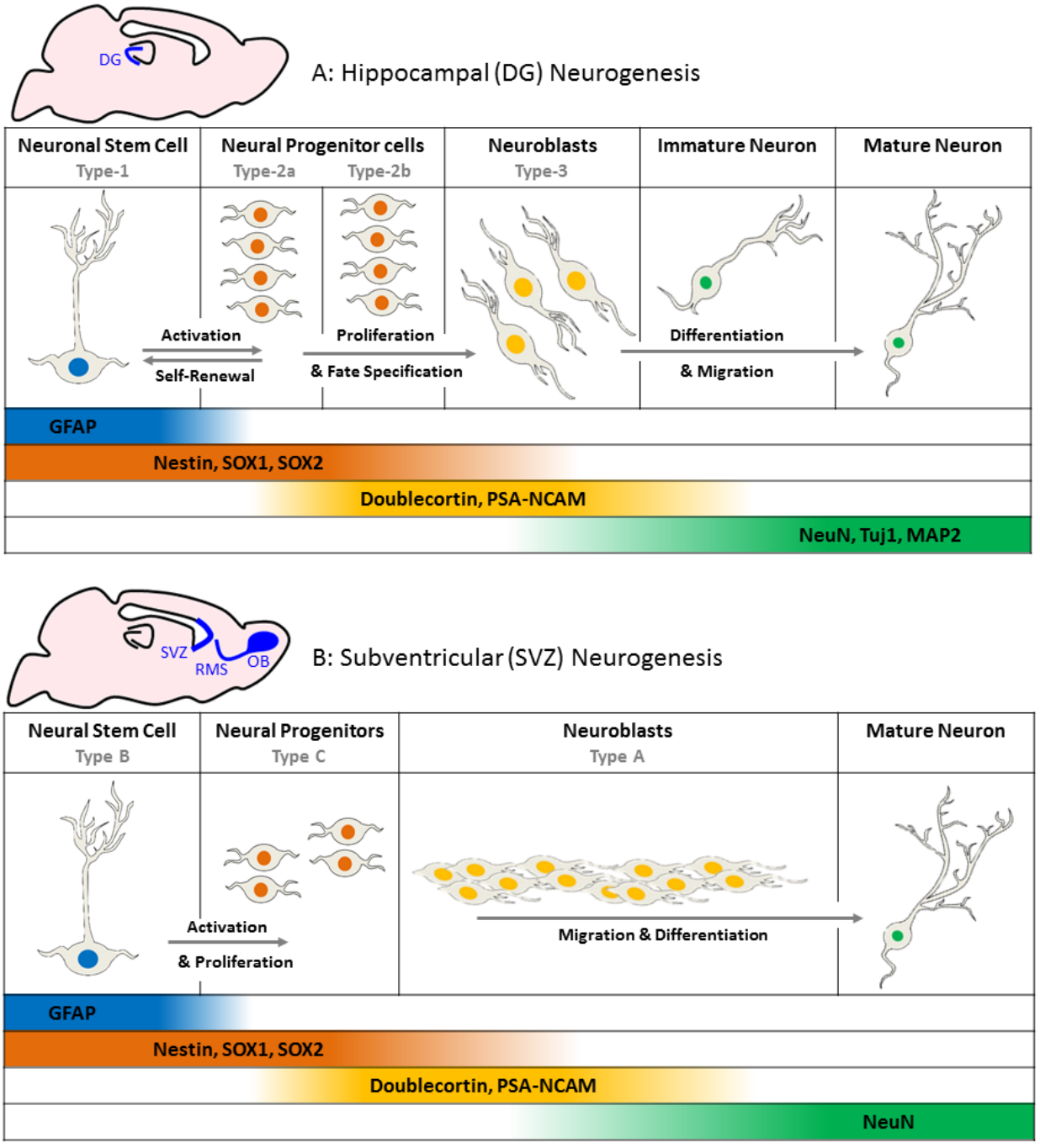

Figure 1.4: Schematic representation of adult neurogenesis in the dentate gyrus (A) and the subventricular zone (B): stages and associated markers. Adapted from Schouten et al. (2012) and Toda et al. (2018)
DG, dentate gyrus; GFAP, glial fibrillary acidic protein; MAP2, microtubule-associated protein 2; NeuN, neuronal nuclei antigen; PSA-NCAM, OB, olfactory bulb; polysialylated neural cell adhesion molecule; RMS, rostal migratory stream; SOX, sry-related HMG box; SVZ, subventricular zone; Tuj1, class III beta-tubulin 1.

1.4.3 Exercise training and brain function

The neurobiological effects of physical activity are numerous. A large body of research in animals and humans over the past decade has demonstrated that regular aerobic activity results in an array of changes affecting brain structure and function (reviewed by Erickson et al., 2015; Paillard et al., 2015). In healthy adults transient cognitive effects are induced after a single exercise session and last for up to 2 hours after physical activity (Basso and Suzuki, 2017). These effects include improvements in attention, working memory, problem solving, decision making, and information processing. When exercise training is maintained for several months these effects become persistent, and spatial memory (required for efficient navigation) is also improved (Smith et al., 2010; Basso and Suzuki, 2017). Aerobic exercise also induces short and long term effects on mood, by decreasing the biological response to acute psychological stress (Rosch, 1985) and by altering positive and negative affectivity: an individual's experience of positive and negative events (Aan het Rot et al., 2009; Krogh et al., 2011).

There are currently several hypotheses explaining how physical activity may bring about its neurocognitive effects. Firstly, exercise increases oxygen supply and angiogenesis in the brain areas required to perform cognitive tasks (Isaacs et al., 1992). Secondly, physical activity increases neurotransmitters such as serotonin and norepinephrine, which facilitate information processing following exercise (Brown et al., 1979). The hypothesis currently generating most excitement, however, is that regular physical activity promotes adult hippocampal neurogenesis (AHN), discussed below.

1.4.4 Exercise training and adult neurogenesis

In 1999, van Praag et al. (1999) elegantly demonstrated elevated levels of DG neuron proliferation and differentiation in running mice compared to sedentary mice. They achieved this using bromodeoxyuridine (BrdU); a synthetic nucleotide analog which they used to detect new nuclear DNA synthesis in the brain (Kuhn et al., 1996). BrdU labelling is now the most commonly adopted technique for studying AHN *in situ*, and has been used by several

publications to demonstrate increased AHN in rodents after exercise training (Allen et al., 2001; Persson et al., 2004; van der Borght et al., 2006). Increased AHN has been correlated in mice with increased blood flow to the dentate gyrus during exercise (Pereira et al., 2007), though exactly what causes AHN to occur following physical activity remains poorly understood. One suggestion is expression of the protein brain-derived neurotrophic factor (BDNF). Physical activity increases BDNF expression in the brain, skeletal muscle, and adipose tissue, and elevated BDNF in the hippocampus activates signalling pathways that drive exercise-dependent enhanced learning and memory formation (Vaynman et al., 2004). BDNF is also a key promoter of neuronal proliferation, differentiation, and survival in the developing brain (Hyman et al., 1991; Poo, 2001; Monteggia et al., 2004) and therefore may be involved in these cellular processes during AHN.

1.5 Secreted Factors

Secreted factors are signalling molecules that are expressed and secreted by an array of cell types under different physiological and pathophysiological conditions. The most studied secreted factors are those that enable cell-cell communication via ligand-receptor signalling. Many secreted factors are found in skeletal muscle and neuronal stem cell niches, and may be involved with the proliferation and differentiation stages of adult myogenesis and neurogenesis.

1.5.1 Secreted Factors and Adult Myogenesis

Several cytokines and growth factors are found in regenerating muscle. Factors thought to be expressed and released specifically by muscle cells are termed 'myokines', and, to name a few, include myostatin, irisin, leukemia inhibitory factor (LIF), and several interleukins (reviewed by Pedersen, 2011). Other non-muscle secreted factors such as hepatocyte growth factor (HGF) and transforming growth factor-β (TGF-β) are trapped and stored in the muscle extracellular matrix, then released or activated upon mechanical stimulation (Thomas et al., 2015). Moreover, some systemic factors are secreted by inflammatory cells that are recruited

to the site of muscle injury, such as insulin-like growth factor 1 (IGF-1), platelet derived growth factor (PDGF), and tumour necrosis factor-α (TNF-α) (Tonkin et al., 2015; Sugg et al., 2017). The precise roles of many of these proteins in satellite cell proliferation and differentiation require further exploration. To date, HGF is the only factor which has been robustly established to stimulate activation of quiescent satellite cells *in vitro* and *in vivo*, via binding of c-met receptors on the satellite cell surface (Allen et al., 1995; Tatsumi et al., 1998).

1.5.2 Secreted Factors and Adult Neurogenesis

Dynamic modulation of the neurogenic niches is aided by neurotransmitters dopamine, serotonin, and gamma-aminobutyric acid (GABA), which all influence proliferation of NSCs in the SVZ and DG (reviewed by Berg et al., 2013). Blood and cerebrospinal fluid (CSF) also contain several hormones, cytokines, and growth factors that participate in neurogenic proliferation and differentiation (Lafon-Cazal et al., 2003; Bunn et al., 2005; Zappaterra and Lehtinen, 2012). Local vasculature can supply NSCs with vascular endothelial growth factor (VEGF) and BDNF, which promote the proliferation and differentiation of NSCs, respectively (Li et al., 2006). Conversely, elevated levels of blood glucocorticoids associated with stress have been shown to lessen neurogenesis in the SVZ (Snyder et al., 2011). Transcriptome analysis of the choroid plexus (from which the CSF originates) have revealed that resident epithelial cells secrete several signalling molecules that can act either as positive (TGF-α, IGF-1, and fibroblast growth factor-2) or negative (VEGF) regulators of adult neurogenesis (Marques et al., 2009; Liddelow et al., 2012).

1.5.3 Exercise Factors

Physical activity results in disruption of homeostasis in a large number of tissues, which in the long term provokes physiological adaptations associated with improved health and wellbeing (Hawley et al., 2014). The ability of exercise to stimulate secreted factor release is therefore of great interest with regards to revealing an 'exercise factor' that mediates the benefits of physical activity. Numerous tissues including skeletal muscle (Barnett et al., 2004), liver (Hansen et al.,

2011, 2015), adipose tissue (Stanford et al., 2015), brain (Lancaster et al., 2004), and bone (Mera et al., 2016) have been shown to secrete signalling molecules during exercise, however due to the complex structure of some of the parent tissues, the relationship between local and circulating levels of these molecules remains unclear.

1.5.4 Extracellular Vesicles as Novel Exercise Factors

In addition to the well-recognised signals discussed above, a novel type of intercellular messenger has been identified in the form of EVs. We now know that EVs allow the transfer of functional molecules between cells and can therefore modify the behaviour of recipient cells (see section 1.2.3).

EVs appear to play significant roles in mesenchymal and cancer stem cell niches (reviewed by Han et al., 2016; Xu et al., 2018), however their importance in adult muscle and neuronal stem cell niches remains virtually unexplored. Aswad et al. (2016) demonstrated that culturing muscle precursor cells in EV-depleted bovine serum reduced their capacity to proliferate and subsequently differentiate compared to culturing them with whole serum. They therefore proposed that blood EVs may mediate recipient satellite cell proliferation independently of classical secreted factors. Likely due to a lack of serum use in culture, similar experiments do not appear to have been conducted with NSCs.

Research regarding the effects of physical activity on EVs in healthy populations is somewhat limited to date, however some studies have shown increases in circulating EVs following acute bouts of strenuous exercise (Frühbeis et al., 2015; Wilhelm et al., 2016; Bei et al., 2017). Although homogeneous populations of EVs can't be reliably obtained from plasma, the vast majority of these studies have focused on larger plasma EVs (pelleted by low speed centrifugation), proposed to be platelet-derived microvesicles. One example where smaller circulating EVs were examined includes the work of Frühbeis et al. (2015), in which a rapid and sustained release of small EVs (presumed to be exosomes) into the circulation was observed during the aerobic phase of cycling and treadmill running interventions. The origin of these small EVs, their cargo, and their potential physiological role has not yet been addressed.

1.6 Project Aims

Circulating EVs increase in number following acute bouts of exercise, and may function as signalling molecules in myogenic and neurogenic stem cell niches. This PhD project therefore aims to:

- Enrich and characterise EVs from the plasma of healthy participants, at rest and following an acute bout of exercise (chapter 3).
- Establish robust *in vitro* models of adult myogenesis and neurogenesis, and treat these models with plasma EVs (chapters 3 & 4).
- Identify and test cargo molecules present in pre- and post-exercise plasma EV populations which may be responsible for modifying stem cell proliferation and differentiation (chapter 4).

Chapter 2

Materials & Methods

2.1 Introduction

Several of the methods outlined in this chapter were adopted for more than one experiment. This chapter therefore outlines all standard protocols used, and additional details specific to each experiment can be found in the relevant results chapters.

2.2 Chemicals and Reagents

Table 2.1: General Chemicals and Reagents - Sources and Abbreviations Used

Item	Abb.	Notes	Supplier
1x Phosphate buffered saline	PBS		Sigma
1x Dulbecco's phosphate buffered saline	DPBS	-magnesium, -calcium	Sigma
PBS-tween	PBST	PBS + 0.05% Tween20	Made in-house
Dulbecco's Modified Eagle Medium	DMEM	High glucose	Gibco
Bovine serum albumin	BSA		Sigma
Enhanced chemilumescent reagent	ECL		Bio Rad
1x Tris buffered saline	TBS		Made in-house
TBS-tween	TBST	TBS + 0.05% Tween20	Made in-house
Dithiothreitol	DTT		Thermo
Resazurin Sodium Salt	Resazurin		Sigma
Hydrochloric acid	HCl	2N concentration	Sigma
5-Bromo-2'-deoxyuridine	BrdU		Sigma
Paraformaldehyde	PFA	4% in PBS	Sigma
Polyethylene glycol	PEG	mw 6000	
Sepharose CL-2B	Sepharose		GE Healthcare
Triton X-100	Triton X		Thermo
Uranyl acetate	UA	2% in ultrapure water	Agar Scientific
Radioimmunoprecipitation assay buffer	RIPA	Sigma	
Sodium dodecyl sulfate	SDS		Sigma
1x Tris-glycine-SDS	TGS		Sigma
Horseradish peroxidase	HRP		n/a
Ethylenediamine tetraacetic acid	EDTA		Sigma

Table 2.2: Cell Culture Solutions and Media

Solution	Components
Wash Solution	DPBS, no calcium, no magnesium
Fixing Solution	Methanol (75%) + acetic acid (25%)
C2C12 Complete Growth Medium	DMEM, 4.5g/L glucose with GlutaMAX ™ supplement + 10% foetal bovine serum (heat inactivated)
C2C12 Serum-Free Medium	DMEM, 4.5g/L glucose with GlutaMAX ™ supplement
C2C12 Differentiation Medium	DMEM, 4.5g/L glucose with GlutaMAX ™ supplement + 2% horse serum (heat inactivated)
C2C12 Freezing Medium	DMEM, 4.5g/L glucose with GlutaMAX ™ supplement + 20% Foetal Bovine Serum (heat inactivated) + 10% Dimethyl sulfoxide
C2C12 Dissociation Solution	DPBS, no calcium, no magnesium + 0.05% trypsin-EDTA
Human Myoblast Complete Growth Medium	Ham's F-10 nutrient mix + 20% foetal bovine serum (heat inactivated) + 500 U/mL penicillin + 500 ug/mL streptomycin
NSC Complete Growth Medium	Neurobasal ™ -A Medium + 1x B-27™ supplement + 1x GlutaMAX ™ supplement + 500 U/mL penicillin + 500 µg/mL streptomycin + 20ng/mL human epidermal growth factor + 20ng/mL human fibroblast growth factor
NSC Differentiation Medium	Neurobasal ™ Medium + 1x B-27 ™ supplement + 1x N-2 supplement + 1x L-glutamine + 0.2% heparin sodium + 500 U/mL penicillin + 500 µg/mL streptomycin
NSC Dissociation Solution	Accutase ®

DPBS, Dulbecco's phosphate buffered saline; DMEM, Dulbecco's Modified Eagle Medium; NSC, neural stem cell.

2.3 Cell Culture

2.3.1 Description of Cell Lines and Primary Cells

C2C12 Mouse Myoblasts

The C2C12 mouse myoblast cell line was kindly provided by Dr Susan Brown and colleagues at the Department of Comparative Biomedical Sciences, Royal Veterinary College, University of London. This cell line is an immortalised subclone of satellite cells originally obtained from the thigh of a female adult C3H mouse 70 hours after a crush injury (Yaffe and Saxel, 1977; Blau et al., 1985). C2C12 cells proliferate in high serum conditions, and readily differentiate into myotubes expressing characteristic muscle proteins in low serum conditions.

Primary Human Myoblasts

Primary human skeletal muscle cells (HSkMCs) were kindly provided by Dr Karl Morten and colleagues at the Nuffield Department of Women's & Reproductive Health, Medical Sciences Division. Cell extraction from human muscle tissue was performed by Dr Karl Morten and colleagues under ethical approval from the University of Oxford's Central University Research Ethics Committee, and in accordance with Human Tissue Authority legislation.

Primary Mouse Neural Stem Cells

Primary neural stem cells were obtained from neurogenic niches in the brains of young mice (aged P4). Mice were kindly provided by Dr Julie Davis in the Department of Physiology, Anatomy and Genetics, Oxford University. Details of primary cell isolation are included in section 2.3.2.

2.3.2 Maintenance and Subculturing

C2C12s and Primary Myoblasts

Muscle cells were cultured in the relevant complete growth medium (table 2.2) in tissue culture treated flasks and/or plates, and were maintained at 37°C and 5% CO_2 in a humidifying

incubator. They were always passaged at less than 70% confluence to avoid cell-cell contact and therefore maintain a myoblastic phenotype. To passage, cells were washed with PBS and incubated for 5 minutes with sufficient dissociation solution (table 2.2) to cover the culture surface. Once cells were rounded and floating, trypsin in the dissociation solution was inactivated with an equal volume of complete growth medium, which was washed over the culture surface several times to collect cells before transferring to a 50 mL centrifuge tube. Cells were pelleted by centrifugation at 500 *xg* for 5 minutes, and the resulting cell pellet was resuspended in complete growth medium (table 2.2 to achieve a seeding density of approximately $2x10^3$ cells/cm^2 in the new culture vessel. C2C12s were used below passage ten and primary myoblasts were used within 5 passages of receipt for all experiments.

NSCs

Mice were euthanised by CO_2 chamber before decapitation, and intact brains were removed by cutting and opening of the skull at the midline. Brains were placed in cold Hanks' balanced salt solution (HBSS, Sigma) and cut into 50 µm coronal sections with a McIlwain tissue chopper before returning to cold HBSS. Under a dissecting microscope, SVZ and DG regions were identified in the relevant brain sections and were extracted using 27G needles with as little contaminating striatum as possible. Separate tubes containing SVZ or DG pieces were briefly centrifuged (15 seconds) to collect tissue which was then cut into smaller pieces with fine Iris scissors. Tissue was then incubated in 1x Accutase solution (table 2.2) for 15 minutes, and single cell suspensions were achieved by vigorous trituration with a P200 pipette. To remove Accutase and wash the cells, 2.5 mL NSC complete growth medium without the growth factors (table 2.2) were added, and cells were centrifuged for 5 minutes at 280 *xg*, 4°C. Cells were washed in this way another two times, then adjusted to a concentration of $1x10^5$ cells/mL in NSC complete growth medium (with the growth factors) and plated at $2x10^5$ cells/well in a non-tissue culture treated six well plate. They were maintained at 37°C and 5% CO_2 in a humidifying incubator.

From their first passage onwards, primary NSCs were grown in non-tissue culture treated six well plates coated with polyheme (Sigma, P-3932) in 95% ethanol, to allow for neurosphere

formation. Passaging of NSCs was carried out twice-weekly. To do this, neurospheres and media were collected from each plate using a 10 mL pipette and transferred to a 50 mL centrifuge tube pooling all wells from the same plate. Cells were pelleted by centrifugation at 300 *xg* for 5 minutes, and then incubated with 1 mL 1x Accutase for 15 minutes at 37°C. A single cell suspension was then achieved by thorough trituration with a P200 pipette. Accutase was inactivated and washed from the cells by addition of 2.5 mL NSC complete growth medium without the growth factors (table 2.2), and cells were centrifuged at 300 *xg* for 5 minutes. Cells were washed in this way another two times, then counted and adjusted to a concentration of $1x10^5$ cells/mL in NSC complete growth medium (with the growth factors) and plated at $2x10^5$ cells/well in a non-tissue culture treated six well plate coated with polyheme. For all experiments they were used within three passages from harvesting.

Freezing and Thawing Cells

To freeze stocks of C2C12s, cells were washed, dissociated and pelleted as per section 2.3.1. Total cells pelleted from one 70% confluent T-175 flask were resuspended in 3 mL freezing medium (table 2.2) and 1 mL aliquots were transferred to labelled cryovials. Cryovials were added to a room-temperature isopropanol freezing chamber which was left at -80°C overnight before cryovials were transferred to liquid nitrogen. To thaw cell stocks, 7 mL complete growth medium (table 2.2) was added to each of two T-25 culture flasks and allowed to equilibrate at 37°C, 5% CO_2 for at least 30 minutes. Cells in freezing medium were retrieved from liquid nitrogen and thawed at 37°C for no more than 2 minutes before transferring to equilibrated growth medium (half a cryovial per flask) and returning to the incubator. Once cells had adhered to the culture surface (approx 6 hours), the medium was exchanged for fresh complete growth medium to remove all remaining DMSO. Primary cells were always used fresh and so did not require freezing or thawing.

Mycoplasma Testing

Cells were grown in a $25cm^2$ flask for 2-3 days with no medium change. Cells were then detached in their growth medium using a cell scraper, and centrifuged at 10,000 *x g* for 15

minutes to pellet cells and any floating microorganisms. The resulting pellet was resuspended in 200 µL PBS. DNA was extracted using a PureLink® Genomic DNA Kit according to the manufacturer's instructions, and eluted in 50 µL genomic elution buffer. The concentration and purity of DNA were measured with a NanoDrop™ One Spectrophotometer (Thermo Scientific), and DNA concentration was normalised to 50 ng/µL. 50 ng of DNA was then amplified using an e-Myco™ Mycoplasma PCR Detection Kit (Intron Biotechnology), following the manufacturer's instructions. PCR products of the cells, positive controls, and negative controls (provided in the kit) were run on a 2% agarose gel with SafeView Nucleic acid stain (NBS Biologicals) alongside a Quick-Load Purple 100 bp DNA Ladder (New England Biolabs). The gel was visualised using a ChemiDoc imaging system (BioRad) to examine the presence of sample control DNA (570 bp), internal control DNA (160 bp) and mycoplasma DNA (270 bp).

2.3.3 Resazurin Cell Viability Assay

Resazurin dye (150 µg/mL in dH_2O) was sterilised with a 0.22 µm syringe-driven filter. A 10% volume of filtered resazurin was then added to the culture medium to give 63 nM per well, and was left to incubate with the cells at 37°C and 5% CO_2 in a humidifying incubator for 2 hours. 100 µL aliquots of incubated resazurin-containing medium were transferred to a clear bottom 96 well plate with black walls, and fluorescence intensity was measured using a plate reader with a 560 nm excitation / 590 nm emission filter set, performing 5 reads per well in a cross formation.

2.3.4 BrdU Incorporation Assay

10 µM BrdU (in complete growth medium) was incubated with cells at 37°C and 5% CO_2 in a humidifying incubator for three hours. Cells were washed three times with PBS to remove unincorporated BrdU before fixation and immunocytochemistry techniques (see section 2.4.1) using a primary antibody against BrdU were performed.

2.3.5 Coating of Culture Surfaces

For neural stem cell differentiation experiments, culture surfaces were pre-treated with Poly-D-lysine and laminin. Wells were coated with 300 µl Poly-D-lysine (200 μg/mL) per cm^2 of culture surface, incubating at 4°C overnight. Excess Poly-D-lysine was removed, then wells were incubated with 100 µL laminin (200 μg/mL) per cm^2 of culture surface for 1 hour at room temperature prior to seeding cells.

2.4 Immunocytochemistry

All immunocytochemisty protocols used a blocking buffer of 1% BSA in PBS. Incubations were all performed at room temperature on a rocking platform, and wash steps were performed for 5 minutes per wash on a rocking platform, unless stated otherwise. Individual details of the different antibody stains used can be found below.

2.4.1 BrdU

Following proliferation tissue culture experiments, coverslips of C2C12 cells were washed twice with sterile PBS then fixed and permeabilised in cell fixing solution (see table 2.2) at 4°C for 10 minutes. Cells were washed three times in PBS, then DNA was hydrolysed by incubating cells with 2N HCl for 30 minutes. HCl was removed and the cells were neutralised by incubation in sodium tetraborate buffer (pH 8.5) for 2 minutes. Cells were then incubated with blocking buffer for 1 hour, followed by primary antibody against BrdU (see table 2.3) diluted 1:50 in blocking buffer for 1 hour. Cells were washed once with blocking buffer and twice with PBS, then incubated with a fluorescent-dye (Alexafluor 488) conjugated secondary antibody targeting mouse IgG (see table 2.4) diluted 1:1000 in blocking buffer for 30 minutes in the dark. Cells were then incubated with Hoechst 33342 nucleic acid stain (1 µM in PBS) for 1 minute and washed three times with PBS, then coverslips were mounted onto slides with aqueous mounting medium (Fluoromount, Diagnostic BioSystems), sealed with clear nail varnish, and stored in the dark at 4°C.

2.4.2 Myosin Heavy Chain

Coverslips of C2C12 cells were washed twice with sterile PBS then fixed and permeabilised in cell fixing solution (see table 2.2) at 4°C for 10 minutes. Cells were washed three times in PBS, then incubated with blocking buffer for 1 hour, followed by primary antibody against myosin heavy chain (see table 2.3) diluted 1:500 in blocking buffer for 1 hour. Cells were washed once with blocking buffer and twice with PBS, then incubated with a fluorescent-dye (Alexafluor 488) conjugated secondary antibody targeting mouse IgG (see table 2.4) diluted 1:1000 in blocking buffer for 30 minutes in the dark. Cells were then incubated with Hoechst 33342 nucleic acid stain (1 µM in PBS) for 1 minute and washed three times with PBS, then coverslips were mounted onto slides with aqueous mounting medium (Fluoromount, Diagnostic BioSystems), sealed with clear nail varnish, and stored in the dark at 4°C.

2.4.3 GFAP, MAP2 and Tuj1

Plates of neural stem cells were washed once with PBS and fixed in 4% PFA for 15 minutes. Cells were washed once more in PBS, and incubated for 1 hour in blocking buffer supplemented with 0.1% (v/v) Triton X-100 to permeabilise. Cells were incubated overnight at 4°C with a cocktail of primary antibodies against GFAP (astrocyte marker, 1:400), MAP2 (oligodendrocyte marker, 1:300) and Tuj1 (neuron marker, 1:1000), all diluted in blocking buffer. Cells were then washed once with PBS and incubated for 1 hour in the dark with corresponding fluorescent-dye conjugated secondary antibodies (anti mouse IgG +Alexafluor 568, anti rat IgG +Alexafluor 488, anti rabbit IgG +Alexafluor 647) all diluted 1:500 in blocking buffer. Cells were again washed once with PBS and incubated for 15 minutes with DAPI (1 µM) before washing once more with PBS. After removing the last wash, the wells of cells were allowed to dry for <5 minutes before one drop of aqueous mounting medium (FluorSave, Merck) was added to the side of every well. The entire plate was covered using a PCR plate seal to prevent evaporation, and Stored in the dark at 4°C.

2.5 Microscopy

2.5.1 Fluorescent Microscopy

Following immunocytochemistry, microscopy slides were imaged at 10x or 40x magnification using Zeiss Axioimager 2 and LSM 880 microscopes. Images were taken in 4x4 tile stitches with the gain and exposure time standardised for relevant fluorescence channels. Plates of cells were imaged at 10x magnification using an LSM 880 microscope, taking four separate images at fixed locations within each well, with the gain and exposure time standardised for relevant fluorescence channels.

2.5.2 Transmission Electron Microscopy

EV samples were adsorbed onto formvar coated nickel grids (Agar Scientific) for 1 hour, fixed with 4% PFA for 15 minutes, and washed three times with ultrapure water. For immunogold labelling, grids were then blocked with 0.1% BSA in PBS buffer for 30 minutes and incubated with primary antibody (see table 2.3) in 0.1% BSA for 1 hour. Grids were then washed three times with PBS buffer and incubated with secondary gold-conjugated antibody (see table 2.4) in 0.1% BSA for 30 minutes followed by another three washes in ultrapure water. Samples were negatively stained in 2% UA for ten minutes and washed three times with ultrapure water before storage. Grids were imaged using a Hitachi H-7650 transmission electron microscope (TEM) and accompanying software.

2.6 Image Analysis

All image analysis was performed using ImageJ (Fiji) software (Schindelin et al., 2012).

2.6.1 Automated Nuclei Counts

Images were split into Individual Fluorescence channels and converted to 8 bit binary, resulting in black particles on a white background. uniformity of particles was improved using the binary - dilate function, and overlapping particles were split using the watershed function. Automated particle counts were then performed on each channel, counting particles 500-1000 pixels in size, with a circularity value of 0.2-1.

2.6.2 Manual Cell Counts

Differentiating Myoblasts

Individual fluorescence channels were imported and merged, and the Cell Counter plugin (DeVos, 2011) was used to mark and count all myosin-positive cells with two or more nuclei vs all mononuclear myosin-positive cells.

Differentiating Neural Stem Cells

individual fluorescence channels were imported and merged. The Cell Counter plugin was used to mark and count all cells positive for each neural cell marker, taking into account typical features of precursor morphology (small nucleus, cell body, and long branched processes for neurons, larger nucleus and medium branched processes for astrocytes, extensive branching for oligodendrocytes).

2.7 Fractionation of Whole blood and Platelet Depletion of Plasma

Trained phlebotomists collected venous blood samples into EDTA vacutainer tubes by cannulation. Whole blood samples were kept upright at room temperature and processed to platelet-depleted plasma within three hours of collection. Blood samples were centrifuged for ten minutes at 1,000 *xg* to fractionate, and the plasma (upper phase) was collected, taking care to avoid disruption of the buffy coat below. Plasma was diluted with an equal volume of PBS and was then centrifuged for 15 minutes at 1,500 *xg* to remove dead cells and cell fragments. The

pellet was discarded and the supernatant was centrifuged for 15 minutes at 2,500 *xg* to deplete platelets. Again the pellet was discarded and the supernatant was centrifuged at 16,000 *xg* to clear it of large microvesicles and apoptotic bodies The resulting platelet-depleted plasma (PDP) was stored at -80°C until further use.

2.8 Enriching EVs from Human Plasma

Total EVs were enriched from 1 mL PDP (equating to 0.5 mL original plasma) by size exclusion chromatography, ultracentrifugation or polymer precipitation. Each enrichment method is described in further detail below.

2.8.1 Differential Centrifugation

PDP was thawed at 4°C and passed through a syringe-driven filter with a pore size of 0.2 µm, pre-blocked with 0.1% (w/v) BSA in PBS. Filtered PDP was transferred to a 5 mL open top ultracentrifuge tube (Beckmann Coulter), topped up with sterile PBS, and centrifuged at 110,000 *xg* using an SW55Ti rotor (Beckmann Coulter) for 70 minutes at 4°C. An aliquot of supernatant was kept as EV-depleted plasma controls, and the EV pellet was resuspended in 100 µL sterile PBS by vortexing for 20 seconds followed by thorough trituration.

2.8.2 Size Exclusion Chromatography

Empty chromatography columns (BioRad) were filled with 14 mL CL-2B Sepharose slurry and topped up with sterile PBS buffer. Sepharose was allowed to settle for 4 hours. A column bed support was placed above each Sepharose column, and columns were primed by allowing 10mL PBS to flow through twice, followed by 10 mL PBST (0.01%). PDP was thawed at 4°C and concentrated to a final volume of 0.5 mL using a Vivaspin2 (GE Healthcare) concentrator column with a molecular weight cutoff of 5 kDa. 0.5 mL concentrated PDP was then pipetted above the column bed support, followed by immediate collection of flow-through from the column. Once PDP had completely entered the Sepharose column, the column was topped up

with 10mL sterile PBST. 3 mL of flow-through was collected from the column and discarded. The next 2 mL of flow-through was then collected into a fresh tube, and labelled the 'EV' fraction. A further 3 mL of flow-through was collected and discarded, then a final 2 mL of flow-through was collected in a new tube and labelled the 'EV-depleted' fraction.

2.8.3 Polymer Precipitation

PDP was thawed at 4°C and combined with 400 µL 50% (w/v) PEG (mw 6000) in 375 mM NaCl. The PDP-PEG solution was triturated thoroughly, and incubated at 4°C for 30 minutes before centrifugation at 1,500 *xg* for 30 minutes at 4°C. The supernatant was kept as an EV-depleted plasma control, and the EV pellet was resuspended in 100 µL sterile PBS by vortexing for 20 seconds followed by thorough trituration.

2.9 Nanoparticle Tracking Analysis

Nanoparticle tracking analysis was performed using a ZetaView 110 instrument and accompanying software (Particle Metrix, GmbH). The instrument was calibrated with known concentrations of 100nm polystyrene particles, then plasma EV samples were diluted 1:1000 in 0.2 µm-filtered PBS to measure the particle size and concentration. At 11 positions within the flow cell, 0.5 second videos were recorded and analysed for two cycles. Temperature was maintained at 23°C.

2.10 EV Fluorescent Labelling

Following DC protocols (section 2.8.1), EV pellets were resuspended in 400 µL PBS and incubated with PKH26 dye in diluent C (Sigma, final concentration 2 µM) for 5 minutes in the dark. An equal volume of 1% BSA was added to quench residual dye, and stained EVs were then centrifuged for 70 minutes at 110,000 *xg*, 4°C. The same procedure was followed with 400 µL PBS as a dye-only control.

2.11 Protein Extraction and Quantification

2.11.1 Protein Extraction

From whole cells

Following relevant tissue culture experiments, culture dishes were placed on ice and cells were washed twice with ice cold PBS buffer. Cells were scraped in cold 1x RIPA lysis buffer + 1% SDS, 1U protease inhibitor cocktail II (Sigma) and 1U phosphatase inhibitor cocktail III (Sigma). They were vortexed several times and incubated on a rocker at 4°C for 30 minutes, then cell lysates were centrifuged at 14,000 *xg* for 20 minutes at 4°C. The resulting pellets were discarded and the supernatants (containing total cell protein) were kept.

From EVs

EVs were lysed by addition of 10x RIPA buffer (final concentration 1x) + 1% SDS and 1U protease inhibitor cocktail II (Sigma) with thorough vortexing followed by 30 seconds probe sonication on ice using 50% amplification and 0.5 second on/off cycles. EV lysates were then heated to 100°C for 5 minutes, and incubated with gentle shaking on ice for 10 minutes.

2.11.2 Protein Quantification

Due to significant differences in protein concentration range, whole cell protein was quantified by BCA assay (Pierce) and EV protein was quantified by micro-BCA assay (Pierce). Samples were compared against serially diluted BSA as standard, prepared as per manufacturer's recommendations (0-2 mg/mL for BCA and 0-0.2 mg/mL for micro-BCA). BSA standards were loaded in triplicate into a 96 well plate, followed by unknown protein samples. For whole cell measurements, 10 µL standard/sample was loaded per well followed by 90 µL BCA working reagent, and the plate was incubated at 37°C for 30 minutes. For EV measurements, 10 µL standard/sample was loaded per well, followed by 10 µL micro-BCA working reagent, and the plate was incubated at 37°C for 2 hours. Absorbance was measured at 562 nm, taking 5 reads per well in a cross format. A curve of standard protein concentration vs absorbance was plotted

and sample values were extrapolated from this curve using a third-order polynomial equation, with r^2 >0.96 for each assay.

2.12 Western Blotting

Protein samples were combined with 4x Laemmli Buffer (BioRad, +DTT for reducing conditions, -DTT for non-reducing conditions) and heated to 100°C for 5 minutes. A total of 5 µg protein was loaded per well of a precast 10% agarose gel, and run at 100V for 1 hour in TGS running buffer. Protein was transferred to a nitocellulose membrane using a TurboBlot device (BioRad) on high mw setting for 10 minutes. Nonspecific binding sites were blocked in blocking buffer (5% (w/v) BSA in PBST) for 1 hour, then cut in relevant sections and incubated with primary antibodies diluted in blocking buffer (see table 2.3 for antibodies and dilutions) for 1 hour at 4°C overnight. Membrane sections were washed once in blocking buffer and four times in PBST (5 minutes per wash), then incubated with HRP-conjugated secondary antibodies diluted in PBST (see table 2.4 for antibodies and dilutions) for 30 minutes at room temperature. Membrane sections were washed four times in PBST (5 minutes per wash), then incubated with ECL substrate for 2 minutes and visualised using a ChemiDoc imaging system (BioRad).

2.13 Dot blot Assays

The concentrations of all protein samples were normalised, and normalised protein was slowly spotted on to nitrocellulose membranes (one for each antibody) in 2 µL aliquots. Membranes were allowed to air dry for 1 hour and non-specific binding sites were blocked with blocking buffer (5% [w/v] BSA in TBST) for 1 hour at room temperature. Membranes were each incubated with relevant primary antibody diluted in blocking buffer for 1 hour at room temperature (antibody dilutions in table 2.3). They were then washed once in blocking buffer and three times in TBST (5 minutes per wash), and incubated with HRP-conjugated secondary antibodies diluted in TBST (antibody dilutions in table 2.4) for 1 hour at room temperature. Membranes were washed three times with TBST, then incubated with ECL reagent for two minutes. Excess

ECL reagent was removed from the membrane surface before visualising using a ChemiDoc imaging system (BioRad).

Table 2.3: Primary Antibodies, Techniques & Dilutions

Target	Host Species	Technique(s)	Dilution(s)	Supplier, Cat no.
CD81	Mouse	Dot blot + WB, TEM	1:1000, 1:200	Abcam, ab79559
CD63	Mouse	Dot blot, TEM	1:50, 1:10	DSHB, H5C6
CD9	Mouse	Dot blot	1:50	DSHB, B2C11
HSP70	Rabbit	Dot blot, WB	1:1000	Abcam, ab79852
Calnexin	Rabbit	Dot blot	1:1000	Abcam, ab22595
CD41	Rabbit	Dot blot	1:2000	Abcam, ab181548
MHC	Mouse	ICC	1:500	Abcam, ab124205
BrdU	Mouse	ICC	1:50	DSHB, G3G4
GFAP	Rat	ICC	1:400	Invitrogen, 130300
MAP2	Mouse	ICC	1:300	Upstate, 05-346
TUJ1	Rabbit	ICC	1:1000	Covance, MRB-435P-100
ApoA-1	Rabbit	Dot blot	1:1000	Proteintech, 14427-1-AP
ApoB-100	Mouse	Dot blot	1:1000	Santa Cruz, sc-13538

Apo, apolipoprotein; BrdU, 5-bromo-2'-deoxyuridine; CD, cluster of differentiation; DSHB, Developmental Studies Hybridoma Bank; GFAP, glial fibrillary acidic protein; HSP70, heat shock protein 70; ICC, immunocytochemistry; MAP2, microtubule-associated protein 2; MHC, major histocompatibility complex; TEM, transmission electron microscopy; TUJ1, class III beta-tubulin 1; WB, western blot.

Table 2.4: Secondary Antibodies, Techniques & Dilutions

Target	Host Species	Conjugate	Technique	Dilution	Supplier
Mouse IgG	Goat	Alexa Fluor 488	ICC	1:1000	Invitrogen, A11001
Mouse IgG	Donkey	Alexa Fluor 568	ICC	1:500	Invitrogen, A10037
Rat IgG	Goat	Alexa Fluor 488	ICC	1:500	Invitrogen, A11006
Rabbit IgG	Goat	Alexa Fluor 647	ICC	1:500	Invitrogen, A20991
Mouse IgG	Goat	10nm gold beads	TEM	1:200	Abcam, ab39619
Mouse IgG	Goat	HRP	WB	1:2000	BioRad, 1706516
Rabbit IgG	Goat	HRP	WB	1:2000	Abcam, ab6721

ICC, immunocytochemistry; Ig, immunoglobulin; HRP, horseradish peroxidase; TEM, transmission electron microscopy; WB, western blot.

Chapter 3

Circulating Vesicles and Adult Myogenesis

3.1 Introduction

3.1.1 Background

Adult myogenesis involves the rapid expansion of muscle resident stem cells, which exhibit an increasingly muscle specific phenotype as they differentiate and fuse to form new myofibers (reviewed by Hernández-Hernández et al., 2017). This process occurs following physical activity to repair or replace myofibers damaged by exertion (Darr and Schultz, 1987). Small circulating EVs increase in a range of physiological and pathological conditions (reviewed by Yuana et al., 2013); it could therefore be reasonably hypothesised that physical activity, which generates a marked systemic response, might also result in a greater number of circulating small EVs. Only a handful of published works to date have addressed changes in circulating EVs following physical activity, and have for the most part concentrated on larger EVs. One group has however demonstrated an increase in circulating small EVs following physical activity (Fruhbeiss, 2015), which is yet to be corroborated by subsequent publications. Moreover, the physiological importance of exercise-induced small EVs has not yet been addressed. Small EVs have been demonstrated to transport functional cargo, including proteins and micro-RNAs with known involvement in the proliferation and differentiation steps of adult myogenesis (Wang and Wang, 2016; Choi et al., 2016), however whether this happens in the context of physical activity remains unexplored.

3.1.2 Aims and Objectives

The experiments described in this chapter aimed to investigate if exercise-induced circulating small EVs could alter the proliferation and differentiation status of recipient muscle progenitor cells. The objectives of this chapter therefore were:

- To establish and optimise reproducible *in vitro* models of myoblast proliferation and differentiation
- To enrich populations of small EVs from the pre- and post-exercise plasma of healthy

volunteers

- To assess myoblast proliferation and differentiation models treated with pre- and post-exercise plasma EVs

3.2 Establishing In vitro Models of Myoblast Proliferation and Differentiation

3.2.1 Experiment Rationale

To test if exercise-induced small EVs play an active regulatory role in myoblast proliferation and differentiation, we aimed to establish robust *in vitro* models of these processes which could be treated with pre- and post-exercise plasma EVs. The immortalised mouse myoblast cell line C2C12 was used as a model cell line for both processes. Several different techniques were selected and optimised to demonstrate proliferative and differentiative status of the cells. Proliferation was quantified by: the total number of cells present; quantification of cellular metabolism (resazurin assay); and the number of cells which were actively synthesising new DNA (BrdU incorporation). Differentiation status was determined by the quantifiable presence of multinucleate myosin-expressing cells (fusion index).

BrdU Incorporation

To measure new DNA synthesis and therefore identify cells representative of an activated satellite cell population, C2C12s were incubated with the synthetic nucleoside Bromodeoxyuridine (BrdU). BrdU is an analog of thymidine which can be incorporated into the newly synthesized DNA of replicating cells during the S phase of cell cycle (Meyn et al., 1973), and can also be passed on to daughter cells upon replication (Kee et al., 2002). Antibodies specific for BrdU can be used to detect its incorporation, thus highlighting cells that were actively replicating their DNA during the incubation period.

Resazurin Assay

Also known as AlamarBlue, resazurin has been available since 1993 and is commonly used to quantitatively measure cell viability and cytotoxicity. It is an oxidation-reduction indicator that undergoes colorimetric change in response to cellular metabolic reduction (Ahmed et al., 1994), and is used to measure both aerobic and anaerobic respiration of cells in vitro (Chen et al., 2015). Respiring cells convert dark blue resazurin to its reduced form, resorufin, which is pink and highly fluorescent. The intensity of fluorescence produced is proportional to the number of respiring cells (Ahmed et al., 1994).

Myoblast Fusion Index

To quantify myoblast differentiation, a "myoblast fusion index" is calculated (Metzinger et al., 1993; Kandalla et al., 2011). This fusion index usually describes the number of nuclei inside MHC-positive myotubes as a percentage of the total nuclei within the field of view (Nishiyama et al., 2004). Problematically, the common phenomena of nuclei clustering and cell overlapping in the culture conditions makes accurate counting of nuclei near impossible for the human eye or for an automated program (Duca et al., 1998; Agley et al., 2012). To improve accuracy and reproducibility, it was instead decided to count the percentage of MHC-expressing myotubes which contained more than one nucleus, and had formed as a result of myoblast fusion. The requirement of myoblasts to exit cell cycle before differentiating and fusing minimised the possibility of counting dividing cells, as only MHC-positive multinucleate cells were counted. This alternative method was demonstrated to reliably distinguish between differentiation status of myoblats at days 0-7 of differentiation before experimental use (section 3.2).

3.2.2 Methods

Proliferation Model

C2C12 cells were maintained as per section 2.3.2 and seeded at $2x10^3$ cells/cm^2 onto untreated sterile glass coverslips. They were allowed to proliferate at 37 °C and 5% CO_2 for 24 hours, before incubation with resazurin dye (2 hours) and with BrdU (3 hours). After the incubation period, 100 µL aliquots of resazurin-containing medium were transferred from every well of

cells to a black-walled 96 well plate and fluorescence intensity of resofurin was measured (section 2.3.3). Cells were then washed three times in PBS to remove unincorporated BrdU and resazurin/resofurin. They were fixed and permeabilised, and DNA was hydrolysed (section 2.4). Immunocytochemistry was then performed using a primary antibody against BrdU plus a Hoechst nuclear counterstain (section 2.4). Tile images of each coverslip were taken with a fluorescent microscopre (section 2.5.1), images were blinded, and automated counts of total nuclei and BrdU positive nuclei were performed (section 2.6).

To test that this model could adequately detect differences in proliferation rate, C2C12 complete growth medium was either replaced with serum-free medium (SFM) or with fresh complete growth medium (GM) once cells had adhered to the culture surface. All BrdU and resazurin assay methods were then performed following a 24 hour incubation in these medium conditions (n=3 technical replicates) (figure 3.1). Means of SFM and GM treated cells were compared by 2-tailed paired students T test.

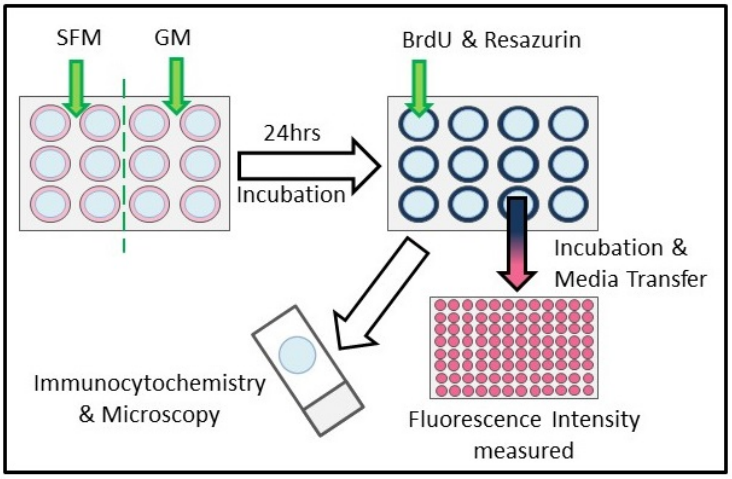

Figure 3.1: Schematic representation of myoblast proliferation model.
BrdU, 5-bromo-2'-deoxyuridine; GM; C2C12 complete growth medium, SFM, C2C12 serum-free medium.

Differentiation Model

C2C12 cells were maintained as per section 2.3.2 and seeded at $1x10^4$ cells/cm^2 onto untreated sterile glass coverslips. They were allowed to reach over 80% confluence for 48 hours, then

the confluent cells were induced to differentiate by exchanging complete growth medium for low-serum differentiation medium (table 2.2). The time of media change was considered time zero, and cells were maintained in differentiation medium (replaced after three days) for a further seven days. Coverslips of cells were washed, fixed, and permeabilised, then immunocytochemistry was performed using a primary antibody against myosin heavy chain (MHC) plus a Hoechst nuclear counterstain (section 2.4). Tile images of each coverslip were taken with a fluorescent microscope (section 2.5.1), all images were blinded, and MHC-positive cells were manually counted (section 2.6) to calculate a myoblast fusion index (MFI) : the percentage of MHC-positive cells with two or more nuclei, which had presumably formed by the differentiation and fusion of two or more individual myoblasts.

To confirm that the chosen methods could reliably and reproducibly detect an increase in myotube formation, fixing and permeabilisation of cells was repeated on days 0, 1, 2, 3, 4 and 7 of differentiation (n=6 technical replicates), to capture early myotube formation over a one week period. Immunocytochemistry was then performed on all fixed coverslips of cells and MFI was calculated for each.

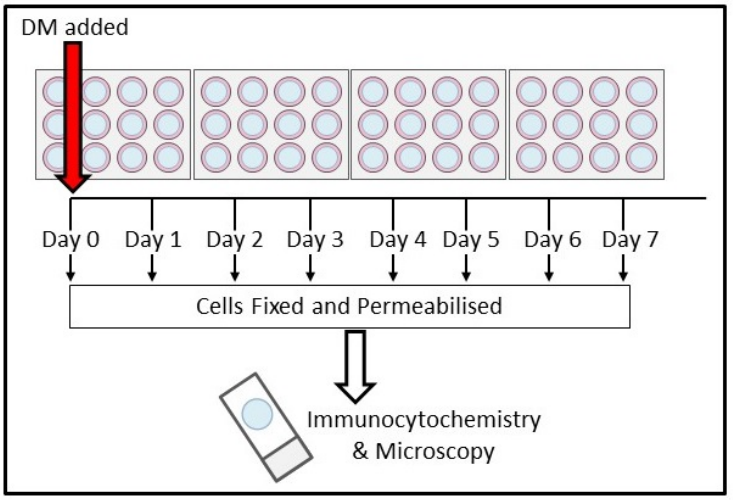

Figure 3.2: Schematic representation of myoblast differentiation model. DM = C2C12 differentiation medium.

Statistical Analysis

Statistical analysis of C2C12 proliferation measures was carried out in the form of a 2-tailed independent samples students T test, to describe differences between cells cultured in complete growth medium and cells cultured in serum-free medium. Differentiation was assessed by one-way ANOVA and subsequent Tukey's honest significant difference test, to demonstrate differences between the mean MFI calculated among cells fixed at multiple time points of the differentiation protocol.

3.2.3 Results

Proliferation Model

C2C12 cells were incubated with complete growth medium or serum-free medium for 24 hours before total cells and BrdU-positive cells were counted and resazurin reduction was quantified. Total cell number, BrdU incorporation, and resazurin reduction were all elevated in cells incubated with complete growth medium compared with serum-free medium, as is demonstrated by figure 3.3. These data indicated that the techniques tested should be sufficient to demonstrate any marked increases or decreases in C2C12 proliferation following 24-hour incubation with plasma EVs.

Differentiation Model

As days of differentiation progressed, cellular expression of MHC increased, as did the amount of myoblast fusion. Individual MHC-expressing myoblasts visibly lined up and fused to form longer multinucleate structures (figure 3.4 A-C). This was reflected by the MFI calculated at each day of differentiation, which consistently showed an increase in myoblast fusion from one day to the next, with a statistically significant increase in MFI first observed at day 3 of differentiation (3.4 D). These data led to the decision that experimental analysis of C2C12 differentiation after plasma EV treatment would be performed on day 3 of the differentiation model.

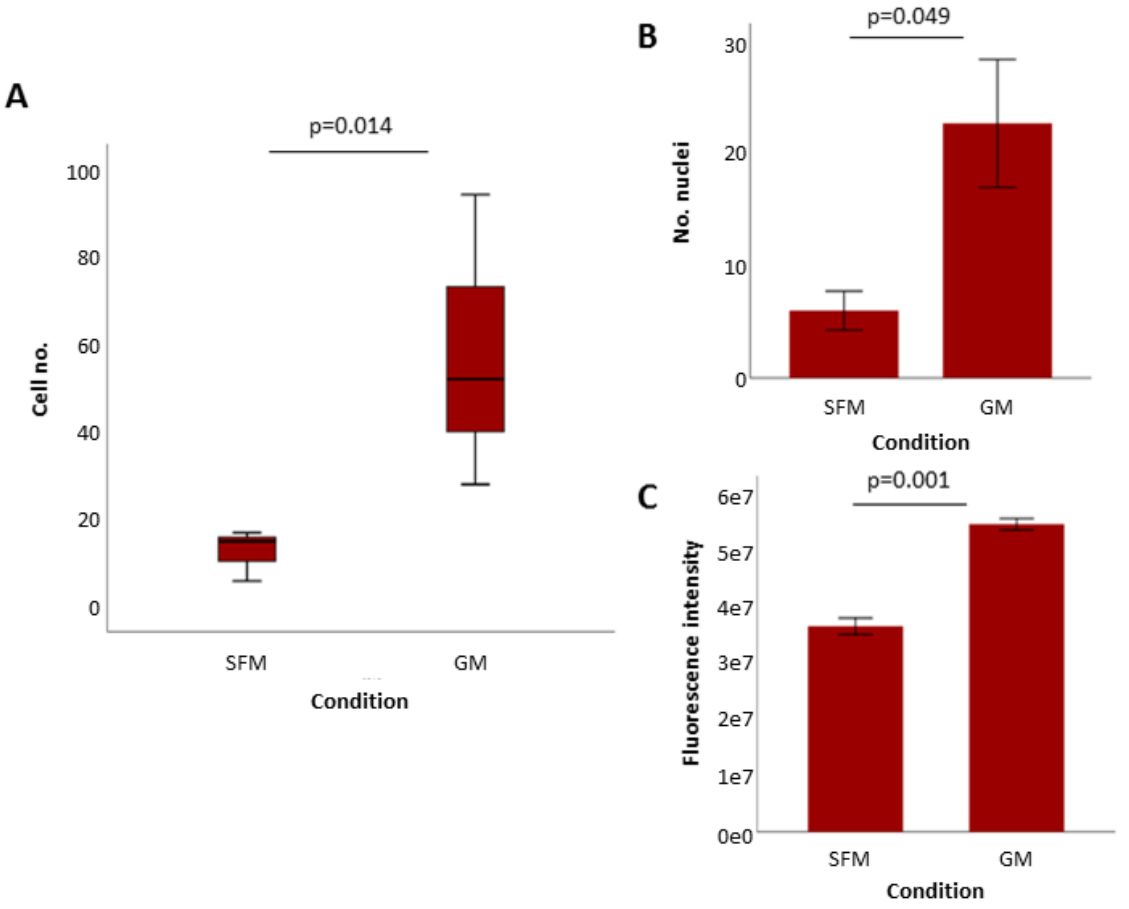

Figure 3.3: Myoblast proliferation model: Total cell number per FOV (A), total BrdU positive nuclei per FOV (B), and resofurin fluorescence intensity (C) of C2C12 cells after 24-hour incubation with GM or SFM. Error bars = +/- 1 SEM, p values generated by 2-tailed independent samples students T test. n=3 technical replicates.
FOV, field of view; GM, C2C12 complete growth medium; SEM, standard error of mean; SFM, C2C12 serum free medium.

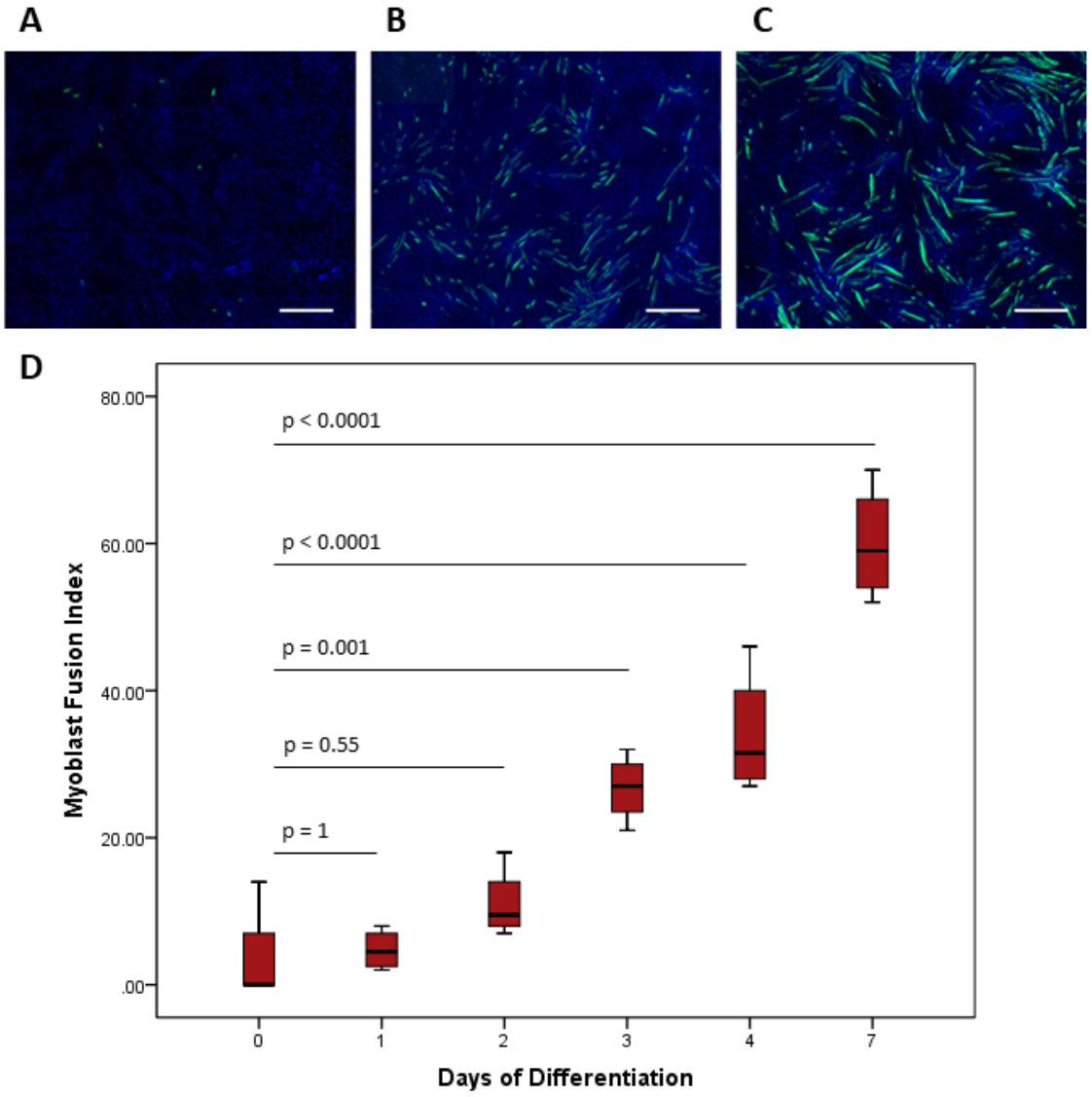

Figure 3.4: Myoblast differentiation model: Representative images of C2C12 myosin heavy chain expression at day 0 (A), day 3 (B) and day 7 (C) of differentiation, scale bars = 500 μm. Calculated myoblast fusion index of C2C12 cells at days 0-7 of differentiation (D). n=6 technical replicates, p values generated by one way ANOVA and subsequent Tukey test.

3.3 Enriching and Counting EVs from Pre- and Post-Exercise Plasma

3.3.1 Experiment Rationale

One published study has demonstrated that circulating small EVs increase in number in response to strenuous physical activity (Fruhbeiss, 2016). They counted EVs by nanoparticle tracking analysis (NTA) following an exhaustive exercise test, and enriched them from plasma by DC methods. To test if a similar increase could be observed following moderate intensity exercise, NTA was used to estimate the diameter and number of EVs enriched from PDP obtained before and after a bout of moderate intensity cycling. NTA utilises the properties of light scattering and Brownian motion to estimate the concentration and size distribution of nanoparticles in liquid suspension. A laser beam is passed through the sample and particles in its path scatter light, allowing them to be visualised by a video camera mounted onto a x20 magnification microscope. The camera captures video files of the particles moving under Brownian motion, and accompanying software tracks individual particles and calculates their hydrodynamic diameters based on this motion (Carr & Wright, 2013).

3.3.2 Methods

Participants and Exercise Protocols

Ethical approval for all exercise interventions and for subsequent *in vitro* experiments using the human blood samples collected was granted by the University research ethics committee. Exercise protocols were designed and implemented by Professor Helen Dawes and Dr Johnny Collett in the Department of Sport, Health Sciences and Social Work, Oxford Brookes University. Young, healthy volunteers performed moderate intensity exercise on a cycle ergometer, maintaining 60% maximum heart rate (HR_{max}) for 15 minutes (for myoblast differentiation experiments), or 40% maximal oxygen consumption (VO_2) for 30 minutes (for myoblast proliferation experiments). Exercise protocols were carried out on fasted individuals (fasted for >8 hours), and parameters including participant age, sex, height and weight were recorded - participant demographics are

outlined in appended section A1.

Blood collection, EV Enrichment and EV counting

Cannulation was performed at each session, and whole blood samples were taken at rest and then at 15, 30, 45 and 60 minutes post-exercise. Whole blood samples were processed to platelet depleted plasma (PDP) as per section 2.7 and stored at -80°C within 3 hours of blood collection. Once all participant interventions had been performed, PDP samples were thawed and EVs were enriched by differential centrifugation (section 2.8). Nanoparticle Tracking Analysis (NTA) was then used to count the number of EVs present in all pre- and post-exercise samples, in addition to measuring their size distribution (section 2.9).

Descriptive analysis of EV numbers revealed that the acquired data was not normally distributed. Consequently, comparison of group means was performed using a Friedman's non parametric test for $\geq$3 related samples.

EV Characterisation

To visualise EV size, morphology and presence of EV markers, plasma EVs were negatively stained and labelled for CD81 with immunogold techniques, then imaged by electron microscopy (section 2.5.2). To further demonstrate the presence of known vesicular proteins in the plasma EV samples, total protein was extracted from the EV preparations and from their originating whole plasma. Protein concentration was normalised across all samples and analysed via dot blot assay using antibodies specific to HSP70, CD63, CD9, and CD81 (section 2.13). Control dot blot assays using antibody specific to Calnexin were also performed, to demonstrate the absence of contaminating cellular compartments. Western blotting was subsequently performed using antibodies specific to CD81 and HSP70, to enable separation of proteins by size in EVs and matched whole plasma (section 2.12).

3.3.3 Results

EV Characterisation

Electron microscopy identified particles with typical EV morphology (figure 3.6 A), which were positive for CD81 following immunogold labelling (figure 3.6 B & C). NTA measured particles of a comparable size distribution to those observed by TEM (figure 3.8). Dot blot assays demonstrated the presence of all tested marker proteins in the EV preparations, though not all markers were notably enriched compared with whole plasma controls (figure 3.5 A). These assays also confirmed a marked reduction in Calnexin in EV samples compared with matched whole plasma controls. Western blotting demonstrated the presence of CD81 and HSP70 proteins in EV samples, this time enriched compared with whole plasma (figure 3.5 B). It appears that by our hands, EVs enriched from human plasma were positive for the tetraspanin CD81.

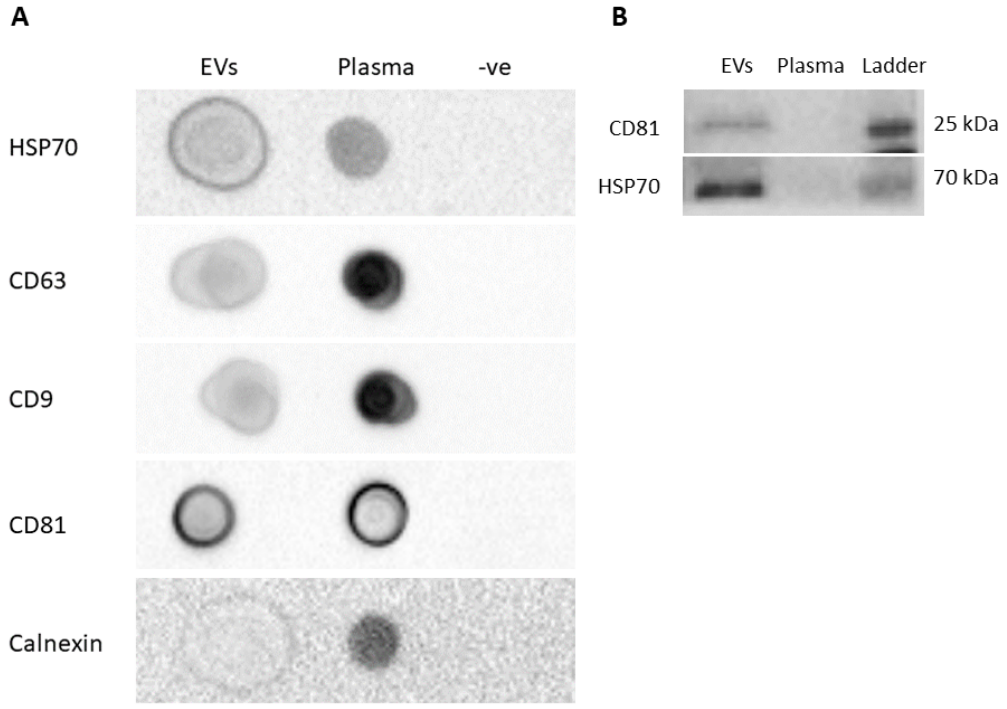

Figure 3.5: Detection of protein markers in EV samples: Dot blot assays for HSP70, CD63, CD9, CD81, and Calnexin with EV protein loaded alongside whole plasma and PBS (-ve) controls (A). Western blot for CD81 and HSP70 with EV protein loaded alongside a protein ladder and a whole plasma control (B).
CD, cluster of differentiation; EV, extracellular vesicle; HSP, heat shock protein; PBS, phosphate buffered saline.

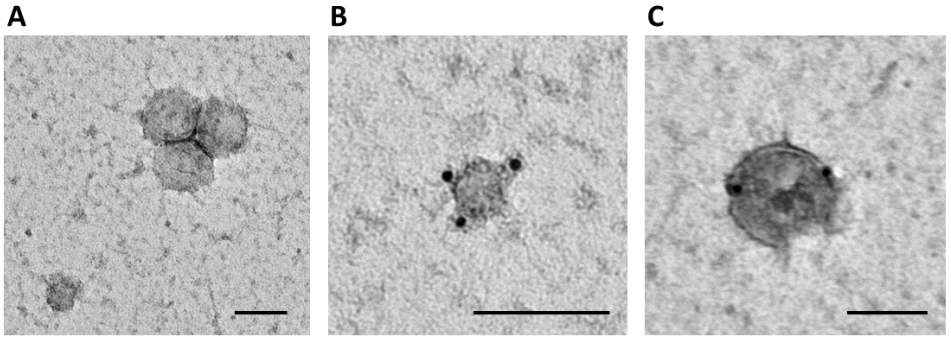

Figure 3.6: Electron microscopy of negatively stained (A) and immunogold labelled (B & C) plasma EVs.
10 nm gold beads label CD81; all scale bars = 100 nm.
EV, extracellular vesicle; CD, cluster of differentiation.

EV Number in pre- and post-exercise Samples

NTA of EV-enriched samples showed no significant change in particle number between pre- and post- exercise samples, and this was true of all time points tested (figure 3.7). Though EV number did not notably increase, it was anticipated that there may still be changes in their cargo rather than their quantity. Consequently, further tests were performed to assess the potential effects of these EVs on recipient muscle progenitors. NTA data also indicated that the particles tracked and counted exhibited size distributions representative of small EVs, possibly exosomes. The size distribution of circulating vesicles did not appear to change between time points (figure 3.8).

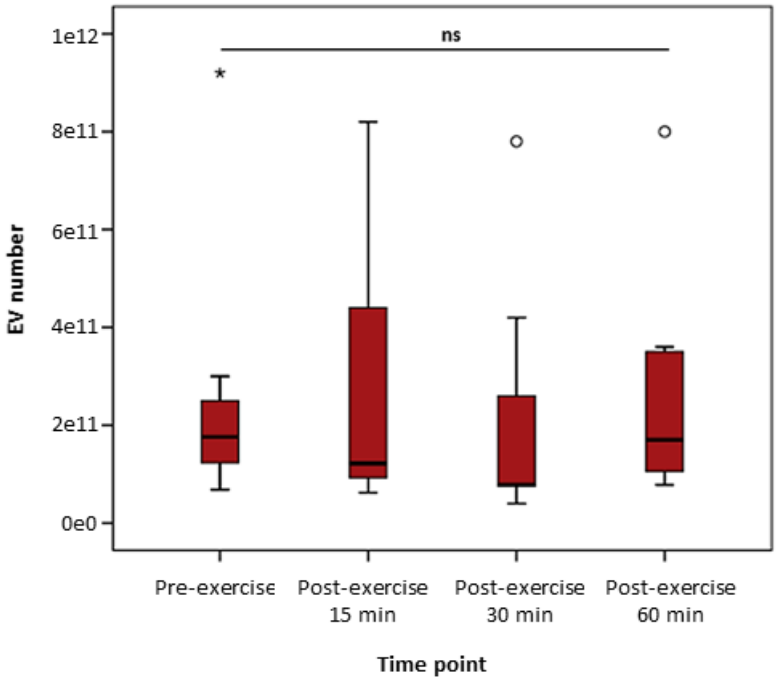

Figure 3.7: Total number of EVs enriched from 1 mL plasma of participants at rest and several time points post-exercise. Outlier extreme upper values labelled with * and °. n=6 biological replicates, statistical significance rejected by Friedman's non parametric test for related samples. EV, extracellular vesicle.

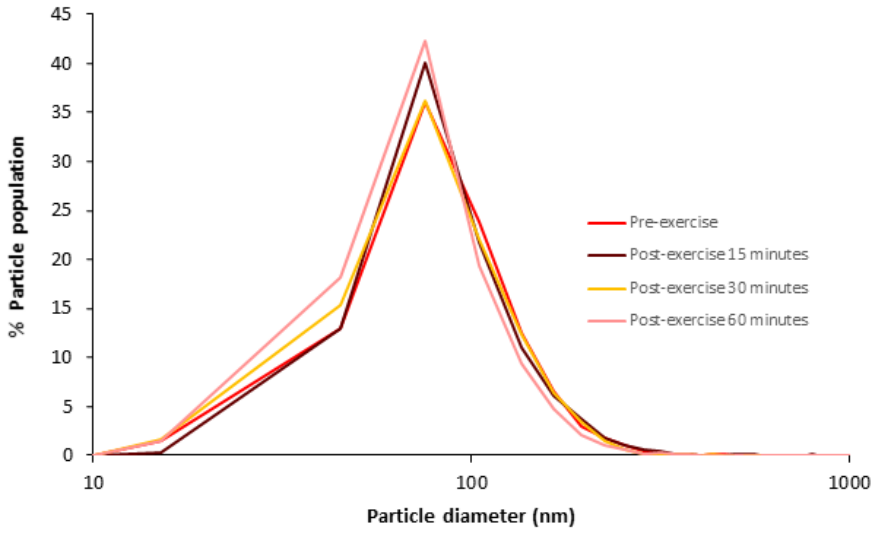

Figure 3.8: Size distribution of EVs enriched from plasma of individuals at rest and several time points post-exercise. n=6 biological replicates. EV, extracellular vesicle.

3.4 Treating Myoblast Proliferation and Differentiation Models with Plasma EVs

3.4.1 Experiment Rationale

To test the effects of pre- and post-exercise plasma EVs on recipient myoblast proliferation and differentiation, the *in vitro* models established in section 3.2 were treated with participant-matched plasma EVs collected pre- and 60 minutes post-exercise. Nanoparticle tracking analysis of EV samples suggested that there was no notable difference in EV number between rest and exercise plasma samples (section 3.3). Accordingly, EV treatments were normalised by original volume of plasma rather than EV number. The 60 minute post-exercise time point was chosen due to good uniformity in EV number across participants compared with other time points (see figure 3.7).

3.4.2 Methods

Proliferation

C2C12 cells were maintained as per section 2.3.2 and seeded at 2x10^3 cells/cm^2 onto untreated sterile glass coverslips. Once cells were adhered to the culture surface, total EVs from 10 µL PDP (equal to 5 µL original plasma) were applied per cm^2 of culture surface (n=6 different participants' plasma EVs), in addition to equal volumes of PBS (no-EV) controls (n=6). EVs and controls were incubated with the cells for 24 hours at 37°C, 5% CO_2. Resazurin and BrdU incorporation assays were then performed as described in section 3.2.2, and images were blinded prior to analysis.

Differentiation

C2C12 cells were maintained as per section 2.3.2 and seeded at 1x10^4 cells/cm^2 onto untreated sterile glass coverslips, then incubated for 48 hours to reach reach >80% confluence. Confluent cells were induced to differentiate by exchanging complete growth medium for differentiation medium (see table 2.2). The time of media change was considered time zero, at which point

total EVs from 10 µL PDP were applied per cm^2 of culture surface (n=6 biological replicates) in addition to equal volumes of no-EV controls (n=6). EVs and no-EV controls were incubated with the cells for 72 hours before immunocytochemistry and image analysis were performed as per section 3.2.2, blinding images prior to analysis. To rule out the possibility that changes in differentiative status were not caused by minor differences in EV number between pre- and post-exercise EV samples, plasma EVs were applied to differentiating myoblasts in equal numbers (n=2 biological replicates) and the differentiation protocol was repeated.

Statistical Analysis

For reproducible comparison, all pre- and post- exercise datasets were expressed as the fold change from no-EV (PBS) controls from the corresponding experiment. Descriptive analysis of all datasets was performed using SPSS-52 software, including a Shapiro-Wilk test for normal distribution. Normal distribution of the majority of datasets allowed for comparison of pre- and post- exercise means with a 2-tailed paired students T test, with the exception of resazurin reduction data which was analysed using a suitable non-parametric alternative (Wilcoxon Signed Rank).

3.4.3 Results

Proliferation

Incubation with post-exercise EVs increased C2C12 proliferation compared with incubation with rest EVs, demonstrated by total cell number (T test, p=0.03), BrdU positive cell number (T test, p=0.07), and resazurin reduction (Wilcoxon signed rank test, p=0.12) after a 24-hour incubation with EVs (figure 3.9). Compared with C2C12s incubated with no-EV controls, those incubated with pre-exercise EVs exhibited at a roughly equal rate of proliferation (fold change from no-EV controls in cell number, BrdU, and resazurin $\sim$1), whereas those incubated with post-exercise EVs proliferated at a faster rate (fold change from no-EV controls $>$1)

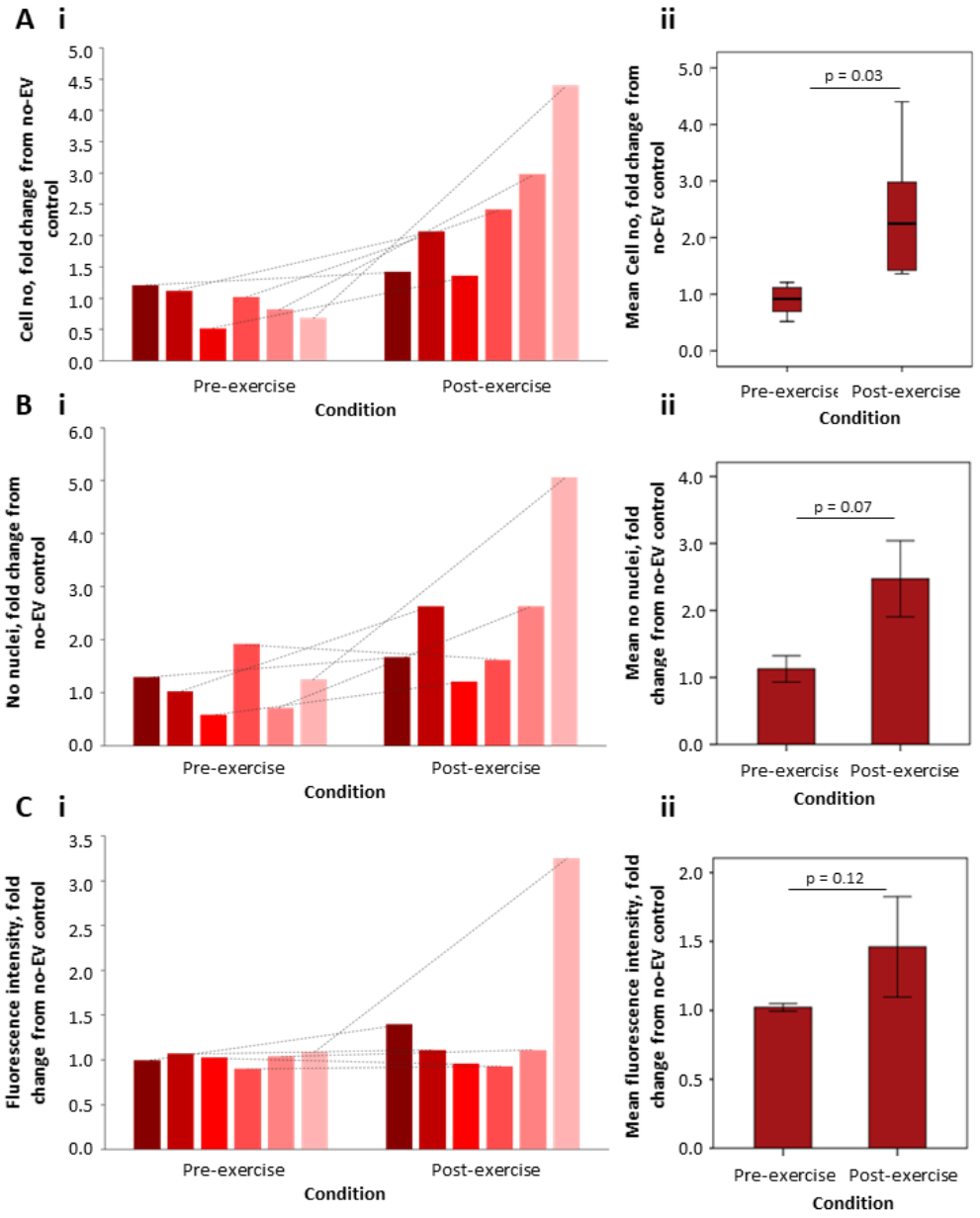

Figure 3.9: Effect of pre- and post-exercise EVs on moyblast proliferation, quantified by total cell number per FOV (A), total BrdU positive nuclei per FOV (B) and resofurin fluorescence intensity (C) of proliferating C2C12s following 24-hour incubation with EVs. Shown for individual participant EVs (i) and overall EV populations (ii). n=6 biological replicates. All measures are expressed as fold change from C2C12s treated with no-EV (PBS) controls. Error bars = +/- 1 SEM, p values generated by 2-tailed paired students T test (A+B) and Wilcoxon signed rank test (C).
BrdU, 5-bromo-2'-deoxyuridine; EV, extracellular vesicle; FOV, field of view; MFI, myoblast fusion index; PBS, phosphate buffered saline; SEM, standard error of the mean.

Differentiation

Incubation with post-exercise EVs decreased differentiation of C2C12s compared with incubation with pre-exercise EVs, as quantified by the MFI of myosin-expressing cells (figure 3.10). Fold change calculations indicated that the differentiative status of C2C12 cells incubated with pre-exercise EVs was similar to those incubated with no-EV controls (mean fold change in MFI = 0.95), whereas the differentiative status of C2C12 cells incubated with post-exercise EVs was lesser than those incubated with no-EV controls (mean fold change in MFI = 0.70). Adding EVs in equal numbers to the myoblasts had the same effect on differentiation, confirming that the previously observed difference was not caused by minor fluctuations in EV number (figure 3.11).

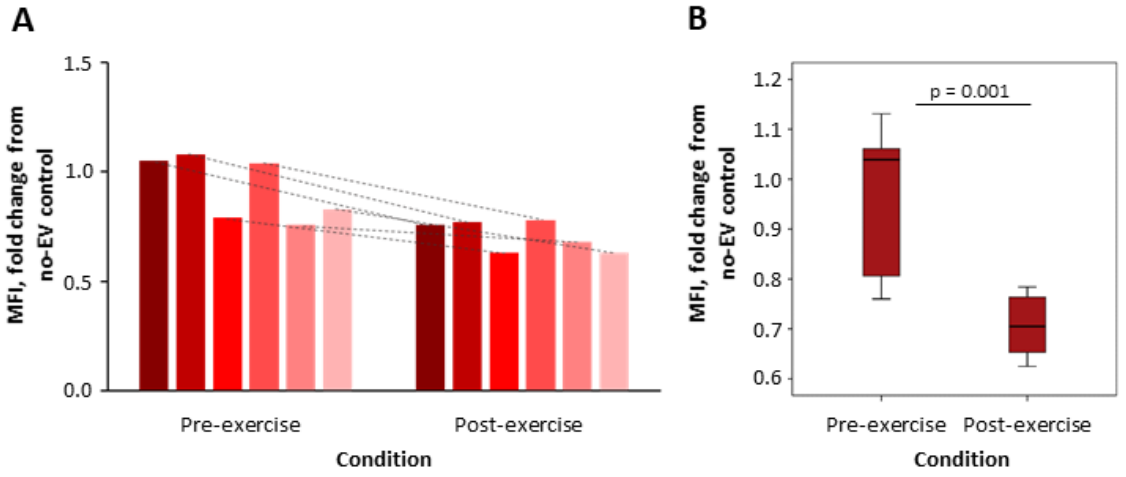

Figure 3.10: Effect of pre- and post-exercise EVs on myoblast differentiation: MFI of C2C12s treated with pre- and post-exercise plasma EVs, expressed as fold change from C2C12s treated with no-EV (PBS) controls. Shown for individual participant EVs (A) and overall EV populations (B). p value generated by 2-tailed paired students T test. n=6 biological replicates.
EV, extracellular vesicle; MFI, myoblast fusion index; PBS, phosphate buffered saline

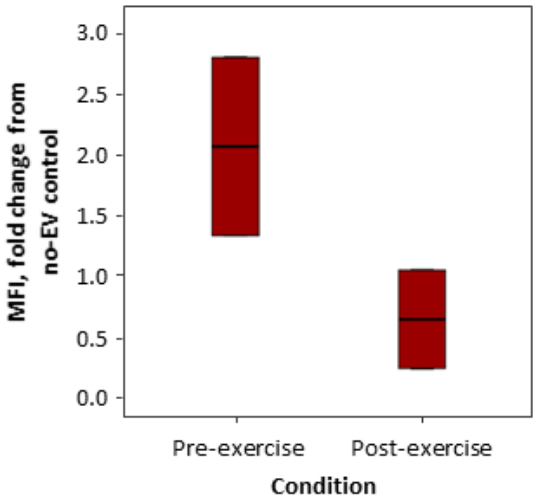

Figure 3.11: Effect of pre- and post-exercise EVs on myoblast differentiation when EV number is normalised across samples: MFI of C2C12s treated with pre- and post-exercise plasma EVs, expressed as fold change from C2C12s treated with no-EV (PBS) controls. n=2 biological replicates.
EV, extracellular vesicle; MFI, myoblast fusion index; PBS, phosphate buffered saline

3.5 Visualising C2C12 Uptake of plasma EVs

3.5.1 Experiment Rationale

To confirm that plasma EVs are in fact incorporated by recipient C2C12 cells, EV samples were labelled with the membrane dye PKH26 and incubated with C2C12 cells before being imaged by fluorescent microscopy. A dye only control was also incubated with the cells, to demonstrate that fluorescent particles observed were not simply micelles of unbound dye.

3.5.2 Methods

Aliquots of participant plasma EVs were labelled with PKH26 as per section 2.10. PKH26 labelled EVs and dye-only controls were then incubated with C2C12s for three hours, and cells were washed, fixed and premeabilised (section 2.4). All fixed cells were briefly incubated with Hoechst to stain nuclei (section 2.4), then imaged by fluorescent microscopy.

3.5.3 Results

Plasma EVs labelled with PKH26 could be observed inside C2C12 cells following the 3-hour incubation. The fluorescent particles observed were distinctly greater in number in cells treated with labelled EVs than in cells incubated with dye-only controls (figure 3.12). However it is not definitive from these images whether the fluorescent particles are inside the cells of interest or are instead bound to the cell surface.

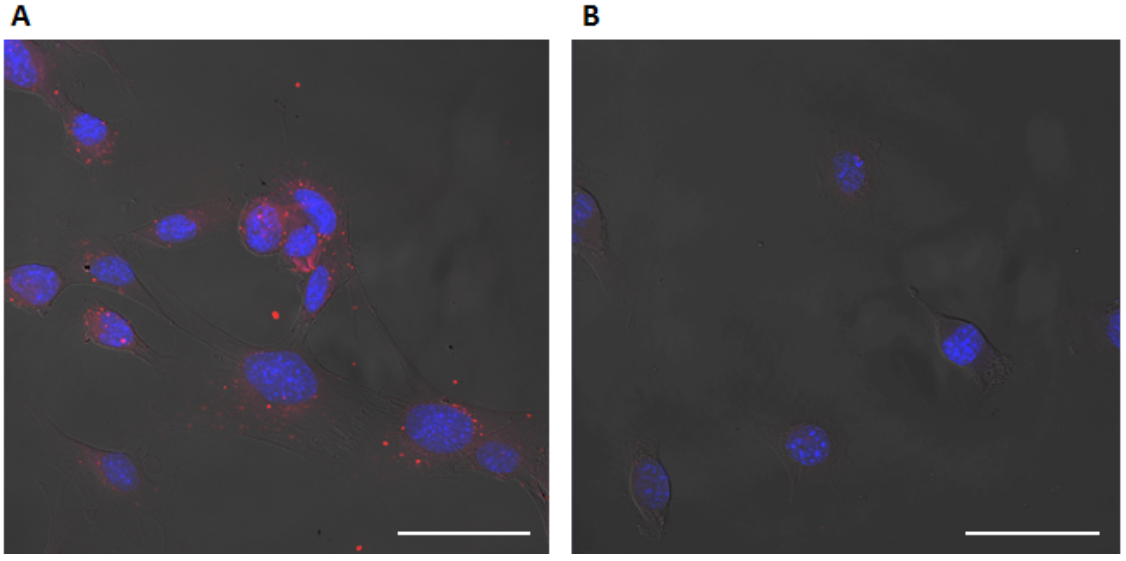

Figure 3.12: C2C12 uptake of labelled plasma EVs (A) vs a dye only control (B).
Blue fluorescence indicates Hoechst staining, red fluorescence indicates PKH26 staining, scale bar = 50 µm.
EV, extracellular vesicle.

3.6 Treating Myoblast Proliferation Model with Other Plasma Components

3.6.1 Experiment Rationale

As an added control, the myoblast proliferation model was treated with pre- and post-exercise EV depleted plasma (DC supernatant) from the same participants as the EV enriched samples. EV depleted plasma samples should contain small blood components other than EVs, such as

free circulating plasma proteins and lipoproteins. It was anticipated that any difference in effect between the EV enriched and EV depleted samples would demonstrate independent actions of these plasma fractions.

3.6.2 Methods

C2C12 proliferation experiments were repeated, this time treating the cells with 10 µL EV-depleted plasma from the pre- and post-exercise blood of matched participants (n=6 biological replicates). An equal volume of PBS was again used for each negative control. All methodology was otherwise performed as per section 3.4.

3.6.3 Results

Treatment with EV depleted plasma from exercised participants did not increase myoblast proliferation compared with pre-exercise EV depleted plasma. This is true of all techniques performed to quantify C2C12 proliferation rate (figure 3.13). If anything this showed a trend towards a suppressive effect.

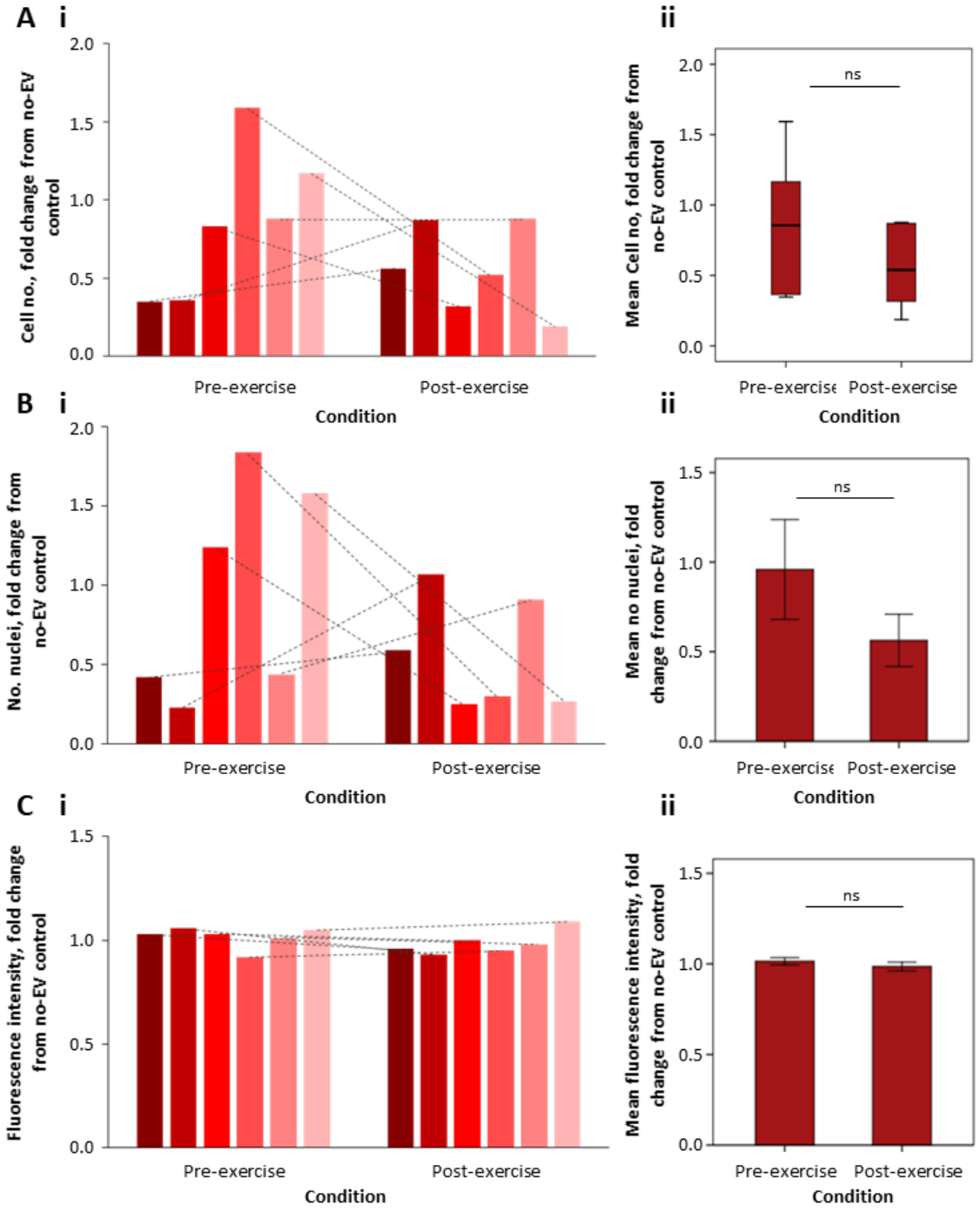

Figure 3.13: Effect of pre- and post-exercise EV depleted plasma on myoblast proliferation, quantified by total cell number (A), BrdU positive nuclei (B) and resazurin fluorescence intensity (C) of proliferating C2C12s following 24-hour incubation with EVs. Shown for individual participant EVs (i) and overall EV populations (ii). All measures are expressed as fold change from C2C12s treated with no-EV (PBS) controls. n=6 biological replicates, error bars = +/- 1 SEM. Statistical significance rejected by 2-tailed paired students T test.
BrdU, 5-bromo-2'-deoxyuridine; EV, extracellular vesicle; PBS, phosphate buffered saline; SEM, standard error of the mean.

3.7 Treating Primary Human Myoblasts with Plasma EVs

3.7.1 Experiment Rationale

To test if the increased proliferation observed in C2C12 cells could be recapitulated in human muscle, primary human myoblasts were incubated with EVs as per C2C12 experiments and total cell number was counted.

3.7.2 Methods

Primary human skeletal myoblasts (HSkMCs) were maintained as per section 2.3.2 and seeded at 2e3 cells/cm^2 in 6 well tissue culture treated plates. Once cells were adhered to the culture surface, total EVs from 10 µL PDP (equal to 5 µL original plasma) were applied per cm^2 of culture surface (n=10 biological replicates), in addition to equal volumes of no-EV controls (n=8). EVs and controls were incubated with the cells for 24 hours at 37°C, 5% CO_2. Cells were then washed and dissociated from the culture surface (section 2.3.2), then counted using a Bio Rad TC20 automated cell counter. All pre- and post- exercise values were expressed as fold changes from the mean no-EV control value from that experiment, and descriptive analysis confirmed normal distribution of data with no outliers. Comparison of pre- and post- exercise means was carried out using a 2-tailed paired students T test.

3.7.3 Results

The increase in HSkMC number after 24 hours incubation was greater for cells incubated with post-exercise EVs than those incubated with pre-exercise EVs (figure 3.14). Fold changes from no-EV controls suggested that overall HSkMCs incubated with pre-exercise EVs proliferate at a rate roughly lower than those incubated with no-EV controls (median fold change <1), whereas HSkMCs incubated with post-exercise EVs proliferated more than those incubated with no-EV controls (median fold change >1)

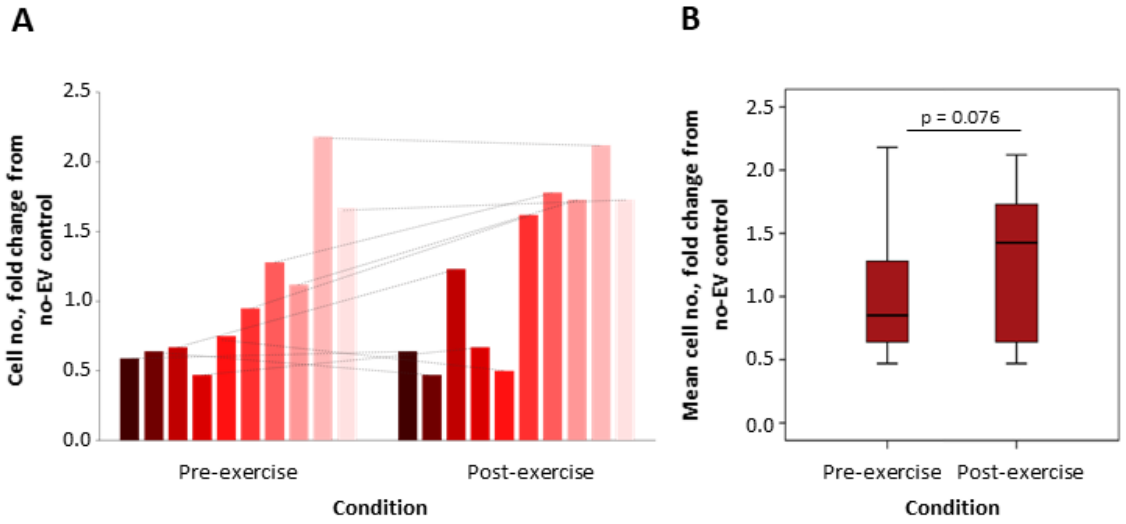

Figure 3.14: Effect of pre- and post-exercise plasma EVs on primary human myoblast proliferation, quantified by number of cells / mL following 24 hour incubation with EVs and expressed as fold change from C2C12s treated with no-EV (PBS) controls. Shown for individual participant EVs (A) and overall EV populations (B) n=10 biological replicates, error bars = +/- 1 SEM, p value generated by 2-tailed paired students T test.
EV, extracellular vesicle; PBS, phosphate buffered saline; SEM, standard error of the mean.

3.8 Discussion

3.8.1 Discussion of Results

To meet the aims of this chapter, *in vitro* models of myoblast proliferation and differentiation were established, and treated with pre- and post-exercise plasma EVs. C2C12 cells were used as a myoblast model cell line, and several complimentary assays were performed to quantify their proliferation and differentiation. Blood EVs were enriched, counted and characterised, and the ability of C2C12 cells to incorporate these EVs was demonstrated by labelling the EVs with a fluorescent dye and visualising their uptake with fluorescent microscopy. Furthermore, effects of the EVs on primary human muscle cell proliferation were also tested, and the likelihood that EVs were acting independently of other plasma components was addressed by treating a C2C12 proliferation model with EV-depleted plasma.

These preliminary results suggest that despite no notable increase in circulating EV number

following moderate intensity cycling, their incubation with muscle progenitor cells results in an increase in myoblast proliferation accompanied by a decrease in differentiation. This alludes to the idea that rather than containing the same cargo but being released in different quantities, EVs released into circulation following physical activity contain different functional molecules to those found in the circulation at rest. Proliferating myoblasts must exit cell cycle in order to differentiate (Walsh and Perlman, 1997); therefore an increase in proliferative status would delay the onset of differentiation. Consistent with this knowledge, we observed an increase in myoblast proliferation accompanied by a decrease in differentiative status in myoblasts treated with post-exercise plasma EVs.

Interestingly, the findings regarding EV number appear to conflict those of Fruhbeis et al. This may be due to considerable differences in exercise intensity: their work focused on a high intensity exercise intervention which was completed by fasted trained male athletes. The work presented here, however, adopted a moderate intensity exercise protocol performed by individuals of both sexes, with varied lifestyles in terms of physical activity (see appendix). Higher intensities of exercise are likely to lead to greater levels of impact associated platelet disruption, and therefore a potential increase in platelet-derived EV release (El-Sayed, 2002). Moreover, it has been hypothesised that trained athletes may have a different EV response compared with untrained individuals (Wardle et al., 2015), and that there might be a difference in EV response between sexes (Gustafson et al., 2015).

EV characterisation studies demonstrated that the particles enriched from whole blood in our hands exhibited size distribution representative of small EVs or exosomes. When testing for EV markers, dot blot assays revealed the presence of HSP70, CD63, CD9, and CD81 proteins in the EV samples. Unusually, significant enrichment of these EV markers was not always observed, though a lack of staining uniformity made it difficult to quantitatively confirm this. The observed lack of enrichment may be reflective of poor EV retention achieved by differential centrifugaiton techniques (Livshits et al., 2015). Alternatively, the presence of contaminant plasma proteins in the EV samples may have had a dampening effect on the detection of marker proteins (further explored in chapter six). The EV marker CD81 appeared to be most highly expressed by the plasma EVs. This can be supported by a much more in-depth

analysis performed by Kowal et al. (2016), who demonstrated that while CD63 and CD9 were moderately enriched in all pellets generated by the differential centrifugation of conditioned medium (2,000 xg, 10,000 xg and 100,000 xg), CD81 was much more highly expressed in smaller EVs (found in the 100,000 xg pellet) than in the cell lysate and all other centrifugation pellets.

A plethora of cell types release EVs, so those found in circulation following exercise could originate from any number of cells and tissues affected by physical activity which come into contact with plasma. It has however been proposed that contracting muscle might contribute the majority of circulating secreted factors due to its major role in performing the physical work of exercise. In support of these EVs originating from muscle, EVs from cultured C2C12 myotubes have been demonstrated to transfer small RNAs into recipient C2C12 myoblasts (Forterre et al., 2014), and EVs from differentiating human skeletal muscle cells were shown to alter the differentiation of recipient human skeletal muscle *in vitro* (Choi et al., 2016). In line with our findings, Guescini et al. (2017) simulated muscle contraction by exposing cultured myotubes to mild oxidative stress (H_2O_2) conditions. Small EVs produced by these myotubes were harvested and incubated with naive differentiating C2C12 cells, and were shown to decrease their differentiative status whilst increasing their proliferative status compared with control EVs. This work elegantly demonstrated that muscle may regulate its own proliferation via EV release. EVs derived from other cell types might also be responsible for the functional effects of plasma EVs on skeletal muscle. For example, EVs derived from mesenchymal stem cells were shown to increase muscle regeneration in an in *vivo* mouse model of muscle injury (Nakamura et al., 2015).

3.8.2 Experimental Limitations

C2C12 Cells

The C2C12 cell line is a subclone of C2 myoblasts originally obtained by Yaffe and Saxel in 1977, with behavioural properties corresponding to those of muscle progenitors (Yaffe and Saxel, 1977). C2C12s were chosen for this project as they are well characterised, and have been extensively used to study mechanistic biochemical pathways in muscle cells *in vitro*.

Dividing C2C12 cells are considered comparable to activated satellite cells in adult muscle, whilst non-dividing cells are representative of quiescent satellite cells (Yoshida et al., 1998). C2C12 cells spontaneously differentiate in culture after serum removal (Blau et al., 1985), and rapidly fuse to form contractile myotubes expressing characteristic muscle proteins such as myosin. They have therefore also been widely adopted as a means of identifying molecules and pathways involved in muscle progenitor differentiation.

One obvious constraint of this cell choice was the use of an immortalised cell line. Immortal cell lines provide a cost effective, relatively quick means of testing hypotheses without ethical concerns associated with the use of animal and human tissue. They also provide a pure population of cells, which in theory aids collection of consistent and reproducible results. Despite being a popular and potentially powerful tool, one must be cautious when extrapolating information from immortalised cell behaviour: any cell lines used should exhibit functional features as close to primary cells as possible, which was considered when choosing a cell line as well characterised as C2C12. However, since cell lines are genetically manipulated, their phenotype, native functions, and their responsiveness to stimuli may be somewhat different to that of their primary cell counterparts.

Primary human myoblasts were treated with pre- and post- exercise EVs to confirm that previous observations were not influenced by the use of an immortalised cell line. Unfortunately, due to the interest of time, the full proliferation and differentiation protocols could not be repeated. Therefore only total cell number was quantified in the human myoblasts, and this was carried out using an automated cell counter on trypsinised cells rather than counting stained nuclei and measuring BrdU incorporation / resazurin reduction. Though the cell counts performed do corroborate an increase in myoblast proliferation following incubation with post-exercise EVs, repeating the full proliferation and differentiation assays would have been preferable.

Controls

PBS was added to the cell models as a no-EV control in each experiment. This allowed myoblast proliferation and differentiation in the presence of rest and exercise EVs to be

compared with these processes in cells incubated with no EVs at all. In a separate experiment, myoblasts treated with equal volumes of rest and exercise EV-depleted plasma were also assessed. It is unclear if the very process of EV depletion might affect other plasma components and therefore their potential impacts on myoblast proliferation and differentiation. Suitable additional controls could therefore include the addition of pre- and post-exercise EV-depleted plasma and whole plasma in every myoblast proliferation and differentiation experiment.

Resazurin Assay

This assay was chosen due to its logistical simplicity: it proved much less time consuming to perform than fixing, staining and imaging cells. A limitation of this assay, however, is its dependence on mitochondrial enzymes (Gonzalez and Tarloff, 2001). Should post-exercise EVs alter the metabolic rate of recipient cells, a change in resazurin reduction disproportionate to the number of cells present might be observed. This assay could therefore only be utilised in conjunction with the more robust techniques of cell counting and BrdU incorporation.

EV Characterisation

Current limitations in available technology mean that characterising and even counting EVs can be problematic. Due to limited quantities of available plasma (and therefore plasma EVs), the presence of characteristic EV protein / RNA markers was not robustly established in our hands. Furthermore, despite being the most widely used EV counting technology available, NTA cannot distinguish between particles of a similar size with different physical properties. It is therefore plausible that pre- and post-exercise EV counts presented here and by the work of Fruhbeiss et al. were compromised by the presence of other blood components such as protein aggregates and lipoproteins, which would also have been captured and tracked by NTA software. This possibility has been further explored by the work presented in chapter six.

EV Labelling and Uptake

PKH26 was used to fluorescently label EVs and visualise their uptake by C2C12 cells. PKH26 is a highly fluorescent and physiologically stable lipophilic dye, which administers little to no

toxic side-effects on recipient cells. Lipophilic dyes stain cell membranes by intercalating their aliphatic portion into the exposed lipid bilayer (Wallace et al., 2008). The use of lipophilic dyes for labelling and tracking cells in *vivo* and *in vitro* is well established, and as the field of extracellular vesicles expands they have also been used to label EV membranes and demonstrate their incorporation by cells (Riches et al., 2014; Franzen et al., 2014). However, the formation of PKH26 dye aggregates can result in false-positive signals for stained EVs that therefore undermine effective interpretation of EV internalization (Dominkuš et al., 2018). In this experiment, PKH26-labelled EVs were compared with a dye-only control, which contained notably fewer fluorescent particles than experimental images. However, it cannot be completely ruled out that some flourescent nanoparticles observed in the labelled EV images were in fact aggregates of unbound dye. It has been recently suggested that for use in EV uptake and functional studies, PKH26-labelled EVs be purified by sucrose-gradient-based isolation to better remove aggregates of PKH26 dye (Dominkuš et al., 2018). Moreover, as highlighted in section 3.6.3, it is not certain from images obtained in a single focal plane whether the fluorescent particles were inside the C2C12s, or instead bound to the cell surface. Establishing this by imaging in several focal planes to generate a series of 'Z stacks' could perhaps suggest whether plasma EVs alter proliferation and differentiation process by binding cell surface receptors, or instead act via incorporation by the target cell.

Dot Blot Assays

Dot blot assays were used to demonstrate the presence of known EV markers in the plasma EV samples. These assays provide a simple means of testing for the presence of a protein of interest and require relatively small amounts of sample, making them particularly suitable for this project. Though dot blot assays rely on the same immunological principles as western blotting, they cannot separate proteins by size. This can therefore limit elimination of false positives, though matched PDP controls and PBS negative controls were used in all assays. As an alternative to a housekeeping control, an assay was performed to test for the presence of Calnexin: a chaperone protein which is confined to the endoplasmic reticulum of cells, and therefore should not be associated with EVs. Calnexin did appear to be notably reduced in EV samples compared with PDP controls (figure 3.5).

Closing Remarks

Though there are certainly experimental limitations to consider, multiple complimentary techniques have been employed in unison to demonstrate as best as possible that the observed changes in myoblast proliferation and differentiation are discernible and meaningful. This part of the project has adopted relatively quick and cost-effective approaches to generate results on which to base further lines of enquiry. The results intriguingly suggest that small ($\sim$100 nm) circulating vesicles positive for common EV protein markers can regulate recipient myoblast behaviour. Further work will aim to address if neural stem cells respond to post-exercise EV treatment in a comparable manner, and which EV cargo molecules might be causing such changes in recipient cell behaviour.

Chapter 4

Circulating Vesicles and Adult Neurogenesis

4.1 Introduction

4.1.1 Background

Adult neurogenesis involves the activation of quiescent neural stem cells (NSCs) to enter cell cycle, proliferation of their progeny, and subsequent commitment of these cells to a neuronal fate as they terminally differentiate into mature functional neurons (reviewed by Gonçalves et al., 2016). Research to date suggests that adult neurogenesis is confined to just two regions of the brain: the DG and the SVZ. Adult neurogenesis increases with regular aerobic exercise (Tharmaratnam et al., 2017) and has been linked to improved learning and memory (Gibbons et al., 2014). Physical activity may increase hippocampal neurogenesis via tissue cross-talk between multiple organs and the brain (Yau et al., 2014; Sleiman et al., 2016; Delezie and Handschin, 2018). Data presented in the previous chapter indicated that circulating small EVs enriched from post-exercise plasma increase the proliferation of recipient myoblasts *in vitro*. Collaborators in the Department of Physiology, Anatomy and Genetics, Oxford University, had well established models of neural stem cell proliferation and differentiation, routinely used to assess the effects of different therapeutic agents on these cellular processes: to test if exercise-induced small EVs could also modify NSC behaviour, EVs were applied to these existing models. NSC models used primary NSCs obtained from both the DG and SVZ neurogenic niches of young mice.

4.1.2 Aims and Objectives

The experiments described in this chapter aimed to investigate if exercise-induced circulating small EVs could alter the proliferation and differentiation status of recipient NSCs. The objective of this chapter therefore was:

- To assess the effect of pre- and post-exercise small plasma EVs on NSC proliferation and differentiation *in vitro*.

4.2 Treating Neural Stem Cell Proliferation and Differentiation models with Plasma EVs

4.2.1 Experiment Rationale

Primary NSCs can be cultured *in vitro* for several passages after harvesting. Culturing on ployhaeme-coated surfaces prevents the cells from adhering to the culture surface and instead encourages formation of 3D neurospheres, the size and number of which can be quantified as a measure of NSC proliferation rate (Jensen and Parmar, 2006). This model was treated with pre- and post-exercise EVs to test their potential effects on NSC proliferation rate.

Culturing on a laminin-coated surface and removing growth factors from the medium encourages NSCs to adhere to the culture surface and begin to differentiate. As NSCs begin to differentiate they can resemble neuronal, astrocyte, or oligodendrocyte fates, each with distinct morphology and expression profile of protein markers (Trujillo et al., 2009) (figure 4.1). It was therefore tested if treating differentiating NSCs with pre- and post-exercise EVs might alter their commitment to each of these cell fates.

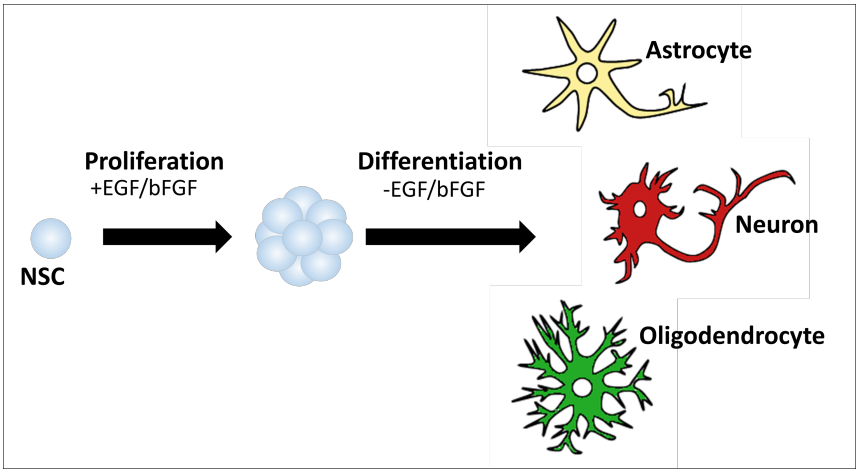

Figure 4.1: Schematic representation of *in vitro* neural stem cell proliferation and differentiation. bFGF, basic fibroblast growth factor; EGF, epidermal growth factor; NSC, Neural stem cell.

4.2.2 Methods

Euthanised mice, plus training in brain dissection and NSC primary culture were kindly provided by Dr Julie Davis in the Department of Physiology, Anatomy and Genetics, Oxford University.

NSC Proliferation

Primary NSCs were obtained from the neurogenic niches of young mice and maintained in culture, as per sections 2.3.1 and 2.3.2. On the third passage of culture, NSCs from DG and SVZ brain regions were plated as single cells at $2.2x10^4$ cells/cm^2 in repellent culture dishes and incubated for 24 hours to allow neurosphere formation. Neurospheres were then incubated with complete growth medium (table 2.2) plus total EVs from 10 µL pre- or post-exercise PDP (equal to 5 µL original plasma) per cm^2 of culture surface (n=5 biological replicates), or an equal volume of PBS for an additional 48 hours. Neurospheres were imaged via light microscopy to assess neurosphere number and size in each treatment.

NSC Differentiation

Primary NSCs were obtained from the neurogenic niches of young mice and maintained in culture, as per section 2.3.2. On the third passage of culture, DG and SVZ NSCs were plated at $3.3x10^4$ cells/cm^2 in laminin coated dishes (section 2.3.5) containing differentiation medium (table 2.2) to induce NSC differentiation. NSCs were immediately treated with pre- and post-exercise plasma EVs (EV amounts as above, n=5 biological replicates) and PBS controls, and incubated for 7 days. On day 7 of differentiation, NSCs were fixed and stained for neuron, astrocyte and oligodendroctye protein markers (section 2.4.3), then imaged via fluorescent microscopy (figure 4.4). Images were blinded, and total cells per field of view expressing protein markers corresponding to neuronal, astrocyte and oligodendrocyte cell fates were counted. In addition to protein staining, cell morphology was used to help inform counting of the precursor cells: smaller cell bodies and nuclei are typically associated with neurons, whereas larger cell bodies and nuceli are associated with astrocytes. Extensive branching of cell processes can be used to identify oligodendricytes.

Three protein markers were used to label differentiating NSCs: Neuron-specific Class III β-Tubulin (TuJ1), Glial fibrillary acidic protein (GFAP), and Microtubule-associate protein-II (MAP-2). These were used to label neuron, astrocyte and oligodentrocyte -type precursors, respectively.

TuJ1 is a tubulin involved specifically during differentiation of neuronal cell types (Lee et al., 1990). Accordingly, immunostaining of TuJ1 is found in the cell bodies, dendrites, axons, and axonal terminations of immature neurons. A powerful advantage associated with TuJ1 immunostaining is the degree to which it is capable of revealing the fine details of neural processes, which can be difficult to otherwise visualise (Tanapat, 2013). Although a form of β-Tubulin is also found in glial cells, it is not recognised by antibodies specific for TuJ1, making this protein an appropriately specific marker for immature neurons (Geisert Jr and Frankfurter, 1989).

GFAP is an intermediate filament protein that provides support and strength to cells whilst controlling their shape, movement, and function (reviewed by Omary et al., 2004). It is one of the most widely used protein markers of astrocytes, and is expressed by neural stem cells with astrocyte properties in the adult brain (Doetsch et al., 1999).

MAP-2 regulates cellular architecture and is expressed in cultured oligodendrocytes and neurons (Müller et al., 1997). Although MAP-2 also is typically expressed by neurons, it is only very weakly expressed by immature/differentiating neuroblasts, and only becomes very prominent in later staged of neuron maturation (reviewed by Dehmelt and Halpain, 2005). Morphology of oligodentrocytes *in vitro* is very distinct from other neural cell types (figure 4.1), which aids their identification in addition to immunostaining.

Statistical Analysis

For reproducible comparison, all cell counts were normalised to the average of no-plasma controls from the corresponding experiment. Descriptive analysis of all datasets was performed using SPSS-25 software, including a Shapiro-Wilk test for normal distribution. Normal distribution of the data allowed for parametric comparison of pre- and post- exercise means with a 2-tailed paired students T test for each cell type.

4.2.3 Results

NSC Proliferation

Unusually, after 48 hours of incubation the NSCs treated with EVs had dissociated from their neurosphere structures and adhered to the culture surface, rendering the initial plan of observing neurosphere size and number impractical. It could be observed, however, that NSCs not treated with EVs maintained neurosphere formation (fig 4.2), whereas those treated with rest or exercise EVs adhered to the culture surface (fig 4.2). This NSC adherence was observed in DG and SVZ cells treated with pre-exercise and with post-exercise EVs, suggesting a role of all circulating EVs in mediating this effect rather than exercise-induced EVs alone. Moreover, some images captured of the SVZ NSCs treated with plasma EVs contained cells which had adhered in quite specific chain formations (figure 4.3). This was not observed in PBS controls or in DG cells.

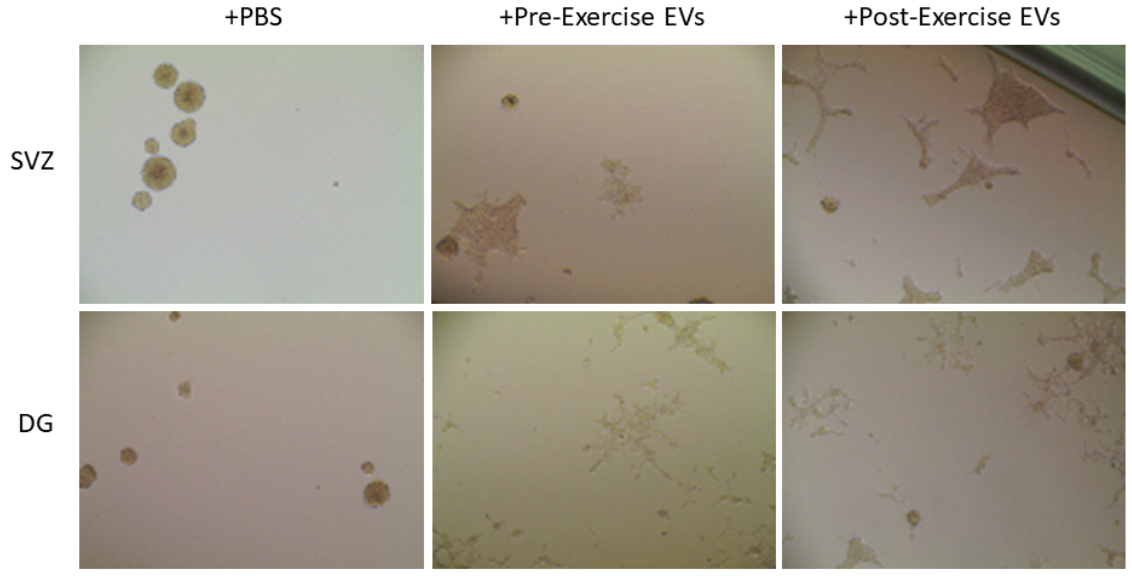

Figure 4.2: Representative images of SVZ and DG neurospheres cultured with participant matched pre- and post-exercise plasma EVs for 48 hours.
DG, dentate gyrus; EV, extracellular vesicle; SVZ, subventricular zone.

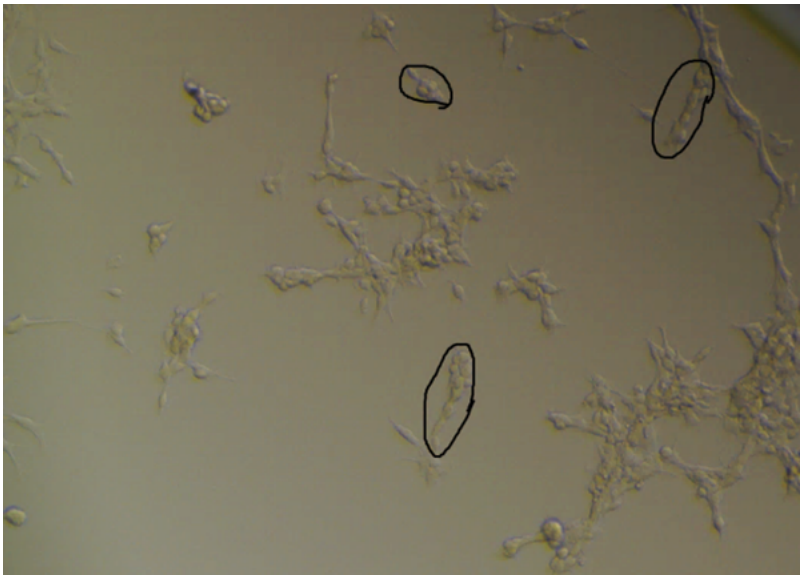

Figure 4.3: Representative image of chain formation in SVZ neurospheres cultured with plasma EVs for 48 hours.
EV, extracellular vesicle; SVZ subventricular zone.

NSC Differentiation

Wells of DG and SVZ cells treated with post-exercise EVs contained a larger number of neuron-like precursors than wells treated with pre-exercise EVs (figures 4.4 and 4.5). This observed difference was greater in SVZ-derived stem cells (2-tailed paired T test, $p=0.016$) than in DG-derived stem cells (2-tailed paired T test, $p=0.098$). Interestingly, the number of cells exhibiting oligodendrocyte and astrocyte morphology and protein markers did not notably change between pre- and post-exercise EV treatments, in SVZ- or DG-derived NSCs (figure 4.5).

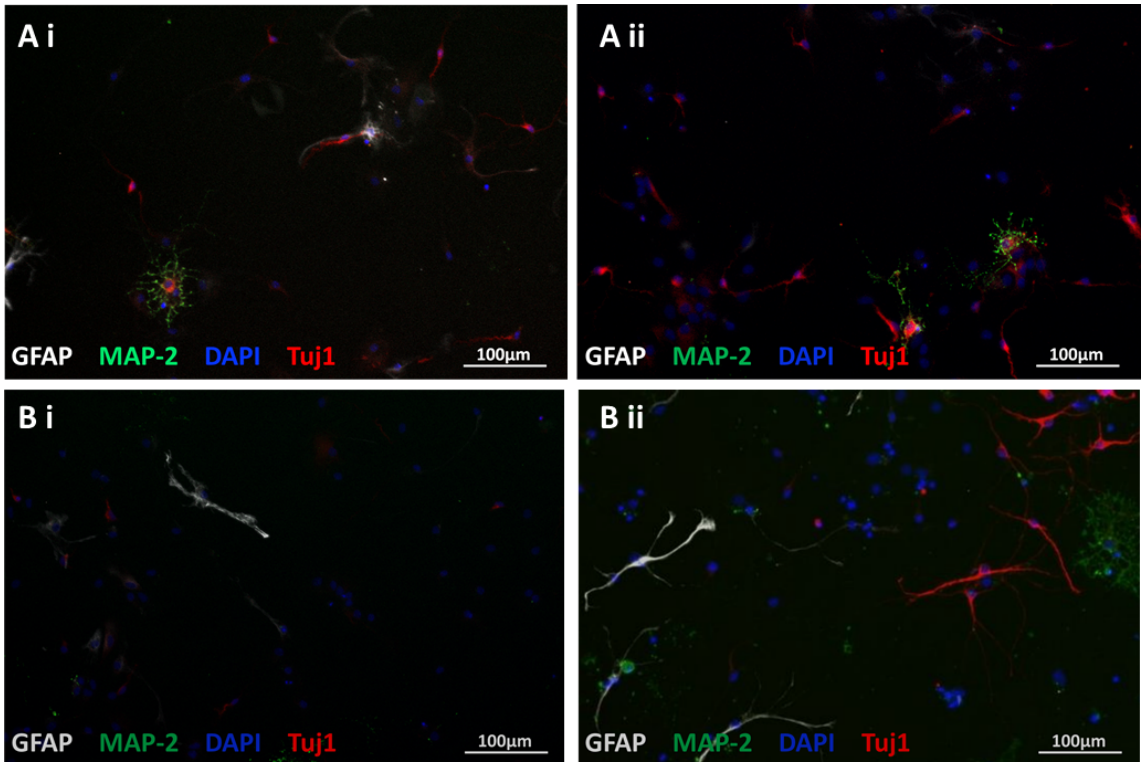

Figure 4.4: Example images of EV-treated NSC staining and morphology. DG (A) and SVZ (B) -derived NSCs treated with pre-exercise (i) and post-exercise (ii) EVs. Neurons seen in red, astrocytes in white, and oligodendrocytes in green.
DAPI, 4′,6-diamidino-2-phenylindole; DG, dentate gyrus; EV, extracellular vesicle; GFAP, Glial fibrillary acidic protein; MAP-2, Microtubule-associated protein-II; NSC, neural stem cell; SVZ, subventricular zone; Tuj1, Neuron-specific Class III β-Tubulin.

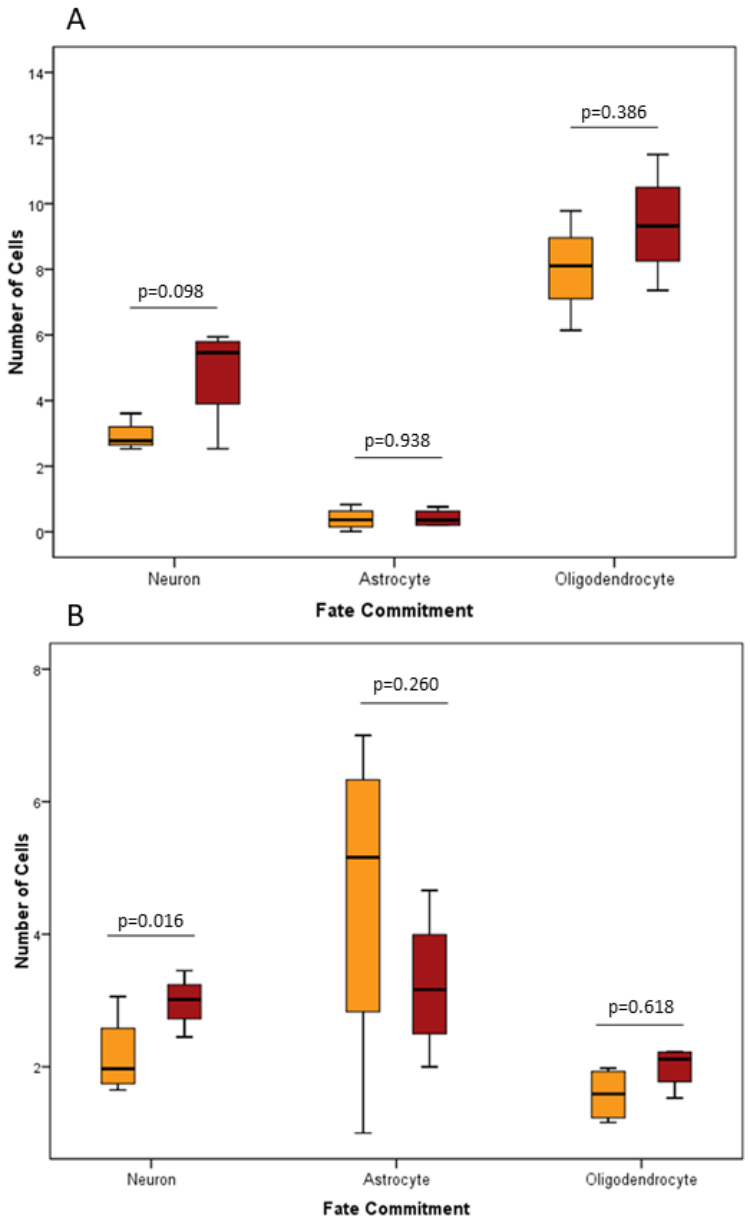

Figure 4.5: Fate Commitment of DG (A) and SVZ (B) neural stem cells treated with pre-exercise (orange) and post-exercise (red) plasma EVs. All cell counts normalised to those of PBS controls. n=5 biological replicates, p value generated by 2-tailed paired students T test.
DG, dentate gyrus; SVZ, subventricular zone.

4.3 Discussion

4.3.1 Discussion of Results

To meet the aims of this chapter, existing *in vitro* models of NSC proliferation and differentiation were treated with pre- and post-exercise plasma EVs. Preliminary results suggest that all plasma EVs promote the dissociation and adherence of proliferating neurospheres, and that exercise-induced plasma EVs encourage the neuronal fate commitment of differentiating NSCs.

Dissociation and Adherence of NSCs

The dissociation and adherence of proliferating NSCs in culture can indicate the onset of their differentiation (Logan, 2015). Interestingly, in other models of NSC behaviour animal sera can be used to drive the differentiation of otherwise proliferating NSCs, resulting in cell behaviour comparable with that observed in our own experiments: NSCs are typically cultured in the absence of foetal bovine serum (FBS), however culturing neurospheres with 1-10% FBS prompts them to dissociate from these structures, adhere to the culture surface, and subsequently differentiate (Logan et al., 2015; Bonnert et al., 2006). It has been demonstrated in other cell types that removal of serum EVs can negatively alter the behaviour of cultured cells usually grown in FBS. For example, myoblasts cultured in EV-depleted FBS exhibit aberrant proliferation and differentiation (Aswad et al., 2016), and T-lymphocytic cell lines cultured in EV-depleted FBS exhibit changes in cell behaviour and viability, which are restored when serum EVs are re-introduced (Liao et al., 2017). These experiments therefore imply that blood EVs may mediate an important portion of the effects of whole serum on cell behaviour. No such experiments have been performed with neural cells. Nonetheless, the evidence gleaned from other cultured cell types poses that here we may see plasma EVs inducing NSC adherence and differentiation just as the addition of serum would.

NSC Chain Formation

An interesting observation of this work is the formation of adherent cell chains amongst some of the SVZ neurospheres treated with plasma EVs. This may be indicative of a well-known

migratory process that occurs throughout life in rodent brains (Altman, 1969): the rostal migratory stream (RMS). The RMS is a movement of neuronal precursor cells through the brain, from the SVZ to the olfactory bulb (OB) . The cells move at high speed (20e30 mm / hr) as a connected chain also bound by astrocytes (Lois et al., 1996), migrating roughly 500 cell diameters in mice before they reach the OB and differentiate to become functional interneurons (Goldman and Luskin, 1998). Migrating cells appear to navigate not only by contact cues such as the neural cell adhesion molecule CD56 (Wang et al., 2011), but also by long range signalling from target cells using molecules including Netrin, Glial cell line-derived neurotrophic factor (GDNF), BDNF and HGF (Sun et al., 2015). This phenomenon has been successfully recapitulated in culture: when plated on Matrigel to mimick the presence of extracellular matrix (ECM), SVZ explants emit long, connected chains of neuronal precursors which are highly motile (Wichterle et al., 1997). Plasma is considered the ECM of blood (Rehfeld et al., 2017), and EVs are known to carry several molecules in common with ECM, such as enzymes and glycoproteins (Vallhov et al., 2011; Esser et al., 2010). It therefore appears that treating neurospheres with plasma EVs may have introduced signalling molecules to the cells, or even mimicked the presence of extracellular matrix (ECM) components which weren't otherwise present in the culture conditions, thus promoting the formation of NSC chains in culture.

The RMS functions to enable refinement of a mammal's sensitivity to smells, particularly in rodents (Hack et al., 2005). Human olfactory sense is much less developed than that of rodents, and therefore the presence and functional relevance of an analogous RMS in adult humans has been difficult to identify. However relatively recent work by Wang et al reported, for the first time, the presence of doublecortin-expressing cells between the SVZ and OB of adult human brains, implying that these cells are indeed migrating along a route comparable to a true RMS. Their complete findings suggested that a human RMS exists, but that only a few migrating neuroblasts follow this stream (Wang et al., 2011). Neuroblasts have also been shown to migrate from the SVZ toward sites of damage following an insult such as stroke or traumatic injury (Zhang et al., 2009). These cells are guided by chemoattractants secreted from the injured area, and migrate in chain formations much like those of the RMS

(Sawada et al., 2014). Though hippocampal neuroblasts do also migrate short distances (Sun et al., 2015), chain formation has not been described in the literature to date as an aspect of hippocampal neuron migration. In conclusion, although its exact physiological significance in humans remains unclear, chain formation is seemingly required for the efficient, coordinated movement of SVZ neuroblasts through adult brain tissue. The recapitulation of such a dynamic process in the NSC models suggests a potent activating effect of EVs on the recipient cells, however the exact physiological importance of this effect remains unclear.

Neuronal Fate Commitment

Treatment of differentiating NSCs with exercise-induced small plasma EVs resulted in increased neuronal fate commitment in both DG and SVZ cells. To our knowledge, this is the first example of plasma EVs contributing to the regulation of NSC fate commitment. Though little work has been carried out in the context of normal or exercise physiology, emerging evidence shows that EV-mediated signalling impacts neuronal firing, synaptic plasticity, and myelin formation, and may also support neuroregeneration and neuroprotection in disease conditions (reviewed by Holm et al., 2018). Intriguingly, such signalling is thought to be mediated not only by neuron and glial cell EVs, but also by periphery-derived EVs which might be found in circulation. For instance, EVs derived from mesenchymal stem cells (MSCs) have been shown to improve neuronal cell survival and regeneration after injury: increased neuronal survival was observed in an *in vitro* stroke model treated before or after injury with MSC EVs, driven by activation of the phosphoinositide 3-kinase (PI3K)/AKT pathway (Scheibe et al., 2012). In accordance with this finding, systemic administration of MSC EVs to an *in vivo* rat model of stroke led to functional recovery and neurovascular plasticity (Xin et al., 2013). Furthermore, mouse fibroblast EVs increased neurite outgrowth in vitro and *in vivo*, via autocrine activation of Wnt10b and consequent activation of mammalian target of rapamycin (mTOR) (Tassew et al., 2017). EVs may therefore embody a targeted inter-organ communication system involving the brain and several other distal organs, which could be implicated in several different physiological and pathological states.

4.3.2 Experimental limitations

Primary Neural Stem Cells

Neurosphere culture was the first *in vitro* system to demonstrate the presence of true neural stem cells in the adult brain (Reynolds et al., 1992). It is widely used to assess NSC proliferation and differentiation and, when performed correctly, provides the best available functional assay for these processes (reviewed by Jensen and Parmar, 2006; Gordon et al., 2013). Though primary cultured cells are the closest *in vitro* forms of the cells that they represent in normal tissues, some disadvantages and limitations are still associated with their use: they have a poor lifespan, and prolonged culture leads to cellular senescence or to the introduction of genetic mutation, both of which will have an adverse effect on reliable quantification of proliferation and differentiation (Jensen and Parmar, 2006). There is therefore only a very narrow window in which to perform experiments following dissection, to ensure optimal health and growth rate of the cells. This greatly restricts the availability of such cells for experimental work. Another observation encountered in primary cultures is that many cells lose their structural and functional characteristics when removed from *in vivo* conditions. Manipulation of the culture environment is used to deplete cell types other than those of interest (Ng and Schantz, 2010; Fauza and Bani, 2016), which may ablate important intercellular communication that occurs *in vivo*. Though cultured as 3D spheres in these models, the primary NSCs may lose several behavioural characteristics otherwise maintained *in vivo* due to a lack of other cell types usually found in the neurogenic niche microenvironment (Jensen and Parmar, 2006).

Blood-Brain Barrier

A key point for consideration is the capacity for plasma EVs to cross the blood-brain barrier (BBB) in an *in vivo* setting. The BBB is formed by a monolayer of specialised endothelial cells separating the blood from the cerebrospinal fluid, which are characterized by high-resistance tight junctions. These cells form a semipermeable membrane which durably restricts the passage of cells, particles, and large molecules into the cerebrospinal fluid (CSF). Inability of small EVs to cross the BBB could of course render any findings regarding their effects on neural stem cells physiologically irrelevant. It is well described that in the context of

neuroinflammation and traumatic injury the integrity of the BBB is compromised by pro-angiogenic factors, allowing easy access of small particles into the CSF and therefore the neural cells it comes into contact with (reviewed by Obermeier et al., 2013). However as properties of the BBB continue to be unravelled, there is still some debate as to whether small EVs can cross the BBB in normal physiology. It has been suggested however that the healthy BBB can undergo periods of local, reversible hyperpermeability in order to support neurogenesis and therefore aid learning and memory (reviewed by Pozhilenkova et al., 2017). Vazana et al. (2016), for example, showed that the action of glutamate through N-methyl-d-aspartate receptors expressed by the BBB can transiently elevate its permeability in the cortex. Moreover, neurogenic niches posses unique characteristics which may make them better able to receive systemic factors than other brain regions. Both the DG and the SVZ contain dense microvasculature to support cell renewal, proliferation, and differentiation, which may aid access to circulating factors in these regions (Bjornsson et al., 2015). Tavazoie et al. (2008) demonstrated that NSCs in the SVZ directly contact blood vessels, and that vascular walls contain fewer tight junctions in this region. They therefore hypothesised that the BBB may exhibit permanently increased permeability in the SVZ, thus exposing this neurogenic niche to circulating particles. Interestingly, our finding that SVZ neuronal fate commitment was more sensitive to plasma EV treatment than that of DG cells is consistent with the idea that the SVZ may receive greater exposure to systemic factors than the DG *in vivo* (Pozhilenkova et al., 2017).

In support of these ideas, several published works have functionally demonstrated that small EVs (exosomes) can in fact cross the BBB and deliver RNA cargo to cells of the central nervous system. This has been demonstrated in inflammatory states, and importantly also under normal physiological conditions (Alvarez-Erviti et al., 2011; Ridder et al., 2014; Chen et al., 2016). Of particular interest, Alvarez-Erviti et al. (2011) demonstrated that the Systemic injection of EVs loaded with *GAPDH* siRNA resulted in delivery of this siRNA to neurons, microglia, and oligodendrocytes in the healthy brain. Villeda et al. (2011) additionally showed that age-related chemokines found in the plasma were able to cross the BBB and consequently regulate neurogenesis in the DG. Further work is required to fully establish exactly how the BBB may permit entry of small molecules to neurogenic niches, however the literature to date

provides some promising evidence that circulating small EVs can access these brain regions.

Closing Remarks

Incubation of neural stem cells derived from DG and SVZ brain regions with plasma EVs resulted in phenotypic changes which allude to a shift toward NSC migration and differentiation. Most excitingly, SVZ-derived NSCs exhibited a statistically significant increase in neuronal fate commitment when incubated with post-exercise EVs. The full functional importance of this phenomenon in the SVZ of humans remains unclear, but adult neurogenesis is important for olfactory- and hippocampus-dependent learning and memory which are enhanced by exercise.

Chapter 5

Investigating Mechanisms of Action

5.1 Introduction

5.1.1 Background

Experimental results reported thus far have suggested that exercise induced circulating EVs have functional effects on recipient muscle and neural stem cells, imparted by specific EV cargo molecules rather than a change in EV concentration. The next logical step was therefore to identify EV cargo molecules which might be responsible for these observations. To further support previous functional experiments, recipient cells were also profiled for modifications in signalling proteins associated with proliferation after a brief incubation with pre- and post-exercise EVs.

5.1.2 Aims and Objectives

The experiments described in this chapter aimed to investigate mechanistic the properties of exercise induced EVs, which we have shown to alter recipient myoblast and NSC proliferation and differentiation. The objectives of this chapter therefore were:

- To profile pre- and post- exercise plasma EVs using proteomic techniques.
- To assess post-translational modifications in signalling proteins of cells treated with pre- and post- exercise plasma EVs *in vitro*.

5.2 Proteomic Profiling of Plasma EVs

5.2.1 Rationale

As experiments thus far have demonstrated that post-exercise plasma EVs have some functional effects on recipient muscle and neural stem cells, this experiment aimed to identify EV-associated proteins which might be responsible for our observations. To do this, total protein was extracted from pre- and post-exercise plasma EVs, and mass spectral analysis was performed by

collaborators at the university of British Columbia. They performed liquid chromatography-tandem mass spectrometry (LC-MS/MS) using label-free quantitation (LFQ) techniques, to minimise sample processing and to enable whole proteome coverage. This method correlates the direct mass spectrometric signal for any given peptide with the absolute protein quantity, to generate an intensity value representative of the protein abundance in the original sample (see Nagara, 2014).

5.2.2 Methods

Exercise Protocol and Blood Processing

Healthy fasted participants cycled for 15 minutes, maintaining 60% HR_{max} throughout (n=5). Blood samples were collected by venepuncture before and 1 hour following exercise and participant age, sex, height and weight were again recorded (see appended section A1). Whole blood samples were processed to PDP as per section 2.7 and stored at -80°C within 3 hours of blood collection. Once all participant interventions had been performed, PDP samples were thawed and EVs were enriched by differential centrifugation (section 2.8).

Mass Spectrometry

Total protein was extracted from pre- and post-exercise plasma EVs as per section (2.11.1). Protein was quantified as per section (2.11.2), and shipped to collaborator Dr Craig Kerr and colleagues in the Department of Biochemistry and Molecular Biology, University of British Columbia, who performed LC-MS/MS using LFQ techniques to compare peptide intensities between pre-exercise and post-exercise EV samples (n=5 biological replicates).

Data Analysis

Once normalised LFQ intensity values were received, proteins with different LFQ intensities between groups (2-tailed paired students T test, p-value <0.05) were identified. A volcano plot was generated, plotting statistical significance vs fold change of LFQ intensity values.

Reactome software (v67) was used to perform a pathways analysis of the proteins significantly

altered in exercise EVs (fold change >2; 2-tailed paired students T test, p value <0.05). Reactome is a manually curated database of pathways and their composite reactions in human biology, a 'reaction' being defined as any event in biology that alters the state of a biological molecule. An in-software Fisher's exact test (suitable for small sample sizes) was performed to determine overrepresentation of pathways associated with the submitted proteins, asking the question 'Does this list contain a greater proportion of proteins that interact with pathway X than would be expected by chance?'. A reactions ratio was used to determine the importance of each matched protein within a pathway, by calculating the number of individual molecules within a given pathway that interact with the inputted protein(s). Finally, the p-value generated for each pathway-protein association was corrected using Benjamini-Hochberg False Discovery Rate (Croft et al., 2013).

To complement these data and ask the same question of known gene ontolgoy (GO) terms, GO analysis was carried out by inputting the gene IDs corresponding to each detected protein into PANTHER classification software (v14.0) (see Mi et al., 2013). The software implemented a Fisher's exact test with Bonferroni correction to identify statistically significant overrepresentation of GO terms. This was performed with all detected proteins, and with any proteins altered by exercise (LFQ fold change >2). Finally, tissue enrichment of differentially detected proteins (LFQ fold change >2) was assessed using the Human Protein Atlas (HPA) : a curated tissue-based map of the human proteome (Uhlén et al., 2015).

5.2.3 Results

GO analysis of all plasma EV samples highlighted that proteins most enriched in the samples were associated with annotations describing vesicles and EVs (figure 5.2 A), thus demonstrating that DC methods had successfully enriched EVs from the plasma (figure 5.2 A). HPA described the majority of increased proteins as known secreted or plasma proteins, confirming removal of cell fragments from the EV preparations. Interestingly, though many of the proteins increased by exercise are expressed in all tissues, a majority of these proteins displayed tissue enrichment in the liver (*Human Protein Atlas Tissue-based map of the human proteome*, n.d.) (figure

5.4).

According to GO analysis, proteins which increased in post-exercise EVs (fold change >2 compared to pre-exercise EVs) displayed an overrepresentation of GO terms associated with complement activation and clot formation (table 5.1, figure 5.2 B), perhaps indicative of EV contamination with other circulating (non EV-associated) plasma proteins. GO analysis also revealed enrichment of terms associated with lipoprotein and chylomicron remodelling (table 5.1, figure 5.2 B), which may represent systemic communication via EVs to the liver or small intestine where lipoproteins are made. This could however also represent contamination of EVs with circulating lipoproteins, which are similar in size and density to small EVs (Yuana et al., 2014).

Four proteins which increased in exercise EVs with a fold change >2 and a p value <0.05 were identified (figure 5.1): Apolipoprotein A4 (ApoA-4), Gelsolin (GSN), Coagulation factor 5 (F5), and Serpin family A member 4 (SERPINA4). Pathway analysis of these proteins using Reactome software did not identify an association between these proteins and pathways involved in cell proliferation or differentiation (figure 5.3). Instead, pathways required for lipoprotein and chylomicron assembly and remodelling, platelet activation, and clot formation were overrepresented. No proteins were decreased by exercise with a fold change >2 and a p value <0.05. Unfortunately this analysis did not highlight any stand-out candidate EV cargo proteins which might be responsible for modulating muscle and neural stem cell proliferation and differentiation following exercise.

Table 5.1: Plasma EV proteins increased by exercise (fold change >2), sorted by p-value

Protein Name	Gene	Fold Increase	P Value
Apolipoprotein A4	APOA4	2.48	0.01
Gelsolin	GSN	2.69	0.01
Coagulation Factor 5	F5	7.42	0.02
Serpin family A member 4	SERPINA4	7.32	0.04
Filamin A	FLNA	6.66	0.08
Complement Factor H	CFH	3.27	0.08
Alpha-1-microglobulin	AMBP	15.67	0.13
Selenoprotein P	SEPP1	9.76	0.13
Fibrinogen alpha chain	FGA	2.72	0.14
Pericentriolar material 1	PCM1	8.79	0.15
Carnosine dipeptidase 1	CNDP1	3.72	0.16
Kininogen 1	KNG1	2.84	0.16
Transforming growth factor beta induced	TGFBI	12.09	0.16
Pre-mRNA processing factor 8	PRPF8	6.92	0.18
Complement C4B	C4B	3.76	0.19

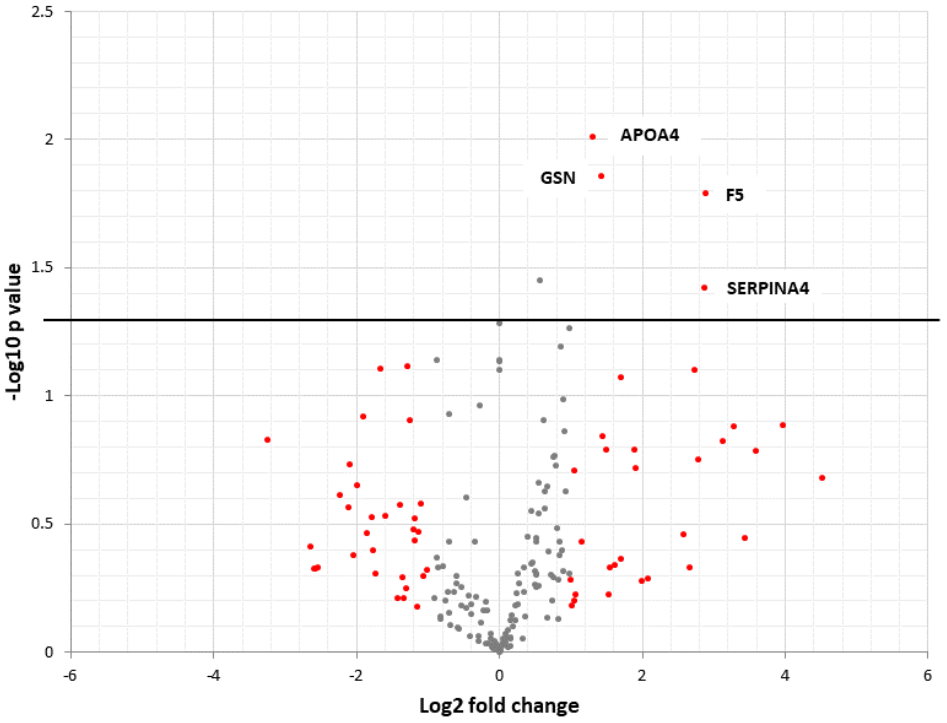

Figure 5.1: Volcano plot of significance vs protein fold change (determined by mass spectrometry) between pre- and post-exercise EVs. n=5 biological replicates. All proteins with a fold change greater than 2 are highlighted in red, line represents p=0.05 (2-tailed paired students T test)
Apo, apolipoprotein; EV, extracellular vesicle; F5, coagulation factor 5; GSN, gelsolin; SERPINA4, kallistatin.

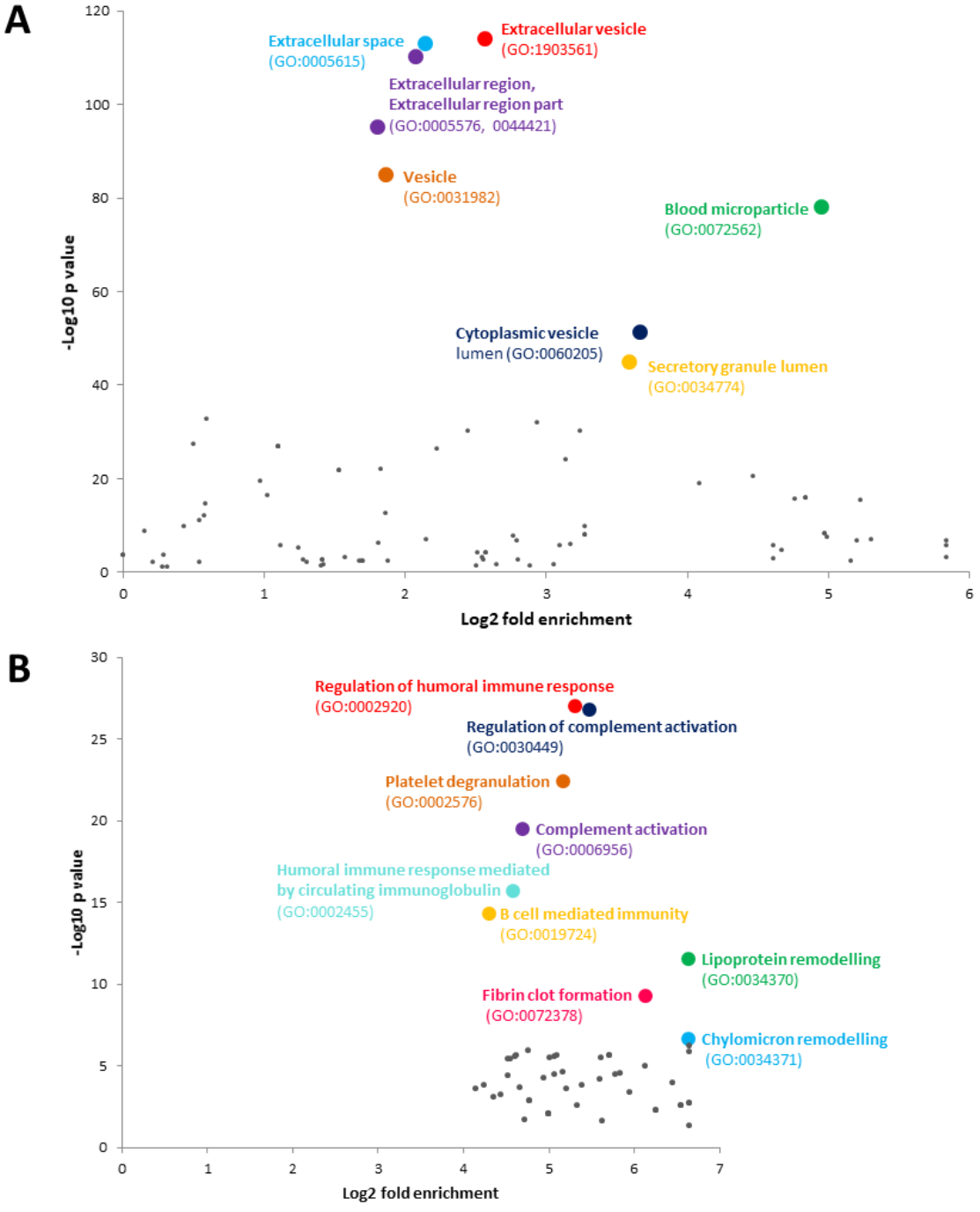

Figure 5.2: GO-terms analysis using Panther (v14.0) software of all proteins detected in plasma EVs (A) and proteins detected at higher intensities in post-exercise plasma EVs (fold change >2) (B). Most significantly enriched proteins have been highlighted and annotated. n=5 biological replicates, p values generated by Fisher overrepresentation test with Bonferroni correction.
EV, extracellular vesicle; GO, gene ontology.

Table 5.2: Pathways associated with ApoA-4, GSN, F5 and Serpina4, detected using Reactome (v67) software, and sorted by p-value.

Pathway Name	**P value**	**Protein(s)**
Assembly of active LPL and LIPC lipase complexes	4.58E-05	APOA4
Plasma lipoprotein remodelling	1.48E-04	APOA4
Amyloid fiber formation	3.91E-04	APOA4, GSN
Plasma lipoprotein assembly, remodeling, and clearance	4.84E-04	APOA4
Platelet degranulation	9.41E-04	F5, SERPINA4
Response to elevated platelet cytosolic Ca2+	0.001	F5,SERPINA4
Platelet activation, signalling and aggregation	0.004	F5, SERPINA4
Caspase-mediated cleavage of cytoskeletal proteins	0.004	GSN
Chylomicron assembly	0.005	APOA4
Chylomicron remodelling	0.006	APOA4
Plasma lipoprotein assembly	0.011	APOA4
Common Pathway of Fibrin Clot Formation	0.012	F5
Cargo concentration to the ER	0.013	F5
Apoptotic cleavage of cellular proteins	0.014	GSN
Formation of Fibrin Clot (Clotting Cascade)	0.018	F5
Apoptotic execution phase	0.019	GSN
COPII-mediated vesicle transport	0.027	F5
Retinoid metabolism and transport	0.028	APOA4
Hemostasis	0.03	F5, SERPINA4
Metabolism of fat-soluble vitamins	0.033	APOA4
Metabolism of proteins	0.036	APOA4, F5, GSN
Post-translational protein phosphorylation	0.038	F5
Transport of small molecules	0.041	APOA4
Regulation of Insulin-like Growth Factor transport and uptake	0.045	F5

Apo, apolipoprotein; F5, coagulation factor 5; GSN, gelsolin; LPL, lipoprotein lipase; LPIC, lysosomal pepstatin insensitive protease; SERPINA4, kallistatin.

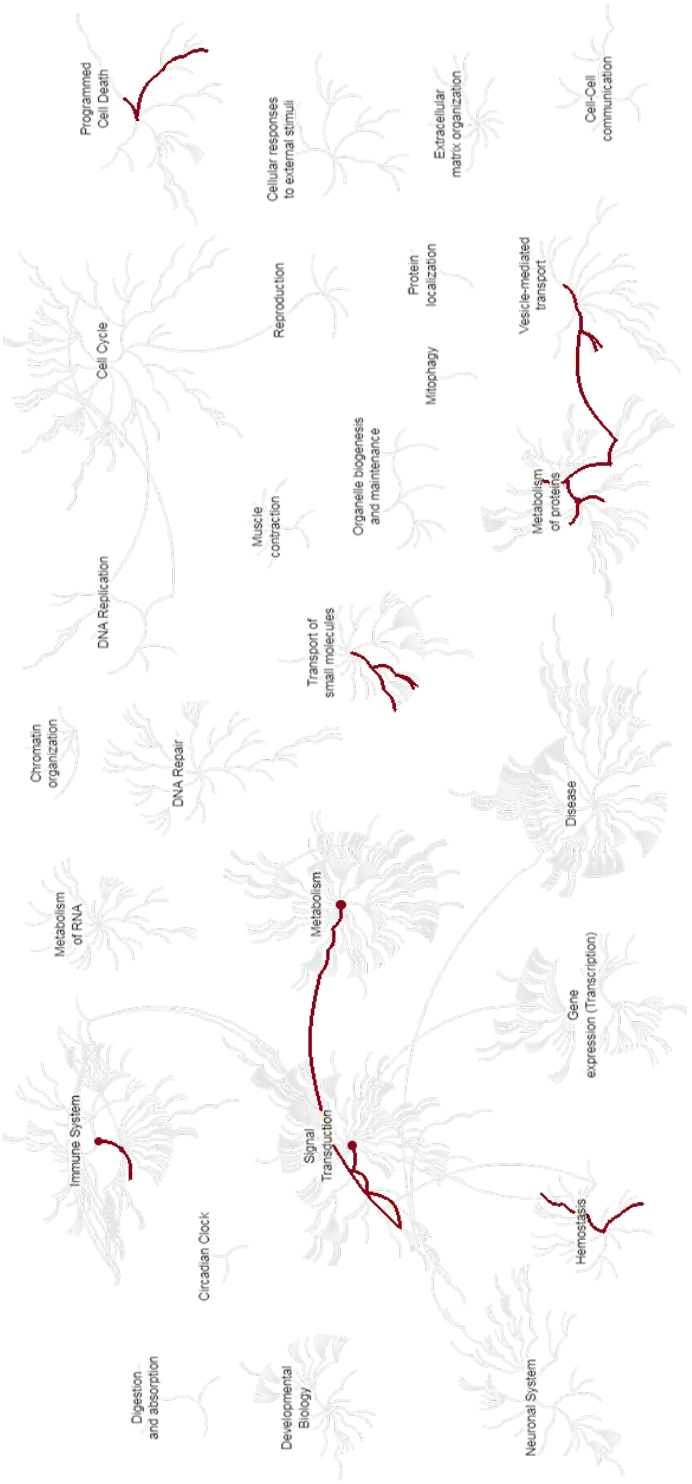

Figure 5.3: Genome-wide overview of pathways associated with proteins significantly increased in post-exercise plasma EVs, generated by Reactome software. Pathways associated with post-exercise proteins highlighted in red.
EV, extracellular vesicle.

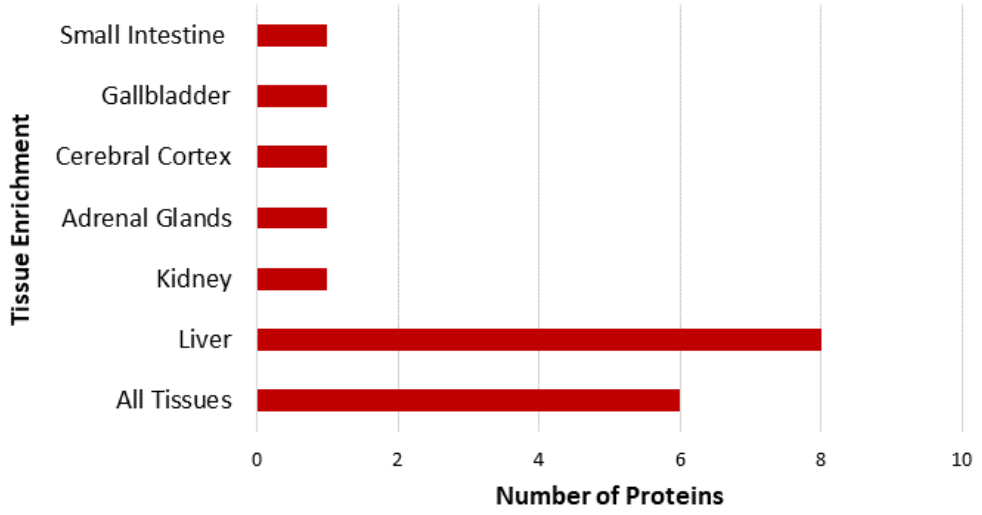

Figure 5.4: HPA tissue enrichment of proteins increased in post-exercise plasma EVs. n=5 biological replicates.
EV, extracellular vesicle; HPA, Human Protein Atlas

5.3 Proteomic Analysis of Myoblasts Treated with Plasma EVs

5.3.1 Rationale

Proteomic analysis of plasma EVs did not reveal protein cargo with an overt involvement in cell proliferation and differentiation, yet the treatment of myogenesis and neurogenesis models with post-exercise EVs resulted in clear modulation of these processes. It was therefore decided to directly investigate if specific pathways were being activated in the recipient cells, rather than relying on association via database analysis. To do this, an antibody array was performed on cells treated with pre- and post-exercise EVs, testing for post-translational protein modifications with known involvement in cell growth proliferation. Cell protein was extracted after a 30 minute incubation of cells with EVs, based on reported protocols for measuring protein phosphorylation which do so 30 and 60 minutes post cell treatment (*RnD Systems Detecting protein phosphorylation*, 2018).

5.3.2 Methods

C2C12 cells were maintained as per section 2.3.2 and plated at 1e4 cells/cm^2 in 6 well plates. The following day, cells were incubated with participant matched pre- and post- exercise plasma EVs (total EVs from 10 µL PDP were applied per cm^2 of culture surface for 30 minutes (n=4 biological replicates). Total protein was then extracted from the cells (section 2.11.1) and applied to a PathScan fluorescent readout intracellular signalling array kit (Cell Signaling Tech) as per manufacturers instructions. A fluorescent image of the slide was then captured with an Innopsys 700 Microarray side scanner and spot intensities were quantified using MAPIX array analysis software. The means of reads generated for pre- and post-exercise EV treated myoblasts were compared using a 2 tailed paired students T test.

5.3.3 Results

Increased modification of several proliferation-associated proteins was observed (figure 5.5) in post-exercise treated myoblasts compared to pre-exercise treated myoblasts. In particular, a very large (approximately 80 times) fold increase in PRAS40 phosphorylation (Thr246; inactivating) was observed, in addition to statistically significant increases in ERK 1/2 (Thr202/ Tyr204; activating), Akt (Ser473; activating) and AMPKα (Thr172; activating) phosphorylation. A full list of proteins and phosphorylation sites can be found in appended section D.5.

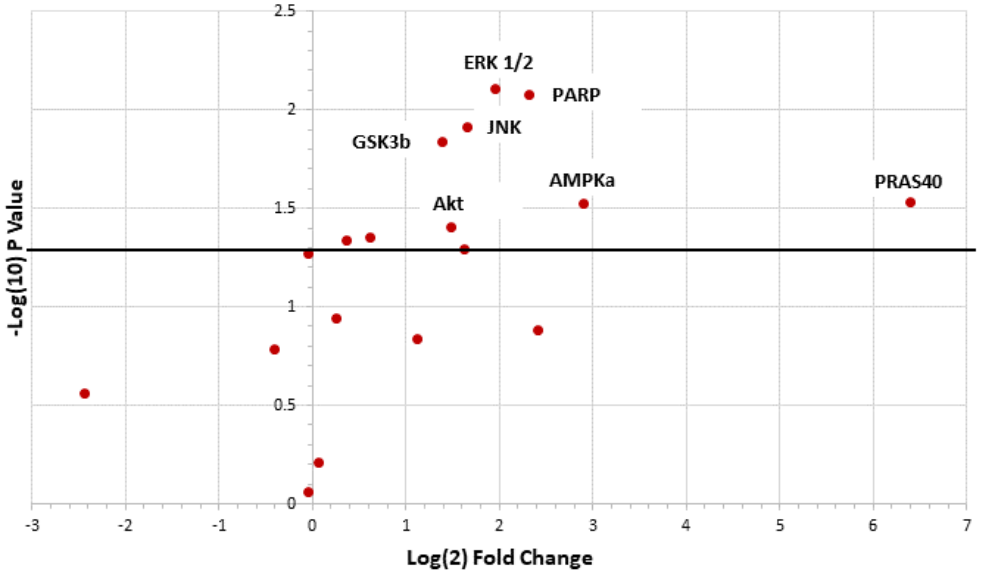

Figure 5.5: Phosphorylation of proliferation-associated proteins in myoblasts incubated with plasma EVs, described by fold change in modified proteins between pre- and post-exercise EV treated myoblasts. Protein modifications with a fold change >2 and a statistically significant p value (2-tailed paired students T test p value <0.05) have been annotated. n=4 biological replicates, line represents p=0.05. Akt, protein kinase B; AMPK, AMP-activated protein kinase; ERK, extracellular-signal-regulated kinase; EV, extracellular vesicle; GSK, Glycogen Synthase Kinase; JNK, c-Jun N-terminal kinase; PARP, Poly (ADP-ribose) polymerase; PRAS40, proline-rich Akt substrate of 40 kDa.

5.4 Discussion

5.4.1 Discussion of Results

Proteomic Analysis of Plasma EVs

Proteomic analysis of EVs enriched from pre- and post-exercise plasma confirmed (via EV-associated GO terms) that EVs were considerably enriched by our hands. An overrepresentation of functional annotations and pathways relating to humoural immune response, complement activation, and lipoprotein remodelling was observed across proteins increased (fold change >2) in post-exercise EV samples.

Just four of these proteins were significantly increased in post-exercise plasma EVs with a fold change >2 ($p<0.05$). These were ApoA-4, GSN, F5 and Serpina4. Consultation of Exocarta

and Vesiclepedia databases (accessed September 2018) and scrutiny of the current literature reveal that all four proteins have been previously found inside or associated with EVs of some kind. ApoA-4 has been found in EVs derived from umbilical cord blood mesenchymal stem cells (Kiplinen, 2013), and very aptly was recently identified as a protein enriched in populations of mesenchymal stem cell EVs which promoted recipient renal tubular cell proliferation and protection from apoptosis (Collino et al., 2017). ApoA-4 is also a major component of high density lipoproteins and chylomicrons synthesised in the small intestine, and is an important mediator of chylomicron and very low density lipoprotein secretion and catabolism (Wang et al., 2015).

GSN has been associated with small EVs enriched from cultured oligodendrocytes (Krämer-Albers et al., 2007), B cells (Buschow et al., 2010), and bone-marrow derived mast cells (Valadi et al., 2007). It was also identified in foetal calf serum EVs (Ochieng et al., 2009). GSN is a calcium-regulated protein which exerts effects both intracellularly and in extracellular fluids (reviewed by Janmey et al., 1998; Yin, 1987). Intracellular GSN helps regulate cellular architecture and motility via severing, capping and nucleating activities on actin filaments (McGough et al., 1998). *Gelsolin* null mice demonstrate that GSN is necessary for dynamic cells such as fibroblasts and platelets to contribute to wound healing and clotting processes (Witke et al., 1995). In agreement, overexpression of GSN in fibroblasts increases their motility (Cunningham et al., 1991). A role of GSN in the context of NPC migration has not yet been explored, but is plausible based on its effects on other motile cell types. F5 has been associated with small EVs obtained from cultured B cells (Meckes et al., 2013), dendritic cells (Kowal et al., 2016), endothelial cells (de Jong et al., 2012) and T lymphocytes (Perez-Hernandez et al., 2013). F5 was also identified in EVs positive for platelet markers which were enriched from human plasma (Al Kaabi et al., 2012). Approximately 20% of circulating F5 is thought to be inside platelets (Kalafatis, 2005). It plays a crucial role in the coagulation cascade, as activated F5 cleaves (and in turn activates) prothrombin to thrombin. Mass spectral analysis identified Serpina4 in small EVs enriched from human plasma from healthy donors (de Menezes-Neto et al., 2015). This protein has also been found in larger EVs positive for platelet markers enriched from plasma (Al Kaabi et al., 2012), and in EVs derived from red

blood cells (Bosman et al., 2008). Serpina4 inhibits tissue kallikrein, a protein involved in regulation of blood pressure (Chai et al., 1993).

Several of these proteins have been found in EVs secreted by B cells, and GO terms associated with the regulation of humoural immune response were enriched in post-exercise EVs. EVs secreted by B-cell lines carry co-stimulatory and adhesion molecules, and maintain the topology of their parent antigen presenting cell (APC) by exposing major histocompatibility (MHC) molecules at the vesicle surface (Raposo et al., 1996). At high concentrations APC-derived EVs bearing MHC complexes can stimulate recipient T cells *in vitro* (Admyre et al., 2007), however, the T-cell stimulatory capacity of APC-derived is much lower than that of the parent APCs (Vincent-Schneider et al., 2002).

Pienimaeki-Roemer et al (2015) performed mass spectral analysis on large (180-260 nm) EVs enriched from platelet concentrates by density gradient centrifugation, and identified ApoA-4, GSN and F5 as proteins present in these EVs. ApoA-4 and GSN have not been reported to date in small or large EVs enriched directly from plasma. The known functions of ApoA-4, GSN, F5 and Serpina4 proteins suggest that they could be shuttled by or associated with circulating EVs, but also that they may have been found in our EV preparations due to contamination with other blood components such as lipoproteins and platelets.

Pathway analysis using Reactome software did not highlight any known associations of these four proteins with cell proliferation or differentiation pathways. Overrepresented pathways instead mostly included those involved in lipoprotein and chylomicron assembly and remodelling, platelet activation, and clot formation. Some interesting observations, however, include:

- ApoA-4 is involved in the assembly of active Lipoprotein lipase (LPL) and hepatic triacylglycerol lipase (LIPC) lipase complexes pathway. ApoA-4 directly activates LPL, which liberates fatty acids from VLDLs and chylomicrons for tissue utilisation (Mead et al., 2002); LPL is especially abundant in adipocytes and skeletal myocytes, and increases following exercise (Seip and Semenkovich, 1998). Moreover, APOA4 has been shown to increase AKT phosphorylation (observed in the C2C12s treated with

post-exercise EVs) in both hepatocytes and adipocytes *in vitro* (He et al., 2018; Li, Wang, Xu, Howles and Tso, 2017).

- F5 is a component the regulation of Insulin-like growth factor (IGF) transport and uptake pathway. IGF proteins promote the proliferation of a range of cell types, including skeletal muscle and neural stem cells (see chapter one).
- GSN mediates actin cytoskeletal remodelling, a process integral to promoting cell motility (Lee and Dominguez, 2010).

Though not within the scope of this project, further investigation into the effects of exercise-induced plasma EVs on recipient muscle and neuronal stem cell metabolism and migration may be warranted based on some of these proteomic data. The known functions and cellular origins of the proteins increased by exercise imply that they may have been detected by ourselves and others in plasma EVs as a result of sample contamination with platelets, plasma proteins, and lipoproteins (further explored in chapter five). Alternatively it is possible that proteins found free in circulation or contained in platelets or lipoproteins are also carried by plasma EVs. However due to a lack of standardisation in the field, it remains unclear which is most likely to be the case.

All proteins increased by exercise were described by HPA as secreted/plasma proteins, and liver tissue enrichment was observed. This may be indicative of tissue-crosstalk between the liver and other tissues following exercise: communication between muscle and liver via circulating factors has been extensively demonstrated (reviewed by Pedersen, 2011). Moreover, a recent study has shown that EVs liberated by exercise display a tendency to localise in the liver (Whitham et al., 2018).

Proteomic Analysis of Myoblasts Treated with Plasma EVs

Phosphorylation assays identified a statistically significant increase in protein modifications pertaining to increased cell proliferation and survival in myoblasts treated with post-exercise EVs (compared to those treated with pre-exercise EVs). Figure 5.6 highlights proliferative pathways in which these proteins are involved according to the current literature, discussed in

more detail below.

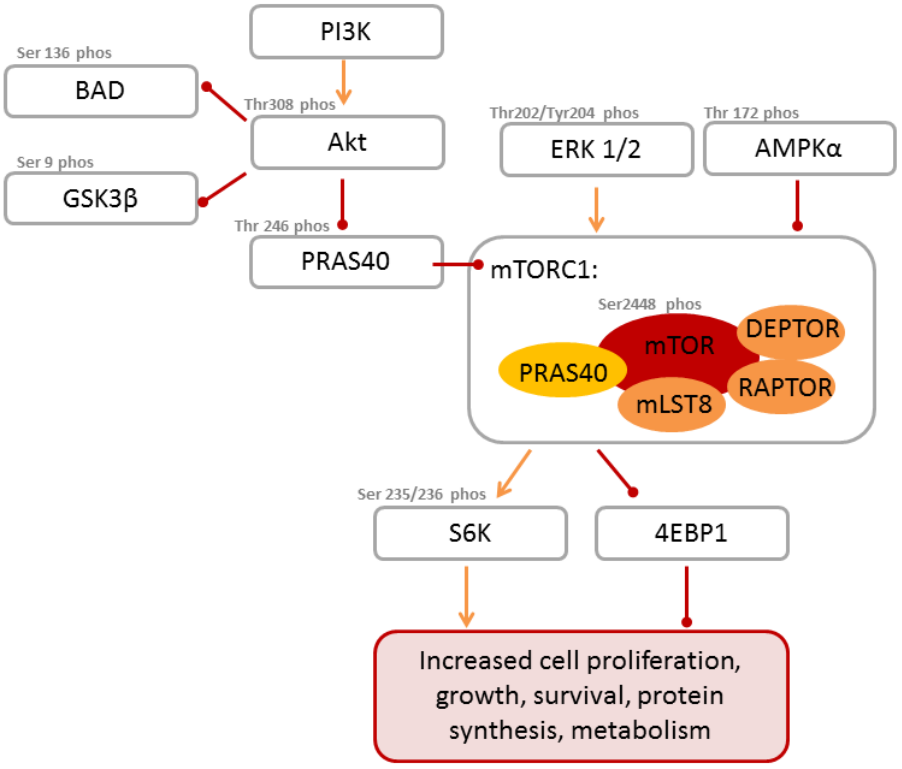

Figure 5.6: Schematic representation of cellular proliferation pathways assessed by PathScan assay. Orange arrows represent protein activation, red lines represent protein inactivation. Proteins are annotated with the modification(s) detected by our hands via PathScan assay.
Akt, protein kinase B; AMPK, AMP-activated protein kinase; BAD, Bcl-2-associated death promoter; DEPTOR, domain-containing mTOR-interacting protein; ERK, extracellular-signal-regulated kinase; EV, extracellular vesicle; GSK, Glycogen Synthase Kinase; JNK, c-Jun N-terminal kinase; mLST8, mammalian lethal with SEC13 protein 8; mTOR, mammalian target of rapamycin; mTORC1, mTOR Complex 1; PI3K, Phosphoinositide-3-kinase; PARP, Poly (ADP-ribose) polymerase; PRAS40, proline-rich Akt substrate of 40 kDa; RAPTOR, Regulatory-associated protein of mTOR.

Statistically significant increases in Protein kinase B (Akt) , Proline-rich AKT1 substrate 1 (PRAS40) and Mammalian target of rapamycin (mTOR) phosphorylation were detected by the PathScan assay in myoblasts incubated with post-exercise plasma EVs. Interestingly, an over 80-fold increase in PRAS40 phosphorylation was observed compared to treatment with pre- exercise EVs. Active PRAS40 inhibits mTOR complex 1 (mTORC1) activity by competitively binding with Raptor, an essential substrate of mTORC1 which acts as a scaffold

to recruit substrates such as 4EBP1 and ribosomal S6 kinase (S6K) to the complex (Nojima et al., 2003). Phosphorylation of PRAS40, however, strongly inhibits its ability to bind Raptor and therefore liberates Raptor for adequate substrate recruitment and subsequent activity of mTORC1 (Sancak et al., 2007). mTORC1 phosphorylates and activates S6K, which in turn phosphorylates multiple components of the cell's translation machinery required for cell growth and proliferation (Howell et al., 2013).

Extracellular-signal-regulated kinases (ERKs) 1 and 2 are 84% identical and share many common functions (Lloyd, 2006), therefore they are often referred to by the single designation ERK1/2. ERK1/2 modulates a diverse collection of functions, including cell cycle progression, proliferation, differentiation, senescence, cell death, migration, actin and microtubule networks and cell adhesion; it is therefore unsurprising that equally diverse mechanisms for ERK1/2 regulation have been proposed in the literature. ERK1/2 activation has predominantly been described at the plasma membrane via growth factor receptors, integrins, and G-protein coupled receptors (Ramos, 2008). Although exact mechanisms remain unclear to date, ERK1/2 is thought to act in parallel with Akt to promote mTORC1 activity (Winter et al., 2011). Unusually, although an increase in ERK1/2 phosphorylation and a very large increase in PRAS40 phosphorylation were observed, anticipated phosphorylation of mTOR was comparatively minimal (fold change 1.19, p=0.114) and downstream phosphorylation of S6K did not increase (fold change -1.0, p=0.053). This may be due to timing of the experiment performed: the phosphorylation snapshot captured at 30 minutes post-treatment was perhaps adequate timing to detect changes in Akt and PRAS40 phosphorylation, but not mTOR or downstream S6K phosphorylation. An alternative explanation is the observed increase in AMP-activated protein kinase (AMPKα) phosphorylation. Activated AMPKα has been shown to bind Raptor, and therefore compete with mTOR for Raptor binding much like PRAS40 (Gwinn et al., 2008). Phosphorylation activates AMPKα thus promoting its binding to Raptor, unlike PRAS40 which is conversely inhibited by phosphorylation. Our finding that AMPKα phosphorylation increases following exercise EV treatment therefore may be indicative of *decreased* myoblast proliferation, however AMPKα inhibition of mTORC1 is also required for metabolic changes which occur under energy stress, another well-established response of muscle cells to exercise (Gwinn et al., 2008).

5.4.2 Experimental Strengths and Limitations

Proteomic Analysis of Plasma EVs

Mass spectral analysis of pre- and post-exercise EV samples identified four proteins which were upregulated in post-exercise EVs, however how these might have related to changes in recipient cell proliferation and differentiation remains unclear. Although the EV samples exhibited an overwhelming enrichment of proteins associated with vesicles and EVs (see figure 5.2), classic 'marker' proteins (eg CD81, CD9, CD63, ALIX etc) were not detected among these samples, with the exception of Heat shock cognate 71 kDa protein (HSC70) . This may be due to a lack of starting material, due to contamination with other blood components that could make identifying comparatively low abundance proteins more challenging, or due to a combination of these two factors.

Mass spectrometry has become a crucial technology for protein identification and quantitation, and enables the comprehensive study of proteins in biological systems (reviewed by Aebersold and Mann, 2003). Label-free methods such as those used by our collaborators are a popular choice for small volume biological samples like plasma, as they enable minimal sample processing and maximum proteome coverage compared to labelling with stable isotopes (Geyer et al., 2016; Patel et al., 2009). A challenge in quantitative proteomics often associated with LFQ is wide-spread missing protein identifications or peptide intensity values. If the abundance of a peptide is below the instrument's limit of detection or if a peptide's source protein is incorrectly identified, then this protein will not be reported as present in the sample (Karpievitch et al., 2012). Analysis techniques that can effectively alleviate this issue remain a work in progress (Wei et al., 2017).

Proteomic Analysis of EV-Treated Myoblasts

An antibody array detected upregulation of several phosphorylation events indicative of pro-proliferative intracellular signalling in post-exercise treated myoblasts. This slide-based array tests for post-translational protein modifications which are well-characterised to play roles in cell growth and proliferation, thus providing a broad snapshot of signalling within the cells of interest. Though antibody cross-reactivity between human and mouse proteins is common, this array

was specifically designed for use on human cells (and therefore the detection of human protein specific post-translational modifications). The results of this assay must therefore be treated with great caution and require extensive further validation, though this was a useful starting point to support previous observations that post-exercise EVs increase recipient myoblast proliferation.

EV Enrichment from Plasma

As discussed above, proteomic analysis of EVs indicated that EV fractions may be contaminated with other blood components. Unfortunately there is still no true standardisation of EV enrichment from plasma in the field (Witwer et al., 2013). Such standardisation would greatly facilitate identification of specific EV-associated molecules which might be mediating the effects observed in functional experiments. Further investigation into the degree of blood component contamination and its potential effects on the results presented in this thesis is presented in chapter six.

Chapter 6

Evaluating Methods of Circulating Vesicle Enrichment

6.1 Introduction

6.1.1 Background

As discussed in chapter one (section 1.2.5), several different methods are used to enrich EVs from biofluids, all with varying degrees of EV recovery and specificity. A global survey performed by the International Society for Extracellular Vesicles in 2015 indicated that at that time, differential centrifugation (DC) was overwhelmingly the most utilised technique, with less than 20% of EV studies adopting any alternative methods (Gardiner et al., 2016). The work reported in this thesis began that year, and consequently began by enriching plasma EVs for functional assays using DC. Subsequent proteomic analysis of the EVs (chapter five), however, suggested that this technique may not be entirely effective for separating EVs from other non-EV associated plasma components.

Naturally, it was questioned if alternative EV enrichment methods could be better suited to the needs of this work. Size exclusion chromatography (SEC) has been proposed as a method better able to separate EVs from contaminant proteins (Nordin et al., 2015), though further investigation is required to assess its true efficacy when enriching EVs from complex media such as human plasma. Polymer precipitation (PP) techniques are still widely used for the enrichment of EVs from biological samples due to the high recovery rate associated with these methods (Deregibus et al., 2016; Nakai et al., 2016; Shin et al., 2015), though the ability of PP to separate EVs from other biofluid components has undoubtedly been challenged (Witwer et al., 2013).

6.1.2 Aims and Objectives

The experiments described in this chapter aimed to investigate the ability of three common EV enrichment techniques to separate small plasma EVs from other blood components. The objectives of this chapter therefore were:

- To test the ability of in-house plasma processing techniques to effectively deplete platelets

from human plasma prior to EV enrichment

- To assess particle retention and plasma protein contamination associated with DC, SEC and PP enrichment methods
- To assess lipoprotein contamination associated with DC, SEC and PP methods

6.2 Platelet Depletion of Plasma

6.2.1 Experiment Rationale

Approximately 25% of plasma EVs are thought to originate from platelets (Arraud et al., 2014). Platelet activation, shear stress, or ineffective depletion of platelets from plasma can however introduce a huge number of additional platelet fragments and/or platelet-derived EVs which make downstream analysis of other small EVs challenging (Heijnen et al., 1999; Holme et al., 1997). It was therefore tested whether plasma samples processed by our hands were effectively depleted of platelets prior to EV enrichment. Plasma was tested for platelet markers at each stage of the depletion process, to test for effective depletion.

6.2.2 Methods

Whole blood (9 mL) was collected by venepuncture from six fasted healthy volunteers. Platelet rich plasma (PRP) was then obtained from whole blood by centrifugation at 1,000 xg for 5 minutes, and was diluted in an equal volume of PBS to reduce viscosity. A 1 mL aliquot of diluted PRP was stored at 4°C until further use. The remaining PRP was centrifuged at 2,500 xg for 15 minutes to deplete cells and a 1 mL aliquot of the resulting cell depleted plasma (CDP) was also stored at 4°C. The remaining CDP was then centrifuged at 10,000 xg for 10 minutes to deplete platelets, and the resulting platelet-depleted plasma (PDP) was stored at 4°C. To test if freezing could also have an effect on this process, or more specifically if platelet depletion *after* freezing could also effectively remove platelet markers, a 1 mL aliquot of PRP was stored at -80°C overnight, then thawed and centrifuged at 2,500 xg and 10,000 xg as above. This

was referred to as 'Frozen PDP'. Platelet markers were then quantified in all plasma aliquots (PRP, CDP, PDP, Frozen PDP) using flow cytometry by collaborator Dr Lisa Ayers at the Radcliffe Department of Medicine, Medical Sciences Division. Lisa performed assays to quantify events positive for platelet markers glycoprotein IIb (CD41) (Mateo et al., 1996; Bagamery et al., 2005) and Annexin V (Walker, 2000) in the plasma samples following incubation with fluorophore-conjugated antibodies specific to CD41 and Annexin V. 1 μm beads were used to gate particle size, so that events $\sim$1 μm in size (corresponding to platelet microvesicles or fragments) were measured. CD41 and Annexin V positive events were compared between samples using a one way ANOVA and subsequent Tukey's honest significant difference test.

6.2.3 Results

CD41 and Annexin V positive events were significantly reduced in all processed plasma compared to PRP. There was no statistical difference in CD41 or Annexin V content between CDP, PDP and Frozen PDP, suggesting that all of these steps depleted platelets to a comparable degree. Some platelet marker was still detectable in all samples (sample medians $<$10 events), demonstrating the presence of some, but very few, CD41 and Annexin V positive particles.

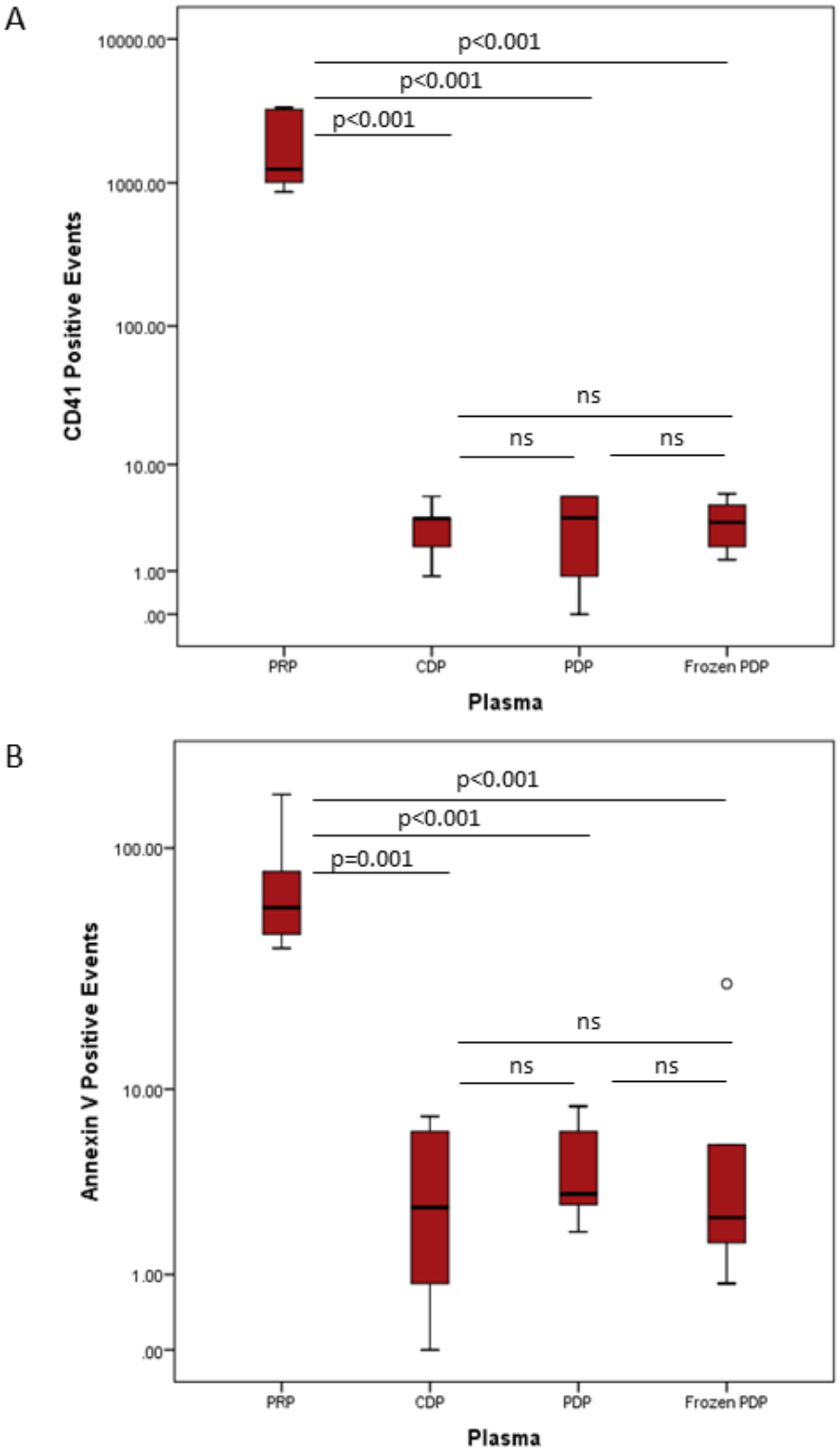

Figure 6.1: Platelet markers CD41 (A) and Annexin V (B) in platelet rich vs platelet depleted human plasma. Outlier extreme upper value labelled with °. n=6 biological replicates, p values determined by one way ANOVA and subsequent Tukey's honest significant difference test.

6.3 EV Retention and Plasma Protein/Lipoprotein Contamination

6.3.1 Experiment Rationale

Though DC is by far the most commonly used EV enrichment technique, it is known to result in contamination with protein aggregates of a similar size to EVs. SEC has been proposed to separate particles by size more efficiently than DC, via the use of sepharose beads containing tiny pores which trap and slow down nanoparticles within a very specific size range (Mori and Barth, 2013). Limited work has been published with regards to the efficiency of these methods in enriching EV populations from human plasma. We therefore compared these methods, along with PP which is still widely used on biofluid samples due to its logistic simplicity, for their ability to enrich EVs from relatively small volumes of human plasma.

Circulating lipoproteins have very similar characteristic sizes and densities to EVs, and can therefore co-enrich with EVs when enriched by methods exploiting these properties (Sódar et al., 2016). To test each enrichment method's ability to separate plasma EVs from lipoproteins, EV samples were tested for the presence of Apolipoprotein B-100 (ApoB-100) and Apolipoprotein A-1 (apoA-1). ApoB-100 is the apolipoprotein found in lipoproteins synthesised by the liver, and is therefore found in very low density lipoproteins (VLDLs), intermediate density lipoproteins (IDLs), low density lipoproteins (LDL) and Lipoprotein A (LP(a)) particles. ApoA-1, on the other hand, is found in lipoproteins synthesised in the small intestine: it is the main component of high density lipoproteins (HDLs) and can also be found in chylomicrons (Feingold and Grunfeld, 2018). Dot blot assays were used to test for the presence of ApoB-100 and ApoA-1, and were chosen not only to minimise the usage of limited EV samples, but also to allow detection of the ApoB-100 protein, which was too large (500 kDa) to effectively separate on a gel using SDS-PAGE by our hands.

6.3.2 Methods

Firstly, SEC was optimised to confirm in which fractions plasma EVs eluted in our hands. SEC was performed on 500 µl aliquots of PDP (section 2.8.2, n=6 biological replicates),

collecting 20 individual 500 µL fractions of flowthrough for each sample. Particles present in SEC fractions 1-20 were counted by NTA (section 2.9), and free protein content of each fraction was quantified by BCA assay (section 2.11.2). Total particles vs free protein were plotted to identify fractions containing the most EVs and the least contaminating protein.

Whole blood (9 mL) was then obtained from six fasted healthy individuals, and processed to PDP as per section 2.7. 500 μL aliquots of PDP were thawed at 4°C, and total EVs were enriched by DC, SEC and PP techniques (sections 2.8.1-3). Total EVs enriched by DC and PP were resuspended in 100 µL PBS, and the 2 mL EV fraction generated by SEC was concentrated to 100 µL with a Vivaspin2 concentrator column (molecular weight cutoff = 5kDa). As a negative control, equal volumes of PBS were also processed by each enrichment method (n=3 technical replicates). The number of particles present in each resulting EV preparation / PBS control were counted by NTA (section 2.9), and the free protein content of each sample was measured by BCA assay (section 2.11.2). To more accurately quantify protein contamination, a ratio of particle count to protein concentration (particle:protein ratio) was calculated for each sample.

Total protein was then extracted from EVs enriched by SEC, DC and PP methods. This protein was applied to dot blot assays (section 2.13) using antibodies specific to ApoB-100 and ApoA-1, also loading protein from whole plasma and PBS as positive and negative controls, respectively. Samples processed by SEC, DC and PP were also imaged using electron microscopy to visualise EVs and contaminants. EV samples were fixed and adhered to formvar coated grids, then negatively stained with uranyl acetate (section 2.5.2). Images were captured at relatively low magnification for EVs (5,000 x), to provide an adequately representative field of view in which to observe contamination levels for each sample.

6.3.3 Results

Particle counts and protein quantification identified SEC fractions 7-10 as those containing the most EVs with the least contaminating plasma protein. These fractions were therefore combined and labelled the EV-containing fraction for all future experiments using SEC.

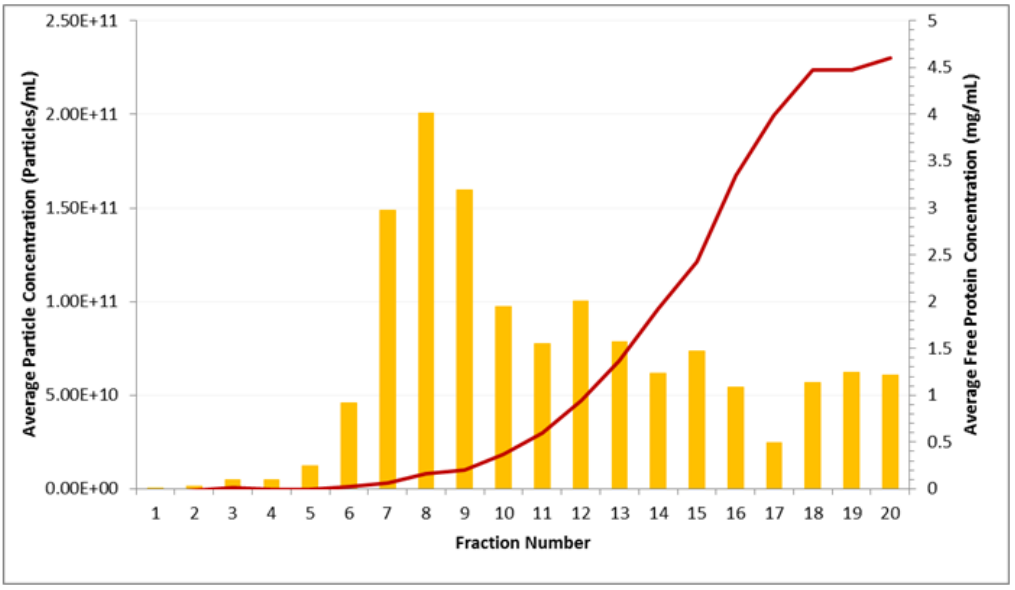

Figure 6.2: Optimisation of SEC to enrich EVs from human plasma: particle counts (bars) vs free protein content (line) of SEC fractions 1-20. n=6 technical replicates.
EV, extracellular vesicle; SEC, size exclusion chromatography

PP methods yielded the greatest number of particles from plasma, followed by SEC and then DC (figure 6.3 A), and NTA of PBS controls demonstrated that the particles counted in the plasma samples were not merely artifacts of the enrichment methods. SEC yielded EVs with the highest particle:protein ratio and therefore the lowest level of plasma protein contamination, followed by PP and DC methods (figure 6.3 C).

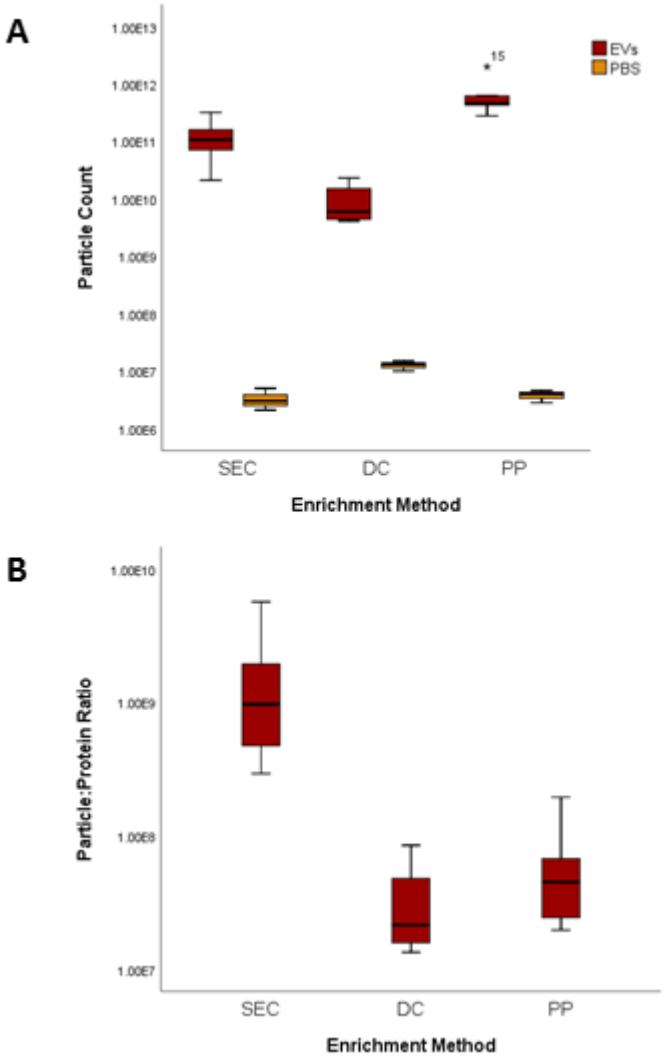

Figure 6.3: Particle retention (A) and protein contamination (B) of EVs enriched from human plasma using SEC, DC and PP techniques. Particle counts and protein measurements are of total particles/protein yielded from a 500 µL starting volume of plasma. Outlier extreme upper value labelled with *. n=6 biological replicates.
DC, differential centrifugation; EV, extracellular vesicle; PP, polymer precipitation; SEC, size exclusion chromatography.

Dot blot assays revealed that PP co-precipitated both HDLs and lower density lipoproteins, evidenced by positive staining for ApoB-100 and ApoA-1. SEC successfully eliminated HDL, denoted by an absence of Apo-A1 staining. Conversely DC was better able to reduce lower density lipoproteins (denoted by very weak ApoB-100 staining compared to SEC and PP).

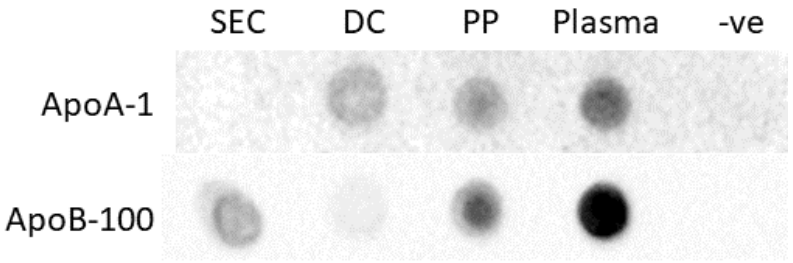

Figure 6.4: Lipoprotein contamination of plasma EVs enriched by SEC, DC and PP methods demonstrated by presence of ApoB-100 and ApoA-1, compared to positive (whole plasma) and negative (PBS) controls.
-ve, negative control; Apo, apolipoprotein; DC, differential centrifugation; EV, extracellular vesicle; PBS, phosophate buffered saline; PP, polymer precipitation; SEC, size exclusion chromatography.

Images generated by TEM showed a definite presence of structures with typical EV morphology in the SEC samples, denoted by black arrows (figure 6.5 A). UC samples contained similar structures, also denoted by black arrows, though the presence of some contaminating material (possibly protein aggregates) masked these structures in places and made it difficult to obtain clear images (figure 6.5 B). PP yielded samples with such high levels of contamination that no structures resembling EVs could be seen. A series of very small bright white vesicles could however be observed, approximately the size of HDL and LDLs and denoted by white arrows (figure 6.5 C).

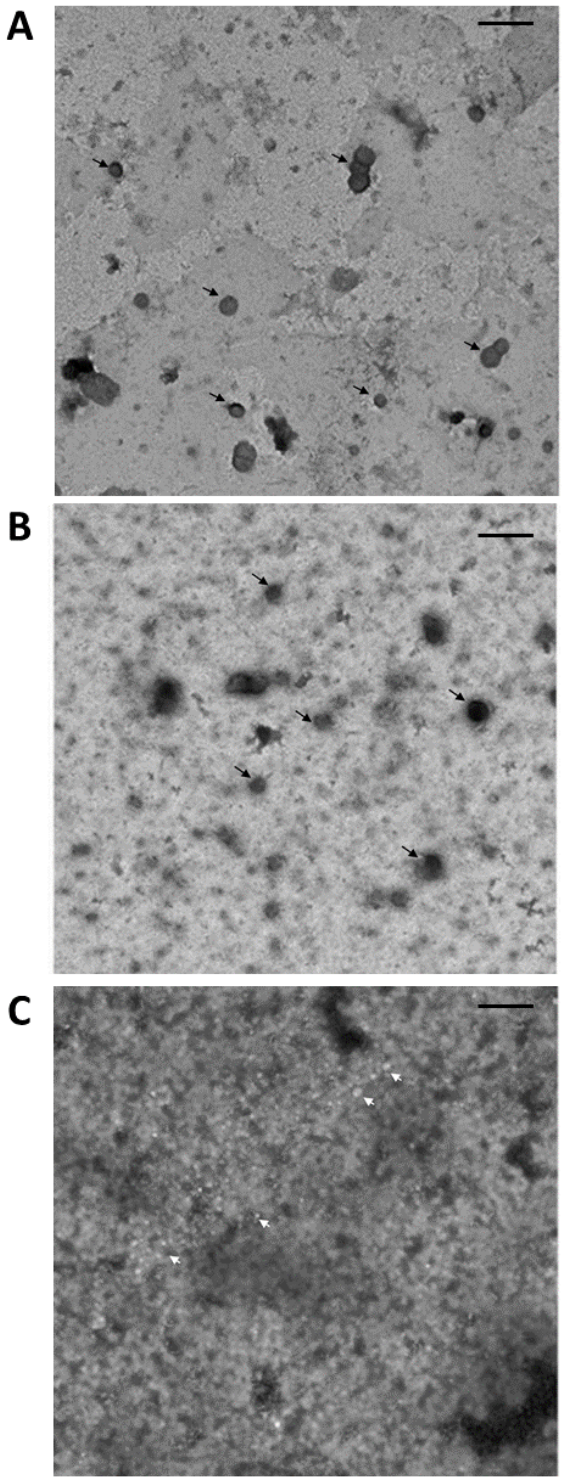

Figure 6.5: Transmission electron microscopy of particles enriched from human plasma by SEC (A), DC (B), and PP (C) techniques. Black arrows denote visible structures assumed to be extracelluar vesicles, and white arrows denote visible structures assumed to be lipoproteins. Scale bar = 200 nm. DC, differential centrifugation; PP, polymer precipitation; SEC, size exclusion chromatography.

6.4 Treating C2C12 Proliferation Model with SEC Plasma EVs

6.4.1 Experiment Rationale

As the work presented so far in this chapter demonstrated that DC and SEC yield EVs with distinct contamination profiles, another logical control was to treat the models with pre- and post-exercise SEC EVs, to test if this would yield comparable results to the DC EVs previously used.

6.4.2 Methods

EVs were enriched from 1 mL aliquots of pre- and post-exercise PDP (section 2.8.2) and C2C12 proliferation experiments were repeated once more, this time treating the cells with EVs enriched by SEC from pre- and post-exercise plasma of matched participants (n=3 biological replicates). The effect of these plasma EVs was compared to myoblast incubation with participant matched protein-containing SEC fractions (fractions 17-20 combined for each sample). All methodology was otherwise performed as per section 3.7. An equal volume of PBS was again used for each negative control, and pre- and post-exercise values were normalised to those of PBS controls.

6.4.3 Results

Plasma EVs enriched by SEC affected myoblast proliferation in a manner comparable to those enriched by DC: a 24 hr incubation with post-exercise SEC EVs increased the total number of C2C12 cells in culture compared to pre-exercise SEC EVs (T test, p=0.02). Incubation with plasma proteins also increased cell number after 24 hours, but to a lesser degree than the EV fractions (T test, p=0.67).

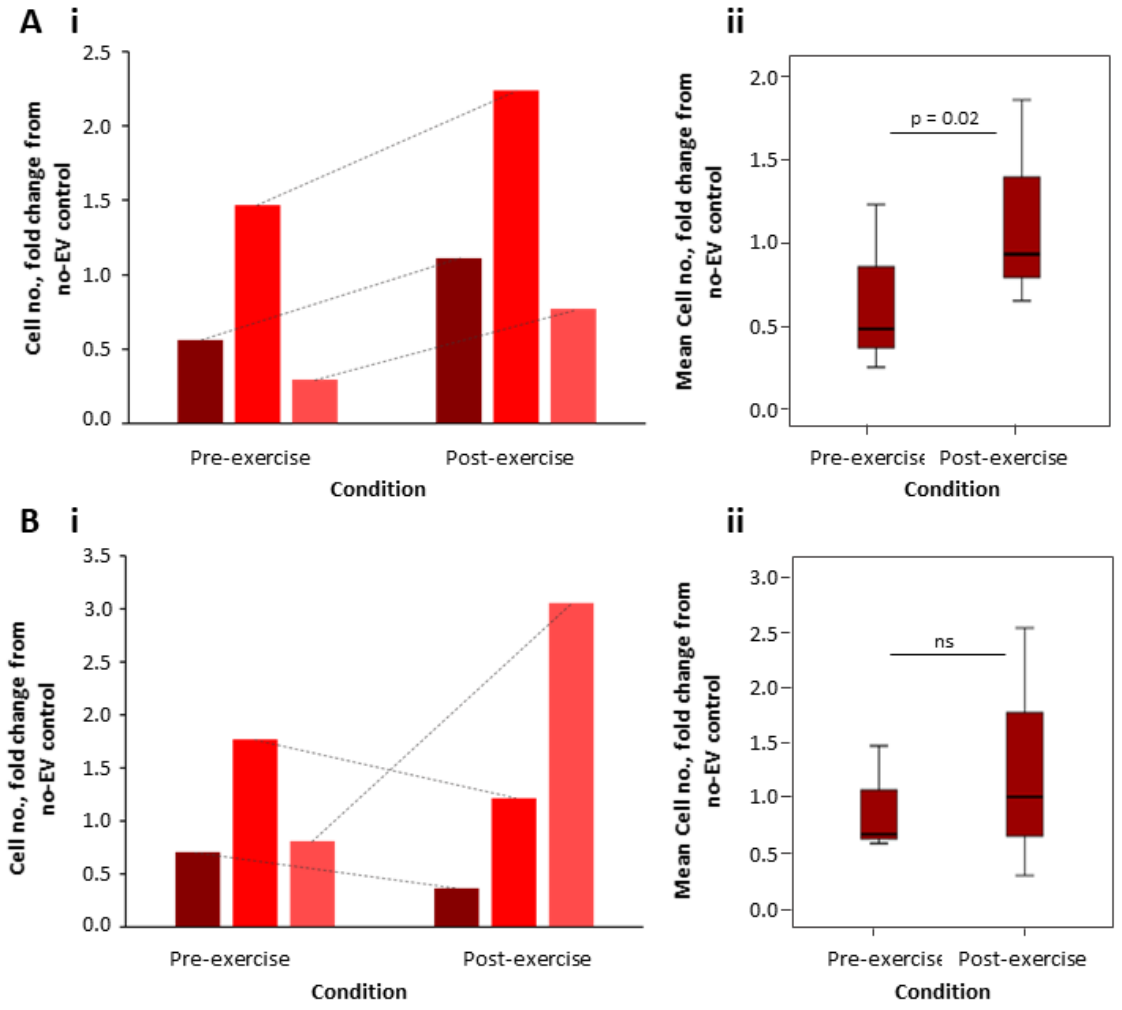

Figure 6.6: Proliferation of C2C12s treated with SEC-enriched plasma EVs (A) and plasma proteins (B), quantified by total cell number after 24 hour incubation, expressed as fold change from C2C12s treated with no-EV (PBS) controls. Shown for individual participant EVs (i) and overall EV populations (ii). n=3 biological replicates, p values generated by 2-tailed paired students T test.
EV, extracellular vesicle; PBS, phosphate buffered saline; SEC, size exclusion chromatography.

6.5 Discussion

6.5.1 Discussion of Results

To meet the aims of this chapter, whole blood was processed to PDP, and platelet markers were measured at several different stages of the process to test for successful platelet depletion. EVs

were enriched from PDP by three different methods commonly used in the field: SEC, DC and PP. EV yield was compared between enrichment methods, and converted to a particle:protein ratio as a measure of EV purity. Levels of plasma protein contamination and lipoprotein contamination were also assessed in EVs yielded by each method using several complimentary techniques. Plasma EVs enriched by SEC from pre- and post-exercise blood samples were then applied to the C2C12 myoblast proliferation model, to compare changes in myoblast proliferation with those previously observed using DC EVs.

Firstly, detection of platelet marker CD41 and platelet activation marker Annexin V by flow cytometry indicated that some activated platelet fragments or platelet-derived EVs were present in the PDP, but at very low levels. Resting platelets are the smallest cellular component of peripheral blood (2–3 μm), and are found at a concentration range of 1–3e8 platelets/mL. Upon activation, they undergo changes in cell surface receptor expression that alter their morphology and adhesive properties, thus promoting the formation of a platelet plug at sites of vascular disruption (Jackson, 2007). Platelet activation is also associated with platelet EV release (reviewed by Antwi-Baffour, 2015). One of the most widely used markers to identify platelets and their EVs via flow cytometry is CD41, an integrin receptor that mediates cell-matrix interactions (Duperray et al., 1989; McMichael et al., 1987; Tao et al., 2017). Annexin V is the major calcium-binding protein found in human platelets. One of the most important signals accompanying platelet activation is a surge in intracellular calcium, which instigates an increase in calcium-binding proteins to relay final platelet responses. Consequently, Annexin V is often used as a marker for platelet activation and apoptosis (Walker, 2000). Depletion of 1 µm sized particles expressing these markers by a single centrifugation step (2,500 xg) implies that this is sufficient to remove platelets and platelet fragments, without inducing significant platelet activation and therefore EV release. Although it was anticipated that these markers would further decrease with subsequent centrifugations, this did not appear to be the case. Moreover, centrifugation of whole plasma after overnight storage at -80°C appeared to deplete platelet fragments and EVs to a level comparable to handling fresh plasma. If a true result, this is particularly promising with regards to the enrichment of EVs from biobanked plasma samples, which have often been stored at -80°C without prior centrifugation steps.

Post-thawing centrifugation would therefore enable enrichment of other plasma EVs without an overwhelming majority of platelet-derived particles muddying subsequent analysis.

When comparing EV enrichment methods, all of the experiments performed strongly indicated that although it is a quick and simple technique, PP is not suitable for enriching plasma EVs without introducing contamination with other plasma components. PP co-pelleted plasma proteins, as demonstrated by BCA assay and the resulting particle:protein ratio. PP also co-pelleted lipoproteins with markers characteristic of high and low density lipoproteins, detected by dotblot assay. Moreover, electron microscopy highlighted the presence of an overwhelming number of contaminating particles, which prevented the clear visualisation of any EV structures in the samples. This finding has been published by Zarovni et al. (2015) using quantitative protein assay and western blotting techniques, but it was useful to confirm that this was also the case in our hands.

DC yielded a very low number of particles compared to the other techniques, as counted by NTA. This has also been observed by Soares Martins et al. (2018), who found that DC of a 250 µl starting volume pf plasma (half of of the volume used here) yielded too few EVs (1x107 particles/ml) to perform adequate downstream analyses. Calculation of particle:protein ratio and visualistion by EM suggested that EVs enriched by DC contained protein aggregates. An additional western blot or dot blot for an abundant plasma protein such as albumin may have aided in confirming this. Western blotting was carried out by Baranyai et al. (2015), who demonstrated the presence of albumin in rat and human plasma EVs enriched by DC with final ultracentrifugation (120,000 $\times$g) steps of varying lengths. Interestingly, they also observed white 'cloudy' areas of protein aggregate contamination in their electron microscopy images. We observed clear presence of HDL (detected via ApoA-1), and a very low level of other lipoproteins (detected via ApoB-100) in EV populations enriched by DC. This can be corroborated by a study performed in 2014, which conversely focused on how EVs can contaminate HDL populations enriched from plasma by density gradient centrifugation (Yuana et al., 2014) They demonstrated via flow cytometry that HDL-containing fractions also

contained small EVs, and proposed that these EVs may contribute to some of the miRNAs thought to be transported by lipoproteins.

SEC appeared to drastically reduce the amount of plasma protein contamination in EV samples, demonstrated by quantitative protein assay, subsequent particle:protein ratio calculation, and by electron microscopy. It was however noticed that SEC co-enriched lipoproteins positive for ApoB-100. Some recent work published toward the end of this project has confirmed that SEC does in fact co-enrich small EVs and lipoproteins, which they demonstrated by a combination of western blotting, electron microscopy, and in-house enzyme-linked immunosorbent assay (Karimi et al., 2018). Unusually, although lipoprotein markers were detected in our SEC EVs, they were not clearly visible in the EV samples by electron microscopy. The three (SEC, DC and PP) EV samples used for this analysis originated from the same participant's plasma, so differences in lipoprotein profiles between individuals cannot explain this observation.

Results presented here together with the emerging work of others demonstrate that alone, SEC, DC and PP cannot yield a pure population of EVs from complex biofluids such as plasma. The field of EV research unfortunately lacks standardisation in this area, and often new techniques are adopted without prior critical evaluation. Past publications such as that of Yuana (2014) have proffered that a combination of density gradient centrifugation (DGC) and SEC may be most optimal for separating EVs from other plasma components: alone, DGC can effectively separate EVs from all lipoprotein classes with the exception of HDLs, and SEC can optimally separate EVs from HDLs and protein aggregates. Karimi et al. (2018) recently demonstrated that this is in fact the case, showing that SEC followed by DGC yielded purer EV populations than all other tested methods. The major drawback of combining these techniques, however, is a distinct lack of EV yield. Though contaminants are effectively removed by combining these techniques, a large percentage of EVs (detected by EV marker proteins) are also lost in the process (Baranyai et al., 2015).

One potential solution to this predicament is the relatively recent development of microfluidic devices for the enrichment of EVs from biofluids. Though this technology is still very much in its infancy, promising early experimental evidence suggests that these devices effectively separate EVs from other blood components without the need for any prior processing, and

do so without losing large quantities of EVs (Davies et al., 2012; Reátegui et al., 2018)). As this technology continues to evolve, it is anticipated that customisable chips will enable the enrichment of increasingly purer EV populations and subpopulations, by exploiting EV characteristics such as electric properties, shape, size and density at the microscale (reviewed by Marrugo-Ramírez et al., 2018; Guo et al., 2018).

It was retrospectively demonstrated that the post-exercise DC EVs observed to alter recipient myoblast and NSC behaviour were likely to have been contaminated with circulating plasma proteins and protein aggregates. This acknowledged, no-EV controls (which contained majority plasma proteins and minority EVs) were not able to induce these same effects (section 3.6). Moreover, the treatment of cultured myoblasts with SEC-enriched plasma EVs replicated the effects imparted by DC-enriched EVs (section 3.6). As DC and SEC -enriched plasma EVs contain different contaminating plasma components (DC EVs containing HDLs and plasma proteins, SEC EVs containing other lipoproteins), the particles they have in common are EVs and some lipoproteins. This implies that either the plasma EV component of each sample, or a molecule found in both HDLs and LDLs, was likely to be the main contributing cause of changes in myoblast and NSC behaviour. Moreover, it cannot yet be excluded that a fraction of lipoprotein markers may be specifically associated with some plasma EVs (Østergaard et al., 2012).

Chapter 7

Discussion & Future Directions

7.1 Summary of Key Findings

Previous work has demonstrated that circulating small EVs increase in number following acute bouts of exercise, and may function as signalling molecules in myogenic and neurogenic stem cell niches. This PhD project therefore aimed to:

- Enrich and characterise EVs from the plasma of healthy volunteers, at rest and following an acute bout of exercise (chapter3).
- Establish robust *in vitro* models of adult myogenesis and neurogenesis, and treat these models with plasma EVs (chapters 3 & 4).
- Identify a mechanistic action of plasma EVs, by identifying cargo molecules present in pre- and post-exercise plasma EV populations and protein modifications in recipient cells (chapter 5).

To meet the aims of this project, whole blood was collected from healthy volunteers at rest and following a short duration of moderate intensity exercise on a cycle ergometer. Whole blood was processed to platelet depleted plasma, and small EVs were enriched by DC techniques. The resulting EV preparations were characterised by a combination of electron microscopy, nanoparticle tracking analysis, and dot blot assay / western blotting for known protein markers. *in vitro* models of myoblast proliferation and differentiation were established with immortalised mouse myoblasts (C2C12s), and pre- and post- exercise plasma EVs were applied to these models. The same EVs were also applied to proliferating primary human myoblasts to test that the results of treating C2C12 cells were reproducible in a more physiologically relevant cell type. Proliferating C2C12 cells were also treated with pre- and post-exercise EV-depleted plasma, to demonstrate localisation of the proliferative effects within distinct plasma fractions. Pre- and post- exercise EVs were then applied to pre-existing models of neuronal stem cell proliferation and differentiation, and were analysed for protein cargo which may be responsible for mediating the changes in myoblast and neural stem cell behaviour observed thus far. Mass spectral analysis of pre- and post-exercise EVs revealed the presence of several potential contaminants in the EV preparations, represented by a mixture of free-circulating proteins and lipoprotein

associated proteins. From this finding, a fourth project aim emerged:

- To compare available EV enrichment methods for their ability to yield circulating small EVs from human plasma with high EV retention and low plasma protein / lipoprotein contamination (chapter 6).

Three EV enrichment techniques (SEC, DC and PP) were therefore tested for their ability to separate small EVs from plasma proteins and lipoproteins when enriching EVs from small (0.5 mL) volumes of platelet-depleted plasma. Flow cytometry was also utilised to assess the ability of whole blood processing protocols to effectively deplete plasma of platelets and platelet fragments / EVs.

The key findings of each results chapter are summarised below:

Chapter 3: Circulating Vesicles and Adult Myogenesis

- Small particles approximately 100 nm in diameter were enriched from pre- and post-exercise plasma, and appeared to be positive for the tetraspanin CD81.
- Particle number and size did not notably change between rest and several time points post-exercise.
- Incubating proliferating mouse myoblasts with post-exercise plasma EVs increased their proliferative status after 24 hours (compared with pre-exercise plasma EVs and PBS). Incubating proliferating mouse myoblasts with pre- and post-exercise EV-depleted plasma did not achieve this same effect.
- Incubating differentiating mouse myoblasts with post-exercise plasma EVs decreased their differentiative status after 72 hours (compared with pre-exercise plasma EVs and PBS).
- Incubating proliferating primary human myoblasts with post-exercise plasma EVs increased their proliferative status after 24 hours (compared with pre-exercise plasma EVs and PBS).

Chapter 4: Circulating Vesicles and Adult Neurogenesis

- Incubating proliferating neurospheres with any plasma EVs caused them to dissociate and adhere to the culture surface after 48 hours.
- SVZ-derived neurospheres were observed to adhere to the culture surface in specific chain formations.
- Incubating differentiating NSCs with post-exercise plasma EVs increased their commitment to a neuronal cell fate (compared with pre-exercise plasma EVs and PBS). This was particularly true of SVZ cells, which in a physiological setting receive greater exposure to circulating factors. NSC commitment to glial cell fates were not altered by post-exercise EVs.

Chapter 5: Investigating Mechanisms of Action

- Proteins enriched in pre- and post-exercise plasma EV fractions have known association with vesicles and EVs according to GO analysis.
- Mass spectral analysis of plasma EVs identified four proteins which were significantly increased (p value <0.05, fold change >2) in post-exercise EVs compared with pre-exercise EVs: ApoA4, GSN, F5 and Serpina4. Results of pathway and GO analysis did not highlight any clear links between these proteins and cell proliferation or differentiation.
- Pathway and GO analysis of mass spectral data instead identified an enrichment of terms associated with platelet activation, compliment activation, and lipoprotein remodelling in post-exercise EV samples.
- Proteomic analysis of recipient myoblasts suggested that incubation with post-exercise EVs activated several pathways involved in cell growth and proliferation, denoted by relevant post-translation modifications of key signalling proteins.

Chapter 6: Evaluating Methods of Circulating Vesicle Enrichment

- Whole blood processing effectively depleted stored plasma of platelets and platelet fragments/EVs, but did not completely remove them. A marker of platelet activation was also detected at low levels in the platelet-depleted plasma.
- Differential centrifugation techniques yielded plasma EVs with a low recovery rate, and co-pelleted free plasma proteins and particles positive for HDL markers.
- Size exclusion chromatography techniques yielded plasma EVs with a high recovery rate and minimal contaminating free protein, but co-eluted particles positive for LDLs/VLDL markers.
- Polymer precipitation techniques yielded a huge number of particles, but co-pelleted large quantities of free protein and lipoprotein markers.
- Incubation of mouse myoblasts with post-exercise plasma EVs enriched by SEC increased their proliferative status (compared with pre-exercise plasma EVs and PBS).

7.2 Discussion and Future Work

Discussion points relevant to each individual experiment have been included in previous chapters. Here they are briefly summarised, along with thoughts to consider regarding the project as a whole.

7.2.1 Sample Size and Exercise Interventions

Sample Size

Experiments performed within this project do to some degree support the hypothesis that exercise-induced circulating small EVs play a role in mediating adult myogenesis and neurogenesis. The preliminary data presented here are indeed promising, and displayed definite trends toward indicating that post-exercise EVs increase myoblast proliferation whilst directing differentiating NSCs toward a neuronal fate. However these data do not always present statistical significance

when using the most appropriate statistical tests. This is likely due to a lack of biological replicates used in each experiment: a retrospective power estimation (appended section C) was performed using experimental BrdU positive cell counts (original data in figure 3.9, p=0.07) and suggested that a minumum of 12 biological replicates be used to achieve statistical significance ($p < 0.05$) with a power value of 0.95. Most experiments presented here have used just five or six biological replicates - unfortunately resource limitations prevented the performance of exercise interventions on a large enough sample size to generate statistically meaningful data.

Exercise Interventions

Moreover, the exercise interventions performed for this study involved short duration moderate intensity cycling, and were therefore not comparable to the high intensity protocols used by the preceding work of Fruhbeiss et al (2015). This may explain why no notable increase in circulating EVs was observed at any time point post-exercise, and it would likely have been interesting to test whether or not exercise of higher intensity had generated a response comparable to the work of others. Using a more potent exercise intervention (which may have a greater effect on subsequent myogenesis and neurogenesis) may also perhaps have been a better starting point for revealing a role of exercise EVs in mediating these processes. Nonetheless, demonstrating that adult myogenesis and neurogenesis are altered by exercise intensities which are easily achievable by untrained individuals can provide a more realistic and transferable dataset in the context of promoting physical activity on a global scale.

Two approaches were used to normalise exercise intensity across participants: for some exercise interventions, exercise intensity was maintained at 60% of the participant's estimated HR_{max}, and for some interventions it was maintained at 40% VO_2 max. Maximum heart rate is commonly used to determine exercise intensity (Benson, 2011). Since directly measuring an individual's HR_{max} imposes a heavy physical burden on the subject, a simple formula based on their age is extensively used to estimate it (Robergs and Landwehr, 2002):

HR_{max} = 220 - age (years)

Unfortunately this is not a particularly accurate estimate, and decreases in accuracy with age (Gellish et al., 2007). This therefore means that exercise interventions normalised for intensity across participants might not always be so well 'normalised' when using this approach. Oxygen consumption is instead considered the 'gold standard' physiological parameter to express the aerobic capacity of an individual (Pinet et al., 2008). It is measured in milliliters of oxygen used in one minute per kilogram of the participant's body weight (mL/kg/min), and is based on the premise that the more oxygen an individual consumes during high-intensity exercise, the more their body will generate energy (in the form of ATP) in cells and therefore the more efficient they will be at performing the exercise (Kenney et al., 2015). VO_2 max is usually tested via a graded exercise test, in which exercise intensity is carefully calibrated and increased over time. VO_2 max is reached when the individual's oxygen consumption plateaus despite a continuing increase in the intensity: at this point a shift from aerobic to anaerobic metabolism occurs, coinciding with the onset of muscle fatigue which forces the individual to cease exercising (Kenney et al., 2015). A flaw of this method is difficulty in accurately determining if a subject has in fact reached maximal oxygen consumption: particularly in untrained individuals, it is common for the subject to cease exercise due to perceived fatigue before maximal oxygen consumption has actually been reached. Incorrect calculation of VO_2 would of course result in incorrect normalisation of the intensity of subsequent exercise interventions across participants.

7.2.2 Blood Collection and Processing

Whole blood samples were collected into EDTA vacutainer tubes, and processed to PDP on the same day as collection. Current guidelines suggest that for the downstream enrichment of EVs, whole blood samples should be collected in sodium citrate tubes (Bæk et al., 2016; Wisgrill et al., 2016) and kept upright at room temperature for no more than 2 hours following collection (Lacroix et al., 2012). Though samples were kept upright at room temperature at all times, the anticoagulant used did not meet these guidelines, and the logistical complication of taking multiple blood samples from each participant meant that earlier time point samples were left waiting at room temperature for different lengths of time before they were fully processed to PDP and stored at -80°C. Platelet marker analysis suggested that although

platelet and platelet activation markers in the PDP were minimal, some CD41 and Annexin V positive events were detectable in these samples, thus implying that not all platelet-derived particles were successfully removed and that some platelet activation had occurred during blood taking or handling. Factors secreted by activated platelets have been demonstrated to increase recipient cancer cell, hepatocyte and smooth muscle cell proliferation (Cirillo et al., 1999; Castle et al., 2016), however their effects on skeletal muscle cells have not yet been reported in the literature. A more detailed assessment of the platelet depletion protocol could be achieved by measuring the percentage of exosome-sized enriched particles positive for CD41 and Annexin V in each sample rather than absolute number of 1000 µm events, perhaps by bead-assisted flow cytometry, or alternatively by using an affinity microarray platform such as the Exoview (nanoview Biosciences) to quantify particles positive for CD41 and EV marker antigens.

Recent MISEV guidelines reinforce that other preanalytical factors including donor age, biological sex, pre/postprandial status, Circadian variations, and body mass index may affect circulating EVs (Théry et al., 2018). These were recorded on the day of each exercise intervention, and factors such as pre/postprandial status and Circadian variations were controlled for by enforcing that all participants were fasted, and performed each exercise intervention between 8 and 10 am.

7.2.3 Enrichment and Characterisation of Plasma EVs

Enrichment Techniques

For functional experiments EVs were enriched from human plasma by DC techniques. NTA indicated that particles with a size distribution representative of small EVs (exosomes) were present in our EV preparations, though this technology cannot differentiate between EVs and lipoproteins or protein aggregates of a similar size. Via TEM particles with classic EV morphology were observed, and these were positive for the EV marker protein CD81 according to immunogold labelling techniques. Dot blots identified the presence of several EV marker proteins, though these were not detected by subsequent mass spectral analysis. This may be due to a lack of antibody specificity in the dot blot assays, or due to a combination of

small sample volume and contamination preventing MS from detecting all proteins present in adequate depth.

We later identified that using DC for plasma samples may introduce considerable levels of plasma protein and lipoprotein contamination. Now, at the time of writing, great effort is being poured into investigating other EV enrichment techniques; particularly in the context of enriching EVs from biofluids such as plasma and urine. There is not yet consensus on a single optimal enrichment method which offers high EV recovery and specificity: density gradient centrifugation (DGC) and immuno-isolation have been proposed as good candidate methods for minimising contamination with non-EV particles, however their very low recovery rates make them suitable only for use on large volumes of plasma (Karimi et al., 2018), rendering them highly impractical for use on limited biofluids. At present the available techniques therefore cannot satisfy the needs of our experimental work, though the data presented in this thesis does demonstrate that some entity within our plasma EV preparations has a functional effect on recipient stem cells. Protease treatment of the plasma EVs could be adopted to help distinguish EV-associated molecules from contaminating proteins, though this approach could strip away EV surface proteins in addition to altering their binding and uptake by recipient cells in subsequent functional studies (Escrevente et al., 2011).

Comparative assessment of EV enrichment techniques suggested that a combination of SEC and DC, or better yet, a combination of SEC and density gradient DC would be best suited to separating plasma EVs and other plasma components into distinct fractions. Future work may therefore benefit from adopting these improved enrichment techniques before performing functional assays, to allow for a more confident assessment of the plasma components responsible for observed effects on myoblast and NSC behaviour. As previously discussed, combining these techniques may lead to a detrimental loss of EV yield, thus rendering them unsuitable for use on small volumes of participant plasma. Alternatively, several EV-specific microfluidic devices are currently in development, which once optimised would be better suited to enriching and characterising EVs from small volumes of biological samples (Chiriacò et al., 2018). For future experiments this technology may provide a more accurate representation of circulating EV number before and after moderate exercise. It may also provide novel insights as to

whether existing enrichment methods that generate purer EV populations (such as density gradient centrifugation and immunoprecipitation) actually do so at the loss of EV yield, or simply appear to produce less EVs as a result of available counting techniques being unable to distinguish between EVs and other contaminant particles.

Proteomic profiling of pre- and post- exercise plasma EVs was performed, however a limitation on time and resources prevented the execution of a comparable RNA analysis. EVs carry several RNA species which are capable of inducing biological effects in recipient cells (see chapter one, section 1.2.3). RNA-Seq analyses of pre- and post-exercise plasma EVs may therefore highlight interesting candidate nucleic acids with roles in regulating cell proliferation and differentiation (Prendergast et al., 2018).

Post-Exercise EVs and Cell Metabolism

MS identified significantly higher levels of ApoA4 in post-exercise plasma EVs, though it remains unclear as to whether changes in this protein were detected due to a genuine association with plasma EVs or due to lipoprotein contamination. ApoA4 is carried by circulating chylomicrons, and activates lipoprotein lipase (LPL) which in turn mediates increases in lipid metabolism following moderate exercise (Ghafouri et al., 2015). Circulating HDL is well established to increase following aerobic exercise in rodents and humans, however the effect of aerobic exercise on circulating levels of chylomicrons has been less investigated (reviewed by Wang and Xu, 2017). Moreover, and increase in AMPKα phosphorylation was observed in myoblasts incubated with post-exercise EVs, potentially indicative of upregulated metabolic processes. Confirming if ApoA4 is also carried by EVs and assessing the effect of post-exercise EVs on metabolic pathways in a range of cell types could therefore be an interesting future pursuit.

7.2.4 In vitro Models of Myogenesis and Neurogenesis

Functional Studies

Plasma EVs were applied to models of myoblast and NSC proliferation and differentiation, and several complimentary techniques were combined wherever possible to demonstrate a

discernible effect of EVs on these processes. We observed increases in myoblast proliferation following incubation with post-exercise EVs, supported by an antibody assay which demonstrated that post-exercise plasma EVs may be increasing recipient myoblast proliferation via activation of PI3K-Akt and ERK1/2 signaling cascades. These preliminary findings require further validation, perhaps via western blotting with primary antibodies specific to phosphorylated forms of the relevant mouse proteins. Phosphorylation of ribosomal protein S6 by mTORC1 has been demonstrated as a process necessary for cell proliferation (Volovelsky et al., 2016; Wittenberg et al., 2016), and can be increased by PI3K-Akt and ERK1/2 signalling. Testing levels of phosphorylated ribosomal protein S6 in pre- and post-exercise EV treated myoblasts may therefore be a good starting point. Optimisation of experimental time points would be required, suggested by results of the antibody assay which detected notable increases in Akt, PRAS40 and ERK1/2 phosphorylation, but not downstream mTOR and S61K modifications.

Incubation with plasma EVs appeared to initiate the differentiation of otherwise proliferating neurospheres, and incubation with post-exercise plasma EVs promoted the commitment of differentiating NSCs to a neuronal fate. PBS controls suggested that NSC adherence was specifically in response to plasma EV treatment rather than general culture conditions, but as several factors can affect NSC adherence it would be wise to repeat this experiment with more biological replicates and on several different batches of NSCs. Should the same effect be observed, development of an automated method to count adherent cells using ImageJ software would be a useful tool.

For initial myoblast work an immortalised mouse cell line was used: primary human myoblasts were later obtained and tested for one measure of proliferative status following EV treatment, which generated results corroborating previous C2C12 experiments. Unfortunately the restrictions of limited human samples and culturing primary cells on our premises prevented further validation in this cell type. Moreover, the proliferation experiment performed using primary human myoblasts adopted the same protocols as those previously performed using C2C12s. A 24 hour incubation of cells with EVs was used as this represents approximately two cell doubling times for C2C12s (Sato et al., 2011). Primary cells generally grow at a slower rate than immortalised cell lines, and so a 24 hour incubation of primary myoblasts with EVs may not have been

sufficient to detect changes in proliferation rate. Had more primary myoblasts been available, initial determination of cell doubling time followed by proliferation experiments with optimised incubation times would have been beneficial.

Another aspect to consider is the majority use of mouse cells in these models, as treating mouse cells with human EVs introduces a level of interspecies complexity which further removes results from a physiologically relevant setting. The mouse cell models used have been well characterised and are thought to accurately reflect the behaviour of their human counterparts, though particularly in the case of NSCs, studies that characterise neurogenic processes in rodents and non-human primates dramatically outweigh those focusing on human tissues to date (reviewed by Braun and Jessberger, 2014). It therefore would have been preferable to use well characterised human cell lines and primary cells had they been available.

Plasma Protein Controls

Initial myoblast experiments used DC supernatant (EV-depleted plasma) as a plasma protein control, and incubating myoblasts with this medium did not increase their proliferative status. This seems unusual, as several growth factors and cytokines known to regulate myoblast proliferation are expected to be present in this plasma fraction. A possible explanation is that for these assays, a volume of EV-depleted plasma equal to the EV volume was applied each time, which is highly unlikely to be physiologically representative as plasma is diluted in large volumes of PBS for ultracentrifugation (110,000 xg) steps. Determining the correct amount of supernatant to use as a control therefore remains a challenge for all researchers using DC as their chosen EV enrichment technique. A later experiment using SEC-enriched EVs and proteins did however demonstrate that both plasma EVs and plasma proteins increased recipient myoblast proliferation (though proteins did not increase proliferation by a statistically significant measure). Perhaps, therefore, SEC is better able to separate EVs and protein contaminants into fractions of more comparable volumes.

7.2.5 Supporting Literature

Evidence in the literature which both supports and contradicts the findings of this project has been reported in previous chapters. Publications of particular interest include that of Fruhbeiss et al. (2015), which demonstrated a sustained increase in circulating small EVs in response to exhaustive exercise, and is one of the only exercise publications to date which focuses on smaller plasma EVs rather than platelet-derived microvesicles. Gusecini et al. (2017) developed an *in vitro* model of muscle contraction by exposing cultured myotubes to mild oxidative stress conditions, and incubated naive differentiating C2C12 cells with the small EVs produced by 'exercised' myotubes. In line with our own findings, recipient cells exhibited a decrease in differentiative status accompanied by an increase in proliferative status compared with control EVs. Alternatively, Whitham et al. (2018) employed quantitative proteomic techniques to characterise assumed EV-contained proteins secreted following a 1 hour bout of cycling exercise in healthy humans. They observed an increase in the circulation of over 300 proteins, and like us noted the enrichment of proteins that compose EVs. They also demonstrated that the plasma EVs they enriched had a tendency to localise in the liver of recipient rodents. This work used DC techniques to enrich plasma EVs, but did not address the possibility that the resulting EV preparations may contain large quantities of lipoproteins or plasma proteins. Performing proteomic analysis on this plasma fraction did however enable adequate separation of relatively low-abundance proteins (which may or may not be packaged in EVs) from highly abundant circulating proteins such as albumin.

7.2.6 Results in Context

Physical activity leads to beneficial physiological adaptation, and as a result is thought to reduce the risk of several major non-communicable diseases (see chapter one). However, the mechanisms by which exercise brings about these benefits are not fully understood. Despite being proposed as a mechanism for the physiological effects of exercise over 60 years ago (Kao and Ray, 1954), the concept of exercise-induced tissue crosstalk has been, until quite recently, largely understudied. Several published works have now explored the possibility of

tissue crosstalk following exercise, and due to its obvious role in facilitating movement, these have mostly focused on signalling molecules that originate from muscle (myokines). Myokines have been demonstrated to facilitate communication between skeletal muscle and adipose tissue (Iizuka et al., 2014), bone (Laurent et al., 2016), immune cells (Pillon et al., 2013), liver (Shimizu et al., 2015), and the brain (Delezie and Handschin, 2018) (see figure 7.1). These non-muscle tissues can also secrete signalling molecules of their own in response to exercise (Terra et al., 2012; Dekker et al., 2017; Weigert et al., 2018; García-Hermoso et al., 2017), though which cells and tissues these molecules then target is yet to be elucidated in many cases. Of special interest, however, increased secretion of molecules from the liver (recently coined 'hepatokines') has been observed during exercise, which may mediate crosstalk between the liver and distal skeletal muscle, brain, and adipose tissues (reviewed by Weigert et al., 2018). In particular, hepatokines Follistatin and heat shock protein 72 are thought to increase recipient skeletal muscle mass and mitochondrial function (Gilson et al., 2009; Gehrig et al., 2012).

While the theory of tissue crosstalk during and after exercise is in itself not novel, the field has thus far focused on uncovering new exercise factors that act in ligand-receptor binding complexes (Whitham and Febbraio, 2016). Growing appreciation for the functional role of EVs in tissue communication, accompanied by understanding that many known signalling molecules can be packaged inside EVs (see chapter 1), suggest that exercise might stimulate EV release and provide a new mechanism to transfer important signalling molecules between affected tissues. Data presented here suggest that post-exercise plasma EVs are enriched in liver proteins, which may be indicative of communication between the liver and muscle/neural stem cells following exercise.

Though not demonstrated within this project, EVs can serve as a means of secreting miRNAs into circulation, thus protecting them from enzymatic degradation in the plasma. MicroRNAs have been found in most body fluids, and there is great excitement surrounding their potential use as biomarkers of physiological or pathological processes (Weber et al., 2010; Wang, 2017). An extensive body of work has demonstrated the importance of miRNAs in a variety of cellular processes including proliferation, differentiation, and glucose homeostasis (reviewed

by Kloosterman and Plasterk, 2006), and the functions of miRNAs in adult myogenesis and neurogenesis are just beginning to come to light. A group of eight muscle specific miRNAs (myomiRs) has been identified, including *miR-1, miR-133a, miR-133b, miR-206, miR-208a, miR-208b, miR-486* and *miR-499*, and a series of studies have shown that many of these are involved in myogenesis (Horak et al., 2016), though their exact roles are yet to be elucidated. Some of these miRNAs are also speculated to increase in response to different types of exercise (reviewed by Kirby and McCarthy, 2013). In the brain, miRNAs can regulate NSC differentiation into neuron, astrocyte, and oligodendrocyte lineages. Specifically, *miR-124* was found to be virtually undetectable in undifferentiated NSCs, but upregulated in differentiating and mature neurons (Shi et al., 2010). NSC proliferation in the adult SVZ and DG is promoted by *miR-184* targeting of Numblike, a protein regulator of NSC division and differentiation (Liu et al., 2010). Given the role of EVs in protecting miRNA cargo, it is plausible that these miRNAs could be found inside circulating EVs, and may be altered by exercise.

Several signalling proteins known to play a role in myogenic and neurogenic processes (discussed in chapter one, section 1.5) have been found inside or associated with EVs. According to Exocarta and Vesiclepedia, two extensive web-based digests of exosomal cargo (Kalra et al., 2012; Keerthikumar et al., 2016), these include BDNF, LIF, interleukins, VEGF, and TGF-β. Interestingly, although HGF and IGF-1 themselves have not been reported in EVs according to these databases, mRNAs encoding their receptors - which are upregulated in activated satellite cells - have been (Exocarta, 2018). Mass spectral analysis performed on plasma EVs enriched by our hands did not identify enrichment of these signalling proteins in post-exercise EVs, however this may simply be due to inadequate removal of other contaminating proteins.

While the idea that exercise can stimulate the release of EVs capable of altering physiological function has been speculated upon in the literature (Egan et al., 2016; Frühbeis et al., 2015; Guescini et al., 2015; Safdar et al., 2016), experimental data are considerably lacking. This project has explored several potential biological functions of exercise-induced plasma EVs, in addition to assessing technical aspects of EV enrichment and characterisation from complex biofluids such as plasma. Considering the relative infancy of the EV field and our current inability to confidently attribute biological effects specifically to plasma EVs, the functional

aspects of this project were perhaps a little ahead of their time. Future work might therefore benefit from taking a step back and using an *in vitro* or animal model of exercise to eliminate some of the many confounding factors associated with using human blood. The data generated do however provide some promise that EVs could form a novel means of tissue crosstalk during exercise, and that exercise-induced EVs may be involved in adult myogenic and neurogenic processes (figure 7.1).

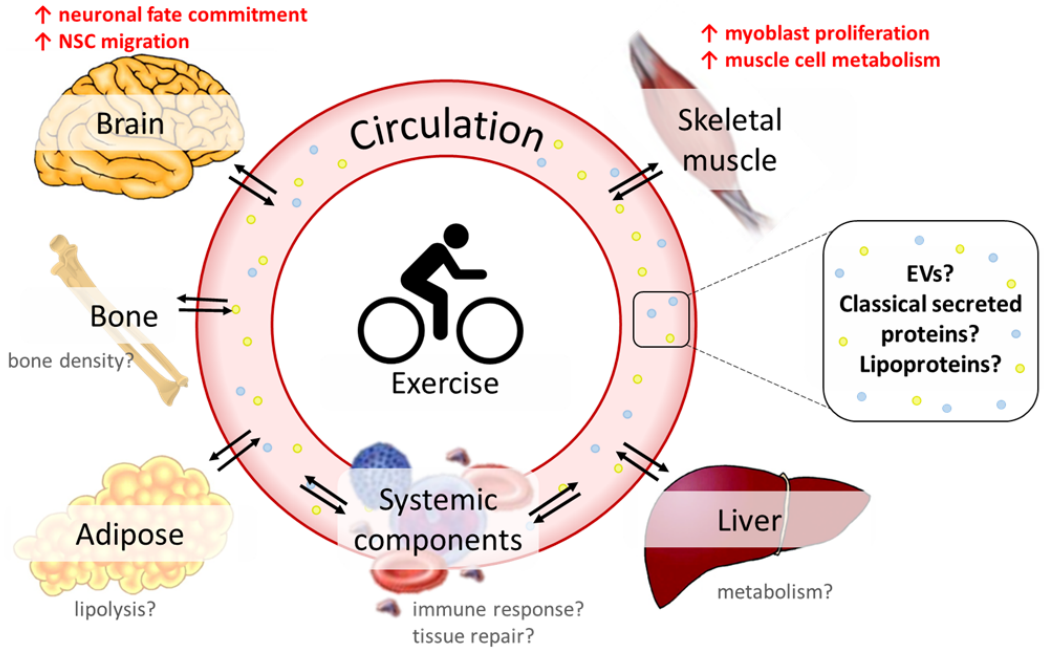

Figure 7.1: Schematic representation of exercise-mediated tissue crosstalk. Speculated functional effects of our post-exercise plasma EV samples are highlighted in red.
EV, extracellular vesicle; NSC, neural stem cell.

Bibliography

Aan het Rot, M., Collins, K. A. and Fitterling, H. L. (2009), 'Physical exercise and depression', *Mount Sinai Journal of Medicine: A Journal of Translational and Personalized Medicine* **76**(2), 204–214.

Admyre, C., Bohle, B., Johansson, S. M., Focke-Tejkl, M., Valenta, R., Scheynius, A. and Gabrielsson, S. (2007), 'B cell–derived exosomes can present allergen peptides and activate allergen-specific t cells to proliferate and produce th2-like cytokines', *Journal of Allergy and Clinical Immunology* **120**(6), 1418–1424.

Aebersold, R. and Mann, M. (2003), 'Mass spectrometry-based proteomics', *Nature* **422**(6928), 198—207.

Agley, C. C., Velloso, C. P., Lazarus, N. R. and Harridge, S. D. (2012), 'An image analysis method for the precise selection and quantitation of fluorescently labeled cellular constituents: application to the measurement of human muscle cells in culture', *Journal of Histochemistry & Cytochemistry* **60**(6), 428–438.

Ahmed, S. A., Gogal Jr, R. M. and Walsh, J. E. (1994), 'A new rapid and simple non-radioactive assay to monitor and determine the proliferation of lymphocytes: an alternative to [3h] thymidine incorporation assay', *Journal of immunological methods* **170**(2), 211–224.

Akers, J. C., Gonda, D., Kim, R., Carter, B. S. and Chen, C. C. (2013), 'Biogenesis of extracellular vesicles (ev): exosomes, microvesicles, retrovirus-like vesicles, and apoptotic bodies', *Journal of neuro-oncology* **113**(1), 1–11.

Al Kaabi, A., Traupe, T., Stutz, M., Buchs, N. and Heller, M. (2012), 'Cause or effect of arteriogenesis: compositional alterations of microparticles from cad patients undergoing external counterpulsation therapy', *PloS one* **7**(10), e46822.

Albertsson, P.-å. and Frick, G. (1960), 'Partition of virus particles in a liquid two-phase system', *Biochimica et biophysica acta* **37**(2), 230–237.

Allen, D. M., van Praag, H., Ray, J., Weaver, Z., Winrow, C. J., Carter, T. A., Braquet, R., Harrington, E., Ried, T., Brown, K. D. et al. (2001), 'Ataxia telangiectasia mutated is essential during adult neurogenesis', *Genes & development* **15**(5), 554–566.

Allen, R. E., Sheehan, S. M., Taylor, R. G., Kendall, T. L. and Rice, G. M. (1995), 'Hepatocyte growth factor activates quiescent skeletal muscle satellite cells in vitro', *Journal of cellular physiology* **165**(2), 307–312.

Altman, J. (1969), 'Autoradiographic and histological studies of postnatal neurogenesis. iv. cell proliferation and migration in the anterior forebrain, with special reference to persisting neurogenesis in the olfactory bulb', *Journal of Comparative Neurology* **137**(4), 433–457.

Altman, J. and Das, G. D. (1965), 'Autoradiographic and histological evidence of postnatal hippocampal neurogenesis in rats', *Journal of Comparative Neurology* **124**(3), 319–335.

Alvarez-Buylla, A. and Garcıa-Verdugo, J. M. (2002), 'Neurogenesis in adult subventricular zone', *Journal of Neuroscience* **22**(3), 629–634.

Alvarez-Erviti, L., Seow, Y., Yin, H., Betts, C., Lakhal, S. and Wood, M. J. (2011), 'Delivery of sirna to the mouse brain by systemic injection of targeted exosomes', *Nature biotechnology* **29**(4), 341.

Anand, K. S. and Dhikav, V. (2012), 'Hippocampus in health and disease: An overview', *Annals of Indian Academy of Neurology* **15**(4), 239.

Andaloussi, S. E., Mäger, I., Breakefield, X. O. and Wood, M. J. (2013), 'Extracellular vesicles: biology and emerging therapeutic opportunities', *Nature reviews Drug discovery* **12**(5), 347.

Arraud, N., Linares, R., Tan, S., Gounou, C., Pasquet, J.-M., Mornet, S. and Brisson, A. R. (2014), 'Extracellular vesicles from blood plasma: determination of their morphology, size, phenotype and concentration', *Journal of Thrombosis and Haemostasis* **12**(5), 614–627.

ASCM (2013), *ACSM's guidelines for exercise testing and prescription*, Lippincott Williams & Wilkins.

Aswad, H., Jalabert, A. and Rome, S. (2016), 'Depleting extracellular vesicles from fetal bovine serum alters proliferation and differentiation of skeletal muscle cells in vitro', *BMC Biotechnology* **16**(1), 32.

Ayers, L., Kohler, M., Harrison, P., Sargent, I., Dragovic, R., Schaap, M., Nieuwland, R., Brooks, S. A. and Ferry, B. (2011), 'Measurement of circulating cell-derived microparticles by flow cytometry: sources of variability within the assay', *Thrombosis research* **127**(4), 370–377.

Bæk, R., Søndergaard, E. K., Varming, K. and Jørgensen, M. M. (2016), 'The impact of various preanalytical treatments on the phenotype of small extracellular vesicles in blood analyzed by protein microarray', *Journal of immunological methods* **438**, 11–20.

Bagamery, K., Kvell, K., Landau, R. and Graham, J. (2005), 'Flow cytometric analysis of cd41-labeled platelets isolated by the rapid, one-step optiprep method from human blood', *Cytometry Part A: The Journal of the International Society for Analytical Cytology* **65**(1), 84–87.

Baj-Krzyworzeka, M., Szatanek, R., Wkeglarczyk, K., Baran, J., Urbanowicz, B., Bra'nski, P., Ratajczak, M. Z. and Zembala, M. (2006), 'Tumour-derived microvesicles carry several surface determinants and mrna of tumour cells and transfer some of these determinants to monocytes', *Cancer Immunology, Immunotherapy* **55**(7), 808–818.

Balaj, L., Lessard, R., Dai, L., Cho, Y.-J., Pomeroy, S. L., Breakefield, X. O. and Skog, J. (2011), 'Tumour microvesicles contain retrotransposon elements and amplified oncogene sequences', *Nature communications* **2**, 180.

Bamman, M. M., Cooper, D. M., Booth, F. W., Chin, E. R., Neufer, P. D., Trappe, S., Lightfoot, J. T., Kraus, W. E. and Joyner, M. J. (2014), Exercise biology and medicine: innovative research to improve global health, number 2, p. 148.

Baranyai, T., Herczeg, K., Onódi, Z., Voszka, I., Módos, K., Marton, N., Nagy, G., Mäger, I., Wood, M. J., El Andaloussi, S. et al. (2015), 'Isolation of exosomes from blood

plasma: qualitative and quantitative comparison of ultracentrifugation and size exclusion chromatography methods', *PloS one* **10**(12), e0145686.

Barnett, C., Carey, M., Proietto, J., Cerin, E., Febbraio, M. and Jenkins, D. (2004), 'Muscle metabolism during sprint exercise in man: influence of sprint training', *Journal of science and medicine in sport* **7**(3), 314–322.

Basso, J. C. and Suzuki, W. A. (2017), 'The effects of acute exercise on mood, cognition, neurophysiology, and neurochemical pathways: a review', *Brain Plasticity* **2**(2), 127–152.

Batagov, A. O. and Kurochkin, I. V. (2013), 'Exosomes secreted by human cells transport largely mrna fragments that are enriched in the 3′-untranslated regions', *Biology direct* **8**(1), 12.

Batista, B. S., Eng, W. S., Pilobello, K. T., Hendricks-Muñoz, K. D. and Mahal, L. K. (2011), 'Identification of a conserved glycan signature for microvesicles', *Journal of proteome research* **10**(10), 4624–4633.

Beauchamp, J. R., Heslop, L., David, S., Tajbakhsh, S., Kelly, R. G., Wernig, A., Buckingham, M. E., Partridge, T. A. and Zammit, P. S. (2000), 'Expression of cd34 and myf5 defines the majority of quiescent adult skeletal muscle satellite cells', *The Journal of cell biology* **151**(6), 1221–1234.

Bei, Y., Xu, T., Lv, D., Yu, P., Xu, J., Che, L., Das, A., Tigges, J., Toxavidis, V., Ghiran, I., Shah, R., Li, Y., Zhang, Y., Das, S. and Xiao, J. (2017), 'Exercise-induced circulating extracellular vesicles protect against cardiac ischemia–reperfusion injury', *Basic Research in Cardiology* **112**(4), 1–15.

Bellingham, S. A., Coleman, B. M. and Hill, A. F. (2012), 'Small rna deep sequencing reveals a distinct mirna signature released in exosomes from prion-infected neuronal cells', *Nucleic acids research* **40**(21), 10937–10949.

Berg, D. A., Belnoue, L., Song, H. and Simon, A. (2013), 'Neurotransmitter-mediated control of neurogenesis in the adult vertebrate brain', *Development* **140**(12), 2548–2561.

Bjornson, C. R., Cheung, T. H., Liu, L., Tripathi, P. V., Steeper, K. M. and Rando, T. A. (2012), 'Notch signaling is necessary to maintain quiescence in adult muscle stem cells', *Stem cells* **30**(2), 232–242.

Bjornsson, C. S., Apostolopoulou, M., Tian, Y. and Temple, S. (2015), 'It takes a village: constructing the neurogenic niche', *Developmental cell* **32**(4), 435–446.

Blau, H. M., Pavlath, G. K., Hardeman, E. C., Chiu, C.-P., Silberstein, L., Webster, S. G., Miller, S. C. and Webster, C. (1985), 'Plasticity of the differentiated state', *Science* **230**(4727), 758–766.

Böing, A. N., Van Der Pol, E., Grootemaat, A. E., Coumans, F. A., Sturk, A. and Nieuwland, R. (2014), 'Single-step isolation of extracellular vesicles by size-exclusion chromatography', *Journal of extracellular vesicles* **3**(1), 23430.

Bonnert, T. P., Bilsland, J. G., Guest, P. C., Heavens, R., McLaren, D., Dale, C., Thakur, M., McAllister, G. and Munoz-Sanjuan, I. (2006), 'Molecular characterization of adult mouse subventricular zone progenitor cells during the onset of differentiation', *European Journal of Neuroscience* **24**(3), 661–675.

Booth, A. M., Fang, Y., Fallon, J. K., Yang, J.-M., Hildreth, J. E. and Gould, S. J. (2006), 'Exosomes and hiv gag bud from endosome-like domains of the t cell plasma membrane', *J Cell biol* **172**(6), 923–935.

Bosman, G. J., Lasonder, E., Luten, M., Roerdinkholder-Stoelwinder, B., Novotnỳ, V. M., Bos, H. and De Grip, W. J. (2008), 'The proteome of red cell membranes and vesicles during storage in blood bank conditions', *Transfusion* **48**(5), 827–835.

Braun, S. M. and Jessberger, S. (2014), 'Adult neurogenesis: mechanisms and functional significance', *Development* **141**(10), 1983–1986.

Braun, T., Buschhausen-Denker, G., Bober, E., Tannich, E. and Arnold, H. (1989), 'A novel human muscle factor related to but distinct from myod1 induces myogenic conversion in 10t1/2 fibroblasts.', *The EMBO journal* **8**(3), 701–709.

Broocks, A., Bandelow, B., Pekrun, G., George, A., Meyer, T., Bartmann, U., Hillmer-Vogel, U. and Rüther, E. (1998), 'Comparison of aerobic exercise, clomipramine, and placebo in the treatment of panic disorder', *American Journal of Psychiatry* **155**(5), 603–609.

Brown, B. S., Payne, T., Kim, C., Moore, G., Krebs, P. and Martin, W. (1979), 'Chronic response of rat brain norepinephrine and serotonin levels to endurance training', *Journal of Applied Physiology* **46**(1), 19–23.

Brown, J. P., Couillard-Després, S., Cooper-Kuhn, C. M., Winkler, J., Aigner, L. and Kuhn, H. G. (2003), 'Transient expression of doublecortin during adult neurogenesis', *Journal of Comparative Neurology* **467**(1), 1–10.

Bunn, R. C., King, W. D., Winkler, M. K. and Fowlkes, J. L. (2005), 'Early developmental changes in IGF-I, IGF-II, IGF binding protein-1, and IGF binding protein-3 concentration in the cerebrospinal fluid of children', *Pediatric research* **58**(1), 89.

Buschow, S. I., Van Balkom, B. W., Aalberts, M., Heck, A. J., Wauben, M. and Stoorvogel, W. (2010), 'MHC class II-associated proteins in b-cell exosomes and potential functional implications for exosome biogenesis', *Immunology and cell biology* **88**(8), 851–856.

Caspersen, C. J., Powell, K. E. and Christenson, G. M. (1985), 'Physical activity, exercise, and physical fitness: definitions and distinctions for health-related research.', *Public health reports* **100**(2), 126.

Castle, J., Smith, R., Davis, B., Klopman, S., Torres, A., Robinson, V. S., Neculaes, V. B. and Garner, A. L. (2016), Pilot study assessing the impact of platelet activation electric stimulation protocols on hematopoietic and mesenchymal stem cell proliferation, *in* 'Power Modulator and High Voltage Conference (IPMHVC), 2016 IEEE International', pp. 88–90.

Chai, K., Chen, L., Chao, J. and Chao, L. (1993), 'Kallistatin: a novel human serine proteinase inhibitor. molecular cloning, tissue distribution, and expression in escherichia coli.', *Journal of Biological Chemistry* **268**(32), 24498–24505.

Chargaff, E. and West, R. (1946), 'The biological significance of the thromboplastic protein of blood', *J Biol Chem* **166**(1), 189–197.

Charras, G. T., Yarrow, J. C., Horton, M. A., Mahadevan, L. and Mitchison, T. (2005), 'Non-equilibration of hydrostatic pressure in blebbing cells', *Nature* **435**(7040), 365.

Chen, C. C., Liu, L., Ma, F., Wong, C. W., Guo, X. E., Chacko, J. V., Farhoodi, H. P., Zhang, S. X., Zimak, J., Ségaliny, A. et al. (2016), 'Elucidation of exosome migration across the blood–brain barrier model in vitro', *Cellular and molecular bioengineering* **9**(4), 509–529.

Chen, J. L., Steele, T. W. and Stuckey, D. C. (2015), 'Modeling and application of a rapid fluorescence-based assay for biotoxicity in anaerobic digestion', *Environmental science & technology* **49**(22), 13463–13471.

Cheung, T. H. and Rando, T. A. (2013), 'Molecular regulation of stem cell quiescence', *Nature reviews Molecular cell biology* **14**(6), 329.

Chiriacò, M., Bianco, M., Nigro, A., Primiceri, E., Ferrara, F., Romano, A., Quattrini, A., Furlan, R., Arima, V. and Maruccio, G. (2018), 'Lab-on-chip for exosomes and microvesicles detection and characterization', *Sensors* **18**(10), 3175.

Choi, J. S., Yoon, H. I., Lee, K. S., Choi, Y. C., Yang, S. H., Kim, I.-S. and Cho, Y. W. (2016), 'Exosomes from differentiating human skeletal muscle cells trigger myogenesis of stem cells and provide biochemical cues for skeletal muscle regeneration', *Journal of Controlled Release* **222**, 107–115.

Cirillo, P., Golino, P., Ragni, M., Battaglia, C., Pacifico, F., Formisano, S., Buono, C., Condorelli, M. and Chiariello, M. (1999), 'Activated platelets and leucocytes cooperatively stimulate smooth muscle cell proliferation and proto-oncogene expression via release of soluble growth factors', *Cardiovascular research* **43**(1), 210–218.

Clark, R. E., Broadbent, N. J., Zola, S. M. and Squire, L. R. (2002), 'Anterograde amnesia and temporally graded retrograde amnesia for a nonspatial memory task after lesions of hippocampus and subiculum', *Journal of Neuroscience* **22**(11), 4663–4669.

Colberg, S. R., Sigal, R. J., Yardley, J. E., Riddell, M. C., Dunstan, D. W., Dempsey, P. C., Horton, E. S., Castorino, K. and Tate, D. F. (2016), 'Physical activity/exercise and diabetes: a position statement of the american diabetes association', *Diabetes care* **39**(11), 2065–2079.

Colcombe, S. and Kramer, A. F. (2003), 'Fitness effects on the cognitive function of older adults: a meta-analytic study', *Psychological science* **14**(2), 125–130.

Collino, F., Pomatto, M., Bruno, S., Lindoso, R. S., Tapparo, M., Sicheng, W., Quesenberry, P. and Camussi, G. (2017), 'Exosome and microvesicle-enriched fractions isolated from mesenchymal stem cells by gradient separation showed different molecular signatures and functions on renal tubular epithelial cells', *Stem Cell Reviews and Reports* **13**(2), 226–243.

Cooper, R., Tajbakhsh, S., Mouly, V., Cossu, G., Buckingham, M. and Butler-Browne, G. (1999), 'In vivo satellite cell activation via myf5 and myod in regenerating mouse skeletal muscle', *J Cell Sci* **112**(17), 2895–2901.

Coskun, Ü., Grzybek, M., Drechsel, D. and Simons, K. (2011), 'Regulation of human egf receptor by lipids', *Proceedings of the National Academy of Sciences* .

Croft, D., Mundo, A. F., Haw, R., Milacic, M., Weiser, J., Wu, G., Caudy, M., Garapati, P., Gillespie, M., Kamdar, M. R. et al. (2013), 'The reactome pathway knowledgebase', *Nucleic acids research* **42**(D1), D472–D477.

Cunningham, C. C., Stossel, T. P. and Kwiatkowski, D. J. (1991), 'Enhanced motility in nih 3t3 fibroblasts that overexpress gelsolin', *Science* **251**(4998), 1233–1236.

Curtis, M. A., Kam, M., Nannmark, U., Anderson, M. F., Axell, M. Z., Wikkelso, C., Holtås, S., van Roon-Mom, W. M., Björk-Eriksson, T., Nordborg, C. et al. (2007), 'Human neuroblasts migrate to the olfactory bulb via a lateral ventricular extension', *science* **315**(5816), 1243–1249.

Dalsky, G. P., Stocke, K. S., Ehsani, A. A., Slatopolsky, E., Lee, W. C. and Birge, S. J. (1988), 'Weight-bearing exercise training and lumbar bone mineral content in postmenopausal women', *Annals of internal medicine* **108**(6), 824–828.

Dalton, A. J. (1975), 'Microvesicles and vesicles of multivesicular bodies versus "virus-like" particles', *Journal of the National Cancer Institute* **54**(5), 1137–1148.

Darr, K. C. and Schultz, E. (1987), 'Exercise-induced satellite cell activation in growing and mature skeletal muscle', *Journal of Applied Physiology* **63**(5), 1816–1821.

Davies, R. T., Kim, J., Jang, S. C., Choi, E.-J., Gho, Y. S. and Park, J. (2012), 'Microfluidic filtration system to isolate extracellular vesicles from blood', *Lab on a chip* **12**(24), 5202–5210.

Davis, R. L., Weintraub, H. and Lassar, A. B. (1987), 'Expression of a single transfected cdna converts fibroblasts to myoblasts', *Cell* **51**(6), 987–1000.

de Jong, O. G., Verhaar, M. C., Chen, Y., Vader, P., Gremmels, H., Posthuma, G., Schiffelers, R. M., Gucek, M. and van Balkom, B. W. (2012), 'Cellular stress conditions are reflected in the protein and rna content of endothelial cell-derived exosomes', *Journal of extracellular vesicles* **1**(1), 18396.

de Menezes-Neto, A., Sáez, M. J. F., Lozano-Ramos, I., Segui-Barber, J., Martin-Jaular, L., Ullate, J. M. E., Fernandez-Becerra, C., Borrás, F. E. and del Portillo, H. A. (2015), 'Size-exclusion chromatography as a stand-alone methodology identifies novel markers in mass spectrometry analyses of plasma-derived vesicles from healthy individuals', *Journal of extracellular vesicles* **4**(1), 27378.

Dehmelt, L. and Halpain, S. (2005), 'The map2/tau family of microtubule-associated proteins', *Genome biology* **6**(1), 204.

Dekker, J., Nelson, K., Kurgan, N., Falk, B., Josse, A. and Klentrou, P. (2017), 'Wnt signaling–related osteokines and transforming growth factors before and after a single bout of plyometric exercise in child and adolescent females', *Pediatric exercise science* **29**(4), 504–512.

Delezie, J. and Handschin, C. (2018), 'Endocrine crosstalk between skeletal muscle and the brain', *Frontiers in neurology* **9**.

Deregibus, M. C., Cantaluppi, V., Calogero, R., Iacono, M. L., Tetta, C., Biancone, L., Bruno, S., Bussolati, B. and Camussi, G. (2007), 'Endothelial progenitor cell–derived microvesicles

activate an angiogenic program in endothelial cells by a horizontal transfer of mrna', *Blood* **110**(7), 2440–2448.

Deregibus, M. C., Figliolini, F., D'antico, S., Manzini, P. M., Pasquino, C., De Lena, M., Tetta, C., Brizzi, M. F. and Camussi, G. (2016), 'Charge-based precipitation of extracellular vesicles', *International journal of molecular medicine* **38**(5), 1359–1366.

DeVos (2011), 'Cell Counter imagej plugin details', `https://imagej.nih.gov/ij/plugins/cell-counter.html`. Accessed: September 2018.

Diamant, M., Nieuwland, R., Pablo, R. F., Sturk, A., Smit, J. W. and Radder, J. K. (2002), 'Elevated numbers of tissue-factor exposing microparticles correlate with components of the metabolic syndrome in uncomplicated type 2 diabetes mellitus', *Circulation* **106**(19), 2442–2447.

Doetsch, F., Caille, I., Lim, D. A., García-Verdugo, J. M. and Alvarez-Buylla, A. (1999), 'Subventricular zone astrocytes are neural stem cells in the adult mammalian brain', *Cell* **97**(6), 703–716.

Dominkuš, P. P., Stenovec, M., Sitar, S., Lasič, E., Zorec, R., Plemenitaš, A., Žagar, E., Kreft, M. and Lenassi, M. (2018), 'Pkh26 labeling of extracellular vesicles: characterization and cellular internalization of contaminating pkh26 nanoparticles', *Biochimica et Biophysica Acta (BBA)-Biomembranes* **1860**(6), 1350–1361.

Dube, D. H. and Bertozzi, C. R. (2005), 'Glycans in cancer and inflammation—potential for therapeutics and diagnostics', *Nature reviews Drug discovery* **4**(6), 477.

Duca, K., Chiu, K., Sullivan, T., Berman, S. and Bursztajn, S. (1998), 'Nuclear clustering in myotubes: a proposed role in acetylcholine receptor mrna expression', *Biochimica et Biophysica Acta (BBA)-Molecular Cell Research* **1401**(1), 1–20.

Duncan, J. J., Farr, J. E., Upton, S. J., Hagan, R. D., Oglesby, M. and Blair, S. N. (1985), 'The effects of aerobic exercise on plasma catecholamines and blood pressure in patients with mild essential hypertension', *Jama* **254**(18), 2609–2613.

Duperray, A., Troesch, A., Berthier, R., Chagnon, E., Frachet, P., Uzan, G. and Marguerie, G. (1989), 'Biosynthesis and assembly of platelet gpiib-iiia in human megakaryocytes: evidence that assembly between pro-gpiib and gpiiia is a prerequisite for expression of the complex on the cell surface', *Blood* **74**(5), 1603–1611.

Egan, B., Hawley, J. A. and Zierath, J. R. (2016), 'Snapshot: exercise metabolism', *Cell metabolism* **24**(2), 342–342.

El-Sayed, M. S. (2002), 'Exercise and training effects on platelets in health and disease', *Platelets* **13**(5-6), 261–266.

Erickson, K. I., Hillman, C. H. and Kramer, A. F. (2015), 'Physical activity, brain, and cognition', *Current opinion in behavioral sciences* **4**, 27–32.

Escrevente, C., Keller, S., Altevogt, P. and Costa, J. (2011), 'Interaction and uptake of exosomes by ovarian cancer cells', *BMC cancer* **11**(1), 108.

Esser, J., Gehrmann, U., D'alexandri, F. L., Hidalgo-Estévez, A. M., Wheelock, C. E., Scheynius, A., Gabrielsson, S. and Rådmark, O. (2010), 'Exosomes from human macrophages and dendritic cells contain enzymes for leukotriene biosynthesis and promote granulocyte migration', *Journal of Allergy and Clinical Immunology* **126**(5), 1032–1040.

Fang, Y., Wu, N., Gan, X., Yan, W., Morrell, J. C. and Gould, S. J. (2007), 'Higher-order oligomerization targets plasma membrane proteins and hiv gag to exosomes', *PLoS biology* **5**(6), e158.

Faulkner, J. A., Brooks, S. V. and Opiteck, J. A. (1993), 'Injury to skeletal muscle fibers during contractions: conditions of occurrence and prevention', *Physical therapy* **73**(12), 911–921.

Fauza, D. O. and Bani, M. (2016), *Fetal stem cells in regenerative medicine: Principles and translational strategies*, Springer.

Feingold, K. R. and Grunfeld, C. (2018), Introduction to lipids and lipoproteins, *in* 'Endotext [Internet]', MDText. com, Inc.

Filippov, V., Kronenberg, G., Pivneva, T., Reuter, K., Steiner, B., Wang, L.-P., Yamaguchi, M., Kettenmann, H. and Kempermann, G. (2003), 'Subpopulation of nestin-expressing progenitor cells in the adult murine hippocampus shows electrophysiological and morphological characteristics of astrocytes', *Molecular and Cellular Neuroscience* **23**(3), 373–382.

Fitzgerald, W., Freeman, M. L., Lederman, M. M., Vasilieva, E., Romero, R. and Margolis, L. (2018), 'A system of cytokines encapsulated in extracellular vesicles', *Scientific reports* **8**(1), 8973.

Forterre, A., Jalabert, A., Berger, E., Baudet, M., Chikh, K., Errazuriz, E., De Larichaudy, J., Chanon, S., Weiss-Gayet, M., Hesse, A.-M. et al. (2014), 'Proteomic analysis of c2c12 myoblast and myotube exosome-like vesicles: a new paradigm for myoblast-myotube cross talk?', *PloS one* **9**(1), e84153.

Franzen, C. A., Simms, P. E., Van Huis, A. F., Foreman, K. E., Kuo, P. C. and Gupta, G. N. (2014), 'Characterization of uptake and internalization of exosomes by bladder cancer cells', *BioMed research international* **2014**.

Frisoni, G. B., Fox, N. C., Jack Jr, C. R., Scheltens, P. and Thompson, P. M. (2010), 'The clinical use of structural mri in alzheimer disease', *Nature Reviews Neurology* **6**(2), 67.

Frühbeis, C., Helmig, S., Tug, S., Simon, P. and Krämer-Albers, E.-M. (2015), 'Physical exercise induces rapid release of small extracellular vesicles into the circulation', *Journal of extracellular vesicles* **4**, 28239.

Füchtbauer, E.-M. and Westphal, H. (1992), 'Myod and myogenin are coexpressed in regenerating skeletal muscle of the mouse', *Developmental Dynamics* **193**(1), 34–39.

Fukuda, S., Kato, F., Tozuka, Y., Yamaguchi, M., Miyamoto, Y. and Hisatsune, T. (2003), 'Two distinct subpopulations of nestin-positive cells in adult mouse dentate gyrus', *Journal of Neuroscience* **23**(28), 9357–9366.

García-Hermoso, A., Ceballos-Ceballos, R., Poblete-Aro, C., Hackney, A., Mota, J. and

Ramírez-Vélez, R. (2017), 'Exercise, adipokines and pediatric obesity: a meta-analysis of randomized controlled trials', *International Journal of Obesity* **41**(4), 475.

Gardiner, C., Vizio, D. D., Sahoo, S., Théry, C., Witwer, K. W., Wauben, M. and Hill, A. F. (2016), 'Techniques used for the isolation and characterization of extracellular vesicles: results of a worldwide survey', *Journal of extracellular vesicles* **5**(1), 32945.

Geeves, M. A. (1991), 'The dynamics of actin and myosin association and the crossbridge model of muscle contraction.', *Biochemical journal* **274**(Pt 1), 1.

Gehrig, S. M., van der Poel, C., Sayer, T. A., Schertzer, J. D., Henstridge, D. C., Church, J. E., Lamon, S., Russell, A. P., Davies, K. E., Febbraio, M. A. et al. (2012), 'Hsp72 preserves muscle function and slows progression of severe muscular dystrophy', *Nature* **484**(7394), 394.

Geisert Jr, E. and Frankfurter, A. (1989), 'The neuronal response to injury as visualized by immunostaining of class iii β-tubulin in the rat', *Neuroscience letters* **102**(2-3), 137–141.

Gellish, R. L., Goslin, B. R., Olson, R. E., McDonald, A., Russi, G. D. and Moudgil, V. K. (2007), 'Longitudinal modeling of the relationship between age and maximal heart rate.', *Medicine and science in sports and exercise* **39**(5), 822–829.

Gercel-Taylor, C., Atay, S., Tullis, R. H., Kesimer, M. and Taylor, D. D. (2012), 'Nanoparticle analysis of circulating cell-derived vesicles in ovarian cancer patients', *Analytical biochemistry* **428**(1), 44–53.

Geyer, P. E., Kulak, N. A., Pichler, G., Holdt, L. M., Teupser, D. and Mann, M. (2016), 'Plasma proteome profiling to assess human health and disease.', *Cell systems* **2 3**, 185–95.

Ghafouri, K., Cooney, J., Bedford, D. K., Wilson, J., Caslake, M. J. and Gill, J. M. (2015), 'Moderate exercise increases affinity of large very low-density lipoproteins for hydrolysis by lipoprotein lipase', *The Journal of Clinical Endocrinology & Metabolism* **100**(6), 2205–2213.

Gibbons, T. E., Pence, B. D., Petr, G., Ossyra, J. M., Mach, H. C., Bhattacharya, T. K., Perez, S., Martin, S. A., McCusker, R. H., Kelley, K. W. et al. (2014), 'Voluntary wheel running, but not a diet containing (-)-epigallocatechin-3-gallate and β-alanine, improves

learning, memory and hippocampal neurogenesis in aged mice', *Behavioural brain research* **272**, 131–140.

Gillies, A. R. and Lieber, R. L. (2011), 'Structure and function of the skeletal muscle extracellular matrix', *Muscle & nerve* **44**(3), 318–331.

Gilson, H., Schakman, O., Kalista, S., Lause, P., Tsuchida, K. and Thissen, J.-P. (2009), 'Follistatin induces muscle hypertrophy through satellite cell proliferation and inhibition of both myostatin and activin', *American Journal of Physiology-Endocrinology and Metabolism* **297**(1), E157–E164.

Goldman, S. A. and Luskin, M. B. (1998), 'Strategies utilized by migrating neurons of the postnatal vertebrate forebrain', *Trends in neurosciences* **21**(3), 107–113.

Gomez, F. A. (2013), 'The future of microfluidic point-of-care diagnostic devices', *Bioanalysis* **5**(1), 1–3.

Gonçalves, J. T., Schafer, S. T. and Gage, F. H. (2016), 'Adult neurogenesis in the hippocampus: from stem cells to behavior', *Cell* **167**(4), 897–914.

Gonzales, P. A., Pisitkun, T., Hoffert, J. D., Tchapyjnikov, D., Star, R. A., Kleta, R., Wang, N. S. and Knepper, M. A. (2009), 'Large-scale proteomics and phosphoproteomics of urinary exosomes', *Journal of the American Society of Nephrology* **20**(2), 363–379.

Gonzalez, R. and Tarloff, J. (2001), 'Evaluation of hepatic subcellular fractions for alamar blue and mtt reductase activity', *Toxicology in vitro* **15**(3), 257–259.

Gordon, J., Amini, S. and White, M. K. (2013), General overview of neuronal cell culture, *in* 'Neuronal Cell Culture', Springer, pp. 1–8.

Gould, G. W. and Lippincott-Schwartz, J. (2009), 'New roles for endosomes: from vesicular carriers to multi-purpose platforms', *Nature reviews Molecular cell biology* **10**(4), 287.

Gould, S. J. and Raposo, G. (2013), 'As we wait: coping with an imperfect nomenclature for extracellular vesicles', *Journal of extracellular vesicles* **2**(1), 20389.

Greist, J. H., Klein, M. H., Eischens, R. R., Faris, J., Gurman, A. S. and Morgan, W. P. (1979), 'Running as treatment for depression', *Comprehensive psychiatry* **20**(1), 41–54.

Guescini, M., Canonico, B., Lucertini, F., Maggio, S., Annibalini, G., Barbieri, E., Luchetti, F., Papa, S. and Stocchi, V. (2015), 'Muscle releases alpha-sarcoglycan positive extracellular vesicles carrying mirnas in the bloodstream', *PloS one* **10**(5), e0125094.

Guescini, M., Genedani, S., Stocchi, V. and Agnati, L. F. (2010), 'Astrocytes and glioblastoma cells release exosomes carrying mtdna', *Journal of neural transmission* **117**(1), 1.

Guescini, M., Maggio, S., Ceccaroli, P., Battistelli, M., Annibalini, G., Piccoli, G., Sestili, P. and Stocchi, V. (2017), 'Extracellular vesicles released by oxidatively injured or intact c2c12 myotubes promote distinct responses converging toward myogenesis', *International journal of molecular sciences* **18**(11), 2488.

Guo, S.-C., Tao, S.-C. and Dawn, H. (2018), 'Microfluidics-based on-a-chip systems for isolating and analysing extracellular vesicles', *Journal of extracellular vesicles* **7**(1), 1508271.

Gustafson, C. M., Shepherd, A. J., Miller, V. M. and Jayachandran, M. (2015), 'Age-and sex-specific differences in blood-borne microvesicles from apparently healthy humans', *Biology of sex differences* **6**(1), 10.

Gwinn, D., B Shackelford, D., Egan, D., Mihaylova, M., Mery, A., Vasquez, D., E Turk, B. and Shaw, R. (2008), 'Ampk phosphorylation of raptor mediates a metabolic checkpoint', *Molecular cell* **30**, 214–26.

Hack, M. A., Saghatelyan, A., De Chevigny, A., Pfeifer, A., Ashery-Padan, R., Lledo, P.-M. and Götz, M. (2005), 'Neuronal fate determinants of adult olfactory bulb neurogenesis', *Nature neuroscience* **8**(7), 865.

Han, C., Sun, X., Liu, L., Jiang, H., Shen, Y., Xu, X., Li, J., Zhang, G., Huang, J., Lin, Z. et al. (2016), 'Exosomes and their therapeutic potentials of stem cells', *Stem cells international* **2016**.

Hansen, J., Brandt, C., Nielsen, A. R., Hojman, P., Whitham, M., Febbraio, M. A., Pedersen, B. K. and Plomgaard, P. (2011), 'Exercise induces a marked increase in plasma follistatin: evidence that follistatin is a contraction-induced hepatokine', *Endocrinology* **152**(1), 164–171.

Hansen, J. S., Clemmesen, J. O., Secher, N. H., Hoene, M., Drescher, A., Weigert, C., Pedersen, B. K. and Plomgaard, P. (2015), 'Glucagon-to-insulin ratio is pivotal for splanchnic regulation of fgf-21 in humans', *Molecular metabolism* **4**(8), 551–560.

Harrison, P., Gardiner, C. and Sargent, I. L. (2014), *Extracellular vesicles in health and disease*, Pan Stanford.

Haskell, W. L. (1986), 'The influence of exercise training on plasma lipids and lipoproteins in health and disease', *Acta Medica Scandinavica* **220**(S711), 25–37.

Hawley, J. A., Hargreaves, M., Joyner, M. J. and Zierath, J. R. (2014), 'Integrative biology of exercise', *Cell* **159**(4), 738–749.

Hazelton, I., Yates, A., Dale, A., Roodselaar, J., Akbar, N., Ruitenberg, M. J., Anthony, D. C. and Couch, Y. (2018), 'Exacerbation of acute traumatic brain injury by circulating extracellular vesicles', *Journal of neurotrauma* **35**(4), 639–651.

He, J., Zhao, J., Yang, Z., Zhang, J., Wei, S., Li, S. and Li, X. (2018), 'Actions of apolipoprotein a-iv on insulin-independent glucose control and activation of akt in mouse liver'.

He, M., Crow, J., Roth, M., Zeng, Y. and Godwin, A. K. (2014), 'Integrated immunoisolation and protein analysis of circulating exosomes using microfluidic technology', *Lab on a Chip* **14**(19), 3773–3780.

Heijnen, H. F., Schiel, A. E., Fijnheer, R., Geuze, H. J. and Sixma, J. J. (1999), 'Activated platelets release two types of membrane vesicles: Microvesicles by surface shedding and exosomes derived from exocytosis of multivesicular bodies and-granules', *Blood* **94**(11), 3791–3799.

Hernández-Hernández, J. M., García-González, E. G., Brun, C. E. and Rudnicki, M. A. (2017), The myogenic regulatory factors, determinants of muscle development, cell identity and regeneration, *in* 'Seminars in cell & developmental biology', Vol. 72, Elsevier, pp. 10–18.

Hilgetag, C. C. and Barbas, H. (2009), 'Are there ten times more glia than neurons in the brain?', *Brain Structure and Function* **213**(4), 365–366.

Holm, M. M., Kaiser, J. and Schwab, M. E. (2018), 'Extracellular vesicles: multimodal envoys in neural maintenance and repair', *Trends in neurosciences* .

Holme, P. A., Ørvim, U., Hamers, M. J., Solum, N. O., Brosstad, F. R., Barstad, R. M. and Sakariassen, K. S. (1997), 'Shear-induced platelet activation and platelet microparticle formation at blood flow conditions as in arteries with a severe stenosis', *Arteriosclerosis, thrombosis, and vascular biology* **17**(4), 646–653.

Horak, M., Novak, J. and Bienertova-Vasku, J. (2016), 'Muscle-specific micrornas in skeletal muscle development', *Developmental biology* **410**(1), 1–13.

Howell, J. J., Ricoult, S. J., Ben-Sahra, I. and Manning, B. D. (2013), 'A growing role for mtor in promoting anabolic metabolism'.

Hristov, M., Erl, W., Linder, S. and Weber, P. C. (2004), 'Apoptotic bodies from endothelial cells enhance the number and initiate the differentiation of human endothelial progenitor cells in vitro', *Blood* **104**(9), 2761–2766.

Huang, X., Yuan, T., Tschannen, M., Sun, Z., Jacob, H., Du, M., Liang, M., Dittmar, R. L., Liu, Y., Liang, M. et al. (2013), 'Characterization of human plasma-derived exosomal rnas by deep sequencing', *BMC genomics* **14**(1), 319.

Human Protein Atlas Tissue-based map of the human proteome (n.d.), `https://www.proteinatlas.org/`. Accessed: September 2018.

Hyman, C., Hofer, M., Barde, Y.-A., Juhasz, M., Yancopoulos, G. D., Squinto, S. P. and Lindsay, R. M. (1991), 'Bdnf is a neurotrophic factor for dopaminergic neurons of the substantia nigra', *Nature* **350**(6315), 230.

Iizuka, K., Machida, T. and Hirafuji, M. (2014), 'Skeletal muscle is an endocrine organ', *Journal of pharmacological sciences* **125**(2), 125–131.

Isaacs, K. R., Anderson, B. J., Alcantara, A. A., Black, J. E. and Greenough, W. T. (1992), 'Exercise and the brain: angiogenesis in the adult rat cerebellum after vigorous physical activity and motor skill learning', *Journal of Cerebral Blood Flow & Metabolism* **12**(1), 110–119.

Jackson, S. P. (2007), 'The growing complexity of platelet aggregation', *Blood* **109**(12), 5087–5095.

Jaiswal, J. K., Andrews, N. W. and Simon, S. M. (2002), 'Membrane proximal lysosomes are the major vesicles responsible for calcium-dependent exocytosis in nonsecretory cells', *J Cell Biol* **159**(4), 625–635.

Janmey, P. A., Stossel, T. P. and Allen, P. G. (1998), 'Deconstructing gelsolin: identifying sites that mimic or alter binding to actin and phosphoinositides', *Chemistry & biology* **5**(4), R81–R85.

Janssen, I., Heymsfield, S. B., Wang, Z. and Ross, R. (2000), 'Skeletal muscle mass and distribution in 468 men and women aged 18–88 yr', *Journal of applied physiology* **89**(1), 81–88.

Jensen, J. B. and Parmar, M. (2006), 'Strengths and limitations of the neurosphere culture system', *Molecular neurobiology* **34**(3), 153–161.

Jin, Y., Chen, K., Wang, Z., Wang, Y., Liu, J., Lin, L., Shao, Y., Gao, L., Yin, H., Cui, C. et al. (2016), 'Dna in serum extracellular vesicles is stable under different storage conditions', *BMC cancer* **16**(1), 753.

Johnstone, R. M., Adam, M., Hammond, J., Orr, L. and Turbide, C. (1987), 'Vesicle formation during reticulocyte maturation. association of plasma membrane activities with released vesicles (exosomes).', *Journal of Biological Chemistry* **262**(19), 9412–9420.

Kalafatis, M. (2005), 'Coagulation factor v: a plethora of anticoagulant molecules', *Current opinion in hematology* **12**(2), 141–148.

Kalra, H., Simpson, R. J., Ji, H., Aikawa, E., Altevogt, P., Askenase, P., Bond, V. C., Borràs, F. E., Breakefield, X., Budnik, V. et al. (2012), 'Vesiclepedia: a compendium for extracellular vesicles with continuous community annotation', *PLoS biology* **10**(12), e1001450.

Kandalla, P. K., Goldspink, G., Butler-Browne, G. and Mouly, V. (2011), 'Mechano growth factor e peptide (mgf-e), derived from an isoform of igf-1, activates human muscle progenitor cells and induces an increase in their fusion potential at different ages', *Mechanisms of ageing and development* **132**(4), 154–162.

Kao, F. F. and Ray, L. H. (1954), 'Regulation of cardiac output in anesthetized dogs during induced muscular work', *American Journal of Physiology-Legacy Content* **179**(2), 255–260.

Karimi, N., Cvjetkovic, A., Jang, S. C., Crescitelli, R., Feizi, M. A. H., Nieuwland, R., Lötvall, J. and Lässer, C. (2018), 'Detailed analysis of the plasma extracellular vesicle proteome after separation from lipoproteins', *Cellular and Molecular Life Sciences* pp. 1–14.

Karpievitch, Y. V., Dabney, A. R. and Smith, R. D. (2012), 'Normalization and missing value imputation for label-free lc-ms analysis', *BMC Bioinformatics* **13**(16).

Kassar-Duchossoy, L., Giacone, E., Gayraud-Morel, B., Jory, A., Gomès, D. and Tajbakhsh, S. (2005), 'Pax3/pax7 mark a novel population of primitive myogenic cells during development', *Genes & development* **19**(12), 1426–1431.

Kee, N., Sivalingam, S., Boonstra, R. and Wojtowicz, J. (2002), 'The utility of ki-67 and brdu as proliferative markers of adult neurogenesis', *Journal of neuroscience methods* **115**(1), 97–105.

Keerthikumar, S., Chisanga, D., Ariyaratne, D., Al Saffar, H., Anand, S., Zhao, K., Samuel, M., Pathan, M., Jois, M., Chilamkurti, N. et al. (2016), 'Exocarta: a web-based compendium of exosomal cargo', *Journal of molecular biology* **428**(4), 688–692.

Kenney, W. L., Wilmore, J. and Costill, D. (2015), *Physiology of sport and exercise 6th edition*, Human kinetics.

Kirby, T. J. and McCarthy, J. J. (2013), 'MicroRNAs in skeletal muscle biology and exercise adaptation', *Free radical biology and medicine* **64**, 95–105.

Kitzmann, M., Carnac, G., Vandromme, M., Primig, M., Lamb, N. J. and Fernandez, A. (1998), 'The muscle regulatory factors myod and myf-5 undergo distinct cell cycle–specific expression in muscle cells', *The Journal of cell biology* **142**(6), 1447–1459.

Kloosterman, W. P. and Plasterk, R. H. (2006), 'The diverse functions of micrornas in animal development and disease', *Developmental cell* **11**(4), 441–450.

Klumperman, J. and Raposo, G. (2014), 'The complex ultrastructure of the endolysosomal system', *Cold Spring Harbor perspectives in biology* p. a016857.

Koivisto, V. A., Yki-Järvinen, H. and DeFronzo, R. A. (1986), 'Physical training and insulin sensitivity', *Diabetes/metabolism reviews* **1**(4), 445–481.

Konoshenko, M. Y., Lekchnov, E. A., Vlassov, A. V. and Laktionov, P. P. (2018), 'Isolation of extracellular vesicles: General methodologies and latest trends', *BioMed research international* **2018**.

Kortebein, P., Symons, T. B., Ferrando, A., Paddon-Jones, D., Ronsen, O., Protas, E., Conger, S., Lombeida, J., Wolfe, R. and Evans, W. J. (2008), 'Functional impact of 10 days of bed rest in healthy older adults', *The Journals of Gerontology Series A: Biological Sciences and Medical Sciences* **63**(10), 1076–1081.

Kowal, J., Arras, G., Colombo, M., Jouve, M., Morath, J. P., Primdal-Bengtson, B., Dingli, F., Loew, D., Tkach, M. and Théry, C. (2016), 'Proteomic comparison defines novel markers to characterize heterogeneous populations of extracellular vesicle subtypes', *Proceedings of the National Academy of Sciences* p. 201521230.

Krämer-Albers, E.-M., Bretz, N., Tenzer, S., Winterstein, C., Möbius, W., Berger, H., Nave, K.-A., Schild, H. and Trotter, J. (2007), 'Oligodendrocytes secrete exosomes

containing major myelin and stress-protective proteins: Trophic support for axons?', *PROTEOMICS–Clinical Applications* **1**(11), 1446–1461.

Krogh, J., Nordentoft, M., Sterne, J. A. and Lawlor, D. A. (2011), 'The effect of exercise in clinically depressed adults: systematic review and meta-analysis of randomized controlled trials', *Journal of Clinical Psychiatry* **72**(4), 529.

Kuang, S., Gillespie, M. A. and Rudnicki, M. A. (2008), 'Niche regulation of muscle satellite cell self-renewal and differentiation', *Cell stem cell* **2**(1), 22–31.

Kuhn, H. G., Dickinson-Anson, H. and Gage, F. H. (1996), 'Neurogenesis in the dentate gyrus of the adult rat: age-related decrease of neuronal progenitor proliferation', *Journal of Neuroscience* **16**(6), 2027–2033.

Lacroix, R., Judicone, C., Poncelet, P., Robert, S., Arnaud, L., Sampol, J. and DIGNAT-GEORGE, F. (2012), 'Impact of pre-analytical parameters on the measurement of circulating microparticles: towards standardization of protocol', *Journal of Thrombosis and Haemostasis* **10**(3), 437–446.

Lafon-Cazal, M., Adjali, O., Galéotti, N., Poncet, J., Jouin, P., Homburger, V., Bockaert, J. and Marin, P. (2003), 'Proteomic analysis of astrocytic secretion in the mouse comparison with the cerebrospinal fluid proteome', *Journal of Biological Chemistry* **278**(27), 24438–24448.

Lancaster, G., Møller, K., Nielsen, B., Secher, N. H., Febbraio, M. A. and Nybo, L. (2004), 'Exercise induces the release of heat shock protein 72 from the human brain in vivo', *Cell stress & chaperones* **9**(3), 276.

Laurent, M. R., Dubois, V., Claessens, F., Verschueren, S. M., Vanderschueren, D., Gielen, E. and Jardí, F. (2016), 'Muscle-bone interactions: from experimental models to the clinic? a critical update', *Molecular and cellular endocrinology* **432**, 14–36.

Laurin, D., Verreault, R., Lindsay, J., MacPherson, K. and Rockwood, K. (2001), 'Physical activity and risk of cognitive impairment and dementia in elderly persons', *Archives of neurology* **58**(3), 498–504.

Lawrie, A., Albanyan, A., Cardigan, R., Mackie, I. and Harrison, P. (2009), 'Microparticle sizing by dynamic light scattering in fresh-frozen plasma', *Vox sanguinis* **96**(3), 206–212.

Lee, M. K., Tuttle, J. B., Rebhun, L. I., Cleveland, D. W. and Frankfurter, A. (1990), 'The expression and posttranslational modification of a neuron-specific β-tubulin isotype during chick embryogenesis', *Cell motility and the cytoskeleton* **17**(2), 118–132.

Lee, S. H. and Dominguez, R. (2010), 'Regulation of actin cytoskeleton dynamics in cells', *Molecules and cells* **29**(4), 311–325.

Li, Q., Ford, M. C., Lavik, E. B. and Madri, J. A. (2006), 'Modeling the neurovascular niche: Vegf-and bdnf-mediated cross-talk between neural stem cells and endothelial cells: an in vitro study', *Journal of neuroscience research* **84**(8), 1656–1668.

Li, W., Li, C., Zhou, T., Liu, X., Liu, X., Li, X. and Chen, D. (2017), 'Role of exosomal proteins in cancer diagnosis', *Molecular cancer* **16**(1), 145.

Li, X., Wang, F., Xu, M., Howles, P. and Tso, P. (2017), 'Apoa-iv improves insulin sensitivity and glucose uptake in mouse adipocytes via pi3k-akt signaling', *Scientific reports* **7**, 41289.

Liao, Z., Muth, D. C., Eitan, E., Travers, M., Learman, L. N., Lehrmann, E. and Witwer, K. W. (2017), 'Serum extracellular vesicle depletion processes affect release and infectivity of hiv-1 in culture', *Scientific Reports* **7**(1), 2558.

Liddelow, S. A., Temple, S., Møllgård, K., Gehwolf, R., Wagner, A., Bauer, H., Bauer, H.-C., Phoenix, T. N., Dziegielewska, K. M. and Saunders, N. R. (2012), 'Molecular characterisation of transport mechanisms at the developing mouse blood–csf interface: a transcriptome approach', *PloS one* **7**(3), e33554.

Liu, C., Teng, Z.-Q., Santistevan, N. J., Szulwach, K. E., Guo, W., Jin, P. and Zhao, X. (2010), 'Epigenetic regulation of mir-184 by mbd1 governs neural stem cell proliferation and differentiation', *Cell stem cell* **6**(5), 433–444.

Livshits, M. A., Khomyakova, E., Evtushenko, E. G., Lazarev, V. N., Kulemin, N. A., Semina, S. E., Generozov, E. V. and Govorun, V. M. (2015), 'Isolation of exosomes by

differential centrifugation: Theoretical analysis of a commonly used protocol', *Scientific reports* **5**, 17319.

Lloyd, A. C. (2006), 'Distinct functions for erks?', *Journal of biology* **5**(5), 13.

Logan, T., Rusnak, M. and Symes, A. (2015), 'Runx1 promotes proliferation and neuronal differentiation in adult mouse neurosphere cultures', *Stem cell research* **15**(3), 554–564.

Lois, C., Garcia-Verdugo, J.-M. and Alvarez-Buylla, A. (1996), 'Chain migration of neuronal precursors', *Science* **271**(5251), 978–981.

Manz, A., Harrison, D. J., Verpoorte, E. M., Fettinger, J. C., Paulus, A., Lüdi, H. and Widmer, H. M. (1992), 'Planar chips technology for miniaturization and integration of separation techniques into monitoring systems: capillary electrophoresis on a chip', *Journal of Chromatography A* **593**(1-2), 253–258.

Marques, F., Sousa, J. C., Coppola, G., Falcao, A. M., Rodrigues, A. J., Geschwind, D. H., Sousa, N., Correia-Neves, M. and Palha, J. A. (2009), 'Kinetic profile of the transcriptome changes induced in the choroid plexus by peripheral inflammation', *Journal of Cerebral Blood Flow & Metabolism* **29**(5), 921–932.

Marrugo-Ramírez, J., Mir, M. and Samitier, J. (2018), 'Blood-based cancer biomarkers in liquid biopsy: a promising non-invasive alternative to tissue biopsy', *International journal of molecular sciences* **19**(10), 2877.

Mateescu, B., Kowal, E. J., van Balkom, B. W., Bartel, S., Bhattacharyya, S. N., Buzás, E. I., Buck, A. H., de Candia, P., Chow, F. W., Das, S. et al. (2017), 'Obstacles and opportunities in the functional analysis of extracellular vesicle rna–an isev position paper', *Journal of extracellular vesicles* **6**(1), 1286095.

Mateo, A., de la Lastra, J. P., Garrido, J. and Llanes, D. (1996), 'Platelet activation studies with cd41/61 monoclonal antibodies', *Veterinary immunology and immunopathology* **52**(4), 357–362.

Matthews, C. E., Ockene, I. S., Freedson, P. S., Rosal, M. C., Merriam, P. A. and Hebert, J. R. (2002), 'Moderate to vigorous physical activity and risk of upper-respiratory tract infection.', *Medicine and science in sports and exercise* **34**(8), 1242–1248.

Mauro, A. (1961), 'Satellite cell of skeletal muscle fibers', *The Journal of biophysical and biochemical cytology* **9**(2), 493.

McGough, A., Chiu, W. and Way, M. (1998), 'Determination of the gelsolin binding site on f-actin: implications for severing and capping', *Biophysical journal* **74**(2), 764–772.

McMichael, A., Beverley, P., Cobbold, S., Crumpton, M., Gilks, W., Gotch, F., Hogg, N., Horton, M., Ling, N., MacLennan, I. et al. (1987), 'Leukocyte typing iii', *White cell differentiation antigens* **3**, 780.

Mead, J. R., Irvine, S. A. and Ramji, D. P. (2002), 'Lipoprotein lipase: structure, function, regulation, and role in disease', *Journal of molecular medicine* **80**(12), 753–769.

Meckes, D. G., Gunawardena, H. P., Dekroon, R. M., Heaton, P. R., Edwards, R. H., Ozgur, S., Griffith, J. D., Damania, B. and Raab-Traub, N. (2013), 'Modulation of b-cell exosome proteins by gamma herpesvirus infection', *Proceedings of the National Academy of Sciences* **110**(31), E2925–E2933.

Mentkowski, K. I., Snitzer, J. D., Rusnak, S. and Lang, J. K. (2018), 'Therapeutic potential of engineered extracellular vesicles', *The AAPS Journal* **20**(3), 50.

Mera, P., Laue, K., Ferron, M., Confavreux, C., Wei, J., Galán-Díez, M., Lacampagne, A., Mitchell, S. J., Mattison, J. A., Chen, Y. et al. (2016), 'Osteocalcin signaling in myofibers is necessary and sufficient for optimum adaptation to exercise', *Cell metabolism* **23**(6), 1078–1092.

Merchant, M. L., Powell, D. W., Wilkey, D. W., Cummins, T. D., Deegens, J. K., Rood, I. M., McAfee, K. J., Fleischer, C., Klein, E. and Klein, J. B. (2010), 'Microfiltration isolation of human urinary exosomes for characterization by ms', *Proteomics–Clinical Applications* **4**(1), 84–96.

Merkle, F. T. and Alvarez-Buylla, A. (2006), 'Neural stem cells in mammalian development', *Current opinion in cell biology* **18**(6), 704–709.

Metzinger, L., Passaquin, A.-C., Warter, J.-M. and Poindron, P. (1993), 'α-methylprednisolone promotes skeletal myogenesis in dystrophin-deficient and control mouse cultures', *Neuroscience letters* **155**(2), 171–174.

Meyn, R., Hewitt, R. and Humphrey, R. (1973), 'Evaluation of s phase synchronization by analysis of dna replication in 5-bromodeoxyuridine', *Experimental cell research* **82**(1), 137–142.

Mi, H., Muruganujan, A., Casagrande, J. T. and Thomas, P. D. (2013), 'Large-scale gene function analysis with the panther classification system', *Nature protocols* **8**(8), 1551.

Miner, J. H. and Wold, B. (1990), 'Herculin, a fourth member of the myod family of myogenic regulatory genes.', *Proceedings of the National Academy of Sciences* **87**(3), 1089–1093.

Mittelbrunn, M., Gutiérrez-Vázquez, C., Villarroya-Beltri, C., González, S., Sánchez-Cabo, F., González, M. Á., Bernad, A. and Sánchez-Madrid, F. (2011), 'Unidirectional transfer of microrna-loaded exosomes from t cells to antigen-presenting cells', *Nature communications* **2**, 282.

Monninkhof, E. M., Elias, S. G., Vlems, F. A., van der Tweel, I., Schuit, A. J., Voskuil, D. W. and van Leeuwen, F. E. (2007), 'Physical activity and breast cancer: a systematic review', *Epidemiology* pp. 137–157.

Monteggia, L. M., Barrot, M., Powell, C. M., Berton, O., Galanis, V., Gemelli, T., Meuth, S., Nagy, A., Greene, R. W. and Nestler, E. J. (2004), 'Essential role of brain-derived neurotrophic factor in adult hippocampal function', *Proceedings of the National Academy of Sciences* **101**(29), 10827–10832.

Montero-Fernandez, N. and Serra-Rexach, J. (2013), 'Role of exercise on sarcopenia in the elderly.', *European journal of physical and rehabilitation medicine* **49**(1), 131–143.

Mori, S. and Barth, H. G. (2013), *Size exclusion chromatography*, Springer Science & Business Media.

Müller, R., Heinrich, M., Heck, S., Blohm, D. and Richter-Landsberg, C. (1997), 'Expression of microtubule-associated proteins map2 and tau in cultured rat brain oligodendrocytes', *Cell and tissue research* **288**(2), 239–249.

Muralidharan-Chari, V., Clancy, J., Plou, C., Romao, M., Chavrier, P., Raposo, G. and D'Souza-Schorey, C. (2009), 'Arf6-regulated shedding of tumor cell-derived plasma membrane microvesicles', *Current Biology* **19**(22), 1875–1885.

Nakai, W., Yoshida, T., Diez, D., Miyatake, Y., Nishibu, T., Imawaka, N., Naruse, K., Sadamura, Y. and Hanayama, R. (2016), 'A novel affinity-based method for the isolation of highly purified extracellular vesicles', *Scientific reports* **6**, 33935.

Nakamura, Y., Miyaki, S., Ishitobi, H., Matsuyama, S., Nakasa, T., Kamei, N., Akimoto, T., Higashi, Y. and Ochi, M. (2015), 'Mesenchymal-stem-cell-derived exosomes accelerate skeletal muscle regeneration', *FEBS letters* **589**(11), 1257–1265.

Ng, K. W. and Schantz, J.-T. (2010), *A Manual for Primary Human Cell Culture, Second Edition*, Vol. 6, World Scientific Publishing.

Nieuwland, R., Berckmans, R. J., McGregor, S., Böing, A. N., Romijn, F. P. T. M., Westendorp, R. G., Hack, C. E. and Sturk, A. (2000), 'Cellular origin and procoagulant properties of microparticles in meningococcal sepsis', *Blood* **95**(3), 930–935.

Nishiyama, T., Kii, I. and Kudo, A. (2004), 'Inactivation of rho/rock signaling is crucial for the nuclear accumulation of fkhr and myoblast fusion', *Journal of Biological Chemistry* **279**(45), 47311–47319.

Nocon, M., Hiemann, T., Müller-Riemenschneider, F., Thalau, F., Roll, S. and Willich, S. N. (2008), 'Association of physical activity with all-cause and cardiovascular mortality: a systematic review and meta-analysis', *European Journal of Cardiovascular Prevention & Rehabilitation* **15**(3), 239–246.

Nojima, H., Tokunaga, C., Eguchi, S., Oshiro, N., Hidayat, S., Yoshino, K.-i., Hara, K., Tanaka, N., Avruch, J. and Yonezawa, K. (2003), 'The mammalian target of rapamycin (mtor) partner, raptor, binds the mtor substrates p70 s6 kinase and 4e-bp1 through their tor signaling (tos) motif', *Journal of Biological Chemistry* **278**(18), 15461–15464.

Nordin, J. Z., Lee, Y., Vader, P., Mäger, I., Johansson, H. J., Heusermann, W., Wiklander, O. P., Hällbrink, M., Seow, Y., Bultema, J. J. et al. (2015), 'Ultrafiltration with size-exclusion liquid chromatography for high yield isolation of extracellular vesicles preserving intact biophysical and functional properties', *Nanomedicine: Nanotechnology, Biology and Medicine* **11**(4), 879–883.

Obermeier, B., Daneman, R. and Ransohoff, R. M. (2013), 'Development, maintenance and disruption of the blood-brain barrier', *Nature medicine* **19**(12), 1584.

Ochieng, J., Pratap, S., Khatua, A. K. and Sakwe, A. M. (2009), 'Anchorage-independent growth of breast carcinoma cells is mediated by serum exosomes', *Experimental cell research* **315**(11), 1875–1888.

Oguma, Y., Sesso, H., Paffenbarger, R. and Lee, I. (2002), 'Physical activity and all cause mortality in women: a review of the evidence', *British journal of sports medicine* **36**(3), 162–172.

Omary, M. B., Coulombe, P. A. and McLean, W. I. (2004), 'Intermediate filament proteins and their associated diseases', *New England Journal of Medicine* **351**(20), 2087–2100.

Ostenfeld, M. S., Jeppesen, D. K., Laurberg, J. R., Boysen, A. T., Bramsen, J. B., Primdal-Bengtson, B., Hendrix, A., Lamy, P., Dagnaes-Hansen, F., Rasmussen, M. H. et al. (2014), 'Cellular disposal of mir23b by rab27-dependent exosome release is linked to acquisition of metastatic properties', *Cancer research* .

Østergaard, O., Nielsen, C. T., Iversen, L. V., Jacobsen, S., Tanassi, J. T. and Heegaard, N. H. (2012), 'Quantitative proteome profiling of normal human circulating microparticles', *Journal of proteome research* **11**(4), 2154–2163.

Ostrowski, M., Carmo, N. B., Krumeich, S., Fanget, I., Raposo, G., Savina, A., Moita, C. F., Schauer, K., Hume, A. N., Freitas, R. P. et al. (2010), 'Rab27a and rab27b control different steps of the exosome secretion pathway', *Nature cell biology* **12**(1), 19.

Paffenbarger Jr, R., Lee, I.-M. and Leung, R. (1994), 'Physical activity and personal characteristics associated with depression and suicide in american college men', *Acta Psychiatrica Scandinavica* **89**, 16–22.

Paillard, T., Rolland, Y. and de Souto Barreto, P. (2015), 'Protective effects of physical exercise in alzheimer's disease and parkinson's disease: a narrative review', *Journal of clinical neurology* **11**(3), 212–219.

Pasco, J. A., Jacka, F. N., Williams, L. J., Brennan, S. L., Leslie, E. and Berk, M. (2011), 'Don't worry, be active: Positive affect and habitual physical activity', *Australian & New Zealand Journal of Psychiatry* **45**(12), 1047–1052.

Patel, V. J., Thalassinos, K., Slade, S. E., Connolly, J. B., Crombie, A., Murrell, J. C. and Scrivens, J. H. (2009), 'A comparison of labeling and label-free mass spectrometry-based proteomics approaches', *Journal of Proteome Research* **8**(7), 3752–3759.

Pavlath, G. K., Dominov, J. A., Kegley, K. M. and Miller, J. B. (2003), 'Regeneration of transgenic skeletal muscles with altered timing of expression of the basic helix-loop-helix muscle regulatory factor mrf4', *The American journal of pathology* **162**(5), 1685–1691.

Pedersen, B. K. (2011), 'Exercise-induced myokines and their role in chronic diseases', *Brain, Behavior, and Immunity* **25**(5), 811–816.

Pereira, A. C., Huddleston, D. E., Brickman, A. M., Sosunov, A. A., Hen, R., McKhann, G. M., Sloan, R., Gage, F. H., Brown, T. R. and Small, S. A. (2007), 'An in vivo correlate of exercise-induced neurogenesis in the adult dentate gyrus', *Proceedings of the National Academy of Sciences* **104**(13), 5638–5643.

Perez-Hernandez, D., Gutiérrez-Vázquez, C., Jorge, I., López-Martín, S., Ursa, A., Sánchez-Madrid, F., Vázquez, J. and Yáñez-Mó, M. (2013), 'The intracellular interactome

of tetraspanin-enriched microdomains reveals their function as sorting machineries to exosomes', *Journal of Biological Chemistry* pp. jbc–M112.

Persson, A. I., Naylor, A. S., Jonsdottir, I. H., Nyberg, F., Eriksson, P. S. and Thorlin, T. (2004), 'Differential regulation of hippocampal progenitor proliferation by opioid receptor antagonists in running and non-running spontaneously hypertensive rats', *European Journal of Neuroscience* **19**(7), 1847–1855.

Pillon, N. J., Bilan, P. J., Fink, L. N. and Klip, A. (2013), 'Crosstalk between skeletal muscle and immune cells: muscle-derived mediators and metabolic implications', *American Journal of Physiology-Heart and Circulatory Physiology* .

Pinet, B. M., Prud'homme, D., Gallant, C. A. and Boulay, P. (2008), 'Exercise intensity prescription in obese individuals', *Obesity* **16**(9), 2088–2095.

Poehlman, E. T., Dvorak, R. V., DeNino, W. F., Brochu, M. and Ades, P. A. (2000), 'Effects of resistance training and endurance training on insulin sensitivity in nonobese, young women: a controlled randomized trial', *The Journal of Clinical Endocrinology & Metabolism* **85**(7), 2463–2468.

Poo, M.-m. (2001), 'Neurotrophins as synaptic modulators', *Nature reviews neuroscience* **2**(1), 24.

Powell, K. E., Paluch, A. E. and Blair, S. N. (2011), 'Physical activity for health: What kind? how much? how intense? on top of what?', *Annual review of public health* **32**, 349–365.

Pozhilenkova, E. A., Lopatina, O. L., Komleva, Y. K., Salmin, V. V. and Salmina, A. B. (2017), 'Blood-brain barrier-supported neurogenesis in healthy and diseased brain', *Reviews in the Neurosciences* **28**(4), 397–415.

Prendergast, E. N., de Souza Fonseca, M. A., Dezem, F. S., Lester, J., Karlan, B. Y., Noushmehr, H., Lin, X. and Lawrenson, K. (2018), 'Optimizing exosomal rna isolation for rna-seq analyses of archival sera specimens', *PloS one* **13**(5), e0196913.

Puhka, M., Takatalo, M., Nordberg, M.-E., Valkonen, S., Nandania, J., Aatonen, M., Yliperttula, M., Laitinen, S., Velagapudi, V., Mirtti, T. et al. (2017), 'Metabolomic profiling of extracellular vesicles and alternative normalization methods reveal enriched metabolites and strategies to study prostate cancer-related changes', *Theranostics* **7**(16), 3824.

Ramos, J. W. (2008), 'The regulation of extracellular signal-regulated kinase (erk) in mammalian cells', *The international journal of biochemistry & cell biology* **40**(12), 2707–2719.

Raposo, G., Nijman, H. W., Stoorvogel, W., Liejendekker, R., Harding, C. V., Melief, C. and Geuze, H. J. (1996), 'B lymphocytes secrete antigen-presenting vesicles.', *Journal of Experimental Medicine* **183**(3), 1161–1172.

Raposo, G. and Stoorvogel, W. (2013), 'Extracellular vesicles: exosomes, microvesicles, and friends', *J Cell Biol* **200**(4), 373–383.

Ratajczak, J., Miekus, K., Kucia, M., Zhang, J., Reca, R., Dvorak, P. and Ratajczak, M. (2006), 'Embryonic stem cell-derived microvesicles reprogram hematopoietic progenitors: evidence for horizontal transfer of mrna and protein delivery', *Leukemia* **20**(5), 847.

Reátegui, E., Vos, K. E., Lai, C. P., Zeinali, M., Atai, N. A., Aldikacti, B., Floyd, F. P., Khankhel, A., Thapar, V., Hochberg, F. H. et al. (2018), 'Engineered nanointerfaces for microfluidic isolation and molecular profiling of tumor-specific extracellular vesicles', *Nature communications* **9**(1), 175.

Record, M., Carayon, K., Poirot, M. and Silvente-Poirot, S. (2014), 'Exosomes as new vesicular lipid transporters involved in cell–cell communication and various pathophysiologies', *Biochimica et Biophysica Acta (BBA)-Molecular and Cell Biology of Lipids* **1841**(1), 108–120.

Rehfeld, A., Nylander, M. and Karnov, K. (2017), *Compendium of Histology: A Theoretical and Practical Guide*, Springer.

Reynolds, B., Tetzlaff, W. and Weiss, S. (1992), 'A multipotent egf-responsive striatal

embryonic progenitor cell produces neurons and astrocytes', *The Journal of neuroscience : the official journal of the Society for Neuroscience* **12**(11), 4565—4574.

Rhodes, S. J. and Konieczny, S. F. (1989), 'Identification of mrf4: a new member of the muscle regulatory factor gene family.', *Genes & development* **3**(12b), 2050–2061.

Riches, A., Campbell, E., Borger, E. and Powis, S. (2014), 'Regulation of exosome release from mammary epithelial and breast cancer cells–a new regulatory pathway', *European journal of cancer* **50**(5), 1025–1034.

Ridder, K., Keller, S., Dams, M., Rupp, A.-K., Schlaudraff, J., Del Turco, D., Starmann, J., Macas, J., Karpova, D., Devraj, K. et al. (2014), 'Extracellular vesicle-mediated transfer of genetic information between the hematopoietic system and the brain in response to inflammation', *PLoS biology* **12**(6), e1001874.

RnD Systems Detecting protein phosphorylation (2018), `https://www.rndsystems.com/resources/articles/methods-detecting-protein-phosphorylation`. Accessed: September 2018.

Robergs, R. A. and Landwehr, R. (2002), 'The surprising history of the" hrmax= 220-age" equation', *Journal of Exercise Physiology Online* **5**(2), 1–10.

Rosch, P. J. (1985), 'Exercise and stress reduction.', *Comprehensive therapy* **11**(4), 10.

Rovio, S., Kåreholt, I., Helkala, E.-L., Viitanen, M., Winblad, B., Tuomilehto, J., Soininen, H., Nissinen, A. and Kivipelto, M. (2005), 'Leisure-time physical activity at midlife and the risk of dementia and alzheimer's disease', *The Lancet Neurology* **4**(11), 705–711.

Ruiz, J. R., Sui, X., Lobelo, F., Morrow, J. R., Jackson, A. W., Sjöström, M. and Blair, S. N. (2008), 'Association between muscular strength and mortality in men: prospective cohort study', *Bmj* **337**, a439.

Safdar, A., Saleem, A. and Tarnopolsky, M. A. (2016), 'The potential of endurance exercise-derived exosomes to treat metabolic diseases', *Nature Reviews Endocrinology* **12**(9), 504.

Sancak, Y., Thoreen, C. C., Peterson, T. R., Lindquist, R. A., Kang, S. A., Spooner, E., Carr, S. A. and Sabatini, D. M. (2007), 'Pras40 is an insulin-regulated inhibitor of the mtorc1 protein kinase', *Molecular cell* **25**(6), 903–915.

Sarker, S., Scholz-Romero, K., Perez, A., Illanes, S. E., Mitchell, M. D., Rice, G. E. and Salomon, C. (2014), 'Placenta-derived exosomes continuously increase in maternal circulation over the first trimester of pregnancy', *Journal of translational medicine* **12**(1), 204.

Sato, K., Meng, F., Glaser, S. and Alpini, G. (2016), 'Exosomes in liver pathology', *Journal of hepatology* **65**(1), 213–221.

Sato, K., Saida, K., Yanagawa, T., Fukuda, T., Shirakura, K., Shinozaki, H. and Watanabe, H. (2011), 'Differential responses of myogenic c2c12 cells to hypoxia between growth and muscle-induction phases: growth, differentiation and motility', *Journal of Physical Therapy Science* **23**(1), 161–169.

Sawada, M., Matsumoto, M. and Sawamoto, K. (2014), 'Vascular regulation of adult neurogenesis under physiological and pathological conditions', *Frontiers in neuroscience* **8**, 53.

Scheibe, F., Klein, O., Klose, J. and Priller, J. (2012), 'Mesenchymal stromal cells rescue cortical neurons from apoptotic cell death in an in vitro model of cerebral ischemia', *Cellular and molecular neurobiology* **32**(4), 567–576.

Schindelin, J., Arganda-Carreras, I., Frise, E., Kaynig, V., Longair, M., Pietzsch, T., Preibisch, S., Rueden, C., Saalfeld, S., Schmid, B. et al. (2012), 'Fiji: an open-source platform for biological-image analysis', *Nature methods* **9**(7), 676.

Schouten, M., Buijink, M. R., Lucassen, P. J. and Fitzsimons, C. P. (2012), 'New neurons in aging brains: molecular control by small non-coding rnas', *Frontiers in neuroscience* **6**, 25.

Seale, P., Sabourin, L. A., Girgis-Gabardo, A., Mansouri, A., Gruss, P. and Rudnicki, M. A. (2000), 'Pax7 is required for the specification of myogenic satellite cells', *Cell* **102**(6), 777–786.

Seip, R. L. and Semenkovich, C. (1998), 'Skeletal muscle lipoprotein lipase: molecular regulation and physiological effects in relation to exercise.', *Exercise and sport sciences reviews* **26**, 191–218.

Shi, Y., Zhao, X., Hsieh, J., Wichterle, H., Impey, S., Banerjee, S., Neveu, P. and Kosik, K. S. (2010), 'Microrna regulation of neural stem cells and neurogenesis', *Journal of Neuroscience* **30**(45), 14931–14936.

Shimizu, N., Maruyama, T., Yoshikawa, N., Matsumiya, R., Ma, Y., Ito, N., Tasaka, Y., Kuribara-Souta, A., Miyata, K., Oike, Y. et al. (2015), 'A muscle-liver-fat signalling axis is essential for central control of adaptive adipose remodelling', *Nature communications* **6**, 6693.

Shin, H., Han, C., Labuz, J. M., Kim, J., Kim, J., Cho, S., Gho, Y. S., Takayama, S. and Park, J. (2015), 'High-yield isolation of extracellular vesicles using aqueous two-phase system', *Scientific reports* **5**, 13103.

Sibley, B. A. and Etnier, J. L. (2003), 'The relationship between physical activity and cognition in children: a meta-analysis', *Pediatric exercise science* **15**(3), 243–256.

Simons, K. and Sampaio, J. L. (2011), 'Membrane organization and lipid rafts', *Cold Spring Harbor perspectives in biology* p. a004697.

Simons, M. and Raposo, G. (2009), 'Exosomes–vesicular carriers for intercellular communication', *Current opinion in cell biology* **21**(4), 575–581.

Simpson, R., Mathivanan, S. et al. (2012), 'Extracellular microvesicles: the need for internationally tecognised nomenclature and stringent purification criteria.', *J Proteomics Bioinform* **5**(2).

Skog, J., Würdinger, T., Van Rijn, S., Meijer, D. H., Gainche, L., Curry Jr, W. T., Carter, B. S., Krichevsky, A. M. and Breakefield, X. O. (2008), 'Glioblastoma microvesicles transport rna and proteins that promote tumour growth and provide diagnostic biomarkers', *Nature cell biology* **10**(12), 1470.

Sleiman, S. F., Henry, J., Al-Haddad, R., El Hayek, L., Haidar, E. A., Stringer, T., Ulja, D., Karuppagounder, S. S., Holson, E. B., Ratan, R. R. et al. (2016), 'Exercise promotes the expression of brain derived neurotrophic factor (bdnf) through the action of the ketone body β-hydroxybutyrate', *Elife* **5**, e15092.

Smith, P. J., Blumenthal, J. A., Hoffman, B. M., Cooper, H., Strauman, T. A., Welsh-Bohmer, K., Browndyke, J. N. and Sherwood, A. (2010), 'Aerobic exercise and neurocognitive performance: a meta-analytic review of randomized controlled trials', *Psychosomatic medicine* **72**(3), 239.

Snell, R. S. (2010), *Clinical neuroanatomy*, Lippincott Williams & Wilkins.

Snyder, J. S., Soumier, A., Brewer, M., Pickel, J. and Cameron, H. A. (2011), 'Adult hippocampal neurogenesis buffers stress responses and depressive behaviour', *Nature* **476**(7361), 458.

Soares Martins, T., Catita, J., Martins Rosa, I., A. B. da Cruz e Silva, O. and Henriques, A. G. (2018), 'Exosome isolation from distinct biofluids using precipitation and column-based approaches', *PloS One* **13**(6), 1–16.

Sódar, B. W., Kittel, Á., Pálóczi, K., Vukman, K. V., Osteikoetxea, X., Szabó-Taylor, K., Németh, A., Sperlágh, B., Baranyai, T., Giricz, Z. et al. (2016), 'Low-density lipoprotein mimics blood plasma-derived exosomes and microvesicles during isolation and detection', *Scientific reports* **6**, 24316.

Spalding, K. L., Bergmann, O., Alkass, K., Bernard, S., Salehpour, M., Huttner, H. B., Boström, E., Westerlund, I., Vial, C., Buchholz, B. A. et al. (2013), 'Dynamics of hippocampal neurogenesis in adult humans', *Cell* **153**(6), 1219–1227.

Stanford, K. I., Middelbeek, R. J. and Goodyear, L. J. (2015), 'Exercise effects on white adipose tissue: beiging and metabolic adaptations', *Diabetes* **64**(7), 2361–2368.

Stepanian, A., Bourguignat, L., Hennou, S., Coupaye, M., Hajage, D., Salomon, L., Alessi, M.-C., Msika, S. and de Prost, D. (2013), 'Microparticle increase in severe obesity:

not related to metabolic syndrome and unchanged after massive weight loss', *Obesity* **21**(11), 2236–2243.

Stoorvogel, W., Strous, G. J., Geuze, H. J., Oorschot, V. and Schwartzt, A. L. (1991), 'Late endosomes derive from early endosomes by maturation', *Cell* **65**(3), 417–427.

Studitsky, A. (1964), 'Free auto-and homografts of muscle tissue in experiments on animals', *Annals of the New York Academy of Sciences* **120**(1), 789–801.

Sugg, K. B., Korn, M. A., Sarver, D. C., Markworth, J. F. and Mendias, C. L. (2017), 'Inhibition of platelet-derived growth factor signaling prevents muscle fiber growth during skeletal muscle hypertrophy', *FEBS letters* **591**(5), 801–809.

Sun, B., Dalvi, P., Abadjian, L., Tang, N. and Pulliam, L. (2017), 'Blood neuron-derived exosomes as biomarkers of cognitive impairment in hiv', *Aids* **31**(14), F9–F17.

Sun, G. J., Zhou, Y., Stadel, R. P., Moss, J., Yong, J. H. A., Ito, S., Kawasaki, N. K., Phan, A. T., Oh, J. H., Modak, N. et al. (2015), 'Tangential migration of neuronal precursors of glutamatergic neurons in the adult mammalian brain', *Proceedings of the National Academy of Sciences* **112**(30), 9484–9489.

Tanapat, P. (2013), 'A comprehensive review of immunohistochemical markers for cns neuronal cell types', *MATER METHODS* **3**, 196.

Tao, S.-C., Guo, S.-C. and Zhang, C.-Q. (2017), 'Platelet-derived extracellular vesicles: an emerging therapeutic approach', *International journal of biological sciences* **13**(7), 828.

Tassew, N. G., Charish, J., Shabanzadeh, A. P., Luga, V., Harada, H., Farhani, N., D'Onofrio, P., Choi, B., Ellabban, A., Nickerson, P. E. et al. (2017), 'Exosomes mediate mobilization of autocrine wnt10b to promote axonal regeneration in the injured cns', *Cell reports* **20**(1), 99–111.

Tatsumi, R., Anderson, J. E., Nevoret, C. J., Halevy, O. and Allen, R. E. (1998), 'Hgf/sf is present in normal adult skeletal muscle and is capable of activating satellite cells', *Developmental biology* **194**(1), 114–128.

Tavazoie, M., Van der Veken, L., Silva-Vargas, V., Louissaint, M., Colonna, L., Zaidi, B., Garcia-Verdugo, J. M. and Doetsch, F. (2008), 'A specialized vascular niche for adult neural stem cells', *Cell stem cell* **3**(3), 279–288.

Taylor, D. D., Zacharias, W. and Gercel-Taylor, C. (2011), Exosome isolation for proteomic analyses and rna profiling, *in* 'Serum/plasma proteomics', Springer, pp. 235–246.

Terra, R., Silva, S. A. G. d., Pinto, V. S. and Dutra, P. M. L. (2012), 'Effect of exercise on immune system: response, adaptation and cell signaling', *Revista Brasileira de Medicina do Esporte* **18**(3), 208–214.

Thakur, B. K., Zhang, H., Becker, A., Matei, I., Huang, Y., Costa-Silva, B., Zheng, Y., Hoshino, A., Brazier, H., Xiang, J. et al. (2014), 'Double-stranded dna in exosomes: a novel biomarker in cancer detection', *Cell research* **24**(6), 766.

Tharmaratnam, T., Civitarese, R. A., Tabobondung, T. and Tabobondung, T. A. (2017), 'Exercise becomes brain: sustained aerobic exercise enhances hippocampal neurogenesis', *The Journal of physiology* **595**(1), 7–8.

Théry, C., Boussac, M., Véron, P., Ricciardi-Castagnoli, P., Raposo, G., Garin, J. and Amigorena, S. (2001), 'Proteomic analysis of dendritic cell-derived exosomes: a secreted subcellular compartment distinct from apoptotic vesicles', *The Journal of Immunology* **166**(12), 7309–7318.

Théry, C., Witwer, K. W., Aikawa, E., Alcaraz, M. J., Anderson, J. D., Andriantsitohaina, R., Antoniou, A., Arab, T., Archer, F., Atkin-Smith, G. K. et al. (2018), 'Minimal information for studies of extracellular vesicles 2018 (misev2018): a position statement of the international society for extracellular vesicles and update of the misev2014 guidelines', *Journal of Extracellular Vesicles* **7**(1), 1535750.

Thomas, K., Engler, A. J. and Meyer, G. A. (2015), 'Extracellular matrix regulation in the muscle satellite cell niche', *Connective tissue research* **56**(1), 1–8.

Toda, T., Parylak, S. L., Linker, S. B. and Gage, F. H. (2018), 'The role of adult hippocampal neurogenesis in brain health and disease', *Molecular psychiatry* p. 1.

Tonkin, J., Temmerman, L., Sampson, R. D., Gallego-Colon, E., Barberi, L., Bilbao, D., Schneider, M. D., Musarò, A. and Rosenthal, N. (2015), 'Monocyte/macrophage-derived igf-1 orchestrates murine skeletal muscle regeneration and modulates autocrine polarization', *Molecular therapy* **23**(7), 1189–1200.

Trujillo, C. A., Schwindt, T. T., Martins, A. H., Alves, J. M., Mello, L. E. and Ulrich, H. (2009), 'Novel perspectives of neural stem cell differentiation: from neurotransmitters to therapeutics', *Cytometry Part A: The Journal of the International Society for Advancement of Cytometry* **75**(1), 38–53.

Tuomilehto, J., Lindström, J., Eriksson, J. G., Valle, T. T., Hämäläinen, H., Ilanne-Parikka, P., Keinänen-Kiukaanniemi, S., Laakso, M., Louheranta, A., Rastas, M. et al. (2001), 'Prevention of type 2 diabetes mellitus by changes in lifestyle among subjects with impaired glucose tolerance', *New England Journal of Medicine* **344**(18), 1343–1350.

Ueba, T., Nomura, S., Inami, N., Nishikawa, T., Kajiwara, M., Iwata, R. and Yamashita, K. (2010), 'Plasma level of platelet-derived microparticles is associated with coronary heart disease risk score in healthy men', *Journal of atherosclerosis and thrombosis* **17**(4), 342–349.

Uhlén, M., Fagerberg, L., Hallström, B. M., Lindskog, C., Oksvold, P., Mardinoglu, A., Sivertsson, Å., Kampf, C., Sjöstedt, E., Asplund, A. et al. (2015), 'Tissue-based map of the human proteome', *Science* **347**(6220), 1260419.

Ung, T. H., Madsen, H. J., Hellwinkel, J. E., Lencioni, A. M. and Graner, M. W. (2014), 'Exosome proteomics reveals transcriptional regulator proteins with potential to mediate downstream pathways', *Cancer science* **105**(11), 1384–1392.

Vagida, M., Arakelyan, A., Lebedeva, A., Grivel, J. C., Shpektor, A., Vasilieva, E. Y. and Margolis, L. (2016), 'Analysis of extracellular vesicles using magnetic nanoparticles in blood of patients with acute coronary syndrome', *Biochemistry (Moscow)* **81**(4), 382–391.

Valadi, H., Ekström, K., Bossios, A., Sjöstrand, M., Lee, J. J. and Lötvall, J. O. (2007), 'Exosome-mediated transfer of mrnas and micrornas is a novel mechanism of genetic exchange between cells', *Nature cell biology* **9**(6), 654.

Vallhov, H., Gutzeit, C., Johansson, S. M., Nagy, N., Paul, M., Li, Q., Friend, S., George, T. C., Klein, E., Scheynius, A. et al. (2011), 'Exosomes containing glycoprotein 350 released by ebv-transformed b cells selectively target b cells through cd21 and block ebv infection in vitro', *The Journal of Immunology* **186**(1), 73–82.

van Dam, R., Van Ancum, J. M., Verlaan, S., Scheerman, K., Meskers, C. G. and Maier, A. B. (2018), 'Lower cognitive function in older patients with lower muscle strength and muscle mass', *Dementia and geriatric cognitive disorders* **45**, 243–250.

van der Borght, K., Ferrari, F., Klauke, K., Roman, V., Havekes, R., Sgoifo, A., van der Zee, E. A. and Meerlo, P. (2006), 'Hippocampal cell proliferation across the day: increase by running wheel activity, but no effect of sleep and wakefulness', *Behavioural brain research* **167**(1), 36–41.

Varki, A. and Lowe, J. B. (2009), Biological roles of glycans, *in* 'Essentials of Glycobiology. 2nd edition', Cold Spring Harbor Laboratory Press.

Vaynman, S., Ying, Z. and Gomez-Pinilla, F. (2004), 'Hippocampal bdnf mediates the efficacy of exercise on synaptic plasticity and cognition', *European Journal of Neuroscience* **20**(10), 2580–2590.

Vazana, U., Veksler, R., Pell, G. S., Prager, O., Fassler, M., Chassidim, Y., Roth, Y., Shahar, H., Zangen, A., Raccah, R. et al. (2016), 'Glutamate-mediated blood–brain barrier opening: implications for neuroprotection and drug delivery', *Journal of Neuroscience* **36**(29), 7727–7739.

Villeda, S. A., Luo, J., Mosher, K. I., Zou, B., Britschgi, M., Bieri, G., Stan, T. M., Fainberg, N., Ding, Z., Eggel, A. et al. (2011), 'The ageing systemic milieu negatively regulates neurogenesis and cognitive function', *Nature* **477**(7362), 90.

Vincent-Schneider, H., Stumptner-Cuvelette, P., Lankar, D., Pain, S., Raposo, G., Benaroch, P. and Bonnerot, C. (2002), 'Exosomes bearing hla-dr1 molecules need dendritic cells to efficiently stimulate specific t cells', *International immunology* **14**(7), 713–722.

Volovelsky, O., Cohen, G., Kenig, A., Wasserman, G., Dreazen, A., Meyuhas, O., Silver, J. and Naveh-Many, T. (2016), 'Phosphorylation of ribosomal protein s6 mediates mammalian target of rapamycin complex 1–induced parathyroid cell proliferation in secondary hyperparathyroidism', *Journal of the American Society of Nephrology* **27**(4), 1091–1101.

Waldenström, A., Gennebäck, N., Hellman, U. and Ronquist, G. (2012), 'Cardiomyocyte microvesicles contain dna/rna and convey biological messages to target cells', *PloS one* **7**(4), e34653.

Walker, Eleni Tzima, J. H. (2000), 'Platelet annexin v: the ins and outs', *Platelets* **11**(5), 245–251.

Wallace, P. K., Tario Jr, J. D., Fisher, J. L., Wallace, S. S., Ernstoff, M. S. and Muirhead, K. A. (2008), 'Tracking antigen-driven responses by flow cytometry: Monitoring proliferation by dye dilution', *Cytometry Part A* **73**(11), 1019–1034.

Walsh, K. and Perlman, H. (1997), 'Cell cycle exit upon myogenic differentiation', *Current opinion in genetics & development* **7**(5), 597–602.

Wang, C., Liu, F., Liu, Y.-Y., Zhao, C.-H., You, Y., Wang, L., Zhang, J., Wei, B., Ma, T., Zhang, Q. et al. (2011), 'Identification and characterization of neuroblasts in the subventricular zone and rostral migratory stream of the adult human brain', *Cell research* **21**(11), 1534.

Wang, F., Kohan, A. B., Lo, C.-M., Liu, M., Howles, P. and Tso, P. (2015), 'Apolipoprotein a-iv: a protein intimately involved in metabolism', *Journal of lipid research* pp. jlr–R052753.

Wang, H. and Wang, B. (2016), 'Extracellular vesicle microrna s mediate skeletal muscle myogenesis and disease', *Biomedical reports* **5**(3), 296–300.

Wang, K. (2017), 'The ubiquitous existence of microrna in body fluids', *Clinical chemistry* **63**(3), 784–785.

Wang, Y. and Xu, D. (2017), 'Effects of aerobic exercise on lipids and lipoproteins', *Lipids in health and disease* **16**(1), 132.

Warburton, D. E. and Bredin, S. S. (2017), 'Health benefits of physical activity: a systematic review of current systematic reviews', *Current opinion in cardiology* **32**(5), 541–556.

Warburton, D. E., Charlesworth, S., Ivey, A., Nettlefold, L. and Bredin, S. S. (2010), 'A systematic review of the evidence for canada's physical activity guidelines for adults', *International Journal of Behavioral Nutrition and Physical Activity* **7**(1), 39.

Warburton, D. E., Nicol, C. W. and Bredin, S. S. (2006), 'Prescribing exercise as preventive therapy', *Cmaj* **174**(7), 961–974.

Wardle, S. L., Bailey, M. E., Kilikevicius, A., Malkova, D., Wilson, R. H., Venckunas, T. and Moran, C. N. (2015), 'Plasma microrna levels differ between endurance and strength athletes', *PloS one* **10**(4), e0122107.

Webber, J. and Clayton, A. (2013), 'How pure are your vesicles?', *Journal of extracellular vesicles* **2**(1), 19861.

Weber, J. A., Baxter, D. H., Zhang, S., Huang, D. Y., Huang, K. H., Lee, M. J., Galas, D. J. and Wang, K. (2010), 'The microrna spectrum in 12 body fluids', *Clinical chemistry* **56**(11), 1733–1741.

Wei, R., Li, G. and Seymour, A. B. (2014), Multiplexed, quantitative, and targeted metabolite profiling by lc-ms/mrm, *in* 'Mass Spectrometry in Metabolomics', Springer, pp. 171–199.

Wei, R., Wang, J., Su, M., Jia, E., Chen, T. and Ni, Y. (2017), 'Missing value imputation approach for mass spectrometry-based metabolomics data', *Nature* .

Weigert, C., Hoene, M. and Plomgaard, P. (2018), 'Hepatokines—a novel group of exercise factors', *Pflügers Archiv-European Journal of Physiology* pp. 1–14.

Weintraub, H., Davis, R., Tapscott, S., Thayer, M., Krause, M., Benezra, R., Blackwell, T. K., Turner, D., Rupp, R., Hollenberg, S. et al. (1991), 'The myod gene family: nodal point during specification of the muscle cell lineage', *Science* **251**(4995), 761–766.

Whitham, M. and Febbraio, M. A. (2016), 'The ever-expanding myokinome: discovery challenges and therapeutic implications', *Nature Reviews Drug Discovery* **15**(10), 719.

Whitham, M., Parker, B. L., Friedrichsen, M., Hingst, J. R., Hjorth, M., Hughes, W. E., Egan, C. L., Cron, L., Watt, K. I., Kuchel, R. P. et al. (2018), 'Extracellular vesicles provide a means for tissue crosstalk during exercise', *Cell metabolism* **27**(1), 237–251.

WHO (2018), 'WHO physical activity fact sheet', `https://www.who.int/news-room/fact-sheets/detail/physical-activity`. Accessed: September 2018.

Wichterle, H., García-Verdugo, J. M. and Alvarez-Buylla, A. (1997), 'Direct evidence for homotypic, glia-independent neuronal migration', *Neuron* **18**(5), 779–791.

Wilhelm, E. N., González-Alonso, J., Parris, C. and Rakobowchuk, M. (2016), 'Exercise intensity modulates the appearance of circulating microvesicles with proangiogenic potential upon endothelial cells', *American Journal of Physiology-Heart and Circulatory Physiology* **311**(5), H1297–H1310.

Winter, J. N., Jefferson, L. S. and Kimball, S. R. (2011), 'Erk and akt signaling pathways function through parallel mechanisms to promote mtorc1 signaling', *American Journal of Physiology-Cell Physiology* **300**(5), C1172.

Wisgrill, L., Lamm, C., Hartmann, J., Preißing, F., Dragosits, K., Bee, A., Hell, L., Thaler, J., Ay, C., Pabinger, I. et al. (2016), 'Peripheral blood microvesicles secretion is influenced by storage time, temperature, and anticoagulants', *Cytometry Part A* **89**(7), 663–672.

Witke, W., Sharpe, A. H., Hartwig, J. H., Azuma, T., Stossel, T. P. and Kwiatkowski, D. J. (1995), 'Hemostatic, inflammatory, and fibroblast responses are blunted in mice lacking gelsolin', *Cell* **81**(1), 41–51.

Wittenberg, A. D., Azar, S., Klochendler, A., Stolovich-Rain, M., Avraham, S., Birnbaum, L., Gallimidi, A. B., Katz, M., Dor, Y. and Meyuhas, O. (2016), 'Phosphorylated ribosomal protein s6 is required for akt-driven hyperplasia and malignant transformation, but not for hypertrophy, aneuploidy and hyperfunction of pancreatic β-cells', *PloS one* **11**(2), e0149995.

Witwer, K. W., Buzas, E. I., Bemis, L. T., Bora, A., Lässer, C., Lötvall, J., Nolte-'t Hoen, E. N., Piper, M. G., Sivaraman, S., Skog, J. et al. (2013), 'Standardization of sample collection,

isolation and analysis methods in extracellular vesicle research', *Journal of extracellular vesicles* **2**(1), 20360.

Wolf, P. (1967), 'The nature and significance of platelet products in human plasma', *British journal of haematology* **13**(3), 269–288.

Wolin, K. Y., Yan, Y., Colditz, G. A. and Lee, I. (2009), 'Physical activity and colon cancer prevention: a meta-analysis', *British journal of cancer* **100**(4), 611.

Xin, H., Li, Y., Cui, Y., Yang, J. J., Zhang, Z. G. and Chopp, M. (2013), 'Systemic administration of exosomes released from mesenchymal stromal cells promote functional recovery and neurovascular plasticity after stroke in rats', *Journal of Cerebral Blood Flow & Metabolism* **33**(11), 1711–1715.

Xu, J., Liao, K. and Zhou, W. (2018), 'Exosomes regulate the transformation of cancer cells in cancer stem cell homeostasis', *Stem cells international* **2018**.

Yaffe, D. and Saxel, O. (1977), 'Serial passaging and differentiation of myogenic cells isolated from dystrophic mouse muscle', *Nature* **270**(5639), 725.

Yau, S. Y., Li, A., Hoo, R. L., Ching, Y. P., Christie, B. R., Lee, T. M., Xu, A. and So, K.-F. (2014), 'Physical exercise-induced hippocampal neurogenesis and antidepressant effects are mediated by the adipocyte hormone adiponectin', *Proceedings of the National Academy of Sciences* **111**(44), 15810–15815.

Yin, H. (1987), 'Gelsolin: calcium-and polyphosphoinositide-regulated actin-modulating protein', *Bioessays* **7**(4), 176–179.

Yoshida, N., Yoshida, S., Koishi, K., Masuda, K. and Nabeshima, Y.-i. (1998), 'Cell heterogeneity upon myogenic differentiation: down-regulation of myod and myf-5 generates 'reserve cells'', *Journal of cell science* **111**(6), 769–779.

Yuana, Y., Levels, J., Grootemaat, A., Sturk, A. and Nieuwland, R. (2014), 'Co-isolation of extracellular vesicles and high-density lipoproteins using density gradient ultracentrifugation', *Journal of extracellular vesicles* **3**(1), 23262.

Yuana, Y., Sturk, A. and Nieuwland, R. (2013), 'Extracellular vesicles in physiological and pathological conditions', *Blood reviews* **27**(1), 31–39.

Zammit, P. S. (2017), Function of the myogenic regulatory factors myf5, myod, myogenin and mrf4 in skeletal muscle, satellite cells and regenerative myogenesis, *in* 'Seminars in cell & developmental biology', Vol. 72, Elsevier, pp. 19–32.

Zappaterra, M. W. and Lehtinen, M. K. (2012), 'The cerebrospinal fluid: regulator of neurogenesis, behavior, and beyond', *Cellular and Molecular Life Sciences* **69**(17), 2863–2878.

Zarovni, N., Corrado, A., Guazzi, P., Zocco, D., Lari, E., Radano, G., Muhhina, J., Fondelli, C., Gavrilova, J. and Chiesi, A. (2015), 'Integrated isolation and quantitative analysis of exosome shuttled proteins and nucleic acids using immunocapture approaches', *Methods* **87**, 46–58.

Zhang, R. L., Chopp, M., Gregg, S. R., Toh, Y., Roberts, C., LeTourneau, Y., Buller, B., Jia, L., Davarani, S. P. N. and Zhang, Z. G. (2009), 'Patterns and dynamics of subventricular zone neuroblast migration in the ischemic striatum of the adult mouse', *Journal of Cerebral Blood Flow & Metabolism* **29**(7), 1240–1250.

Appendices

A.1 Participant Demographics

Participant age, sex, height, and weight were recorded, along with a cardiopulmonary exercise testing (CPET) score. The CPET score (also VO_2 max) is measured in milliliters of oxygen used in one minute per kilogram of the participant's body weight (mL/kg/min).

Table A.1: Participant Demographics

Variable	Mean (SD)	or	Count (%)
Age (years)	32.6 (10.7)		
Biological Sex			
Male			6 (37.5)
Female			10 (62.5)
Height (cm)	171.3 (9.5)		
Weight (kg)	72.7 (11.1)		
CPET* (mL/kg/min)	34.5 (6.6)		

*derived from VO_2 max test.

CPET, cardiopulmonary exercise testing score.

B.1 Mycoplasma Testing

Rationale

Mycoplasma contamination is a common issue associated with immortalized cell lines, and can persist undetected in cell cultures for a long period of time whilst causing considerable adaptations in cell growth, metabolism and morphology. To minimise the risk of such contamination modulating moblast behaviour, C2C12 cells were routinely tested for mycoplasma contamination using PCR-based detection methods (see section XXXX).

Results

C2C12 cells were confirmed negative for mycoplasma contamination before experimental use: an example image of PCR-based mycoplasma testing is shown in figure B.1. Internal control bands of 160 bp were visible in the positive and negative controls, and 270 bp mycoplasma DNA was visible in the positive control only. Sample control DNA (570 bp) was detected only in the C2C12 sample (figure B.1).

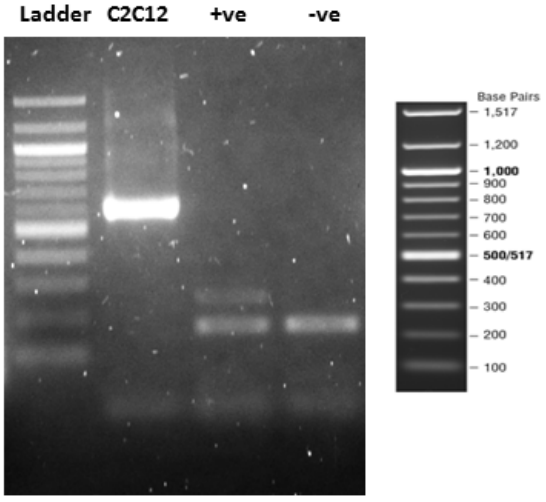

Figure B.1: PCR-based mycoplasma testing of C2C12 cells alongside a 100 bp DNA Ladder and positive (+ve) and negative (-ve) controls

C.1 Power Estimation

Methods

Proliferation data for BrdU positive cells (figure 3.9) was used to perform a retrospective power estimation with G*Power software (v 3.1.9.2). Software was used to predict the sample size required to generate statistically significant results ($p<0.05$ when comparing two paried/dependent means) with a recommended power value of 0.95 (figure C.1).

Results

G*Power software estimated that a minimum of 12 biological replicates should be used for statistically meaningful testing in this instance (figure C.1)

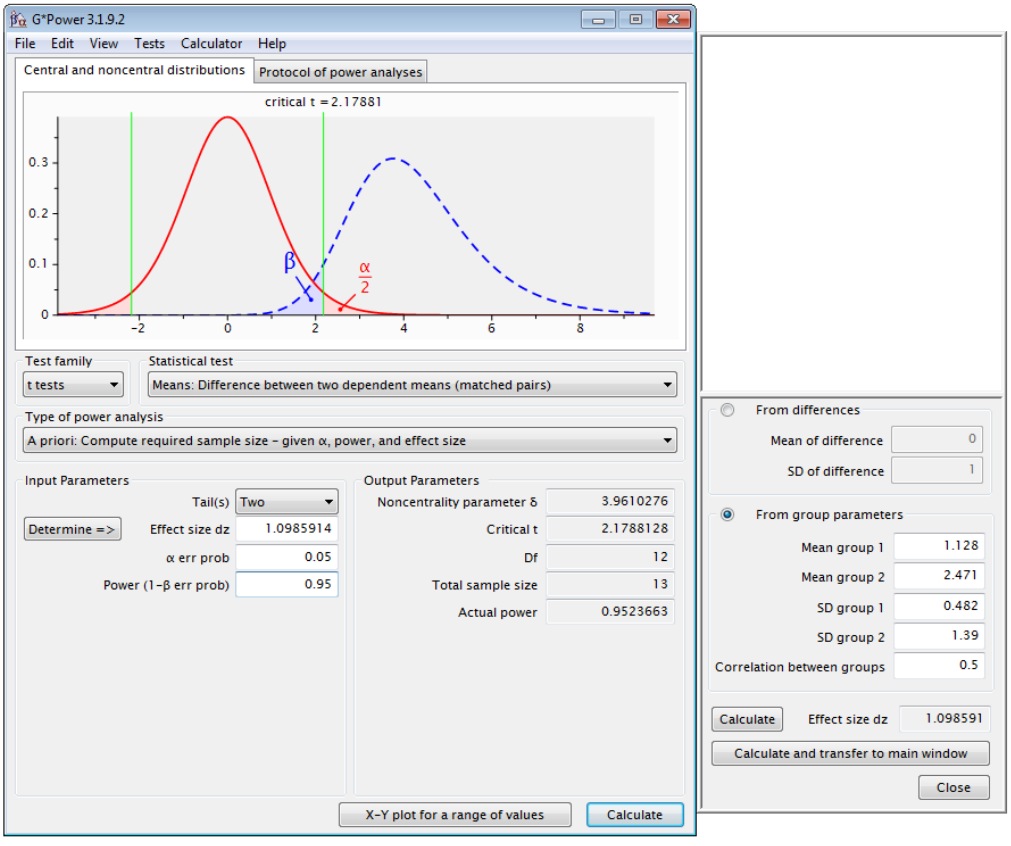

Figure C.1: Power estimation for experimental biological replicates - generated using G*Power (v 3.1.9.2) software

D.1 Spectral analysis of pre- and post-exercise plasma EVs

Table D.1: Plasma EV proteins increased or decreased with exercise - listed here by corresponding gene name, arranged by fold change.

Gene name	Fold Change (rest to exercise)	P Value	Gene name	Fold Change (rest to exercise)	P Value
AMBP	15.667	0.131	AFM	1.660	0.503
TGFBI	12.086	0.165	FGG	1.612	0.405
CD5L	10.896	0.361	CP	1.605	0.226
SEPP1	9.758	0.132	ATIC	1.593	0.739
PCM1	8.793	0.151	FCN3	1.564	0.237
F5	7.423	0.016	APOC3	1.554	0.278
SERPINA4	7.316	0.038	LUM	1.535	0.126
PRPF8	6.915	0.178	SERPINA3	1.486	0.036
FLNA	6.658	0.080	C3	1.477	0.220
LMNB1	4.257	0.519	AGT	1.474	0.555
C4B	3.756	0.193	APOC2	1.471	0.289
CNDP1	3.720	0.163	HBB	1.442	0.558
CFH	3.268	0.085	C8A	1.437	0.498
EEF1A1	3.247	0.432	SERPINF2	1.437	0.371
CLEC3B	3.082	0.460	SERPINF1	1.432	0.359
FCGBP	2.924	0.469	VWF	1.427	0.499
STIP1	2.890	0.596	F2	1.424	0.550
KNG1	2.844	0.163	IGHG1	1.410	0.483
FGA	2.720	0.144	TTR	1.378	0.450
GSN	2.694	0.014	APOE	1.364	0.456
APOA4	2.475	0.010	C6	1.363	0.283
C2	2.298	0.404	A2M	1.320	0.356
HABP2	2.221	0.374	RBP4	1.296	0.733
LRPPRC	2.098	0.596	C1R	1.272	0.584
ATP5B	2.028	0.663	LGALS3BP	1.270	0.470
ORM1	2.003	0.521	FCGR3A/B	1.262	0.891
SPTBN1	1.981	0.497	C8B	1.214	0.541
C1QA	1.968	0.055	APOA1	1.202	0.656
CLU	1.916	0.238	FN1	1.193	0.494
C7	1.893	0.139	PON1	1.179	0.592
GC	1.873	0.104	ITIH1	1.177	0.754
SERPINA6	1.857	0.483	HPX	1.171	0.663
F13A1	1.851	0.404	SERPINA1	1.141	0.800
APOB	1.829	0.065	APCS	1.133	0.718
SERPIND1	1.793	0.420	TFRC	1.121	0.883
TBCA	1.777	0.747	C1QB	1.118	0.755
CFI	1.770	0.525	SF3A3	1.117	0.947
TF	1.754	0.331	IGHM	1.117	0.888
C5	1.746	0.187	F13B	1.098	0.956
CFB	1.717	0.172	ITIH2	1.097	0.826
BCHE	1.697	0.513	CPN1	1.081	0.874
VIM	1.688	0.174	ATRN	1.071	0.849
CA1	1.669	0.633	HRG	1.063	0.917

Gene name	Fold Change (rest to exercise)	P Value	Gene name	Fold Change (rest to exercise)	P Value
C9	1.048	0.939	LDHB	0.597	0.631
CPN2	1.045	0.918	HBD	0.581	0.463
IGFALS	1.040	0.890	PKM	0.567	0.742
C1S	1.022	0.951	HBA1/2	0.549	0.429
HSP90B1	1.017	0.992	IGLC2	0.547	0.073
C8G	1.013	0.945	C4BPA	0.477	0.509
PROS1	1.012	0.973	CLTC	0.467	0.264
KNG1	1.004	0.998	GPX3	0.458	0.340
GPLD1	1.003	0.989	IPO5	0.451	0.670
VTN	0.982	0.963	CPB2	0.443	0.301
APOC1	0.980	0.974	IGKC	0.443	0.368
HPR	0.972	0.929	IGKV1-5	0.438	0.333
LRG1	0.970	0.956	IGHG4	0.419	0.125
GAPDH	0.963	0.982	IGJ	0.410	0.077
ITIH4	0.960	0.910	FASN	0.404	0.566
SAA1/2	0.949	0.939	HSP90AB1	0.397	0.621
HSP90AA1	0.949	0.975	IGLC3	0.383	0.269
XRCC5	0.933	0.963	CAP1	0.372	0.615
PRKDC	0.927	0.894	APOA2	0.333	0.295
APOL1	0.924	0.850	SERPINA5	0.317	0.079
HP	0.898	0.929	GANAB	0.300	0.495
SERPINA7	0.887	0.690	EEF2	0.293	0.298
F10	0.884	0.931	F12	0.277	0.346
PGLYRP2	0.877	0.639	IGHG2	0.266	0.121
PLG	0.863	0.689	HNRNPM	0.251	0.223
KLKB1	0.837	0.771	CCT2	0.245	0.419
SERPINC1	0.832	0.109	C1QC	0.235	0.185
APOM	0.822	0.871	ACTB	0.232	0.274
PLEC	0.819	0.906	HSPA8	0.172	0.467
MASP2	0.789	0.374	EIF3B	0.169	0.475
FGB	0.768	0.711	ENO1	0.167	0.473
LBP	0.767	0.655	IGHG3	0.160	0.387
CALU	0.750	0.866	ECM1	0.000	0.052
IGHA1	0.745	0.605	SERPINA10	0.000	0.073
SERPING1	0.732	0.250	APOH	0.000	0.074
APOD	0.726	0.678	F11	0.000	0.080
BTD	0.694	0.658	APOF	0.000	0.178
ITIH3	0.691	0.561	PSMD3	0.000	0.178
HSPD1	0.674	0.816	SSB	0.000	0.179
LDHA	0.672	0.807	SAA4	0.000	0.179
AZGP1	0.660	0.507	S100A9	0.000	0.181
ORM2	0.648	0.586	DDX5	0.000	0.183
DCD	0.621	0.785	QSOX1	0.000	0.184
EIF3A	0.619	0.703	SEC31A	0.000	0.191
AHSG	0.618	0.374	VCL	0.000	0.201
A1BG	0.614	0.118	F9	0.000	0.203
FCN2	0.606	0.587	IGLL1/5	0.000	0.236

Gene name	Fold Change (rest to exercise)	P Value	Gene name	Fold Change (rest to exercise)	P Value
PUF60	0.000	0.239	GDI2	0.000	0.374
USP7	0.000	0.243	HBG1/2	0.000	0.374
ALDOA	0.000	0.323	NPEPPS	0.000	0.374
HSPA5	0.000	0.350	GLUD1/2	0.000	0.374
IGLC7	0.000	0.374	SEC23IP	0.000	0.374
C4B	0.000	0.374	RPTOR	0.000	0.374
ALDOA	0.000	0.323	TRAP1	0.000	0.374
HSPA5	0.000	0.350	NUP153	0.000	0.374
IGLC7	0.000	0.374	CAD	0.000	0.374
C4B	0.000	0.374	YLPM1	0.000	0.374
NUP133	0.000	0.374	LYZ	0.000	0.374
IGHV4OR15	0.000	0.374	TKT	0.000	0.374
NOC3L	0.000	0.374	MST1	0.000	0.374
MATR3	0.000	0.374	PA2G4	0.000	0.374
EIF3L	0.000	0.374	C6orf229	0.000	0.374
TNXB;TNXA	0.000	0.374	MPI	0.000	0.374
VARS	0.000	0.374	CHD8	0.000	0.374
CFHR1/2	0.000	0.374	SHBG	0.000	0.374
TXNRD1	0.000	0.374	AGRN	0.000	0.374
PDIA3	0.000	0.374	TCERG1	0.000	0.374
IGFBP3	0.000	0.374	PFAS	0.000	0.374
PLTP	0.000	0.374	ACTN4	0.000	0.374
PPP2R1A	0.000	0.374	NARS	0.000	0.374
GTF2I	0.000	0.374	PPL	0.000	0.374
PROC	0.000	0.374	DNAJC13	0.000	0.374
RAP1A/B	0.000	0.374	GLRX3	0.000	0.374
PGD	0.000	0.374	IGHV3-23	0.000	0.374
DPYSL2	0.000	0.374	PIGR	0.000	0.374
FUS	0.000	0.374	IGHA2	0.000	0.374
MOB1A/B	0.000	0.374	IGHD	0.000	0.374
COPS3	0.000	0.374	PPBP	0.000	0.374
HADHB	0.000	0.374	PF4	0.000	0.374
TRIT1	0.000	0.374	LCAT	0.000	0.374
PDIA6	0.000	0.374	HLA-A	0.000	0.374
UNC79	0.000	0.374	GSN	0.000	0.374
FETUB	0.000	0.374	GPI	0.000	0.374
ITIH4	0.000	0.374	TPM3	0.000	0.374
MRPL39	0.000	0.374	P4HB	0.000	0.374
FGG	0.000	0.374	LPA	0.000	0.374
SCLT1	0.000	0.374	SNRPA	0.000	0.374
RAPGEF6	0.000	0.374	DBH	0.000	0.374
UFSP2	0.000	0.374	C4B;C4A	0.000	0.374
MCM4	0.000	0.374	LAMC1	0.000	0.374
COL6A3	0.000	0.374	MBL2	0.000	0.374
TKT	0.000	0.374	LAMP1	0.000	0.374
EIF4B	0.000	0.374	TOP1	0.000	0.374

Gene name	Fold Change (rest to exercise)	P Value	Gene name	Fold Change (rest to exercise)	P Value
CDH5	0.000	0.374	TUBB4B	0.000	0.374
PRG4	0.000	0.374	HNRNPU	0.000	0.374
C1RL	0.000	0.374	RPL18A	0.000	0.374
GP1BA	0.000	0.374	NUCB1	0.000	0.374
SND1	0.000	0.374	LMNB2	0.000	0.374
ZNF587B	0.000	0.374	EML5	0.000	0.374
COL6A1	0.000	0.374	NSUN2	0.000	0.374
TPR	0.000	0.374	BPTF	0.000	0.374
SELL	0.000	0.374	AIMP1	0.000	0.374
IGLL1	0.000	0.374	ACACA	0.000	0.374
ZNF8	0.000	0.374	SPP2	0.000	0.374
PFKL	0.000	0.374	PSMD2	0.000	0.374
PGAM1	0.000	0.374	MAD2L1	0.000	0.374
PZP	0.000	0.374	IFIT5	0.000	0.374
HNRNPA2B1	0.000	0.374	COTL1	0.000	0.374
PROZ	0.000	0.374	DYNC1H1	0.000	0.374
SFPQ	0.000	0.374	PRPSAP1	0.000	0.374
ATP5A1	0.000	0.374	PON3	0.000	0.374
PSMA3	0.000	0.374	ADIPOQ	0.000	0.374
DDX6	0.000	0.374	PCK2	0.000	0.374
PTBP1	0.000	0.374	LSM12	0.000	0.374
CALR	0.000	0.374	ECM29	0.000	0.374
CANX	0.000	0.374	VASN	0.000	0.374
PRDX5	0.000	0.374	CYFIP1/2	0.000	0.374
CMPK1	0.000	0.374	ARMC9	0.000	0.374
SHMT2	0.000	0.374	ABCA13	0.000	0.374
MYH9	0.000	0.374	ALYREF	0.000	0.374
PSMC2	0.000	0.374	CAND1	0.000	0.374
MDH2	0.000	0.374	LEMD2	0.000	0.374
IARS	0.000	0.374	AFG3L2	0.000	0.374
NAMPT	0.000	0.374	NUBPL	0.000	0.374
PSMC4	0.000	0.374	NSMCE1	0.000	0.374
VDAC2	0.000	0.374	GBF1	0.000	0.374
USP5	0.000	0.374	HSPH1	0.000	0.374
STT3A	0.000	0.374	GCN1L1	0.000	0.374
NES	0.000	0.374	ANKS1A	0.000	0.374
AARS	0.000	0.374	COPS5	0.000	0.374
LIG3	0.000	0.374	USP9X	0.000	0.374
SERPINH1	0.000	0.374	MYDGF	0.000	0.374
MMP16	0.000	0.374	FERMT2	0.000	0.374
YARS	0.000	0.374	LRRC59	0.000	0.374
CSE1L	0.000	0.374	SUCLG2	0.000	0.374
LAMB2	0.000	0.374	PHB2	0.000	0.374
ATP5I	0.000	0.374	TMX1	0.000	0.374
EIF4A1	0.000	0.374	TEX10	0.000	0.374
ARF1;ARF3	0.000	0.374	DNAH2	0.000	0.374
HNRNPK	0.000	0.374	RRBP1	0.000	0.374

Gene name	Fold Change (rest to exercise)	P Value
TMSB4X	0.000	0.374
RPL10A	0.000	0.374
PPIA	0.000	0.374
YWHAZ	0.000	0.374
TUBA1A/B	0.000	0.374
CLIC4	0.000	0.374
TBK1	0.000	0.374
SLC25A13	0.000	0.374
UBQLN1	0.000	0.374
GSTK1	0.000	0.374
TLN1	0.000	0.374

D.2 Pathways analysis of proteins increased in post-exercise EVs

Table D.2: Pathways enrichment in proteins significantly increased in post-exercise EVs (fold change >2; T test, p<0.05)

Pathway name	Reactions ratio	P Value	Protein(s)
Assembly of active LPL and LIPC lipase complexes	2.13E-03	4.53E-05	APOA4
Plasma lipoprotein remodeling	3.84E-03	1.46E-04	APOA4
Amyloid fiber formation	6.26E-03	3.87E-04	GSN;APOA4
Plasma lipoprotein assembly, remodeling, and clearance	6.97E-03	4.79E-04	APOA4
Platelet degranulation	9.74E-03	9.31E-04	SERPINA4;F5
Response to elevated platelet cytosolic Ca2+	1.02E-02	1.03E-03	SERPINA4;F5
Caspase-mediated cleavage of cytoskeletal proteins	8.54E-04	4.26E-03	GSN
Platelet activation, signaling and aggregation	2.14E-02	4.39E-03	SERPINA4;F5
Chylomicron assembly	9.96E-04	4.97E-03	APOA4
Chylomicron remodeling	1.21E-03	6.03E-03	APOA4
Plasma lipoprotein assembly	2.13E-03	1.06E-02	APOA4
Common Pathway of Fibrin Clot Formation	2.63E-03	1.31E-02	F5
Cargo concentration in the ER	2.63E-03	1.31E-02	F5
Apoptotic cleavage of cellular proteins	2.70E-03	1.34E-02	GSN
Apoptotic execution phase	3.84E-03	1.91E-02	GSN
Formation of Fibrin Clot (Clotting Cascade)	3.91E-03	1.94E-02	F5
COPII-mediated vesicle transport	5.48E-03	2.71E-02	F5
Retinoid metabolism and transport	5.62E-03	2.78E-02	APOA4
Hemostasis	5.90E-02	3.09E-02	SERPINA4;F5
Metabolism of fat-soluble vitamins	6.69E-03	3.30E-02	APOA4
Metabolism of proteins	1.68E-01	3.61E-02	GSN;APOA4;F5
Post-translational protein phosphorylation	7.75E-03	3.82E-02	F5
Transport of small molecules	6.83E-02	4.06E-02	APOA4
Insulin-like Growth Factor transport and uptake	9.03E-03	4.44E-02	F5
ER to Golgi Anterograde Transport	1.17E-02	5.70E-02	F5
Visual phototransduction	1.19E-02	5.83E-02	APOA4
Apoptosis	1.33E-02	6.48E-02	GSN
Programmed Cell Death	1.39E-02	6.75E-02	GSN
Transport to the Golgi and subsequent modification	1.56E-02	7.55E-02	F5
Metabolism of vitamins and cofactors	2.71E-02	1.28E-01	APOA4
Asparagine N-linked glycosylation	2.99E-02	1.41E-01	F5
Neutrophil degranulation	3.41E-02	1.59E-01	GSN
G alpha signalling events	4.03E-02	1.86E-01	APOA4
Membrane Trafficking	4.73E-02	2.15E-01	F5
Vesicle-mediated transport	5.86E-02	2.61E-01	F5
Innate Immune System	9.42E-02	3.90E-01	GSN
GPCR downstream signalling	9.64E-02	3.98E-01	APOA4
Signaling by GPCR	1.05E-01	4.27E-01	APOA4
Post-translational protein modification	1.13E-01	4.52E-01	F5
Immune System	1.89E-01	6.50E-01	GSN
Signal Transduction	2.27E-01	7.24E-01	APOA4
Metabolism	2.55E-01	7.70E-01	APOA4

D.3 Enrichment of Cellular Components in All Plasma EVs

Table D.3: Cellular component GO terms enrichment in plasma EV proteins (pre- and post-exercise). Determined by Fisher overrepresentation test with Bonferroni correction

GO cellular component	Fold Enrichment	Corrected P-value
extracellular vesicle (GO:1903561)	5.96	1.38E-114
extracellular organelle (GO:0043230)	5.95	1.66E-114
extracellular exosome (GO:0070062)	5.99	2.69E-114
extracellular space (GO:0005615)	4.45	2.25E-113
extracellular region part (GO:0044421)	4.24	9.69E-111
extracellular region (GO:0005576)	3.52	1.05E-95
vesicle (GO:0031982)	3.65	1.80E-85
blood microparticle (GO:0072562)	31.1	1.15E-78
cytoplasmic vesicle lumen (GO:0060205)	12.73	8.53E-52
vesicle lumen (GO:0031983)	12.69	1.03E-51
secretory granule lumen (GO:0034774)	12.12	2.44E-45
membrane-bounded organelle (GO:0043227)	1.51	1.12E-33
extracellular matrix (GO:0031012)	7.62	9.29E-33
collagen-containing extracellular matrix (GO:0062023)	9.45	5.03E-31
secretory granule (GO:0030141)	5.45	5.16E-31
organelle (GO:0043226)	1.41	3.28E-28
organelle lumen (GO:0043233)	2.14	1.02E-27
intracellular organelle lumen (GO:0070013)	2.14	1.02E-27
membrane-enclosed lumen (GO:0031974)	2.14	1.02E-27
secretory vesicle (GO:0099503)	4.68	3.59E-27
endoplasmic reticulum lumen (GO:0005788)	8.79	7.13E-25
cytoplasmic vesicle part (GO:0044433)	3.55	5.60E-23
cytoplasmic vesicle (GO:0031410)	2.88	1.05E-22
intracellular vesicle (GO:0097708)	2.88	1.17E-22
platelet alpha granule lumen (GO:0031093)	22.13	2.27E-21
protein-containing complex (GO:0032991)	1.96	2.58E-20
platelet alpha granule (GO:0031091)	16.92	1.02E-19
endomembrane system (GO:0012505)	2.03	2.97E-17
lipoprotein particle (GO:1990777)	28.51	9.75E-17
plasma lipoprotein particle (GO:0034358)	28.51	9.75E-17
protein-lipid complex (GO:0032994)	27.09	2.07E-16
high-density lipoprotein particle (GO:0034364)	37.29	2.88E-16
cytoplasmic part (GO:0044444)	1.5	1.39E-15
cell surface (GO:0009986)	3.63	2.41E-13
intracellular organelle part (GO:0044446)	1.49	4.96E-13
organelle part (GO:0044422)	1.45	5.91E-12
ficolin-1-rich granule lumen (GO:1904813)	9.66	1.11E-10
cytoplasm (GO:0005737)	1.35	1.54E-10
cellular component (GO:0005575)	1.11	9.80E-10
triglyceride-rich plasma lipoprotein particle (GO:0034385)	31.36	3.04E-09
very-low-density lipoprotein particle (GO:0034361)	31.36	3.04E-09
melanosome (GO:0042470)	9.68	6.60E-09
pigment granule (GO:0048770)	9.68	6.60E-09
ficolin-1-rich granule (GO:0101002)	6.78	1.66E-08

GO cellular component	Fold Enrichment	Corrected P-value
endocytic vesicle lumen (GO:0071682)	31.68	2.90E-08
external side of plasma membrane (GO:0009897)	4.44	6.03E-08
chylomicron (GO:0042627)	39.48	7.07E-08
myelin sheath (GO:0043209)	6.91	1.07E-07
platelet dense granule lumen (GO:0031089)	36.66	1.14E-07
spherical high-density lipoprotein particle (GO:0034366)	57.02	1.17E-07
side of membrane (GO:0098552)	3.51	3.34E-07
immunoglobulin complex, circulating (GO:0042571)	9	1.00E-06
endoplasmic reticulum (GO:0005783)	2.16	1.23E-06
platelet dense granule (GO:0042827)	24.44	1.80E-06
membrane attack complex (GO:0005579)	57.02	1.88E-06
immunoglobulin complex (GO:0019814)	8.55	1.89E-06
endoplasmic reticulum part (GO:0044432)	2.37	5.43E-06
pore complex (GO:0046930)	25.34	1.22E-05
vacuolar lumen (GO:0005775)	5.7	3.99E-05
azurophil granule (GO:0042582)	5.92	6.30E-05
primary lysosome (GO:0005766)	5.92	6.30E-05
intrinsic component of membrane (GO:0031224)	0.57	1.53E-04
intracellular organelle (GO:0043229)	1.22	1.67E-04
integral component of membrane (GO:0016021)	0.57	1.68E-04
intermediate-density lipoprotein particle (GO:0034363)	57.02	4.94E-04
nuclear periphery (GO:0034399)	5.83	5.31E-04
vacuolar part (GO:0044437)	2.97	5.69E-04
low-density lipoprotein particle (GO:0034362)	24.44	1.13E-03
endoplasmic reticulum compartment (GO:0005793)	5.88	1.26E-03
azurophil granule lumen (GO:0035578)	6.97	1.94E-03
ribonucleoprotein complex (GO:1990904)	2.42	1.98E-03
lysosome (GO:0005764)	2.66	2.14E-03
lytic vacuole (GO:0000323)	2.66	2.20E-03
focal adhesion (GO:0005925)	3.25	2.34E-03
fibrinogen complex (GO:0005577)	35.64	2.42E-03
cell-substrate adherens junction (GO:0005924)	3.22	2.63E-03
cell-substrate junction (GO:0030055)	3.19	3.07E-03
endocytic vesicle (GO:0030139)	3.66	3.74E-03
cytosol (GO:0005829)	1.45	5.80E-03
vacuole (GO:0005773)	2.46	5.91E-03
intracellular part (GO:0044424)	1.16	7.08E-03
collagen trimer (GO:0005581)	6.27	1.39E-02
anchoring junction (GO:0070161)	2.68	1.40E-02
tertiary granule lumen (GO:1904724)	8.29	1.74E-02
adherens junction (GO:0005912)	2.65	2.44E-02
Golgi lumen (GO:0005796)	5.65	3.21E-02
specific granule lumen (GO:0035580)	7.36	3.82E-02
membrane (GO:0016020)	1.24	4.28E-02
intracellular membrane-bounded organelle (GO:0043231)	1.21	4.39E-02

D.4 Enrichment of Biological Processes in post-exercise EVs

Table D.4: Biological process GO terms enrichment of proteins increased in post-exercise EVs. Determined by Fisher overrepresentation test with Bonferroni correction

GO Biological Process complete	Fold Enrichment	Corrected P-value
chylomicron remodeling (GO:0034371)	100	2.44E-07
complement activation, alternative pathway (GO:0006957)	100	3.38E-12
regulation of very-low-density lipoprotein particle remodeling (GO:0010901)	100	4.93E-02
chylomicron assembly (GO:0034378)	100	6.47E-07
triglyceride-rich lipoprotein particle clearance (GO:0071830)	100	1.98E-03
chylomicron remnant clearance (GO:0034382)	100	1.98E-03
triglyceride-rich lipoprotein particle remodeling (GO:0034370)	100	1.49E-06
positive regulation of cholesterol esterification (GO:0010873)	93.52	2.84E-03
very-low-density lipoprotein particle remodeling (GO:0034372)	93.52	2.84E-03
phospholipid efflux (GO:0033700)	87.67	1.10E-04
regulation of triglyceride catabolic process (GO:0010896)	76.52	5.39E-03
regulation of cholesterol esterification (GO:0010872)	76.52	5.39E-03
blood coagulation, fibrin clot formation (GO:0072378)	70.14	6.06E-10
protein activation cascade (GO:0072376)	70.14	6.06E-10
reverse cholesterol transport (GO:0043691)	70.14	1.05E-05
cytolysis (GO:0019835)	70.14	6.06E-10
high-density lipoprotein particle remodeling (GO:0034375)	61.89	4.61E-04
fibrinolysis (GO:0042730)	57.39	2.91E-05
cholesterol efflux (GO:0033344)	54.89	3.65E-05
plasma lipoprotein particle remodeling (GO:0034369)	52.61	2.25E-06
protein-lipid complex remodeling (GO:0034368)	52.61	2.25E-06
blood coagulation, intrinsic pathway (GO:0007597)	49.51	2.31E-02
protein-containing complex remodeling (GO:0034367)	49.1	3.42E-06
plasma lipoprotein particle assembly (GO:0034377)	48.56	6.88E-05
regulation of complement activation (GO:0030449)	44.69	1.68E-27
protein-lipid complex assembly (GO:0065005)	42.08	1.46E-04
triglyceride catabolic process (GO:0019433)	40.47	2.88E-03
regulation of humoral immune response (GO:0002920)	39.85	1.06E-27
regulation of triglyceride metabolic process (GO:0090207)	37.13	2.83E-04
platelet degranulation (GO:0002576)	36.17	4.28E-23
acute-phase response (GO:0006953)	35.93	2.35E-05
negative regulation of blood coagulation (GO:0030195)	34.35	2.24E-06
negative regulation of hemostasis (GO:1900047)	33.67	2.59E-06
plasma lipoprotein particle organization (GO:0071827)	33.48	3.65E-05
negative regulation of coagulation (GO:0050819)	32.37	3.43E-06
triglyceride homeostasis (GO:0070328)	31.88	8.28E-03
acylglycerol homeostasis (GO:0055090)	31.88	8.28E-03
acylglycerol catabolic process (GO:0046464)	31.88	8.28E-03
neutral lipid catabolic process (GO:0046461)	31.88	8.28E-03
protein-lipid complex subunit organization (GO:0071825)	30.69	6.29E-05
regulation of cholesterol transport (GO:0032374)	27.45	1.43E-03
regulation of sterol transport (GO:0032371)	27.45	1.43E-03
negative regulation of wound healing (GO:0061045)	27.05	1.12E-06

GO Biological Process complete	Fold Enrichment	Corrected P-value
plasma lipoprotein particle clearance (GO:0034381)	26.3	1.96E-02
complement activation (GO:0006956)	25.86	3.42E-20
cholesterol transport (GO:0030301)	25.4	2.08E-04
complement activation, classical pathway (GO:0006958)	24.68	1.26E-16
regulation of blood coagulation (GO:0030193)	24.59	2.44E-06
regulation of hemostasis (GO:1900046)	24.28	2.71E-06
humoral immune response mediated by circulating immunoglobulin (GO:0002455)	23.94	2.14E-16
regulation of coagulation (GO:0050818)	23.38	3.69E-06
negative regulation of response to wounding (GO:1903035)	23.09	4.07E-06
acute inflammatory response (GO:0002526)	23.06	3.98E-05
sterol transport (GO:0015918)	21.66	5.70E-04
regulation of plasma lipoprotein particle levels (GO:0097006)	20.46	8.20E-04
immunoglobulin mediated immune response (GO:0016064)	19.89	5.33E-15
B cell mediated immunity (GO:0019724)	19.69	6.33E-15
retinoid metabolic process (GO:0001523)	18.91	1.68E-04
diterpenoid metabolic process (GO:0016101)	17.72	2.70E-04
cholesterol homeostasis (GO:0042632)	16.19	2.53E-02
regulation of wound healing (GO:0061041)	16.19	1.07E-05
sterol homeostasis (GO:0055092)	15.98	2.72E-02
terpenoid metabolic process (GO:0006721)	15.73	6.42E-04
lymphocyte mediated immunity (GO:0002449)	15.32	4.98E-13
negative regulation of endopeptidase activity (GO:0010951)	15.27	3.73E-12
humoral immune response (GO:0006959)	15.2	3.63E-18
negative regulation of peptidase activity (GO:0010466)	14.74	6.70E-12
adaptive immune response based on somatic recombination of immune receptors (GO:0002460)	14.7	1.02E-12
regulation of lipid localization (GO:1905952)	13.92	2.55E-04
regulation of lipid transport (GO:0032368)	13.9	9.58E-03
regulation of response to wounding (GO:1903034)	13.66	4.96E-05
isoprenoid metabolic process (GO:0006720)	13.36	2.10E-03
regulation of immune effector process (GO:0002697)	13.09	3.68E-19
blood coagulation (GO:0007596)	12.33	7.14E-10
coagulation (GO:0050817)	12.25	7.94E-10
hemostasis (GO:0007599)	12.13	9.29E-10
organic hydroxy compound transport (GO:0015850)	12.11	4.27E-03
negative regulation of proteolysis (GO:0045861)	11.29	9.63E-11
regulation of blood vessel size (GO:0050880)	10.99	4.21E-02
regulation of tube size (GO:0035150)	10.91	4.41E-02
regulation of endopeptidase activity (GO:0052548)	10.29	9.50E-11
regulation of peptidase activity (GO:0052547)	10.18	2.30E-11
activation of immune response (GO:0002253)	10.13	1.38E-15
negative regulation of hydrolase activity (GO:0051346)	9.73	5.39E-11
regulation of lipid biosynthetic process (GO:0046890)	9.35	2.72E-02
post-translational protein modification (GO:0043687)	9.3	2.38E-07

GO Biological Process complete	Fold Enrichment	Corrected P-value
extracellular structure organization (GO:0043062)	9.22	2.68E-07
wound healing (GO:0042060)	8.47	1.29E-08
receptor-mediated endocytosis (GO:0006898)	8.39	1.01E-03
regulation of body fluid levels (GO:0050878)	8.23	2.11E-08
regulated exocytosis (GO:0045055)	8.2	2.32E-13
positive regulation of immune response (GO:0050778)	8.09	3.75E-15
negative regulation of response to external stimulus (GO:0032102)	8.04	4.02E-04
regulation of proteolysis (GO:0030162)	7.71	4.22E-12
adaptive immune response (GO:0002250)	7.68	1.75E-08
regulation of immune response (GO:0050776)	7.56	1.72E-19
response to wounding (GO:0009611)	7.47	2.81E-08
leukocyte mediated immunity (GO:0002443)	7.46	2.26E-12
innate immune response (GO:0045087)	7.36	1.20E-11
exocytosis (GO:0006887)	7.27	4.20E-12
inflammatory response (GO:0006954)	6.62	9.27E-05
negative regulation of catalytic activity (GO:0043086)	6.38	3.60E-09
defense response (GO:0006952)	6.31	1.95E-17
positive regulation of immune system process (GO:0002684)	6.12	1.78E-12
immune effector process (GO:0002252)	6.08	2.12E-12
secretion by cell (GO:0032940)	6.01	1.10E-10
regulation of lipid metabolic process (GO:0019216)	5.9	2.85E-02
response to inorganic substance (GO:0010035)	5.63	2.05E-03
secretion (GO:0046903)	5.57	2.20E-10
regulation of immune system process (GO:0002682)	5.54	1.40E-16
endocytosis (GO:0006897)	5.42	1.56E-04
negative regulation of molecular function (GO:0044092)	4.92	9.87E-08
negative regulation of protein metabolic process (GO:0051248)	4.68	2.00E-06
import into cell (GO:0098657)	4.66	1.30E-03
regulation of hydrolase activity (GO:0051336)	4.62	5.84E-08
vesicle-mediated transport (GO:0016192)	4.51	2.04E-13
negative regulation of cellular protein metabolic process (GO:0032269)	4.35	1.15E-04
regulation of response to external stimulus (GO:0032101)	4.24	2.39E-02
positive regulation of transport (GO:0051050)	3.97	5.36E-03
immune response (GO:0006955)	3.94	1.32E-08
negative regulation of multicellular organismal process (GO:0051241)	3.6	5.38E-03
positive regulation of response to stimulus (GO:0048584)	3.54	4.20E-09
chemical homeostasis (GO:0048878)	3.53	2.82E-02
proteolysis (GO:0006508)	3.47	2.52E-03
immune system process (GO:0002376)	3.37	7.54E-10
response to stress (GO:0006950)	3.32	6.75E-14
regulation of response to stress (GO:0080134)	3.13	4.37E-02
regulation of catalytic activity (GO:0050790)	3.01	3.26E-05
regulation of cellular protein metabolic process (GO:0032268)	2.89	2.75E-05
positive regulation of multicellular organismal process (GO:0051240)	2.86	3.31E-02

GO Biological Process complete	Fold Enrichment	Corrected P-value
regulation of protein metabolic process (GO:0051246)	2.85	1.07E-05
transport (GO:0006810)	2.61	1.16E-09
regulation of biological quality (GO:0065008)	2.58	2.49E-07
establishment of localization (GO:0051234)	2.54	3.68E-09
regulation of response to stimulus (GO:0048583)	2.49	2.57E-07
regulation of molecular function (GO:0065009)	2.42	1.37E-03
protein metabolic process (GO:0019538)	2.41	1.36E-06
regulation of multicellular organismal process (GO:0051239)	2.33	1.59E-02
organonitrogen compound metabolic process (GO:1901564)	2.2	8.93E-07
localization (GO:0051179)	2.14	1.66E-06
response to chemical (GO:0042221)	2.14	1.32E-03
negative regulation of cellular process (GO:0048523)	2.02	5.95E-03
response to stimulus (GO:0050896)	2.01	8.25E-12
positive regulation of biological process (GO:0048518)	1.93	3.53E-04
macromolecule metabolic process (GO:0043170)	1.93	1.35E-04
nitrogen compound metabolic process (GO:0006807)	1.8	4.82E-04
organic substance metabolic process (GO:0071704)	1.74	1.64E-04
metabolic process (GO:0008152)	1.72	6.34E-05
primary metabolic process (GO:0044238)	1.71	2.71E-03
biological regulation (GO:0065007)	1.5	5.01E-06
regulation of biological process (GO:0050789)	1.5	1.21E-04

D.5 Protein Modifications in Mouse Myoblasts Treated with Pre- and Post-Exercise EVs

Table D.5: Protein modifications antibody array raw data - fold change of spot intensities in C2C12 cells treated with pre- and post-exercise EVs. P value generated by 2-tailed student's T test

Target	Modification	Fold Change (pre- to post-exercise)	P value
Erk1/2	thr202/Tyr204 phos	2.848	6.92E-05
STat1	Tyr701 phos	0.523	8.50E-03
Stat3	Tyr705 phos	2.078	3.96E-03
Akt	Thr308 phos	1.793	1.85E-03
Akt	Ser473 phos	0.046	3.42E-01
AMPKalpha	Thr172 phos	6.445	2.28E-03
S6 Ribosomal Protein	Ser235/236 phos	-2.336	3.71E-02
mTOR	Ser2448 phos	0.190	2.90E-02
HSP27	Ser78 phos	4.270	1.40E-02
Bad	Ser112 phos	1.173	2.92E-02
p70 S6 Kinase	Thr389 phos	-2.039	3.33E-03
PRAS40	Thr246 phos	83.037	3.63E-03
p53	Ser15 phos	-6.469	1.08E-01
p38	Thr180/Tyr182 phos	-0.038	4.13E-01
SAPK/JNK	Thr183/Tyr185 phos	2.138	3.38E-03
PARP	Asp214 Cleavage	3.973	1.63E-03
Caspase-3	Asp175 Cleavage	0.280	4.73E-03
GSK-3beta	Ser9 phos	1.597	9.82E-04